

TECHNISCHE UNIVERSITÄT MÜNCHEN

Fakultät für Chemie

Institut für Siliciumchemie

**Synthesis, Isolation and Reactivity of
Silyl-Substituted Functionalized Silylenes**

Gizem Dübek Bengi

Vollständiger Abdruck der von der Fakultät für Chemie der Technischen Universität München zur Erlangung des akademischen Grades eines

Doktors der Naturwissenschaften (Dr. rer. nat.)

genehmigten Dissertation.

Vorsitzender: Prof. Dr. Lukas Hintermann

Prüfer der Dissertation: 1. Prof. Dr. Shigeyoshi Inoue

2. Prof. Dr. Angela Casini

Die Dissertation wurde am 26.06.2020 bei der Technischen Universität München eingereicht und durch die Fakultät für Chemie am 23.07.2020 angenommen.

Acknowledgements

First of all, I am grateful to Shige (Prof. Dr. Shigeyoshi Inoue) for giving me this opportunity to pursue my PhD study in his research group. I deeply appreciate his constant guidance and support through my scientific journey that helped me in developing both scientifically and personally in TU München.

I would like to thank Dr. Thomas Renner, Dr. Richard Weidner, Dr. Elke Fritz-Langhals, Dr. Jan Tillmann and Dr. Niklas Wienkenhöver of WACKER Chemie AG for their joint project work, many technical discussions, the productive as well pleasant atmosphere at the regular meetings.

I am thankful to all members of AK Inoue who helped me throughout this journey and also for introducing me with Bavarian culture (*Servus!*). I especially thankful to members of our “*Lunch club*”, *Amelie Porzelt*, *Dr. Catherine Weetman* and *Dr. Daniel Franz* for nice (and mostly funny) conversations during lunch time. In particular, many thanks to *Amelie* and *Cath* for helping me in proof reading this thesis and most importantly their constant encouragement and motivation during our “*fresh air breaks*” that ease not only my PhD journey but also everyday life problems.

I would also like to thank you to my life-long friends; *Nagme*, *Nil*, *Dr. Merve* and *Zeynep* for showing me that the almost 2000 km distance is nothing to keep me motivated and create smile in my face and also in my heart. I am also thankful to my friends in Bochum; *Derya*, *Nesli* and *Secil*. I especially thank *Nesli* for regular long hours Skype talks that starting with chemistry, evolving to being an international and finalizing with discussion on delicious foods in Turkish cuisine.

Finally, I would like to thank my dear parents for believing, understanding and supporting me all the time. Especially to the most colorful sister in the world, *Cisem*, for her constant support and help while preparing TOC pictures. Last but not least, I am grateful to my husband, *Burak*, for his patience, understanding and also his immense support in every way he can. I am the luckiest to have you all.

List of Abbreviations

Ad	Adamantane (C ₁₀ H ₁₆)
Ar	Aryl group
B(Ar ^F) ₄	Tetrakis[3,5-bis(trifluoromethyl)phenyl]borate
BCF	Tris(pentafluorophenyl)borane
<i>c</i> AAC	Cyclic alkyl(amino)carbene
COD	1,5-Cyclooctadiene (C ₈ H ₁₂)
Cp	Cyclopentadienyl
Cp*	Pentamethylcyclopentadienyl
Cy	Cyclohexane (C ₆ H ₁₂)
DFT	Density Functional Theory
Dipp	2,6-di- <i>iso</i> -propylphenyl (2,6- <i>i</i> Pr ₂ -C ₆ H ₃)
dippe	1,2-Bis(di- <i>iso</i> -propylphosphino)ethane
DMAP	4-Dimethylaminopyridine ((CH ₃) ₂ NC ₅ H ₄ N)
dmpe	1,2-bis(dimethylphosphino)ethane
dms	Dimethylsulphide
E	Element
e. g.	Latin (<i>exempli gratia</i>): for example
Eind	1,1,3,3,5,5,7,7,-octaethyl-s-hydrindacen-4-yl
Et	Ethyl
<i>et al.</i>	Latin (<i>et alii</i>): and others
etc	Latin (<i>et cetera</i>): and the rest
EWG	Electron withdrawing group
h	Hour
HOMO	Highest occupied molecular orbital
hν	Photolysis, irradiation
^{<i>i</i>} Pr ₂ Me ₂	1,3-bis(<i>iso</i> -propyl)-4,5-dimethylimidazol-2-ylidene
IEt ₂ Me ₂	1,3-bis(ethyl)-4,5-dimethylimidazol-2-ylidene
IMe ₄	1,3,4,5-Tetramethylimidazol-2-ylidene
^{<i>i</i>} Pr	<i>iso</i> -propyl
kcal	Kilocalorie
K-Selectride	Potassium tri- <i>sec</i> -butylborohydride
L	Ligand

LUMO	Lowest unoccupied molecular orbital
M	Metal
m.p.	Melting point
Me	Methyl
Mes	2,4,6-Trimethylphenyl (2,4,6-Me ₃ -C ₆ H ₂)
mmol	milli-mole
MO	Molecular orbital
mol	moles
NHC	<i>N</i> -Heterocyclic carbene
NHI	<i>N</i> -Heterocyclic imine
NHSi	<i>N</i> -Heterocyclic silylene
NMR	Nuclear magnetic resonance
OTf	Triflate, trifluoromethanesulfonate (CF ₃ SO ₃ ⁻)
Ph	Phenyl
ppm	Parts per million
R	Functional group
r.t.	Room temperature
<i>s</i> -Bu	<i>sec</i> -butyl (C ₄ H ₉)
SC XRD	Single-crystal X-ray diffraction
Tbb	C ₆ H ₂ -2,6-[CH(SiMe ₃) ₂] ₂ -4- <i>t</i> Bu
<i>t</i> Bu	<i>tert</i> -butyl
THF	Tetrahydrofuran
Tipp	2,4,6-tri- <i>iso</i> -propylphenyl (2,4,6- ^{<i>i</i>} Pr ₃ -C ₆ H ₂)
TM	Transition metal
tmps	MeSi(CH ₂ PMe ₂) ₃
TMS	Trimethylsilyl
UV-vis	Ultraviolet-visible spectroscopy
X	Halogen atom and related substituent

Publication List

- C. Eisenhut, T. Szilvási, G. Dübek, N. C. Breit, S. Inoue, *Inorg. Chem.* **2017**, *56*, 10061-10069.
“Systematic Study of *N*-Heterocyclic Carbene Coordinate Hydrosilylene Transition-Metal Complexes”
- G. Dübek, D. Franz, C. Eisenhut, P. J. Altmann, S. Inoue, *Dalton Trans.* **2019**, *48*, 5756-5765.
“Reactivity of an NHC-stabilized pyramidal hydrosilylene with electrophilic boron sources”
- G. Dübek, F. Hanusch, S. Inoue, *Inorg. Chem.* **2019**, *58*, 15700-15704.
“NHC-Stabilized Silyl-Substituted Chlorosilylene”
- G. Dübek, F. Hanusch, D. Munz, S. Inoue, *Angew. Chem. Int. Ed.* **2020**, *59*, 5823-5829.
“An Air-Stable Heterobimetallic Si₂M₂ Tetrahedral Cluster”

Table of Contents

Acknowledgements	I
List of Abbreviations	II
Publication List	IV
Table of Contents	V
1 Introduction.....	1
1.1 Low-Valent Heavier Main Group Elements	1
2 Carbenes	3
2.1 <i>N</i> -Heterocyclic Carbenes (NHCs).....	4
2.2 NHCs in Low-Valent Main Group Chemistry	5
3 Silylenes.....	8
3.1 <i>N</i> -Heterocyclic Silylene (NHSi)	10
3.2 Acyclic Silylene	11
3.3 Base Stabilized Silylene.....	12
4 Functionalized Stable Silicon(II) Compounds.....	13
4.1 Silicon(II) Halides.....	13
4.2 Silicon (II) Hydrides	19
5 Silicon-Transition Metal Multiple Bonds	23
6 Motivation of This Work.....	30
7 Reactivity of an NHC-stabilized pyramidal hydrosilylene with electrophilic boron sources ...	32
8 NHC-Stabilized Silyl-Substituted Chlorosilylene	43
9 An Air-stable Heterobimetallic Si₂M₂ Tetrahedral Cluster	49
10 Summary and Outlook	57
11 Bibliography	62
12 Appendix.....	66
12.1 Supporting Information for Chapter 7	66
12.2 Supporting Information for Chapter 8	97
12.3 Supporting Information for Chapter 9	119
12.4 Licenses for Copyrighted Content	183

1 Introduction

1.1 Low-Valent Heavier Main Group Elements

The life on earth depends on the element carbon (C), it is a versatile element that finds itself in everything from DNA to materials in everyday use. As carbon is extensively distributed in nature, it has been subject of intense research by scientists for more than 200 years and hence its properties are widely known. Not only in nature, that we come in contact with everyday life, the existence of low-valent carbon plays a crucial role in interstellar space among Group 14 elements and is particularly important in astrochemistry.^[1] In comparison to carbon, the chemistry of low-valent heavier group 14 elements (Si, Ge, Sn, Pb) only began to be investigated in the last three decades of the twentieth century. Due to the close proximity between carbon and silicon in the periodic table, it could be predicted that they would have similar electronic properties. However, there are fundamental differences between the lighter (C) and heavier elements (Si, Ge, Sn), as the covalent radii increases by nearly 50% from C (0.77 Å) to Si (1.11 Å) (Figure 1).^[2-3] Due to the increased radii, the tendency to form hybridized orbitals vanishes for silicon atom. In addition, Group 14 represents the sole group which contains all three major classification of elements: non-metal, metalloid and metal (Figure 1). Since the beginning of the twenty-first century, spectacular discoveries in heavier-main group chemistry have led to them being described as “transition-metal like”.^[4-6] Stable low-valent derivatives of heavier main group elements have either open or quasi-open coordination sites, which classifies them as highly reactive species and thus they bear the ability to mimic transition metals. Regarding their chemical reactivity, this transition metal like nature has enabled the activation of small molecules under mild conditions and recent achievements have showcased their catalytic ability.^[5, 7]

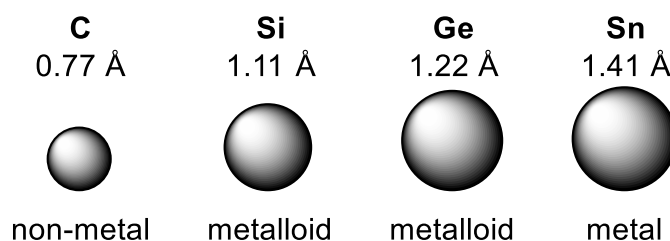


Figure 1. Variation in covalent radii and metallic character upon descending group 14.

The key factor, enabling major breakthroughs in low-valent main group chemistry, has been due to smart ligand design. Sterically demanding ligand motifs provide kinetic stabilization, whilst use of electron donating groups provide electronic stabilization. Consideration of both of these features has allowed for the isolation of stable low coordinate and/or low oxidation state systems and subsequently investigations into their reactivity. The discovery of a variety of simple, easily prepared ligands, which meet the above criteria, has allowed for an increasing number of low-valent main group species. In addition, this has led to the discovery of room-temperature stable main group complexes with astonishing properties, reactivity and catalytic ability. Many of the heavier group 14 elements display high reactivity towards utilization of small molecules such as dihydrogen^[8-10], C^{II} and C^{IV} oxides^[11-13] or ethylene^[14-15] which generally had been reported only for transition-metal species. These reports highlight main group elements compounds showcasing transition-metal like reactivity and open the door to a fruitful and also challenging area of main group catalysis as a replacement for precious and toxic transition metals.

2 Carbenes

Carbenes (general formula, $R_2C:$) are electronically neutral species. The central carbon's six-electron valence shell is covalently bonded through two σ orbitals, with two remaining electrons as a non-bonding electron pair. These two non-bonding electrons can occupy the degenerate p_x and p_y orbitals in a linear carbene structure which includes sp -hybridization (Figure 2, left). Alternatively, they can distribute as spin-paired (singlet) or spin-non-paired (triplet) in a bent structure carbene with a sp^2 -hybridized carbon atom (Figure 2, middle and right). Due to their incomplete electron octet, synthesis and isolation of free, uncoordinated carbenes have been synthetic targets since 1835.^[16]

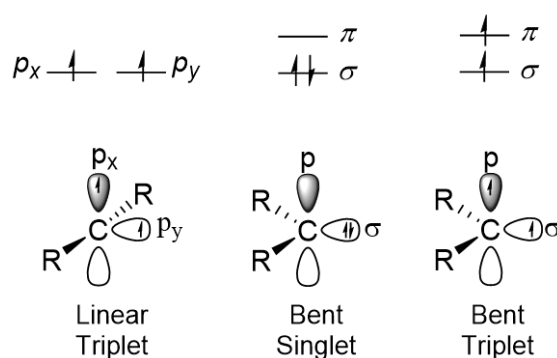


Figure 2. Schematic representation of the different electronic configurations of carbenes ($R_2C:$).

A pioneering study was reported by Bertrand and co-workers in the late 1980s, on isolation of the first acyclic carbene **S2.1** that is stabilized by phosphino and silyl substituents (Figure 3).^[17] Shortly after, in 1991, Arduengo *et al.* reported the first “bottleable” carbene **S2.2** (Figure 3) that is integrated into a nitrogen heterocycle, namely a *N*-heterocyclic carbene (NHC). This was achieved via deprotonation of 1,3-di-1-adamantylimidazolium chloride with sodium hydride in THF.^[18]

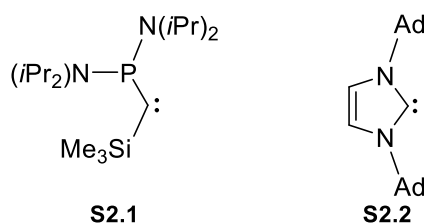


Figure 3. The first reported acyclic (phosphino)(silyl)carbene (**S2.1**, left) and first *N*-heterocyclic carbene (**S2.2**, right).

2.1 N-Heterocyclic Carbenes (NHCs)

After their discovery in 1991, room temperature isolable carbenes, in particular NHCs have played a key role in developing modern organometallic chemistry. Various contributions have been made by several research groups in the development of NHCs and as a result its applications are widely exploited.^[19-23] NHCs have found application not only in homogeneous or organo-catalysis^[24-25], but also in material science^[26-28] and medicinal chemistry^[29-30].

One of the main applications of NHCs are their use as ligands for metal-based catalytic reactions. Since they are strong σ -donors and weak π -acceptors, NHCs are comparable to the ligand class of phosphanes. In fact, it was found that NHCs have various advantages over phosphanes, since they form particularly stronger metal-carbon σ -bonds than the corresponding phosphine complexes. Comparison of the NHC-stabilized second generation Grubbs` catalyst [(SIMEs)(PCy₃)RuCl₂(CHPh)] versus the phosphane-stabilised first generation Grubbs` Catalyst [(PCy₃)₂RuCl₂(CHPh)] shows the strong σ -donation ability and *trans* effect of the coordinated NHC.^[31] This results in enhanced stability and catalytic activity in olefin metathesis.

Although NHCs are mostly known as excellent ligands for metal-based catalysis, another major field of application is the use of nucleophilic carbenes as organocatalysts.^[32] Metal-free catalyzed processes are attractive alternatives to classical metal-based reactions due to their economical low cost and reduced environmental impact. The application of NHCs in organocatalysis first started with benzoin-type reactions (benzoin condensations).^[33-34] Since this initial reactivity several new types of NHC-based organocatalysis has developed rapidly, for example transesterification^[35], ring opening polymerizations (ROPs)^[36] and 1,2-addition reactions.^[37]

The main application of NHCs that has most relevance to this thesis is their use in low-valent main group element chemistry. NHCs have proven to be superior ligands in terms of stabilization of low-oxidation and/or low-coordinate main group elements compared to Lewis base ligands. Thanks to the their tunable steric and electronic properties, numerous remarkable achievements have been reported in the low-valent chemistry of group 13, 14 and 15, which are addressed in detail in the Chapter 2.2.

2.2 NHCs in Low-Valent Main Group Chemistry

Although the majority of scientific contributions focus on the coordination of NHCs to transition metals and their use in organocatalysis, in the last two decades, it was shown that NHCs can also efficiently stabilize low oxidation state Group 13, 14 and 15 elements. One of the main features of the NHCs, in low-valent main group chemistry, is the σ -donation of the NHC to a free σ -accepting orbital of the low valent p-block element.²¹ In addition to their high σ -donor ability, NHCs can be sterically flexible depending on the size of the “wingtip” substituents. Moreover, the electronic characteristic of NHCs can be tuned by altering the number of nitrogen atoms adjacent to carbene carbon atom in the heterocyclic structure, as well as ring size or ring constitution (Figure 4). For example, in 2005, Bertrand *et al.* reported a new type of carbene, by replacing one of the NR groups in the cyclic framework with a CR₂ group, namely cyclic alkyl(amino) carbene (*cAAC*).^[38-41] Due to presence of σ -donating CR₂ group next to the carbene carbon instead of nitrogen, *cAAC*s are stronger σ -donors as well as better π -acceptor ligands than classical NHCs. Furthermore, *cAAC*s are also able to activate small molecules like H₂, NH₃ or CO due to the small HOMO–LUMO separation.^[42] As an additional member of the carbene family, we can also count an isomeric NHC, namely, “abnormal” NHCs (aNHC) are better σ -donors and weaker π -acceptors than the classical isomer due to the reduced heteroatom stabilization.^[43-46] Whilst “normal” NHCs can bind to the metal/element at the C(2) position (NC(2)N), aNHCs can bind through either C(4) or C(5) positions.

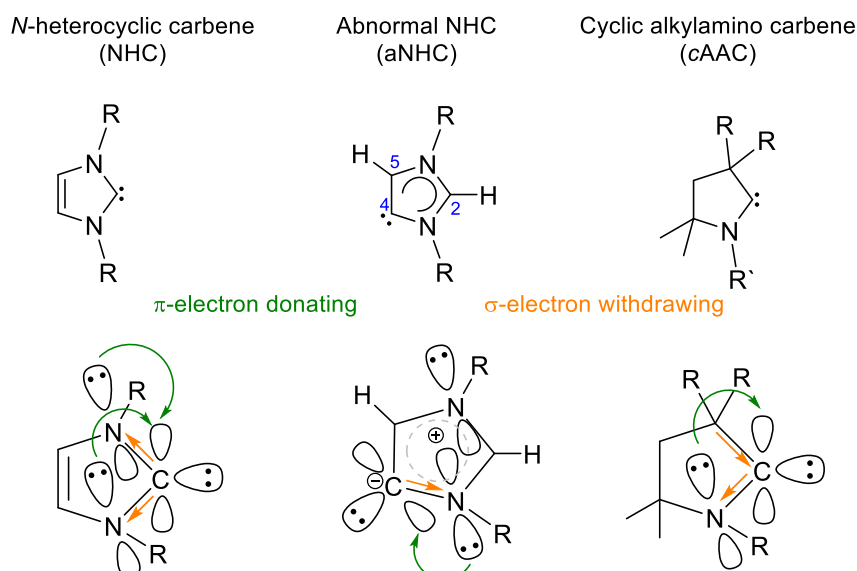


Figure 4. Electronic properties of classical NHC, aNHC and *cAAC* ligands.

Pioneering work in stabilization ability of NHCs to low-valent group 14 elements was carried out by Robinson and co-workers in 2008.^[47] This enabled the isolation of a stable silicon (0) species by the reduction of NHC-stabilized silicon tetrachloride. The obtained disilicon complex **S2.6** (Figure 5) consists of two silicon atoms each exhibiting a non-bonding electron pair. In 2013, the group of Driess reported the synthesis of cyclic silylone **S2.7** (Figure 5), this was made possible by usage of a bidentate NHC ligand in which the NHCs are connected via a methylene bridge.^[48] In the same year, Stalke, Roesky and Frenking *et al.* also described a *cAAC* stabilized biradicaloid silicon atom in the formal oxidation state of zero.^[49] In addition to neutral low-valent main group compounds, NHCs have also led the way to accessing positively charged silicon (II) cations, namely silyliumylidene ions. The groups of Tokitoh, Sasamori and Matsuo as well as Inoue have described numerous examples of silyliumylidene ions **S2.8** (Figure 5) with various ligands and NHCs on the cationic silicon atom.^[50-54] A rare example of silicon (II) dication was reported by Filippou in which three IMe_4 (1,3,4,5-Tetramethylimidazol-2-ylidene) ligands are coordinated to the low-valent silicon center.^[55]

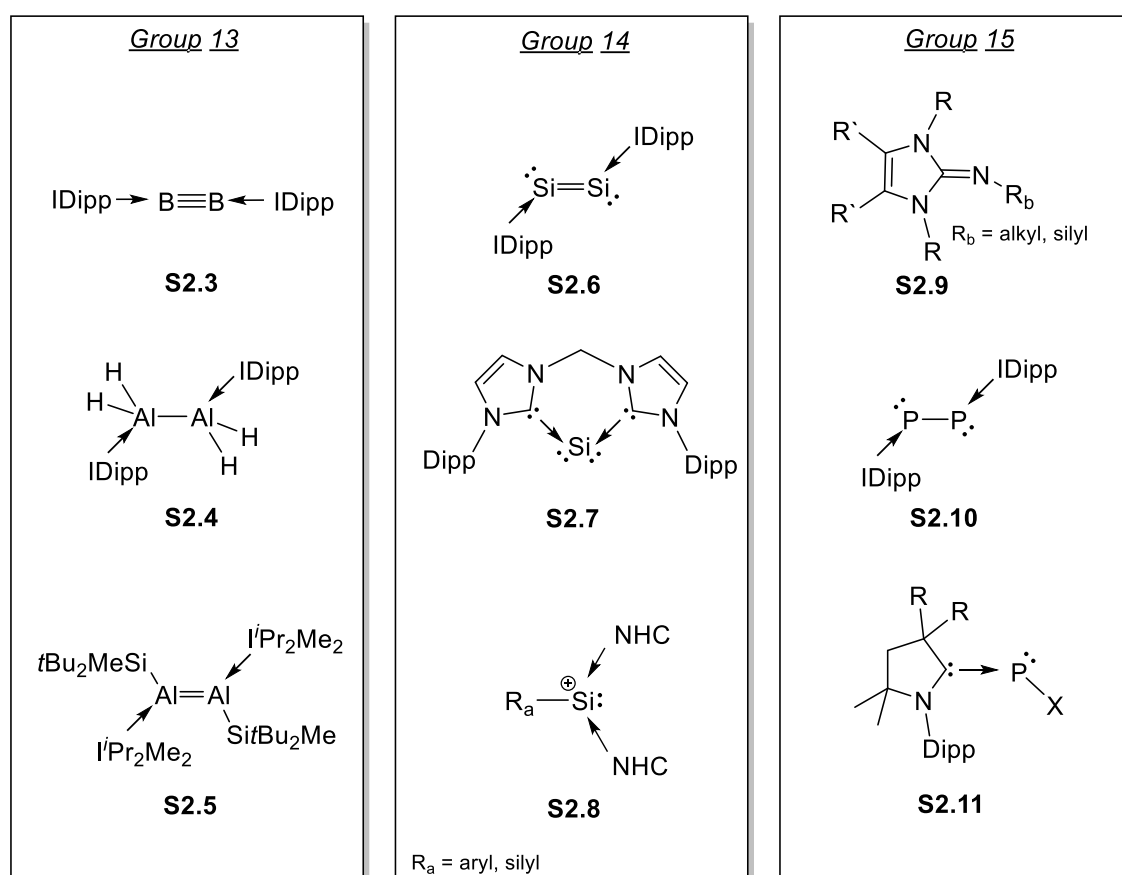


Figure 5. Selected examples of low-valent main group compounds stabilized by NHCs.

3 Silylenes

Silylenes $R_2Si(II)$, the heavier congeners of carbenes, are electronically neutral silicon compounds with a non-bonding electron pair at the divalent silicon center. Despite the close relationship in the periodic table, silylenes differ massively in their electronic properties from their lighter carbon congener. If you consider the calculated molecular structure and electronic configuration of the two divalent parent systems, methylene ($H_2C:$) and silylene ($H_2Si:$), methylene mainly favors the triplet ground state due to very low, indeed negative, singlet-triplet gap ($\Delta E_{S,T} = -14$ kcal/mol). On the other hand, silylene ($H_2Si:$) has a greater single-triplet gap ($\Delta E_{S,T} = 16.7$ kcal/mol)^[66] separation that results in a low tendency to form hybrid orbitals, hence favoring the singlet ground state (Figure 7).

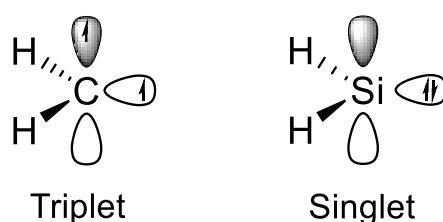


Figure 7. Molecular structure and electronic configuration of methylene ($H_2C:$) and silylene ($H_2Si:$).

Due to the electron configuration of singlet silylenes, the p_z orbital remains unoccupied which makes them susceptible to oligomerization. This results in the formation of disilenes which are still extremely reactive species. Thus, kinetic and/or thermodynamic stabilization is essential to isolate the low-valent silicon center in silylenes. Thermodynamic stabilization can be achieved by donation from the π -donor ligands to the empty p -orbital and kinetic stabilization by introducing sterically demanding ligands (Figure 8).

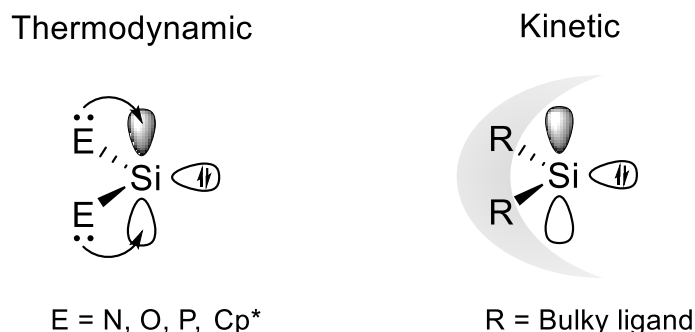


Figure 8. Thermodynamic stabilization of silylenes by π -donor ligands (left) and kinetic stabilization by sterically encumbered ligand (right).

In 1964, the group of Goldstein reported a dimethylsilylene ($(\text{CH}_3)_2\text{Si}:$) in the gas phase as a short-lived intermediate upon reduction of dimethyldichlorosilane ($(\text{CH}_3)_2\text{SiCl}_2$) with sodium-potassium vapor at 260-280 °C.^[67] Over the subsequent two decades, silylenes were thought only to be stable under inert matrices at cryogenic temperatures.^[68] In 1986, Jutzi *et al.* reported the first room temperature stable silicon(II) compound, decamethylsilicocene **S3.1**, from the reduction of the corresponding dihalide with alkali metal (Figure 9).^[69] This report was a great breakthrough in the history low-valent silicon chemistry and has been the subject of recent research.^[70-71] In 1990, Karsch *et al.* reported a four-coordinate stable bis-donor stabilized silylene **S3.2** with a stereochemically active lone pair at the silicon center (Figure 9).^[72] Although these compounds are counted as milestones in low valent silicon chemistry, they are not recognized as “true silylenes” due to their high coordination numbers.

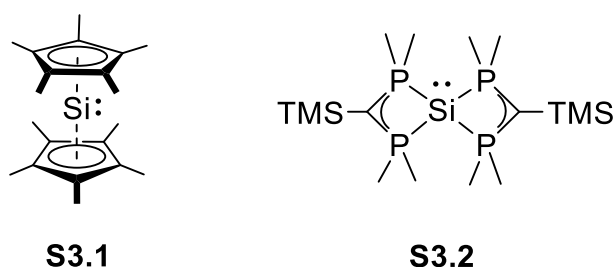


Figure 9. First examples of room temperature isolable divalent Si(II) compounds

3.1 *N*-Heterocyclic Silylene (NHSi)

In 1991, Arduengo *et al.* reported the first NHC **S2.2** (Figure 3) and led the way to the numerous applications not only in academic but also in industrial research. One year later, the first bis(amino)silylene ($\text{Me}_2\text{Si}(\text{N}t\text{Bu})_2\text{Si}:$) was reported by Veith upon photolysis of silicon diazide ($\text{Me}_2\text{Si}(\text{N}t\text{Bu})_2\text{Si}(\text{N}_3)_2$) in an argon matrix at cryogenic temperatures.^[73] Unfortunately, this compound was only stable up to 77 K. Finally, in 1994, Denk and West successfully isolated the first room temperature stable divalent *N*-Heterocyclic Si(II) compound (NHSi) **S3.3**, also known as “West’s silylene”, from the reduction of the corresponding silicon(IV) dichloride precursor with elemental potassium (Figure 10).^[74] Compound **S3.3** is the first member of the divalent cyclic silicon(II) species, which is stabilized by two π -donating amino groups and kinetically supported by two sterically demanding *tert*-butyl groups (Figure 8). Subsequently, the same group also isolated a saturated analog via a similar reduction method.^[75] This analog is more reactive than the unsaturated silylene, and as such it is distinctly less thermally stable.

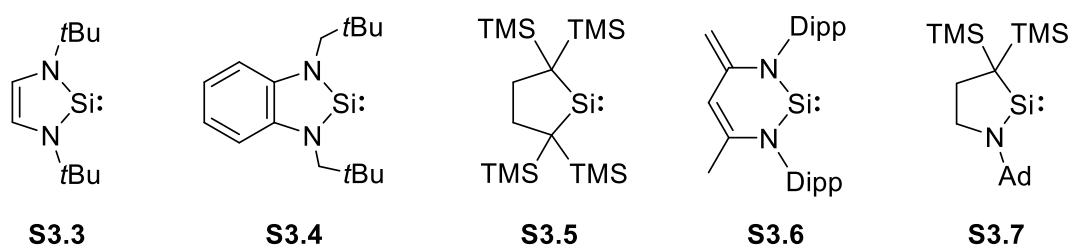


Figure 10. Selected examples of stable *N*-heterocyclic silylenes (NHSi).

Following the isolation of the first NHSi, further examples were described through modifications of the ligand backbone or the amino substituents. For example, in 1995, Lappert and Gerhus reported a new silylene **S3.4** that employed a benzo-fused backbone (Figure 10).^[76] Also in 2006, Driess and co-workers isolated the β -diketimidato-stabilized silylene **S3.6** (Figure 10), this showed ambivalent reactivity towards nucleophiles due to its ylide-like electronic resonance structures.^[77] Roesky, in 2006, reported the first stable chlorosilylene **S4.1** (Figure 13) that is electronically stabilized by a chelating amidinato ligand.^[78] Due to the relevance of this thesis, it will be separately discussed in detail in the Chapter 4.1. As a notable example, Kira *et al.* described a carbocyclic bis(alkyl)silylene **S3.5** (Figure 10). Within this achievement, they showed that stable silylenes do not necessarily need π -donor ligands, which had been previously achieved through use of nitrogen substituents, and can therefore be stabilized only by steric protection.^[79] Very recently, in 2016, the group of Iwamoto reported the synthesis of a novel cyclic(alkyl)(amino)silylene

(*cAASi*) **S3.7** (Figure 10) which is similar to established carbon derivative (*cAACs*).^[80] Compound **S3.7** shows improved thermal stability in comparison to the prior bis(alkyl)silylenes, whilst maintaining similar observed reactivity.

3.2 Acyclic Silylene

Until 2012, stable two-coordinate silylenes were limited to compounds that exhibited the silicon atom as part of a rigid cyclic framework (i.e. NHSi) or high coordination number at silicon(II) center. Although room temperature stable heavier Group 14 tetrylenes ((SiMe₃)₂N)₂E: (E = Ge, Sn) have been known since 1970s,^[81-82] the stable acyclic silylene remained elusive. In 2003, West and Müller reported a semi-stable acyclic bis(bis(trimethylsilyl)amino)silylene (((SiMe₃)₂N)₂Si:) which is stable at -20 °C yet rapidly decomposes above 0 °C.^[83] Finally in 2012, the group of Power succeeded in generating an acyclic thiolate substituted silylene **S3.8** (Figure 11).^[84] Within the same issue, the groups of Aldridge and Jones reported the synthesis of a new acyclic silylene **S3.9** (Figure 11) that bears one amino group and an electropositive σ -donating ligand.^[8] The latter group also implemented a silyl group (Si(SiMe₃)₃) instead of a boryl ligand to be able to synthesize silyl-substituted acyclic silylene **S3.10** (Figure 11).^[85] Two years later, the same groups also reported a new-type isolable acyclic silylene **S3.11** (Figure 11) that bears an extremely bulky boryl-amide ligand.^[86] Thanks to the bulky peripheral substituents, all below compounds **S3.8–11** (Figure 11) are kinetically stabilized and hence thermally robust.

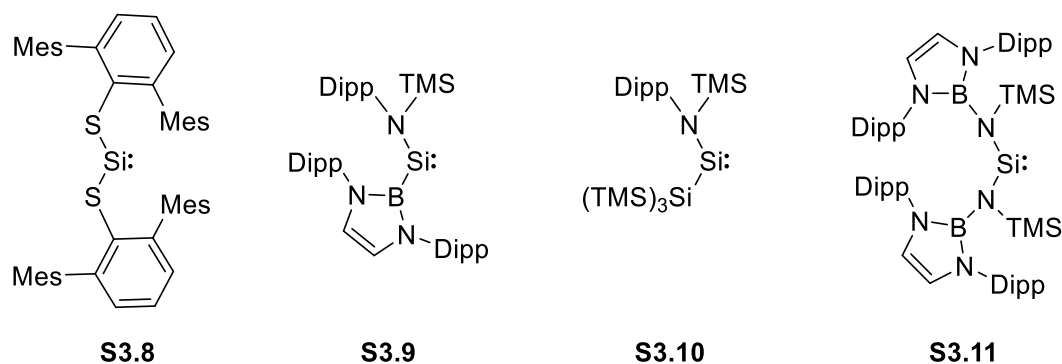


Figure 11. Selected examples of room temperature stable acyclic silylenes.

Acyclic silylenes are thought to be more promising candidates in terms of reactivity towards small molecule activation and/or oxidative addition reactions than NHSi's due to their coordinative flexibility rather than the rigid cyclic framework. In fact, boryl(amino) silylene **S3.9** can activate dihydrogen even at 0 °C.^[8] Similarly, the silyl coordinated silylene **S3.10** (Figure 11) can also split

dihydrogen at room temperature to give corresponding dihydrosilane. Very recently, the same group reported the reductive coupling of CO and CO₂ with **S3.9** (Figure 11).^[87] Inoue and Rieger reported a very reactive acyclic iminosilylsilylene that reversibly inserts into an aromatic C=C double bond to form silacycloheptatriene (silepin).^[88] This silepin can be used as a synthetic equivalent to acyclic silylene. Indeed, treatment of silepin with N₂O successfully furnished the first examples of isolable acyclic, neutral and three-coordinate silanone, which has enhanced stability in both solution and solid state, due to the π -donating NHI ligand and σ -donating silyl groups.^[65]

3.3 Base Stabilized Silylene

The first NHC-adduct of an acyclic bis(silyl)silylene **S3.12** was reported by Sekiguchi in 2012 by reductive dehalogenation of (tBu₃Si)₂SiBr₂ in the presence of IMe₄ (Figure 12).^[89] This compound gained particular interest among the silicon chemistry community, since compound **S3.12** is a rare example of silyl-substituted silylenes. Recently, Cowley and co-workers isolated a NHC-stabilized bis(silyl)silylene **S3.13** (Figure 12) from a donor-supported disilene.^[90] Not only NHCs, but also milder Lewis bases like DMAP can also support reactive acyclic silylenes **S3.14** (Figure 12) as very recently demonstrated by the Inoue group.^[91]

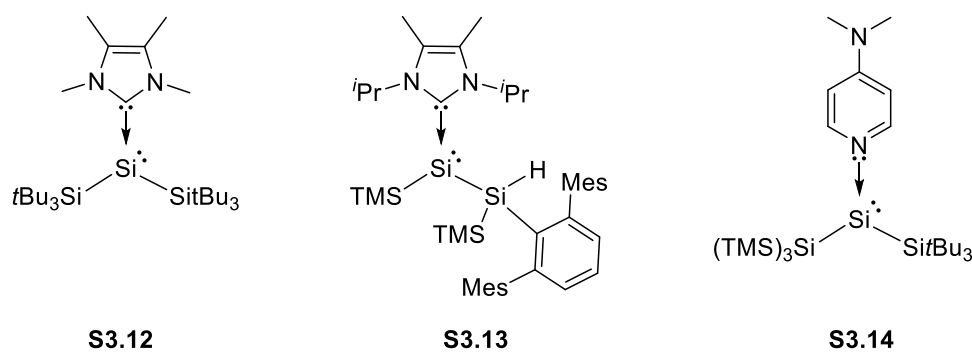


Figure 12. Selected examples of NHC-stabilized acyclic silyl-substituted silylenes.

In addition to acyclic silylenes, Robinson and co-workers reported NHC-stabilized bis-silylenechloride (NHC:(Cl)Si–Si(Cl):NHC) upon reduction of a NHC adduct of SiCl₄ in hexane.^[47] In recent years, NHCs have contributed greatly towards allowing access to a large number of novel low-valent silicon(II) complexes especially in terms of functionalized silylenes, which will be discussed in details in following Chapter 4.

4 Functionalized Stable Silicon(II) Compounds

Over the past 30 years, NHSi ligands have been studied extensively in terms of their synthesis, reactivity and applications in transition-metal like catalysis. A handful of reviews based on the reactivities of bare silylenes have been reported so far^[75, 92-95], however, in contrast much less is known about substituted/functionalized silylenes. In particular, α -substituted three-coordinate silylenes, in which an additional reactive site is gained due to labile substituents, are expected to have distinct reactivity compared to two-coordinate silylenes.

4.1 Silicon(II) Halides

Among functionalized silylene compounds, chloro-substituted silylenes are the most developed class due to the presence of a labile Si-Cl bond. These compounds are prone to undergo salt metathesis type reactions and hence indispensable building blocks for synthetic organosilicon chemistry. The first stable monomeric chlorosilylene **S4.1** (Figure 13) was reported by Roesky and co-workers in 2006, via reduction of amidinato trichlorosilane with finely divided potassium at room temperature in a 10% yield.^[78] The following chemistry of this particular chlorosilylene was limited due to its low yield, yet the same group reported an improved synthesis four years later from the direct reaction of amidinato dichlorohydrosilane with bis-trimethyl silyl lithium amide ($\text{LiN}(\text{TMS})_2$), this increased the isolated yield to 90%.^[96] Compound **S4.1** is kinetically stabilized by sterically hindered amidinato ligand and displays a trigonal pyramidal geometry suggesting the presence of an active lone pair at the silicon center.

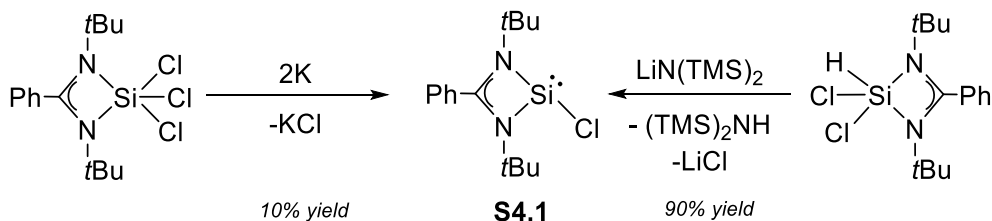


Figure 13. Two alternative synthetic approaches for amidinato chlorosilylene **S4.1**.

Since the successful isolation of the first chlorosilylene (**S4.1**, Figure 13), numerous reactivity investigations have been carried out. Treatment of **S4.1** with biphenyl alkyne at room temperature successfully formed silicon-containing cyclic compound 1,2-disilacyclobutene **S4.2** via oxidative addition (Figure 14). This can be further fluorinated upon using trimethyltin fluoride to form fluoro-substituted disilacyclobutene.^[96] Upon introduction of a less hindered alkyne (methylphosphaalkyne) formation of a five-membered cyclic cation was observed, which consists of silicon, carbon and phosphorus centers.^[97] In 2011, Roesky and co-workers showed that compound **S4.1** can activate P_4 to form a zwitterionic amidinato ligand stabilized Si_2P_2 four membered unit **S4.5** (Figure 14).^[98] Interestingly, in the same year, Inoue and Driess reported the isolation of same Si_2P_2 -cycloheterobutadine **S4.5** that is derived from the reaction of phosphasilene **S4.3** with dichlorotriphenylphosphorane Ph_3PCl_2 .^[99] Treatment of compound **S4.1** with N_2O at room temperature furnished the six-membered Si_3O_3 ring **S4.4**, whilst treatment with benzophenone afforded a monosilaoxirane type complex (Figure 14).

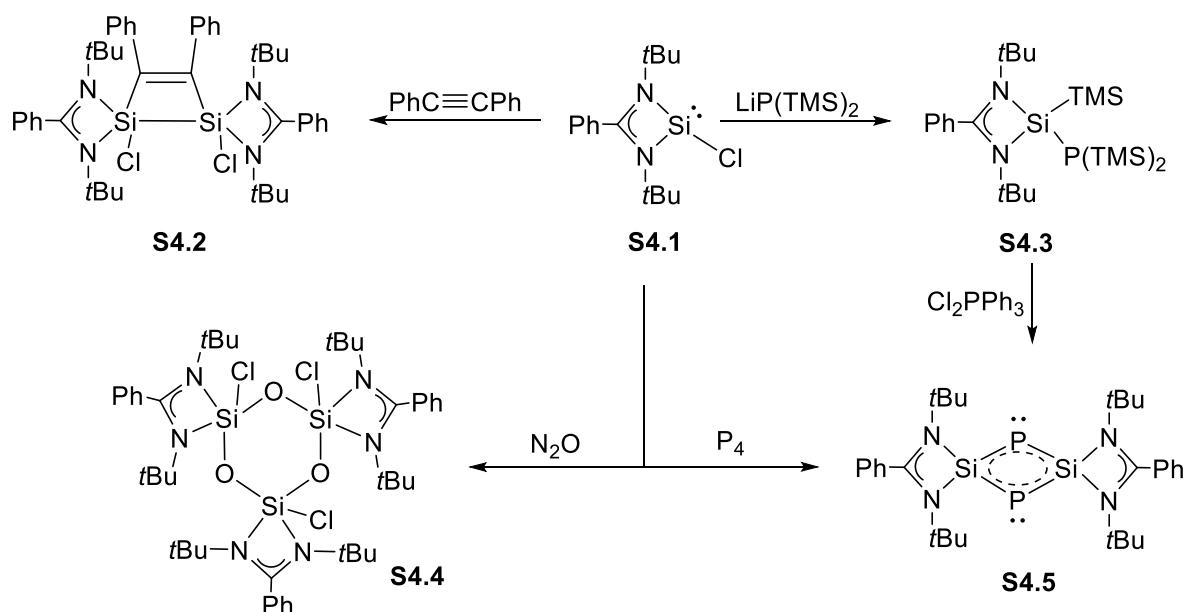


Figure 14. Selected reactivities of amidinato chlorosilylene **S4.1**.

In 2010, Baceiredo and Kato reported a phosphine-stabilized chlorosilylene **S4.6** that shows delightful reactivity, enabling the isolation of a variety of novel silicon containing compounds (Figure 15).^[100] The reaction of chlorosilylene with lithiated phosphinodiazomethane affords phosphino(silyl)diazomethane, this allowed for access to the first isolable phosphine-stabilized silyne ($Si\equiv C$) complex upon photolysis.^[100] The obtained compound **S4.7** is stable up to $-30\text{ }^\circ\text{C}$ and has a very

short silicon-carbon bond that compares well with theoretical predictions for silicon-carbon triple bonds. By using the same synthetic analogy, they also considered to obtain a silylene-substituted azide as a potential precursor for silanitride ($\text{Si}\equiv\text{N}$) species. Unfortunately, reaction of chlorosilylene **S4.6** with sodium azide did not yield the corresponding azide yet it formed 1,3-diaza-2,4-disilacyclobutidine **S4.8** (Figure 15) with an exceptionally short but non-bonded $\text{Si}\cdots\text{Si}$ distance, which lies in the range for that of a $\text{Si}=\text{Si}$ double bond.^[101] This Si_2N_2 four-membered unit can be considered as the dimeric form of the desired silanitride. Recently, the same group also reported the formation of a donor-stabilized silavinylidene phosphorene **S4.9** upon treatment of chlorosilylene with P,S-bis-ylide which results in a remarkably high electron density on the carbon center (Figure 15). Hence, compound **S4.9** can also be considered as a silylene/phosphine supported C(0) center.^[102]

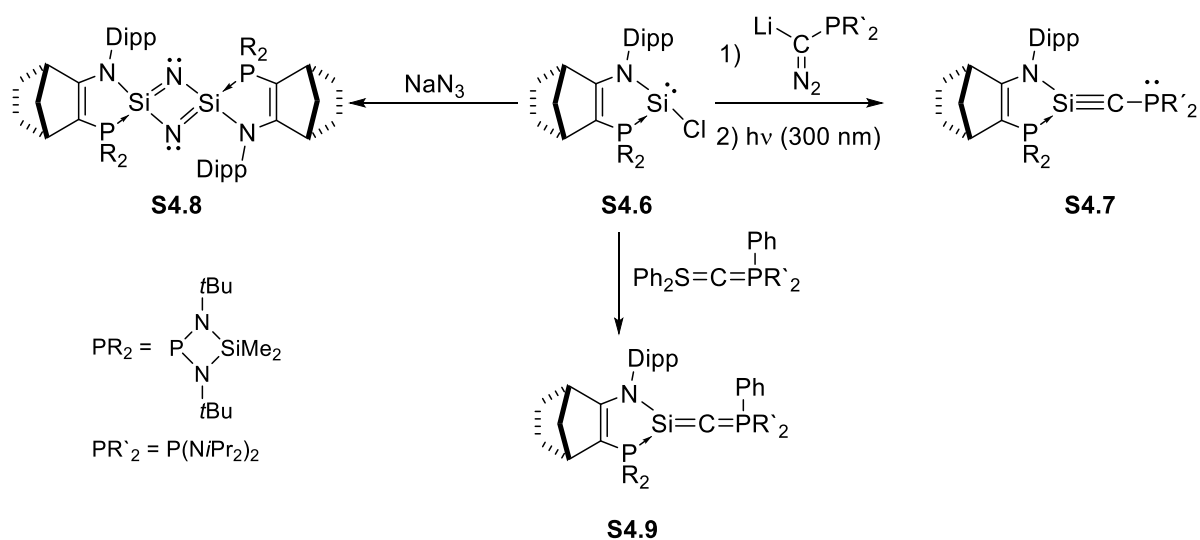


Figure 15. Selected reactivity of a phosphine-stabilized chlorosilylene **S4.6**.

Recently, Driess and co-workers described the isolation of a β -diketiminato chlorosilylene **S4.10** (Figure 16) via the use of a bulky NHC as a dehydrochlorination reagent.^[103] In the same year, Aldridge and co-workers reported a substituted β -ketiminato ligand stabilized chlorosilylene **S4.11**, (nacnac)^{Dipp}SiCl ((nacnac)^{Dipp} = $\text{HC}(\text{Me}_2\text{N})\text{C}(\text{Dipp})\text{N}_2$) that is mildly oxidized with N_2O at room temperature to form a sila-acyl chloride **S4.12** (Figure 16) without the presence of a stabilizing Lewis acid.^[104] Furthermore, nucleophilic substitution of the $\text{Si}(\text{O})\text{Cl}$ unit with either $\text{K}[\text{HBET}_3]$ or KO^tBu successfully furnishes a sila-aldehyde **S4.13** (borane-stabilized) and a sila-ester **S4.14**, respectively (Figure 16).^[104]

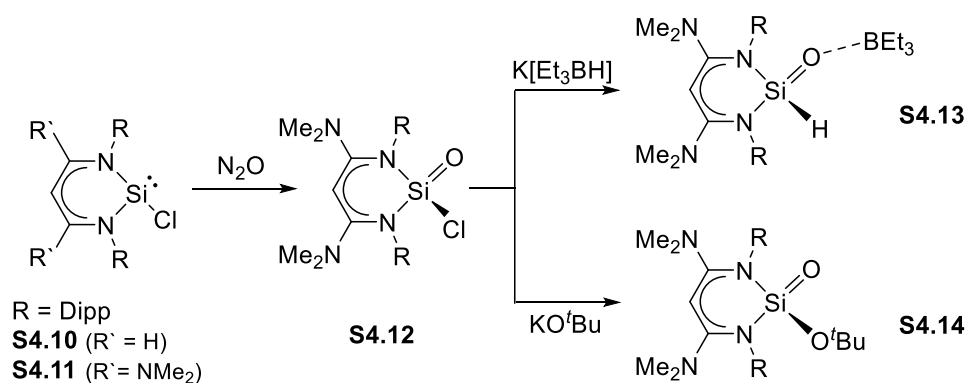


Figure 16. Formation of sila-acyl chloride, sila-aldehyde and sila-ester compounds from β -ketimino chlorosilylene **S4.11**.

In addition to intramolecular Lewis-donor stabilized chlorosilylenes, external Lewis-bases, more precisely NHCs can be also used to support such functionalized silylenes. The first example of a NHC-adduct of chlorosilylene was reported by Filippou *et al.* in 2010.^[105] Whilst one of the two equivalents of NHC selectively dehydrochlorinate the arylchlorosilanes SiArHCl_2 ($\text{Ar} = \text{C}_6\text{H}_3\text{-2,6-Mes}_2$; $\text{C}_6\text{H}_3\text{-2,6-Trip}_2$), the other equivalent externally stabilizes the chlorosilylene **S4.15** (Figure 17). One of the breathtaking compounds derived from **S4.15**, was the first isolable transition metal-silylyne complex ($\text{Si}\equiv\text{M}$) which will be described in detail in Chapter 5. One year later, Cui and co-workers described a new donor-stabilized aminochlorosilylene **S4.16** $\text{RCiSi}\leftarrow\text{NHC}$ ($\text{R} = 2,6\text{-iPr}_2(\text{C}_6\text{H}_3)(\text{SiMe}_3)\text{N}$) via the same method. Compound **S4.16** can be used as a reagent enabling stereoselective bis-silylation of terminal alkynes containing electron withdrawing groups (EWG) to afford compound **S4.18** (Figure 17).^[106-107] Treatment of **S4.16** with various enolizable ketones afforded silicon bis-enolates, whilst use of SiCl_4 yielded different reactions products depending on the reaction conditions.^[108-109] For example, under ambient temperature in Et_2O it formed a rare example of a NHC-stabilized silimine, whereas in hot toluene it transformed to a dimer of dichlorosilimine ($\text{ArN}=\text{SiCl}_2$) that consists of a planar Si_2N_2 central ring. In 2012, Rivard group synthesized amidochlorosilylene **S4.17** (Figure 17) by treating NHC- SiCl_2 adduct with $\text{Li}[\text{NHDipp}]$.^[110] The reaction of compound **S4.17** with a hydride source (LiBH_4) afforded a Si(II) hydride (borane substituted) complex **S4.19** (Figure 17). The same group also reported the heavier congeners (Ge, Sn) via the same synthetic approach. In 2016, Müller group reported another synthetic approach to reproduce Filippou's arylchlorosilylene **S4.15** that involves NHC-induced fragmentation of 7-chloro-7-silanorbornadiene with IME_4 .^[111] Although obtained chlorosilylene was proven to be same compound spectroscopically, it decomposed due to the reaction conditions.

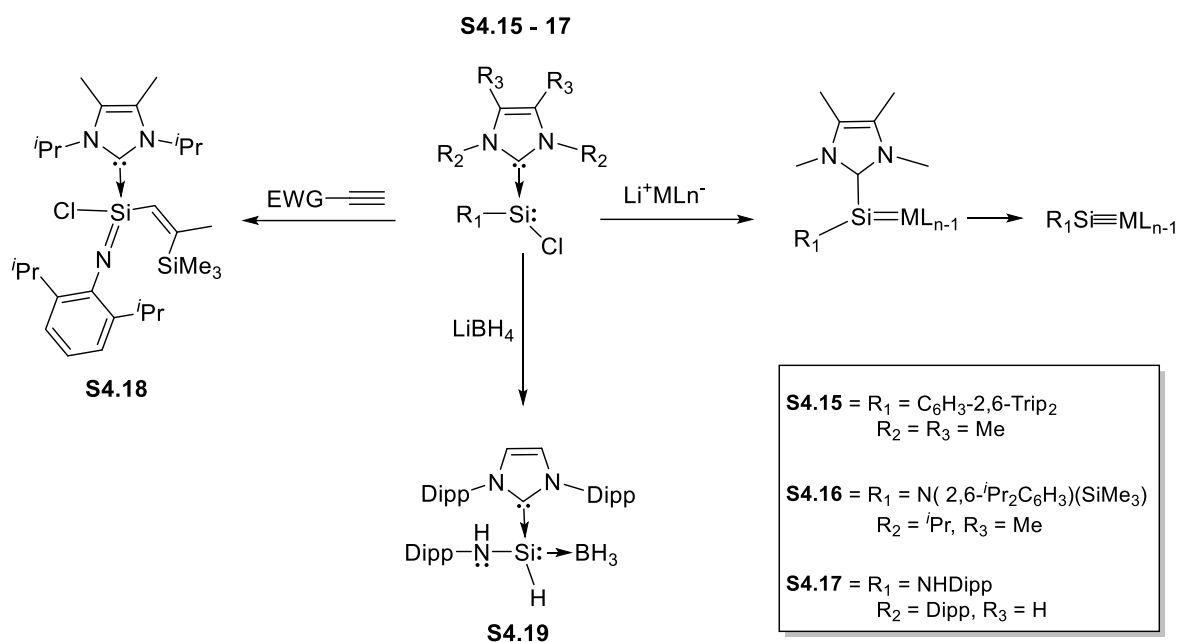


Figure 17. Selected reactivity products of NHC-stabilized chlorosilylenes.

In addition to monochlorosilylene, dihalosilylenes (SiX_2 , $\text{X} = \text{Cl}, \text{Br}, \text{I}$) are an important class of compounds due to their roles in industrial applications such as in microelectronic devices as well as purification of silicon, the so-called Siemens process.^[112] Earlier attempts by Schenk, Schmeisser, Margrave and others to isolate dihalide silylenes at room temperature resulted in mostly polymeric species $(\text{SiX}_2)_n$.^[113-115] In several reports, it was noted that SiX_2 can be generated in gas phase yet it is stable only at very low temperatures.^[116-118] Finally, the first room temperature stable dichlorosilylene **S4.20-Cl** was reported with NHC stabilization by the group of Roesky *et al.* in 2009.^[119] In fact, they have reported two synthetic procedures for the desired $\text{IDipp} \rightarrow \text{SiCl}_2$ (Figure 18). In a similar fashion to the monochlorosilylenes, dehydrohalogenation of trichlorosilane (HSiCl_3) with two equivalents of NHC directly yielded the NHC-stabilized dichlorosilylene in 79% yield.

Another multistep synthetic approach was also described within the same report. It is also obtainable via formation of NHC-stabilized SiCl_4 followed by concomitant reduction of the adduct $\text{IDipp} \rightarrow \text{SiCl}_4$ with two equivalents of KC_8 . The ^{29}Si NMR shift of this dichlorosilylene ($\delta = 19.06$) is in line with those for monochlorosilylenes.^[78, 103, 105, 110-111, 120-121] Similarly, disproportionation of Si_2Cl_6 also results in both the base-stabilized SiCl_2 and SiCl_4 complexes.^[122] The compound $\text{IDipp} \rightarrow \text{SiCl}_2$ can be converted to the novel dichlorosilimine upon treatment with RN_3 which is then further reduced to yield a dimeric silaisonitrile $(\text{RNSi:})_2$.^[123] Within the same issue, Filippou's group reported the analogous $\text{IDipp} \rightarrow \text{SiBr}_2$ **S4.20-Br** via reduction of the ionic complex $[\text{IDipp} \rightarrow \text{SiBr}_3]\text{Br}$ with potassium graphite.^[124] Four years later, Filippou also reported diiodosilylene **S4.20-I** utilizing the same method

(Figure 18).^[55] Aside from usage of NHCs as a HCl scavenger to obtain dihalosilylenes, halogenation of the Si=Si double bond of base-stabilized Si(0) compounds with 1,2-dihaloethanes (1,2-C₂H₄X₂, X = Cl, Br, I) has proven to be an efficient method to access dihalosilylenes. Indeed, in 2015, Filippou and co-workers reported the synthesis of a series of complexes **S4.20-X** (X = Cl, Br, I) (Figure 18) via comproportionation of (IDipp)₂Si₂. These can be further used as precursors for NHC-stabilized silazines and silanimines.^[125-126]

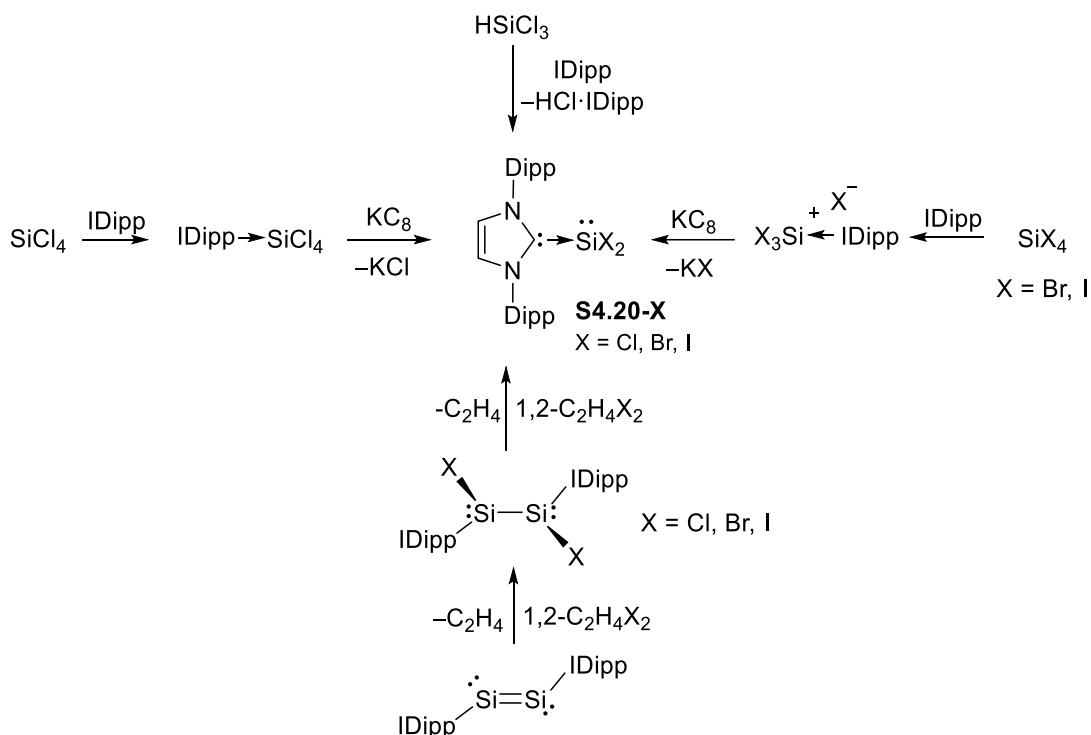


Figure 18. Different synthetic approaches to obtain NHC-stabilized dihalosilylenes (NHC→SiX₂).

Other than NHC ligands, different bases such as *cAAC*s can be also used to support these reactive dihalosilylenes externally. Although, attempts to prepare *cAAC*→SiCl₂ resulted in polymorphic structures for Roesky's group,^[127-128] So and co-workers were able to isolate a stable *cAAC*→SiI₂ upon reduction of *cAAC*→SiI₄ with two equivalents of KC₈ in toluene.^[129] It is important to note that, formation of desired compound is solvent dependent and no product formation was observed when THF was used instead of toluene.

4.2 Silicon (II) Hydrides

Hydrosilylenes, with the generic name as $\text{H}_2\text{Si:}$, are silicon(II) compounds that exhibit minimum one α -substituted hydrogen. These species have only been studied either at very high temperatures or in an argon matrix at cryogenic temperatures, due to the highly reactive silicon center with an unoccupied p -orbital and an active lone pair. In addition to that, the lability of the terminal Si-H bond, which is negatively polarized towards hydrogen ($\text{Si}^{\delta+}-\text{H}^{\delta-}$), makes such elusive species even more reactive in comparison to the tetravalent silicon(IV) hydrides. Hydrosilylenes are important intermediates in the industrial manufacturing process for amorphous silicon and silicon films via the pyrolysis of silane (SiH_4).^[130-131] These hydrosilylenes become valuable synthetic targets due to their great potential in synthetic chemistry such as hydrosilylation reactions. So far, several room temperature-stable silicon(II) hydrides are reported, the majority were synthesized via donor-acceptor stabilization.

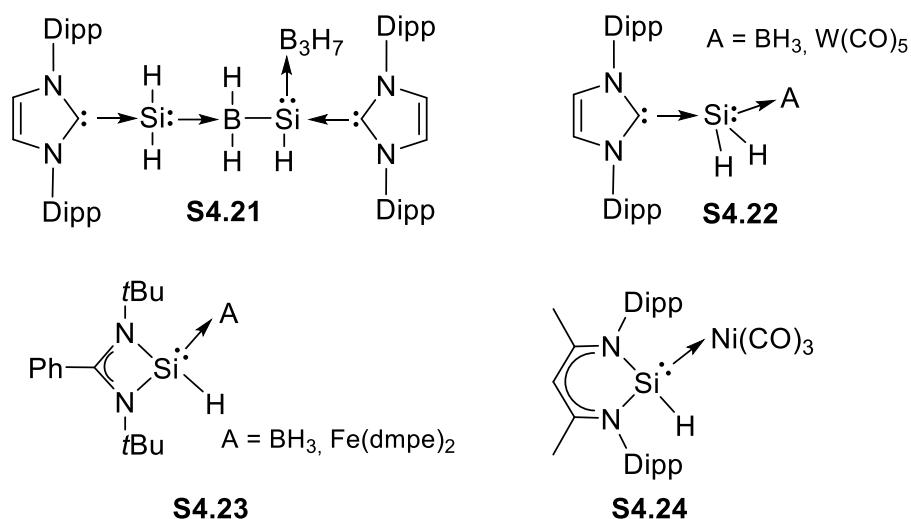


Figure 19. Selected examples for isolated silylene(II) hydrides that adopt donor-acceptor (push-pull) stabilization.

In 2011, the group of Robinson succeeded to isolate the parent silylene **S4.21** ($\text{H}_2\text{Si:}$) unit by “push-pull” stabilization, employing NHC and boranes for the respective push-pull unit (Figure 19). This was achieved by the borane-induced Si-Si bond cleavage of the NHC-adduct of disilicon ($\text{NHC}\rightarrow\text{Si}=\text{Si}\leftarrow\text{NHC}$, $\text{NHC} = \text{IDipp}$).^[132] One year later, the group of Rivard introduced an alternative route to access parent silylenes via the reaction of NHC-stabilized dichlorosilylene complex (IDippSiCl_2) with LiAlH_4 to afford the NHC-stabilized silicon(II) dihydride-borane **S4.22** adduct (Figure 19).^[133] Interestingly, this complex reacts with $\text{W}(\text{CO})_5\cdot\text{THF}$ to yield a dihydride-tungsten complex ($\text{IDipp}\cdot\text{SiH}_2\cdot\text{W}(\text{CO})_5$) via a silylene group transfer mechanism (Figure 19). Furthermore, the

same group reported the synthesis of a silicon(II) amidohydride adduct via chloride/hydride metathesis reaction of the corresponding amido chloro silylene with LiBH_4 .^[110]

The first mononuclear stable Lewis acid-base stabilized Si(II) hydride **S4.23** (Figure 19) was reported by Roesky and Stalke via the reaction of the corresponding silicon(II) chloride **S4.1** (Figure 13) with borane THF adduct ($\text{BH}_3 \cdot \text{THF}$) in 2011.^[134] With the help of the stabilizing chelating amidinato ligands, the obtained Lewis acid-base stabilized monochlorosilylene was converted to monohydridosilylene **S4.23** with hydrogenating agent potassium K-selectride ($\text{K}[(s\text{-Bu})_3\text{BH}]$). One year later, by employing the same chlorosilylene as precursor, Driess and Inoue succeeded in isolating the first example of a bis(hydrido)silylene complex which is also stabilized by means of a push-pull methodology. The reaction of titanium complex $[\text{Cp}_2\text{Ti}(\text{PMe}_3)_2]$ with two equivalents of chlorosilylene resulted in the formation of the bis(chlorosilylene)titanium complex that is subsequently converted into the bis-silylenehydride complex upon treatment with $\text{Li}(\text{HBEt})_3$.^[135] This report also demonstrates that not only Lewis acids, but also transition metal fragments, can be also used as protecting groups in order to stabilize Si(II) hydride complexes. Similarly, the reaction of the Fe(0) complex $[(\text{dmpe})_2\text{Fe}(\text{PMe}_3)]$ ($\text{dmpe} = 1,2\text{-bis}(\text{dimethylphosphino})\text{ethane}$) with chlorosilylene yielded the new chlorosilylene-iron complex, which can be further converted to the corresponding hydridosilylene-iron complex with $\text{Li}(\text{HBEt})_3$ via halide-hydride exchange.^[136]

In addition to the amidinate ligand class, the β -ketiminate ligand stabilized silylene hydride **S4.24** (Figure 19) was also reported. Driess *et al.* reported the formation of $\text{Ni}(\text{CO})_3$ coordinated NHSi . The reaction of the silylene-nickel complex with hydrogen chloride (HCl) afforded the chlorosilylene-nickel complex quantitatively, followed by an exchange of the chloride by hydride with $\text{Li}(\text{HBEt})_3$ to afford desired isolable silicon(II) hydride-nickel complex **S4.24**.^[137] The afforded hydrosilylene complex was also accessible through treatment with a hydrogen source, like ammonia-borane, with the NHSi -nickel complex. In the same report, it was shown that compound **S4.24** is suitable as a hydrosilylation agent for diaryl-substituted alkynes. A second example of a hydridosilylene with β -diketiminato ligand was obtained by the reaction of NHSi with the iridium hydride complex $[\text{Cp}^*\text{IrH}_4]$.^[138] This resulted in the formation of the first silyl-iridium complex via oxidative addition into the iridium-hydrogen bond followed by rearrangement to hydridosilylene in 24 hours at room temperature.

In contrast to various examples of donor-acceptor stabilized silicon(II) hydrides, the isolation of an acceptor free system remained elusive until 2011. The group of Kato and Baceiredo successfully synthesized the first acceptor free phosphine-stabilized silylene(II) hydride **S4.25** (Figure 20) by reductive dehalogenation of the corresponding dichlorosilane derivative with elemental magnesium.^[139]

Interestingly, treatment of NHC-silylene hydride with half an equivalent of Ni(COD)₂, results in the two NHC-ligands, that were formerly attached to the Si(II) center, being transferred to the Ni center, furnishing the first example of a dihydrosilene Ni(0) complex **S4.27** (Figure 21). Compound **S4.26** undergoes [2+2+1] cycloaddition reactions with phenyl acetylene and diphenyl acetylene to form 1-alkenyl-1-alkynylsilane and 2,3,4,5-tetraphenyl-1-(tri-*t*Bu-silyl)-1*H*-silole, respectively.^[141] Furthermore, treatment of silylene (II) hydride with excess CO₂ affords the cyclotrisiloxane **S4.28** in 82% yield (Figure 21).^[142] Recently, the same group also presented the novel iron and tungsten carbonyl complexes **S4.29** (Figure 21) that exhibit exceptionally long silicon-metal bond lengths due to the zwitterionic resonance structures.^[143] In 2016, Müller group described a new synthetic approach to access Lewis base stabilized hydridosilylenes. This described the formation of NHC supported aryl-substituted silylene (II) hydride via NHC-induced fragmentation of silanorbornadiene derivatives which forms hydrosilylene iron complex upon treatment with diironnanocarbonyl (Fe₂(CO)₉).^[111]

5 Silicon-Transition Metal Multiple Bonds

Multiple bonds between transition metals and main-group elements have gained considerable attention, since their discovery in 1964.^[144-145] The first transition metal carbene complex $[(CO)_5W=CMe(OMe)]$ was reported by E. O. Fischer followed by R. R. Schrock with the isolation of $(tBuCH_2)_3Ta=CH(tBu)$ in 1974. Since these seminal discoveries, numerous examples of transition metal carbene complexes have been reported. In terms of their application, these complexes have been widely utilized in alkene metathesis and cross coupling reactions.^[146] The most far-reaching reactivity of metal-carbene complexes is their contributions to the olefin metathesis reactions, which resulted in a Nobel Prize in chemistry in 2005.^[31] Olefin metathesis is one of the versatile methods in the synthesis of new carbon-carbon bonds in not only organic and polymer chemistry but also in pharmaceutical manufacturing.^[147] Grubbs' catalysts are chosen widely in industrial applications^[148-151] for olefin cross-metathesis (CM), ring-opening metathesis polymerization (ROMP), ring-closing metathesis (RCM) and acyclic diene metathesis (ADMET) reactions due to its functional group tolerance, stereoselectivity and catalyst longevity.^[152-153]

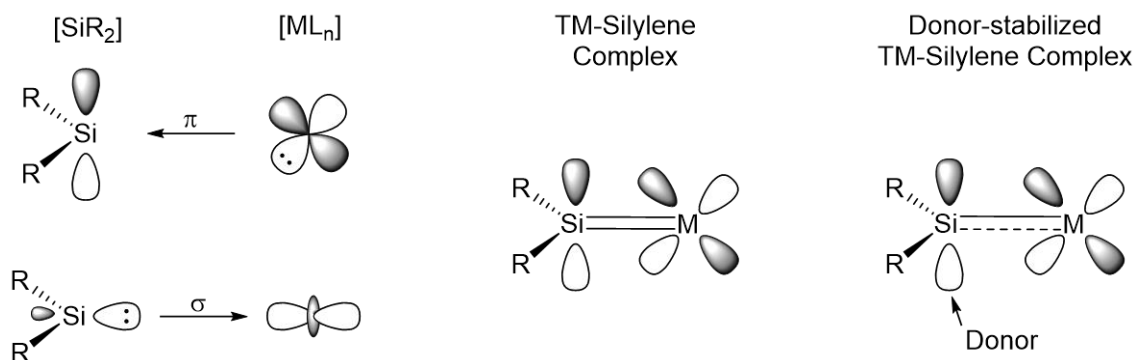


Figure 22. Schematic representation of the orbital interactions in TM-Silylene and a donor-stabilized TM-Silylene Complexes according to Dewar-Chat-Duncanson model.

Among group 14 elements, many attempts have focused on the ability to isolate silicon analogs of transition metal-carbene multiply bonded complexes, due to the close proximity of carbon and silicon in the periodic table. Transition metal-silylene complexes ($LTM=SiR_2$) can be described as complexes displaying planar geometries, with the TM-Si bond displaying double bond character. The bonding situation can be illustrated by Dewar-Chat-Duncanson model similar to metal-carbene complexes (Figure 22).^[154] A σ -bond occurs between the lone pair of the silicon center and empty orbital of the transition metal. A π -bond forms via back donation from a filled d-orbital of the metal to the empty p-orbital of the silicon. Due to the higher electrophilicity of silicon center compared to the carbon

analogue in $\text{TM}=\text{E}$ ($\text{E} = \text{p-block}$) complexes, silylene complexes can also be donor stabilized via coordination of Lewis bases. This results in elongation of the bond between silicon and metal. Transition metal-silylene complexes are sought to be observed as reactive intermediates or in the gas phase in molecular beam experiments. Although they were synthetic targets since the 1960s, earlier attempts did not provide successful results. Thus, further supporting the justification that these complexes are very reactive compared to lighter carbene complexes.

The first isolated transition metal-silylene complexes were donor-stabilized, reported by the two independent groups of G. Müller (**S5.1**) and D. Tilley (**S5.2**) in 1987 (Figure 23).^[155-156] These complexes have a considerably long metal-silicon bond and distorted tetrahedral geometry and hence feature silyl complexes. In addition to base-stabilized silylene complexes, several base-free metal-silylene complexes with different substituents at silicon were discovered.

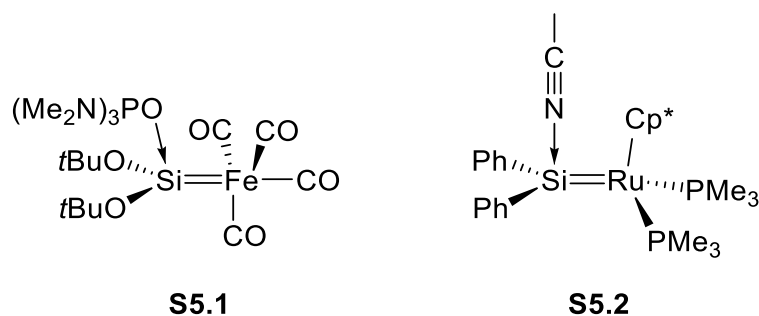


Figure 23. First examples of donor-stabilized transition metal-silylene complexes.

The first base-free silylene complex **S5.3** ($[\text{Cp}^*(\text{PMe}_3)_2\text{Ru}=\text{Si}(\text{SR})_2][\text{BPh}_4]$ ($\text{R} = \text{Et}, -\text{C}_6\text{H}_3-4\text{-Me}$)) was isolated by abstraction of an anionic group (OTf^-) from $[\text{Cp}^*(\text{PMe}_3)_2\text{Ru}-\text{Si}(\text{SR})_2\text{OTf}]$ (**A**, Figure 24).^[157] Abstraction of an anionic group produces a cationic silylene complex and is a reliable procedure to generate silylene complexes. Alternatively, other general synthetic approaches have developed these either involve coordination of a free silylene (**S5.4, B**, Figure 24)^[158] or α -substituent (mostly hydrogen) migration (**S5.5, C**, Figure 24).^[159]

Metal-silylene complexes that are mentioned above can be classified as Fischer-type with the bond highly polarized in a $\text{M}^{\delta-}=\text{Si}^{\delta+}$ manner. Since compounds **S5.1-5** have highly electrophilic silicon and nucleophilic metals, they are thought to be more reactive than the metal-carbene complexes in particular towards nucleophiles.^[160] Moreover, metal-silylene complexes are intriguing to investigate due to their possible roles in metal-catalyzed transformations (i.e. dehydrogenative coupling of hydrosilanes, scrambling of substituents in silanes).^[161-165] Indeed, Glaser and Tilley reported that the cationic ruthenium-hydrosilylene complex is catalytically active in hydrosilylation of alkenes.^[166] TM-

silylene complexes have now been accessible for more than three decades and the chemistry of various silylene complexes including stoichiometric and catalytic transformation reactions have made a steady progress.^[167-175]

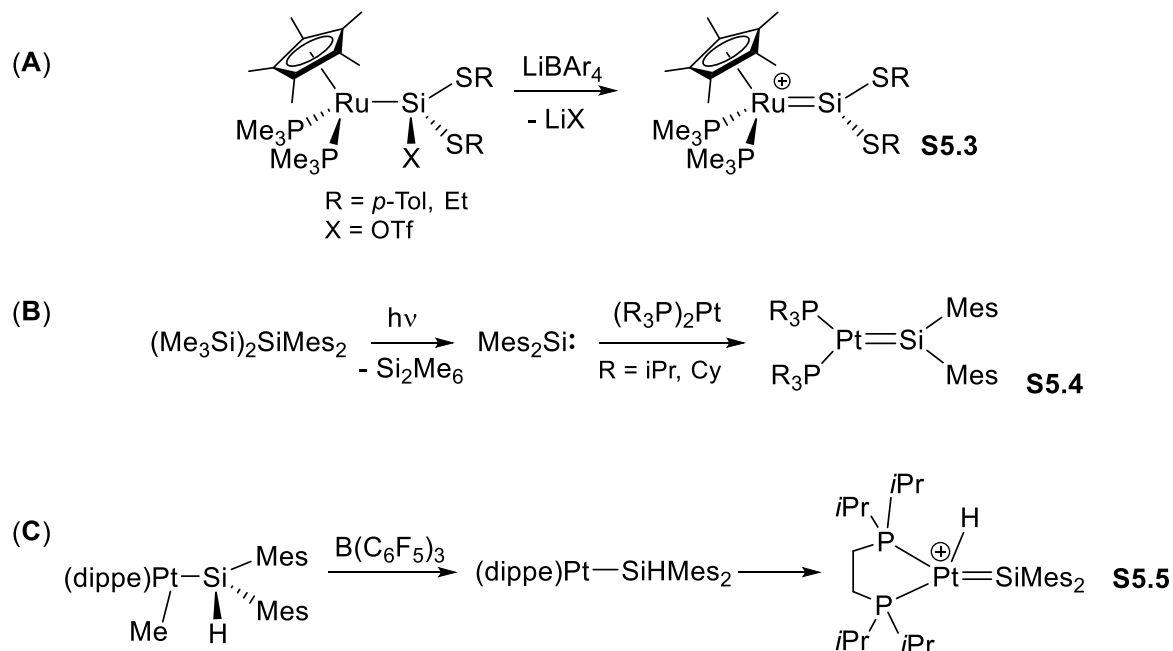


Figure 24. Synthetic routes for base-free silylene complexes by (A) substituent abstraction, (B) coordination of a free silylene to a TM, (C) α -Hydrogen migration.

Although most of the metal-silylene complexes are Fischer-type, a limited number of Schrock-type metal-silylenes were also described. In 2006, the group of Sekiguchi reported the first Schrock-type Hafnium-silylene complex **S5.6** (Figure 25) via the coupling reaction of 1,1-dilithiosilane ($(\text{Si}(\text{Li})_2(t\text{Bu}_2\text{MeSi})_2)$) with $(\eta\text{-C}_5\text{H}_4\text{Et})_2\text{HfCl}_2$. The obtained 16-electron hafnium-silylene complex is thermally unstable and rapidly decomposed at 0 °C, yet could be isolated as 18-electron hafnium-silylene phosphine complex **S5.6-PMe₃** upon addition of PMe_3 to the hafnium center (Figure 25).^[176] Later in 2013, the same group isolated the new Schrock type titanium-silylene complex with bicyclic silylene ligand **S5.7** and explored its reactivity towards simple unsaturated substrates.^[177-178] Compound **S5.7** undergoes [2+2] cycloaddition with terminal alkynes to afford silatitanacyclobutenes **S5.8** as [2+2] cycloaddition products (Figure 25). Due to the use of an early transition metal and electropositive silyl substituent at the silylene center, the bond in compound **S5.6** is polarized in an opposite manner as $\text{M}^{\delta+}=\text{Si}^{\delta-}$. Therefore, complexes **S5.6-7** undergo nucleophilic attack at the silicon atom instead of the transition metal as would be expected from classical Schrock-type TM complexes of main group elements.

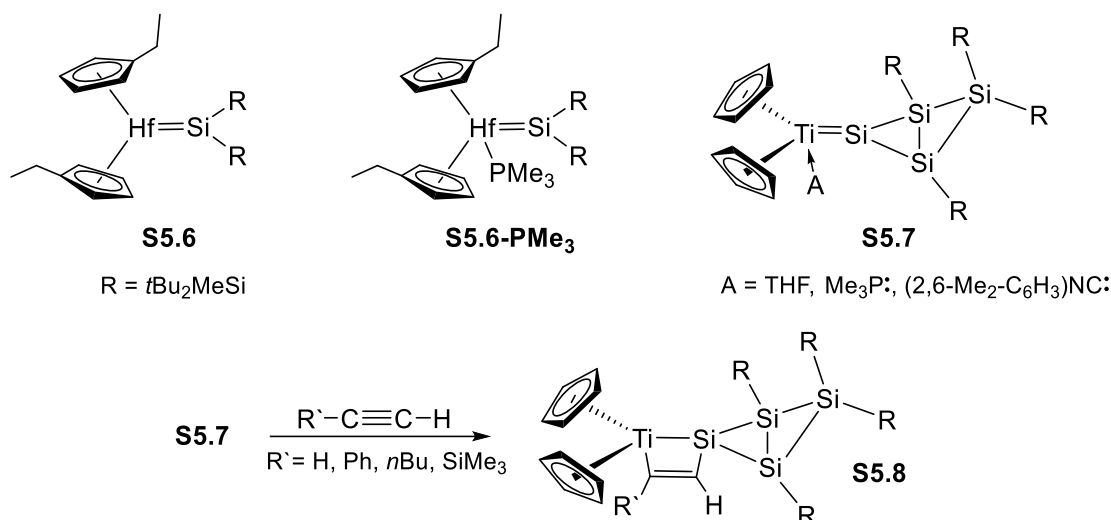


Figure 25. Schrock-type transition metal-silylene complexes and [2+2] cycloaddition reaction of titanium-silylene complex **S5.7**.

Unlike metal-silylene complexes,^[160, 179-180] the chemistry of metal-silylyne complexes featuring a triple bond between silicon and a transition metal center (Si≡M) is relatively unexplored, due to the lack of suitable Si(II) precursors. A notable silylyne complex [Cp*(dmpe)(H)MoSiMes][B(C₆F₅)₄] (dmpe = PMe₂CH₂CH₂PMe₂) was reported by Mork and Tilley in 2003 upon subsequent chloride abstraction from chlorosilylene Cp*(dmpe)(H)Mo=SiClMes with Li[B(C₆F₅)₄].^[181] Although this complex has very short Mo–Si bond length of 2.219(2) Å and downfield shifted resonance in the ²⁹Si NMR spectrum at δ = 289 ppm, it was not considered a “true” metal-silylyne complex, due to the presence of an agostic hydrogen interaction between the transition metal and silicon center.

Later in 2010, a genuine Mo≡Si triple bonded complex **S5.9** (Figure 26) was successfully isolated by the group of Filippou from the base-stabilized silicon(II) halide.^[182] The treatment of NHC–SiCl(R) (R = C₆H₃-2,6-Trip₂) with lithium metallate (Li[CpMo(CO)₃]) furnished the NHC-stabilized metal-silylene complex upon salt metathesis. Subsequent abstraction of the NHC via the Lewis acidic borane (B(*p*-Tol)₃) affords the neutral molybdenum-silylyne complex **S5.9** Cp(CO)₂Mo≡Si(C₆H₃-2,6-Trip₂) with the bond length between silicon and molybdenum being 2.2241(7) Å (A, Figure 26).^[182] In addition to the base-stabilized Si(II) halides, half an equivalent of dihalosilenes can be used as a halosilylene synthetic equivalent as recently described by Filippou in the synthesis of [(κ³-tmps)(CO)₂Nb≡Si(Tbb)] (Tbb = C₆H₂-2,6-[CH(SiMe₃)₂]₂-4-*t*Bu).^[183-184] A cationic silylyne complex was reported by Tilley as having an Os≡Si triple bond **S5.10** which was formed by hydride abstraction with the strong Lewis acid B(C₆F₅)₄ from the hydrosilylene complex [Cp*(^{*i*}Pr₃P)(H)Os=Si(H)Trip] (B, Figure 26).^[185] A similar synthetic route to obtain a triple bond between silicon and transition metal was reported by Tobita and co-workers via dehydrogenation from

a metal-silylene complex containing a (H)W=Si(H) moiety. They reported the synthesis of a neutral $\text{Cp}^*(\text{CO})_2\text{W}\equiv\text{SiTsi}$ ($\text{Tsi} = \text{C}(\text{SiMe}_3)_3$) via the stepwise proton and hydride abstraction utilizing Lewis bases (NHC) and Lewis acids ($\text{B}(\text{C}_6\text{F}_5)_3$), respectively.^[186] Using the same methodology, it was found that the dimeric structure of $[\text{Cp}^*(\text{CO})_2\text{W}\equiv\text{Si}(\text{Eind})]_2$ (**S5.13**, Figure 27) is in equilibrium with its monomer.^[187] Very recently, a new synthetic approach to access metal-silylyne **S5.11** complexes was reported by Filippou. In contrast to previous routes which used silicon halides or hydride/halogen abstraction from the corresponding metal-silylene complexes, this new method involves the direct transfer of a silyliumylidene ion to form the metal-silylyne complexes (**C**, Figure 26).^[70]

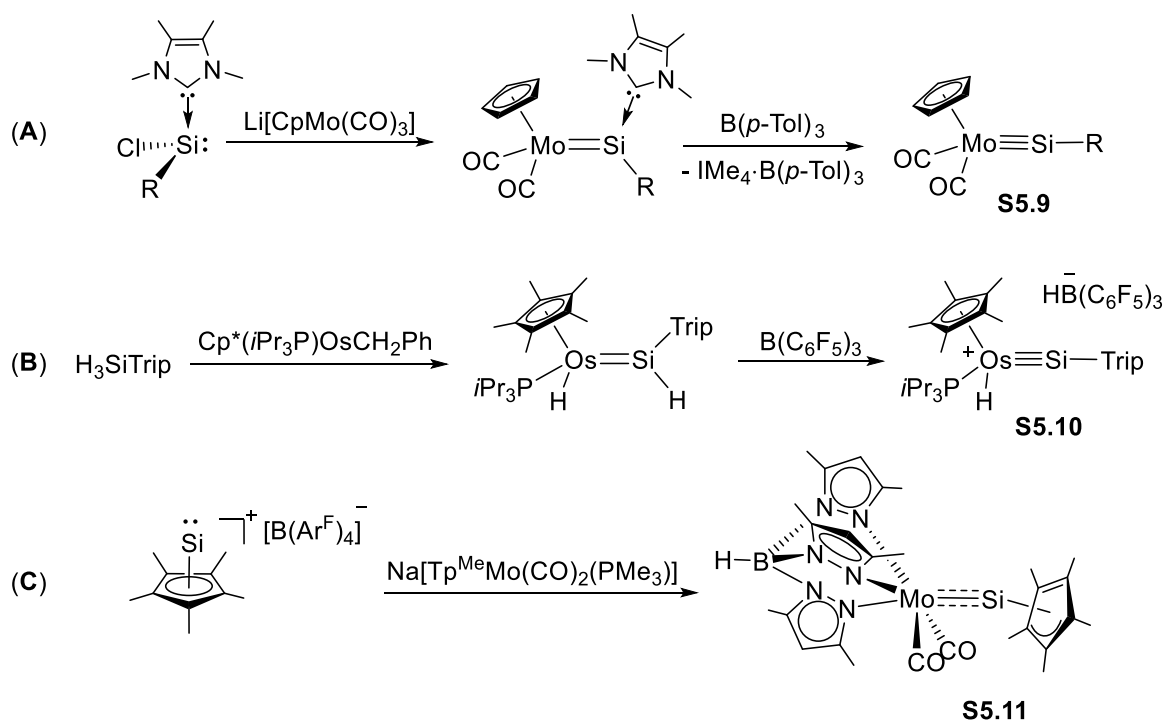


Figure 26. Selected synthetic approaches for novel transition metal-silylyne complexes. (A), starting from base-stabilized Si(II) halides via salt metathesis; (B), starting from silicon (IV) hydrides via abstraction of hydride group from hydro-silylene complex; (C), starting from silyliumylidene ions.

The most important reactivity of $\text{TM}=\text{C}$ complexes is their reactivity with various unsaturated organic substrates and the ability to undergo metathesis reactions, as represented by olefin and alkyne metathesis. Although many reviews are well documented regarding the stoichiometric and catalytic reactions of metal-carbyne complexes,^[188-189] the chemistry of heavier analogues ($\text{M}=\text{Si}$) is still in its infancy.

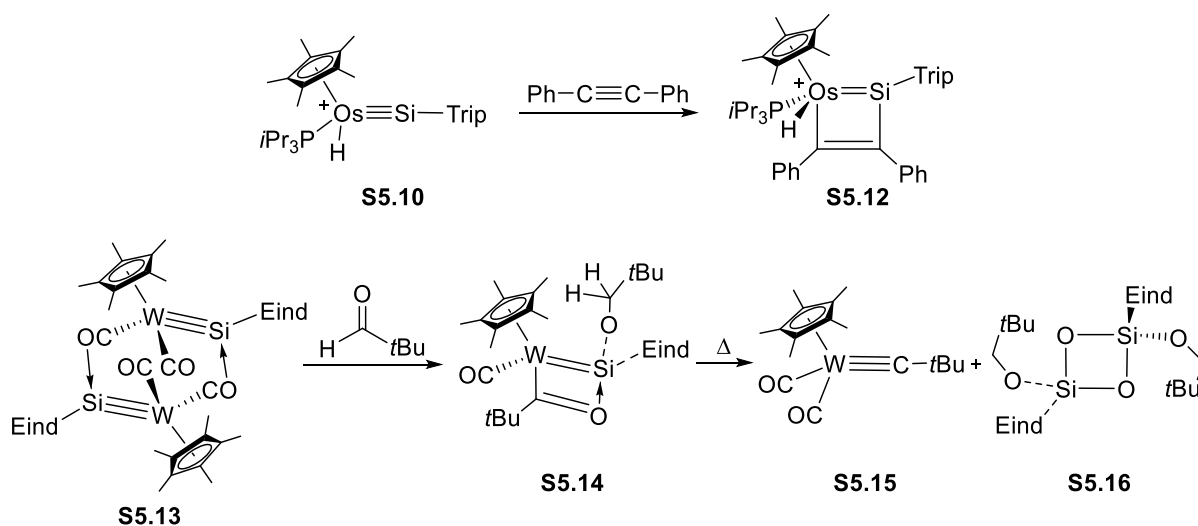


Figure 27. Reactions of silylyne ($\text{TM}=\text{Si}$) towards alkyne to form thermally stable metalocycle (**S5.12**) and towards aldehyde to lead to metathesis-like fragmentation (**S5.15**).

In 2013, Tilley and co-workers reported the formation of metallosilacyclobutadiene **S5.12** (Figure 27) via the [2+2] cycloaddition reaction between compound **S5.10** and an alkyne ($\text{PhC}\equiv\text{CPh}$).^[185] In a general metathesis reaction, formation of four-membered metalocycle is proposed to be the key intermediate. However, in the case of Tilley the obtained product is thermally stable and further conversion could not be obtained. Very recently, the Hashimoto and Tobita groups introduced the reactions of a tungsten silylyne complex with aldehydes and their metathesis like fragmentation.^[190] According to their report, treatment of a half equivalent of compound **S5.13** with pivalaldehyde undergoes a [2+2] cycloaddition reaction to yield the four-membered $\text{W}-\text{Si}-\text{O}-\text{C}$ metalocycle **S5.14** (Figure 27). This is then further converted to a carbyne complex **S5.15** and 1,3-cyclodisiloxane **S5.16** upon gentle heating (Figure 27). In addition to the reactivity of metal-silylyne complexes towards unsaturated organic complexes, a handful of examples have shown reactions towards nucleophiles^[191], bond activations mediated by electron-transfer^[191] and carbonylation reactions^[192]. Since their discovery, the synthesis and chemistry of transition metal-silylyne complexes is one of the exciting yet challenging research fields over the last two decades.^[193]

In addition to TM-Silicon multiple bonded systems, bimetallic complexes with bridging silicon units are considered to be an important class in organo-transition metal chemistry since they are alleged key intermediates in various transition-metal catalyzed transformations^[194-196] like dehydrocoupling of hydrosilanes and the metathesis of olefins.^[197-198] Hybrid clusters including group 14 elements with M_2C_2 core are well known after the first discovery in the bonding ability of acetylenes across metal-metal triple bonds to form quasi-tetrahedral compounds.^[199-201] After that various $M(\mu-C_2R_2)M$ dimetallatetrahedrane complexes were reported not only with acetylenes but also with alkynes that are known as catalytically active in the polymerization of alkynes^[202-211] and in hydroboration reactions.^[212] Among the heavier analogues, many M_2Si_2 dimeric binuclear complexes with various transition-metals ($M = Ti, W, Co, Rh, Ni, \text{etc.}$) were reported including their catalytic activities since 1900s.^[197, 213-234] In 1988, the group of Young reported a Pt_2Si_2 complex **S5.17** (Figure 28) which is a potential key intermediate in the platinum-catalyzed dehydrocoupling of hydrosilanes. Later in 2000, Mol and co-workers suggested that the W_2Si_2 cluster **S5.18** (Figure 28) can act as a catalyst precursor for terminal olefin metathesis under irradiation.^[197-198] Thus far reported complexes with M_2Si_2 core bearing a planar, diamond-shaped or butterfly type environment, but neutral bimetallic tetrahedral structures remain elusive.

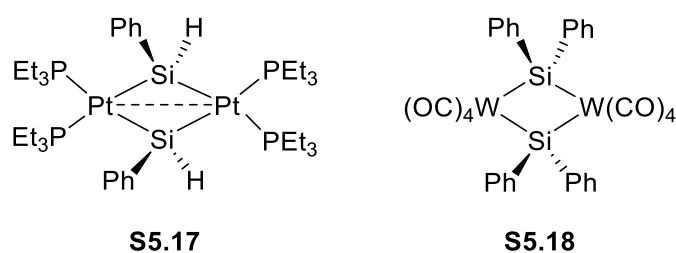


Figure 28. Selected examples of reported planar clusters with M_2Si_2 core.

6 Motivation of This Work

As highlighted in the introduction, unlike the rich field of organic chemistry, relating to the carbon-based systems, the chemistry of heavier main group elements like silicon remains under studied despite silicon being more abundant within the Earth's crust. Undoubtedly, the last two decades have witnessed remarkable achievements in new strategies for synthesis and application of low-valent heavier main group species. Sterically demanding ligand design is one of the key factors for isolating these reactive species. In respect to smart ligand choice, electropositive and sterically demanding silyl substituents (R_3Si-) have become principal ligands in organosilicon chemistry, since they have enabled access to seminal examples in main group chemistry. For instance, it was reported that the σ -donating silyl group is one of the key factors for the enhanced stability of the first neutral acyclic three-coordinate silanone **S2.13** (Figure 6).^[65] Furthermore, silyl groups have also proven effective ligands across the p-block, as highlighted by the isolation of the first neutral dialumene **S2.5** (Figure 5).^[59]

Among low-valent main group species, functionalized silylenes, particularly chlorosilylenes are an intriguing class of compounds. Due to the presence of a labile Si–Cl bond, as well as their empty lone pair, chlorosilylenes are ideal candidates for building blocks towards novel organosilicon compounds, as shown in Chapter 4.1. So far various ligands have been utilized to support the reactive chlorosilylenes via differing kinetic and thermodynamic stabilization strategies,^[78, 100, 103, 110, 120] yet chlorosilylenes bearing silyl-substituents are the still missing pieces. This work aims to close this gap to uncover the combined effect of chloro- and silyl-substitution onto the central silicon atom. With this ligand combination, a good understanding to further versatile silylene reactivity and an access to variety of low-valent functionalized silylenes are anticipated (Figure 29).

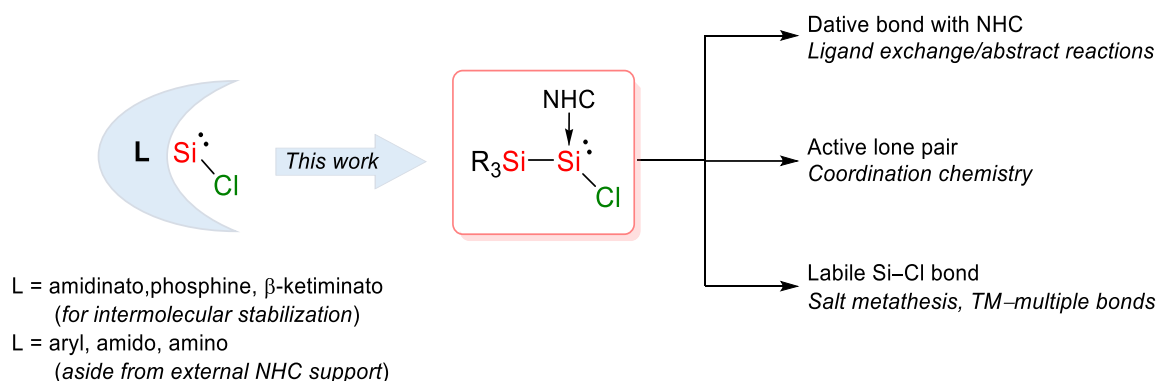


Figure 29. Aims of this thesis: Synthesis of silyl(chloro)silylenes and examination of its reactivity according to the potential reactive sites.

To achieve this challenging task, in addition to the silyl-ligand, further stabilization will be sought via NHCs as they bring easily tunable steric and electronic properties. With the targeted class of compound in hand, it is investigated concerning its reactivity towards a variety of Lewis acids and bases, which will be discussed in Chapter 8. It is moreover an ideal candidate giving access to novel silicon-transition metal multiple bonded species, discussed in Chapter 9.

Moreover, the only reported NHC-stabilized monohydride and silyl-substituted functionalized silylene **S4.26** (Figure 20) will be further surveyed concerning its potential to build up silicon-boron bonds. Initial reactivity investigations with **S4.26** highlighted its coordination chemistry with regards to transition metal^[140, 143] and functional organic groups such as carbonyls and alkynes^[141-142]. Usage of this particular silylene to achieve silicon-boron bonds is rather uncommon despite of numerous studies on silylene-derived silicon-element bond formation. Known silicon coordinated borane moieties bear “acceptor stabilization” as shown for the compounds **S4.21–23** (Figure 19) or those compounds are even not accessible, as silylenes were often found to be prone to insertion of the silicon atom into the boron-heteroatom bond. Thus, we envisaged the use of silylene hydride as ideally suited as a reaction partner with electrophilic boron sources, enabling the build-up of silicon-boron bond, which is discussed in Chapter 7.

7 Reactivity of an NHC-stabilized pyramidal hydrosilylene with electrophilic boron sources

Title: Reactivity of an NHC-stabilized pyramidal hydrosilylene with electrophilic boron sources

Status: Research Article, published online April 3, 2019

Journal: Dalton Transactions, 2019, 48, 5756-5765.

Publisher: Royal Society of Chemistry

DOI: 10.1039/C9DT00608G

Authors: Gizem Dübek, Daniel Franz, Carsten Eisenhut, Philipp J. Altmann and Shigeyoshi Inoue*

Content: Silylenes with an active lone pair on the Si(II) atom have been frequently used as electron-pair donors towards boron-centered electrophiles. In this report, we investigated the reactivity of silylene hydride towards various types of boron-centered electrophiles that are commonly encountered in molecular chemistry. Reaction of silylene hydride with BX_3 ($X = H, F, Cl, Br$) lead in most cases to formation of the Lewis acid-base adducts of silylene hydride ($R_3SiSi(H) \rightarrow BX_3$). Depending on the Lewis acidity of BX_3 an equilibrium to the auto-ionized products $[R_3SiSi(H)BX_2]^- [BX_4]^+$ ($X = F, Cl$) was found. Interestingly, treatment of Si(H) with ammonia borane ($H_3N \cdot BH_3$) led to formation of a NHC adduct of $R_3SiSiH_2NHBH_2$. This was formed through the dehydrogenation of $H_3N \cdot BH_3$ yielding H_2NBH_2 , followed by silylene insertion into the N–H bond concomitant with the migration of NHC from the Si center to the B atom. Accordingly, a similar adduct formation ($R_3SiSi(H) \rightarrow B(Ar)$) was also observed in the case of the organoboranes (BPh_3 or BPh_2Br). As a major result of this study, the stability of the silylene adduct correlates to the relative Lewis acidity of the borane sources and resembles with the stability of the corresponding dimethylsulphide (dms) complexes of boranes.

G. Dübek, D. Franz, C. Eisenhut, P. J. Altmann, S. Inoue, *Dalton Trans.* **2019**, 48, 5756-5765. Reproduced by permission of the Royal Society of Chemistry.

* G. Dübek and D. Franz planned all experiments and co-wrote the manuscript. G. Dübek conducted 70% and C. Eisenhut contributed with 30% of the experimental work including analysis. P. Altmann conducted all SC XRD measurements and managed the processing of the respective data. All work was performed under the supervision of S. Inoue.

Cite this: *Dalton Trans.*, 2019, **48**, 5756

Reactivity of an NHC-stabilized pyramidal hydrosilylene with electrophilic boron sources†

Gizem Dübek,^a Daniel Franz,^a Carsten Eisenhut,^b Philipp J. Altmann^a and Shigeyoshi Inoue^{a*}

Silylenes have become an indispensable tool for molecular bond activation. Their use for the construction of silicon–boron bonds is uncommon in comparison to the numerous studies on silylene-derived silicon–element bond formations. Herein we investigate the reactivity of the pyramidal NHC-coordinated hydrosilylene $t\text{Bu}_3\text{SiSi}(\text{H})\text{L}^{\text{Me}4}$ (**1**; NHC = N-heterocyclic carbene, $\text{L}^{\text{Me}4}$ = 1,3,4,5-tetramethylimidazolin-2-ylidene) with various boron-centered electrophiles. The reaction of **1** with $\text{THF}\cdot\text{BH}_3$ or $\text{H}_3\text{N}\rightarrow\text{BH}_3$ afforded the silylene complex $\mathbf{1}\rightarrow\text{BH}_3$ or the product of insertion of the silicon(II) atom into an N–H bond with concomitant dehydrogenation along the HN–BH moiety (**2**). The respective conversion of **1** with BPh_3 yields $\mathbf{1}\rightarrow\text{BPh}_3$ which readily reacts with excess $\text{L}^{\text{Me}4}$ to form the more stable complex $\text{L}^{\text{Me}4}\rightarrow\text{BPh}_3$ with release of **1**. Treatment of **1** with the haloboranes $\text{Et}_2\text{O}\rightarrow\text{BF}_3$, BCl_3 , BBr_3 and $\text{Me}_2\text{S}\rightarrow\text{BBr}_3$ resulted in the formation of the Lewis acid base adducts $\mathbf{1}\rightarrow\text{BX}_3$ (X = F, Cl, Br) and an equilibrium with their auto-ionization products $[\mathbf{1}_2\text{BX}_2]^+[\text{BX}_4]^-$ slowly develops. The ratio of $\mathbf{1}\rightarrow\text{BX}_3$ significantly increases with rising atomic number of the halide, thus $\mathbf{1}\rightarrow\text{BF}_3$ majorly transforms within hours while $\mathbf{1}\rightarrow\text{BBr}_3$ is near-quantitatively retained over time. Accordingly, the complex $\mathbf{1}\rightarrow\text{BPhBr}_2$ was isolated after conversion of **1** with PhBBr_2 .

Received 9th February 2019,
Accepted 3rd April 2019DOI: 10.1039/c9dt00608g
rsc.li/dalton

Introduction

There has always been a strong link between the chemistry of silicon and boron as implied by the diagonal relationship of these metalloids in the Periodic Table of Elements. Boron-doped silicon semiconductors are a prominent example from materials science in which the combination of these elements fostered tremendous innovation.^{1–3} Molecular chemistry benefits from the particular properties of the silicon–boron bond. It is sufficiently stable to craft durable compounds but also susceptible to mild methods of chemoselective cleavage to enable metallyl group transfer, thus, enriching the ever-growing library of organometallic synthesis.^{4–6} The ylidenic compound class of silylenes are a subtype of molecular silicon complexes with one lone pair majorly located at the metalloid center. As a result, the formal oxidation number +II is assigned to the silicon atom. Silylenes have gained outstanding atten-

tion as key compounds to bring forward new ways for bond activation and catalysis.^{4,7–15} In particular, silylenes may act as ligands to enhance the catalytic activity of transition metal complexes.^{9,10,14} Moreover, the potentially ambiphilic silicon(II) atom itself may engage in bond activations *via* addition and insertion pathways. Taking into account their ylidenic character it does not come as a surprise that there has been made frequent use of silylenes as electron-pair donors towards boron-centered electrophiles. An early report of Metzler and Denk from 1996 described the formation of the adduct between a five-membered ring N-heterocyclic silylene (NHSi) and $\text{B}(\text{C}_6\text{F}_5)_3$ which slowly transforms to the product of Si-insertion into a B–C bond.¹⁶ However, neither the adduct nor the insertion product were structurally characterized in the solid state (*i.e.* XRD study, XRD = X-ray diffraction). In fact, more than 20 years later, one can easily survey the stock of compounds in which conversions of a silylene with an electrophilic borane derivative resulted in the structural characterization of a species that contained a silicon–boron bond.^{17–39} Often a silicon-coordinated borane moiety affords isolation of an otherwise elusive kind of silylene (*i.e.* “acceptor stabilization”). A prominent example for this concept is the silylene dihydride **A**¹ described by Rivard and coworkers (Fig. 1).³⁰ Structurally related compounds have also been reported (**A**², **A**³).^{29,33} Bis(guanidato)-, as well as bis(amidinato)silylenes tend to switch between isomers with a three- or with a four-

^aDepartment of Chemistry, WACKER-Institute of Silicon Chemistry and Catalysis Research Centre, Technische Universität München, Lichtenbergstr. 4, 85748 Garching bei München, Germany. E-mail: s.inoue@tum.de

^bInstitut für Chemie, Technische Universität Berlin, Straße des 17. Juni 135, Sekr. C2, 10623 Berlin, Germany

† Electronic supplementary information (ESI) available: Depiction of analysis spectra and crystallographic details. CCDC 1896328–1896331. For ESI and crystallographic data in CIF or other electronic format see DOI: 10.1039/c9dt00608g

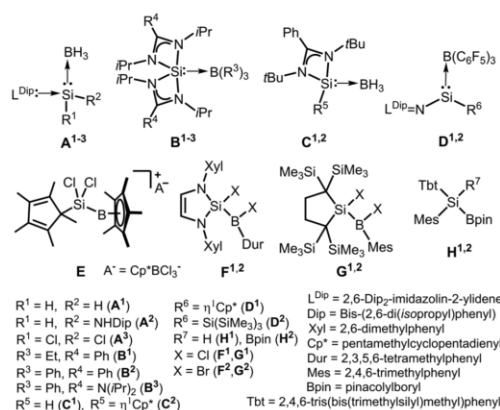
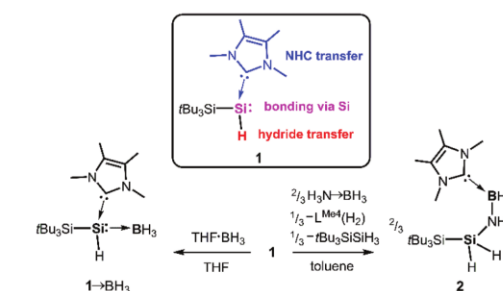


Fig. 1 Selected examples for outcomes of conversions of silylenes with various boron sources.

coordinate silicon atom. The high-coordinate species may be stabilized in the form of borane adducts of type **B**¹⁻³ (Fig. 1).^{23,26} The amidinato ligand was also implemented in four-coordinate adducts between silylene and the trihydroborane group (**C**^{1,2}, Fig. 1).^{21,31} Similar to type **B** the silylene adducts **D**^{1,2} are observed in solution whereas for the respective “free” silylenes (with no borane moiety attached) the coordination number of the silicon centers rapidly changes (Fig. 1).^{17,28}

Despite these various examples for “acceptor stabilization” silylenes were often found to be prone to insertion of the silicon atom into boron-heteroatom bonds as implied by the pioneering study of Metzler and Denk (*vide supra*).¹⁶ Jutzi and coworkers described the insertion of the high-coordinate silylene center of Cp^{*}Si into boron-chloride bonds upon its conversion with Cp^{*}BCl₂ to afford **E** (Fig. 1).³⁸ In agreement with the high reactivity of bonds between boron and the heavier halides (*e.g.* Cl, Br, I) this type of insertion was also observed for low-coordinate silylenes (*i.e.* two-coordinate NHSi) as demonstrated by Braunschweig and coworkers with the isolation of **F**^{1,2} and by the group of Iwamoto (**G**^{1,2}, Fig. 1).²⁴ As verified by the synthesis of **H**^{1,2}, the ylidenic center in silylenes may also insert into boron-hydrogen bonds, as well as unpolarized boron-boron bonds (Fig. 1).³⁷ Interestingly, the group of Chiu reported the conversion of a two-coordinate bulky NHSi with borabicyclo[3.3.1]nonyl triflate (9-(OTf)BBN) to furnish the product of boron-oxygen insertion.³⁹ Obviously, the triflate group complies to its pseudohalide character and, thus, the reactivity of the ambiphilic NHSi with the boron-triflate functionality is reminiscent of Braunschweig’s study on treating NHSi with organoborohalides. In addition to these synthetic examples the reader is also referred to theoretical studies on the insertion of silylene into boron-element bonds.⁴⁰ In consideration of the hitherto outlined scope of compounds we were surprised that systematic investigations of



Scheme 1 Reactive sites at the NHC-stabilized hydrosilylene **1** and its conversions with trihydroboranes.

one particular silylene’s reactivity towards different types of boron sources is rather uncommon with a respective report of Cui being a rare example.²⁵ In the context of discussing silylene-borane adducts one should note the small number of boryl-substituted silylenes, as well as the exceptional reaction of a disilicon(0) complex with THF·BH₃ to outstanding silylene-borane complexes.^{34,41,42} Moreover, silicon-silicon multiple bonded systems with boryl functionalities have been reported.⁴³⁻⁴⁷

Recently, we have isolated the NHC-stabilized hydrosilylene **1** and studied its reactivity towards transition metal complexes (*e.g.* Ni(COD)₂, Fe(CO)₅, W(CO)₅; COD = 1,5-cyclooctadiene) and functional organic groups (*e.g.* carbonyls, alkynes; Scheme 1).⁴⁸⁻⁵² As a distinct characteristic **1** marks three sites that may react with boron-centered electrophiles: (i) the ylidenic site at the silicon center, (ii) the dative bond between the NHC and the silicon atom which may be cleaved by electrophilic attack, and (iii) the Si-H functionality which may readily transfer a hydrogen atom (Scheme 1). Considering the importance of silicon-borane compounds to the community it was apparent to systematically study the reactivity of **1** towards various types of electrophilic boron-sources commonly encountered in molecular chemistry (*e.g.* hydro-, organo-, halo-boranes). We took the marked scarceness of reports on simple Lewis acid base adducts of silylenes with haloboranes as a particular motivation for our investigation.

Results and discussion

Conversions with trihydroborane complexes

A plethora of chemical transformations has derived from complexes of NHCs with the parent borane (*i.e.* NHC→BH₃).⁵³⁻⁵⁶ In sharp contrast, only few silylene adducts with the trihydroborane group are known as outlined above. In fact, two-coordinate silylenes do not commonly form simple and stable Lewis acid base adducts upon reaction with borane complexes (*e.g.* THF·BH₃, Me₂S→BH₃, H₃N→BH₃; here stable means to be isolatable at room temperature in the condensed phase). This will be majorly due to the enhanced Lewis acidity of low-

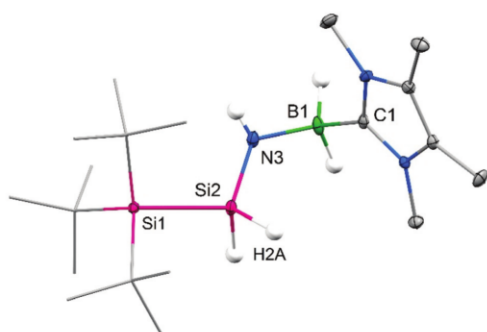
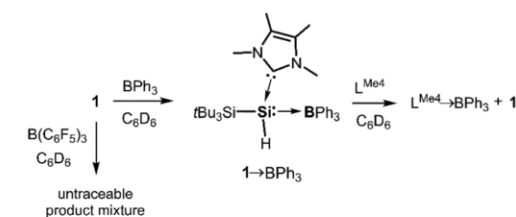


Fig. 3 Ellipsoid plot (30% level) of the molecular structure of **2** in the single crystal. H-atoms omitted (except on B, N, Si). Wireframe model for *tert*-butyl groups. Selected interatomic distances [Å] and angles [°]: Si2–N3 = 1.703(3), B1–N3 = 1.542(4), B1–C1 = 1.635(4); Si1–Si2–N3 = 114.4(1), Si2–N3–B1 = 123.2(2), N3–B1–C1 = 110.2 (2).

(FLP) chemistry).^{60–65} In order to probe the bulky silylene **1** for FLP characteristics, it was converted with the archetypical boron-centered Lewis acids triphenylborane and tris(pentafluorophenyl)borane (Scheme 2). The conversion of **1** with BPh₃ was expected to afford the complex L^{Me4}→BPh₃ which may easily form *via* abstraction of the NHC from the silylene.⁶⁶ The cleavage of the dative type bond between silicon and NHC by virtue of triarylborane has previously been reported to afford such type of NHC–borane adducts.^{25,66,67} However, when repeating the conversion in C₆D₆ in an NMR sample tube and monitoring the course of the reaction we recognized the formation of the proposed complex **1**→BPh₃. A signal at 4.38 ppm is assigned to the SiH hydrogen in the ¹H NMR analysis which is reminiscent of the respective chemical shift in **1**→BH₃. The ¹¹B NMR spectrum reveals a signal at –3.2 ppm. Hence, the signal of the three-coordinate borane precursor (*cf.* BPh₃; δ(¹¹B) = 67 ppm in Et₂O)⁶⁸ is shifted to a value for the chemical shift typical of four-coordinate boron nuclei. Another persuasive hint towards the putative **1**→BPh₃ is given by the ¹H¹³C HMBC correlation experiment in which a cross-peak is given rise to by coupling between the *ipso*-carbon atoms of the BPh₃ group and the SiH hydrogen atom. We verified the stabi-



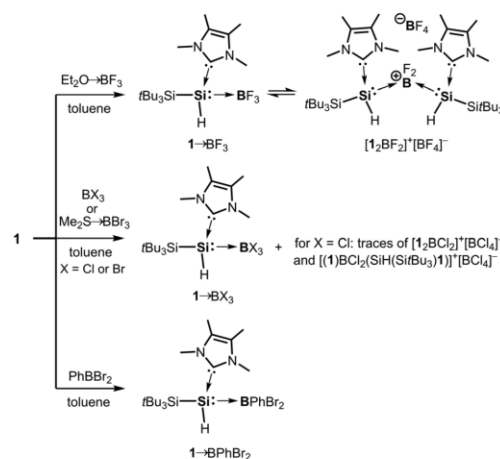
Scheme 2 Conversions of the hydrosilylene **1** with triarylboranes.

lity of the complex in C₆D₆ solution at 50 °C for a period of two days. Nevertheless, the “free” silylene **1** is readily released upon conversion of **1**→BPh₃ with L^{Me4} and the overtly more stable L^{Me4}→BPh₃ is furnished. Interestingly, when bringing **1** into contact with the more potent Lewis acid B(C₆F₅)₃ we were not able to assign any silicon-containing species neither in the product mixture nor as a temporary intermediate.

Conversions with haloboranes

In contrast to the boron sources mentioned in the previous paragraphs (*e.g.* trihydroboranes, triarylboranes) the conversion of silylenes with haloboranes is majorly limited to examples of the groups of Jutzi, of Braunschweig, and of Iwamoto as pointed out in the introduction. In addition, a respective study of Tokitoh and coworkers is to be highlighted in particular.³⁶ In these cases insertion of the silicon atom into a boron–halide bond occurs.

Considering the isolation of **1**→BH₃ after exposing **1** to the parent borane source THF·BH₃ we decided to probe boron halide reagents going from lower to higher atomic number. When the three-coordinate silylene **1** in toluene solution was brought into contact with Et₂O→BF₃ a colorless precipitate rapidly formed (Scheme 3). The solid was obtained in 87% yield after a period of 2 h and redissolved in deuterated fluorobenzene. The ¹¹B NMR analysis reveals a quartet at 4.8 ppm which is produced by a BF₃ group and deviates from the precursor (note: Et₂O→BF₃ is the external standard for the 0 ppm value of the ¹¹B nucleus). Moreover, weaker signals were observed at 10.5 ppm (triplet) and 0.4 ppm (sharp singlet), respectively. The shifts agree with four-coordinate boron centers and the resonances are diagnostic for a BF₂ group and [BF₄][–]. In fact, the intensity of the weaker signals significantly increased upon storage of the sample tube for a period of 20 h while the ratio of the BF₃ species decreased in the mixture.



Scheme 3 Reactions of the hydrosilylene **1** with different haloboranes.

Accordingly, a signal pattern assigned to one $t\text{Bu}_3\text{SiSi}(\text{H})\text{L}^{\text{Me}4}$ moiety had been observed in the ^1H NMR spectrum after 2 h reaction time and two additional signals in a 1:1 ratio rose after storage of the sample for 20 h. From the NMR study we conclude that the initial product $1 \rightarrow \text{BF}_3$ slowly transforms into $[\text{1}_2\text{BF}_2]^+[\text{BF}_4]^-$. Notably, the transformation equilibrates over time and full reaction to the auto-ionization product was not observed.

Moving our systematic investigation to the next heavier halide we treated a yellow colored solution of **1** in toluene with one equivalent of BCl_3 (as a 1 M solution in heptane, Scheme 3). As expected a colorless solid was isolated in 71% yield and combustion elemental analysis confirmed the stoichiometric composition of the trichloroborane compound $1 \cdot \text{BCl}_3$. The ^1H NMR analysis revealed the product to contain one major type of the $t\text{Bu}_3\text{SiSi}(\text{H})\text{L}^{\text{Me}4}$ moiety and additional species are hardly found. The ^{11}B NMR analysis (in CD_2Cl_2) showed a resonance at 5.5 ppm which is in accordance with a four-coordinate boron nucleus and suggests the formation of the Lewis acid base adduct $1 \rightarrow \text{BCl}_3$ (note: uncomplexed BCl_3 produces a resonance at about 40–46 ppm depending on the analytic setup). Nevertheless, a very weak signal at 6.9 ppm hints towards the presence of $[\text{BCl}_4]^-$ in solution. Due to the discrepancy in the intensity ratio (a strong and a weak signal) it is precluded that the 5.5 ppm signal is produced by $[\text{1}_2\text{BCl}_2]^+$ the formation of which *via* auto-ionization of $1 \rightarrow \text{BCl}_3$ should coincide with the $[\text{BCl}_4]^-$ content. Most likely, the observation of the minor amounts of $[\text{1}_2\text{BCl}_2]^+$ is hampered by signal broadening. Thus, we surmise that $1 \rightarrow \text{BCl}_3$ is prone to a similar auto-ionization process as presumed for $1 \rightarrow \text{BF}_3$ but the equilibrium is shifted more to the $1 \rightarrow \text{BCl}_3$ side. Notably, from the literature a few examples can be retrieved for bidentate nitrogen-based ligands to exert auto-ionization on BCl_3 to furnish $[\text{BCl}_4]^-$ salts of chelate fashioned boronium dichloride cation complexes.^{69–72} For carbene or silylene ligands, however, salts of the type $[(\text{ligand})_2\text{BX}_2][\text{BX}_4]$ (with X = halogen) are to the best of our knowledge scarcely reported in the literature. The formation of chloroborane species bearing one or two groups of **1** was corroborated by our ESI mass spectrometric analysis (positive mode) in which signals were assigned to $[\text{1} \cdot \text{BCl}_2]^+$, $[\text{1} \cdot \text{BCl}_2(\text{L}^{\text{Me}4})]^+$, and the auto-ionization product $[\text{1}_2\text{BCl}_2]^+$. Furthermore, the spectrum includes two peaks correlated with the stoichiometries $[(\text{1})\text{BHCl}(\text{SiH}(\text{Si}t\text{Bu}_3)\text{1})]^+$ and $[(\text{1})\text{BCl}_2(\text{SiH}(\text{Si}t\text{Bu}_3)\text{1})]^+$. In fact, we obtained crystalline batches of $1 \cdot \text{BCl}_3$ and from these single crystals of $1 \rightarrow \text{BCl}_3$, as well as $[(\text{1} \rightarrow \text{BCl}_2 \leftarrow \text{SiH}(\text{Si}t\text{Bu}_3) \leftarrow \text{1})]^+[\text{BCl}_4]^-$ have been picked. Unfortunately, the insufficient quality of these data prohibits discussion of the respective structural parameters (see the ESI† for details on mass spectrometry and structure depiction). It is also worth noting that incremental addition of BCl_3 (as a 1 M solution in heptane) to an NMR sample of $1 \cdot \text{BCl}_3$ in CDCl_3 did not change the ^{11}B NMR spectrum except for the rising of a signal at 46 ppm produced by “free” BCl_3 . This suggests that the auto-ionization proceeds very slowly.

As expected, a colorless precipitate also formed upon treatment of a yellow solution of the pyramidal silylene **1** in

toluene solution with BBr_3 (Scheme 3). The ^1H NMR spectrum of the isolated solid (in CD_2Cl_2) diagnoses one product species and the elemental combustion analysis agrees with the proposed stoichiometric composition $1 \cdot \text{BBr}_3$. A proton resonance at 4.76 ppm is assigned to the SiH hydrogen atom (Si, H -satellites: $^1J(\text{Si}, \text{H}) = 168$ Hz) which proves that the conceivable hydride-abstraction from the hydrosilylene by the Lewis acid is no relevant side reaction. Interestingly, while we isolated the product in moderate yield upon conversion of **1** with BBr_3 (50%) the use of the milder boron tribromide source $\text{Me}_2\text{S} \rightarrow \text{BBr}_3$ resulted in higher amounts of obtained product (74%). This also means that **1** possesses a higher affinity to BBr_3 than dimethyl sulphide. The ^{11}B NMR analysis of $1 \cdot \text{BBr}_3$ (in CD_2Cl_2) shows the presence of a four-coordinate boron center as implied by a signal at -11.8 ppm (95 Hz) which is significantly shifted to higher field with respect to BBr_3 (39 ppm in CD_2Cl_2) and also with regard to the value of 4.5 ppm for the presumed $1 \rightarrow \text{BF}_3$, as well as 5.5 ppm for $1 \rightarrow \text{BCl}_3$. The upfield shift is easily explained by the “heavy atom effect” that is imposed by bromine to inflict an upfield shift on the NMR signals of attached nuclei.⁷³ For comparison the ^{11}B nucleus of the NHC adduct $\text{L}^{\text{iPr}} \rightarrow \text{BBr}_3$ had been reported to resonate at -15 ppm (in C_6D_6 , $\text{L}^{\text{iPr}} = 1,3$ -diisopropyl-4,5-dimethyl-imidazolin-2-ylidene). A signal produced by $[\text{BBr}_4]^-$ (expected at about -24 ppm) is not observed. The structural formulation of $1 \cdot \text{BBr}_3$ as the Lewis acid base complex $1 \rightarrow \text{BBr}_3$ is supported by the XRD study conducted on single crystals grown from a concentrated solution of $1 \cdot \text{BBr}_3$ in a 1:1 mixture of dichloromethane with hexane (Fig. 4). The Si–B distance amounts to 2.045(3) Å and, thus, is very similar to the respective distance in $1 \rightarrow \text{BH}_3$. The Si–C_{NHC} bond length is determined to 1.922(3) Å which is only marginally shorter than observed in the trihydroborane complex, hence, the

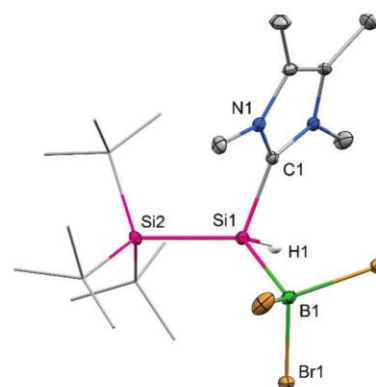


Fig. 4 Ellipsoid plot (30% level) of the molecular structure of $1 \rightarrow \text{BBr}_3$ in the single crystal. H-atoms omitted (except on Si). Wireframe model for *tert*-butyl groups. Selected interatomic distances [Å] and angles [°]: Si1–B1 = 2.045(3), Si1–C1 = 1.922(3); Si2–Si1–B1 = 130.1(1), C1–Si1–B1 = 104.9(1), Si2–Si1–C1 = 113.6(1).

bonding situation within the SiL^{Me_4} fragment seems to be affected only to a small degree by the Lewis acidity of the attached borane group. At this point it is to emphasize that we are not aware of any structural report on a simple Lewis acid base adduct between a silylene and a haloborane group as related examples commonly involve transfer of a halide from the boron- to the silicon atom.

We conclude that the susceptibility of the system consisting of **1** and a boron trihalide to auto-ionization decreases with a rise in atomic number of the halide. This agrees with the general trend reported for complexes between boron and diorganyl compounds of the heavier chalcogens (*i.e.* $\text{R}_2\text{E} \rightarrow \text{BX}_3$ with $\text{E} = \text{S}, \text{Se}, \text{Te}$ and $\text{X} = \text{halogen}$). The complex stabilities of these increase in the order $\text{F} < \text{Cl} < \text{Br}$ for the respective chalcogen.^{74–76} Moreover, the pronounced stability of the widely employed $[\text{BF}_4]^-$ anion explains why the boron fluoride system is particularly prone to auto-ionization.

Because we had studied the triarylborane complex $\mathbf{1} \rightarrow \text{BPh}_3$ and the trihaloborane adducts $\mathbf{1} \rightarrow \text{BX}_3$ it was obvious that the study of a mixed system, that is an arylhaloborane, needed to be included in our systematic investigation. Further reason was given by the recent reports of Braunschweig and coworkers who have disclosed various insertions of two-coordinate NHCs into boron–halide bonds of arylhaloboranes and we sought to contrast these reactivities by employing a three-coordinate silylene in organohaloborane chemistry.^{22,24} Thus, we brought PhBBr_2 into contact with **1** in toluene solution and, reminiscent of the related conversions described above, we observed discoloration and formation of a precipitate (Scheme 3). A sample of the isolated product (70% yield isolated) in CDCl_3 solution exhibited a resonance at -1 ppm in the ^{11}B NMR analysis which is deshielded in comparison to $\mathbf{1} \rightarrow \text{BBR}_3$ and corresponds to the typical chemical shift expected for four-coordinate boron nuclei. Additionally, the observation of the prominent SiH signal at 4.50 ppm in the ^1H NMR spectrum and the ^{13}C NMR resonance assigned to the silicon-bonded carbene center provides evidence that ligand exchange reactions between the metalloid centers are inhibited. We surmise that the silylene Lewis acid base adduct $\mathbf{1} \rightarrow \text{BPhBr}_2$ forms in similar fashion as found in the related reaction between **1** and BBR_3 . This is confirmed by the structural characterization of single crystals of $\mathbf{1} \rightarrow \text{BPhBr}_2$ (Fig. 5). Geometric parameters concerning metalloid coordination differ only by increments from the tribromoborane congener $\mathbf{1} \rightarrow \text{BBR}_3$, that is the Si–B bond and the Si– C_{NHC} are slightly elongated (2.074(3) Å and 1.931(3) Å) with respect to the higher brominated derivative. This can be attributed to the small increase of steric repulsion caused by the phenyl group rather than differences in the Lewis acidities of the tribromoborane and phenyldibromoborane fragments. Notably, the silicon–boron bond length of 2.024(3) Å in \mathbf{F}^2 is shorter by about 0.05 Å in comparison to that in $\mathbf{1} \rightarrow \text{BPhBr}_2$. The respective bond length in \mathbf{G}^2 , however, amounts to 2.077(2) Å which is very similar to our new complex. Consequently, it can hardly be concluded on the type of silicon–boron interaction (*e.g.* dative bond, single bond) from this structural parameter on the scarce basis of reported examples. We envisaged

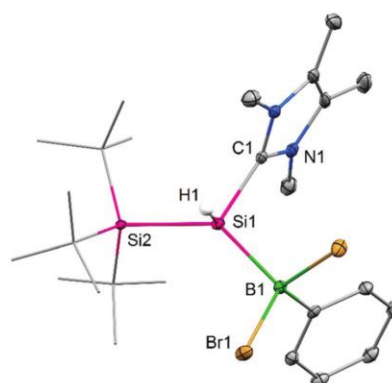


Fig. 5 Ellipsoid plot (30% level) of the molecular structure of $\mathbf{1} \rightarrow \text{BPhBr}_2$ in the single crystal. H-atoms omitted (except on Si). Wireframe model for *tert*-butyl groups. Selected interatomic distances [Å] and angles [°]: Si1–B1 = 2.074(3), Si1–C1 = 1.931(3); Si2–Si1–B1 = 131.9(1), Si2–Si1–C1 = 113.1(1), C1–Si1–B1 = 103.0(1).

that $\mathbf{1} \rightarrow \text{BPhBr}_2$ constitutes a promising precursor for reductive debromination, as well as bromide abstraction experiments to produce novel types of silylene-stabilized organoborylene systems and borenium cation species. In fact, Lin, Xie and coworkers have reported a borylene complex stabilized by a bis(silylene) ligand with four-coordinate silicon centers bearing amidino groups. Unfortunately, our attempts of exposing $\mathbf{1} \rightarrow \text{BPhBr}_2$ to common reducing agents (*e.g.* KC_8 , sodium naphthalenide, $\text{NaSi}t\text{Bu}_3$) afforded ill-defined product mixtures. Similarly, treating $\mathbf{1} \rightarrow \text{BPhBr}_2$ with bromide scavengers (*e.g.* $\text{Ag}[\text{Al}(\text{OC}(\text{CF}_3)_3)_4]$, $\text{K}[\text{B}(\text{C}_6\text{F}_5)_4]$) yielded an untraceable product.

Conclusions

The build-up of silicon–boron bonds by reaction of a three-coordinate silylene with electrophilic boron sources was systematically investigated. We treated the NHC-stabilized pyramidal hydrosilylene $t\text{Bu}_3\text{SiSi}(\text{H})\text{L}^{\text{Me}_4}$ (**1**, $\text{L}^{\text{Me}_4} = 1,3,4,5$ -tetramethyl-imidazolin-2-ylidene) with trihydroboranes, organoboranes and haloboranes. The reaction of **1** with $\text{THF} \cdot \text{BH}_3$ or $\text{H}_3\text{N} \rightarrow \text{BH}_3$ afforded the silylene complex $\mathbf{1} \rightarrow \text{BH}_3$ or the product (**2**) of ammoniaborane dehydrogenation with concomitant insertion of the silicon(II) atom into an N–H bond. Conversion of **1** with BPh_3 leads to the formation of $\mathbf{1} \rightarrow \text{BPh}_3$ complex which readily converts with additional L^{Me_4} to $\text{L}^{\text{Me}_4} \rightarrow \text{BPh}_3$ and “free” silylene **1**. Treatment of **1** with the haloboranes $\text{Et}_2\text{O} \rightarrow \text{BF}_3$, BCl_3 , BBR_3 and $\text{Me}_2\text{S} \rightarrow \text{BBR}_3$ resulted in formation of the Lewis acid base adducts $\mathbf{1} \rightarrow \text{BX}_3$ ($\text{X} = \text{F}, \text{Cl}, \text{Br}$) which slowly equilibrated to the auto-ionization products $[\mathbf{1}_2\text{BX}_2][\text{BX}_4]$. The ratio of $\mathbf{1} \rightarrow \text{BX}_3$ significantly increased with rising atomic number of the halide. Accordingly, the complex $\mathbf{1} \rightarrow \text{BPhBr}_2$ was isolated after conversion of **1** with PhBBr_2 . The

relative stability of $1 \rightarrow \text{BE}_3$ (E = H, F, Cl, Br), as well as $1 \rightarrow \text{BPhBr}_2$ strongly correlates with the relative stability of respective borane dimethyl sulphide adducts.

We envisage that the use of complexes between silylenes and boranes will complement the toolkit of organometallic synthesis similar to the ubiquitous compound class of carbene–borane complexes. The silylene–haloborane compounds in particular provide high prospect for access to hitherto unknown low-coordinate silicon–boron complexes *via* dehalogenation methods.

Experimental section

General considerations

All experiments and manipulations were carried out under an atmosphere of dry argon using standard Schlenk techniques or an MBraun glovebox workstation. Glassware was heat dried under vacuum prior to use. Solvents were dried by standard methods. NMR spectra at ambient temperature (298 K) were recorded on a Bruker AV400US, DRX400, AVHD300, or AV500C device. $\delta(^1\text{H})$ and $\delta(^{13}\text{C})$ were referenced internally to the relevant residual solvent resonances. $\delta(^{11}\text{B})$ was referenced to $\text{Et}_2\text{O} \rightarrow \text{BF}_3$ as an external standard. $\delta(^{29}\text{Si})$ was referenced to tetramethylsilane (TMS) ($\delta = 0$ ppm) as an external standard. Abbreviations: s = singlet, q = quartet, n.o. = not observed. Elemental analyses (EA) were conducted with a EURO EA (HEKA tech) instrument equipped with CHNS combustion analyzer. The silylene⁴⁸ **1**, $\text{Me}_2\text{S} \cdot \text{BBr}_3$ ⁷⁶ and PhBBr_2 ⁷⁷ were prepared according to literature procedures. $\text{THF} \cdot \text{BH}_3$, $\text{H}_3\text{N} \rightarrow \text{BH}_3$, BCl_3 (1.0 M in heptane) and BBr_3 were purchased and used as received. $\text{Et}_2\text{O} \rightarrow \text{BF}_3$ was distilled and stored in a fridge under argon. BPh_3 was sublimed at 80 °C in vacuum prior to use.

Synthesis of $1 \rightarrow \text{BH}_3$

A solution of $\text{THF} \cdot \text{BH}_3$ (1.0 M, 0.3 mL, 0.30 mmol) in THF was added to a solution of silylene **1** (80 mg, 0.23 mmol) in THF (5 mL) at ambient temperature dropwise. The color of the solution changed from yellow to colorless immediately. The reaction solution was stirred for additional 30 min. All volatiles were removed in vacuum to give $1 \rightarrow \text{BH}_3$ as colorless solid (77 mg, 93%). Colorless crystals suitable for single crystal X-ray diffraction analysis were obtained at ambient temperature from a benzene solution. ^1H NMR (400.1 MHz, C_6D_6 , 298 K): δ [ppm] = 4.31 (q, $^3J(\text{H},\text{H}) = 4.8$ Hz, Si,H-satellites: $^1J(\text{Si},\text{H}) = 150$ Hz, 1H, Si–H), 3.71 (s, 3H, N–CH₃), 3.09 (s, 3H, N–CH₃), 1.36 (s, 27H, C(CH₃)₃), 1.29 (s, 3H, C–CH₃), 1.19 (s, 3H, C–CH₃), n.o. (BH). ^{11}B NMR (128.4 MHz, C_6D_6 , 298 K): δ [ppm] = –40.8 (q, $^1J(\text{B},\text{H}) = 93$ Hz, BH₃). $^{13}\text{C}\{^1\text{H}\}$ NMR (100.6 MHz, C_6D_6 , 298 K): δ [ppm] = 161.8 (:CN₂), 127.0 (C–CH₃), 126.9 (C–CH₃), 35.0 (N–CH₃), 34.1 (N–CH₃), 32.1 (C(CH₃)₃), 24.5 (C(CH₃)₃), 8.5 (C–CH₃), 8.1 (C–CH₃). $^{29}\text{Si}\{^1\text{H}\}$ INEPT NMR (79.5 MHz, C_6D_6 , 298 K): δ [ppm] = –77.0 (Si–H), 13.1 (*t*Bu₃Si). APCI-MS $m/z = 365.2977$ [M – H]⁺, calc: 365.2974. IR (KBr) $\tilde{\nu}$ [cm^{–1}] = 2974 (w), 2950 (w), 2885 (w), 2852 (s), 2311 (br, B–H), 2238 (w, B–H), 2083 (m, Si–H), 1914 (w),

1648 (w), 1468 (m), 1437 (m), 1385 (s), 1364 (m), 1131 (w), 1021 (s), 931 (w), 888 (s), 814 (s), 775 (m), 591 (s).

Synthesis of **2**

To a solution of silylene **1** (250 mg, 0.71 mmol) in 10 mL toluene, $\text{NH}_3 \cdot \text{BH}_3$ (22 mg, 0.71 mmol) in 5 mL toluene was added dropwise at ambient temperature. The yellow solution turned colorless immediately. The reaction mixture stirred additional 3 hours; toluene was removed under vacuum, hexane was added (2 × 15 mL) and it was filtered. Hexane was removed in vacuum to afford a colorless solid. Yield: 40 mg, 46%. Colorless crystals suitable for X-ray diffraction analysis were obtained from a toluene : pentane (1 : 1) mixture at 5 °C. ^1H NMR (400.1 MHz, C_6D_6 , 298 K): δ [ppm] = 5.24 (d, $^3J(\text{H},\text{H}) = 4$ Hz, 2H, Si–H₂), 3.30 (s, 6H, N–CH₃), 1.37 (s, 27H, C(CH₃)₃), 1.21 (s, 6H, C–CH₃). ^{11}B NMR (128.4 MHz, C_6D_6 , 298 K): δ [ppm] = –17.8 (t, BH₂, $^1J(\text{B},\text{H}) = 94$ Hz). $^{13}\text{C}\{^1\text{H}\}$ NMR (100.6 MHz, C_6D_6 , 298 K): δ [ppm] = 122.6 (C–CH₃), 31.8 (C(CH₃)₃), 31.1 (N–CH₃), 23.7 (C(CH₃)₃), 7.8 (C–CH₃), n.a. (:CN₂). $^{29}\text{Si}\{^1\text{H}\}$ NMR (79.5 MHz, C_6D_6 , 298 K): δ [ppm] = –46.3 (SiH₂), 2.4 ppm (*t*Bu₃Si). APCI-HRMS $m/z = 380.3093$ [M – H]⁺, calc: 380.3083.

Synthesis of $1 \rightarrow \text{BPh}_3$

Freshly sublimed triphenylborane (BPh_3) (34.4 mg, 0.14 mmol) and silylene **1** (45 mg, 0.13 mmol) were added to a NMR sample tube and dissolved in C_6D_6 (0.5 mL). After sealing the NMR-tube the spectroscopic investigation was processed. ^1H NMR (400.1 MHz, C_6D_6 , 298 K): δ [ppm] = 7.81 (d, 6H, C^{2,6}–H, C₆H₅), 7.22 (t, 6H, C^{3,5}–H, C₆H₅), 7.12 (m, 3H, C¹–H, C₆H₅), 4.38 (s, Si,H-satellites: $^1J(\text{Si},\text{H}) = 149$ Hz, 1H, Si–H), 2.90 (s, 3H, N–CH₃), 2.62 (s, 3H, N–CH₃), 1.17 (s, 27H, C(CH₃)₃), 1.14 (s, 3H, C–CH₃), 1.07 (s, 3H, C–CH₃). ^{11}B NMR (160.5 MHz, C_6D_6 , 298 K): δ [ppm] = –3.2 (BPh_3). $^{13}\text{C}\{^1\text{H}\}$ NMR (125.8 MHz, C_6D_6 , 298 K): δ [ppm] = 161.8 (:CN₂), 156.6 (PhC), 136.8 (PhCH), 127.5 (C–CH₃), 126.5 (PhCH), 126.3 (C–CH₃), 123.6 (PhCH), 36.0 (N–CH₃), 33.8 (N–CH₃), 32.4 (C(CH₃)₃), 24.6 (C(CH₃)₃), 8.4 (C–CH₃), 7.7 (C–CH₃). $^{29}\text{Si}\{^1\text{H}\}$ NMR (99.4 MHz, C_6D_6 , 298 K): δ [ppm] = –76.6 (Si–H), 24.4 (*t*Bu₃Si). Isolated in 60% yield. Elemental analysis (%): calcd for C₃₇H₅₅BN₂Si₂: C, 74.71; H, 9.32; N, 4.71. Found: C, 73.58; H, 9.51; N, 4.42.

Synthesis of $1 \cdot \text{BF}_3$

$\text{Et}_2\text{O} \rightarrow \text{BF}_3$ (0.05 mL, 0.36 mmol) was added dropwise to a yellow solution of **1** (86 mg, 0.25 mmol) in 10 mL toluene. Immediate decolorization followed by formation of a colorless precipitate occurred. The suspension was stirred for 2 hours at room temperature and the phases were separated. The colorless solid was washed with pentane (10 mL) and dried in vacuum to give $1 \cdot \text{BF}_3$ (90 mg, 87%). Mono-adduct: ^1H NMR (300.1 MHz, $\text{C}_6\text{D}_5\text{F}$, 298 K): δ [ppm] = 4.39 (s, 1H, Si–H), 4.01 (s, 3H, N–CH₃), 3.58 (s, 3H, N–CH₃), 1.79 (s, 6H, C–CH₃), 1.50 (s, 27H, C(CH₃)₃). ^{11}B NMR (96.3 MHz, $\text{C}_6\text{D}_5\text{F}$, 298 K): δ [ppm] = 4.85 (q, $J = 85.3$ Hz). ^{19}F NMR (376.5 MHz, C_6D_6 , 298 K): δ [ppm] = –138.12 (q, $^1J(\text{B},\text{F}) = 36$ Hz). $^{29}\text{Si}\{^1\text{H}\}$ NMR

(99.4 MHz, C₆D₆F, 298 K): δ [ppm] = -84.0 (*Si-H*), 19.4 (*tBu₃Si*). Elemental analysis (%): calcd for C₁₉H₄₀BF₃N₂Si₂: C, 54.27; H, 9.59; N, 6.66. Found: C, 52.79; H, 9.61; N, 6.22 (the low value for C is reasoned by the formation of incombustible boron- and silicon carbides).

Synthesis of 1-BCl₃

To a solution of **1** (100 mg, 0.28 mmol) in 10 mL toluene, BCl₃ (1 M in heptane, 0.3 mL, 0.3 mmol) was added dropwise at ambient temperature. The yellow solution turned colorless immediately and a colorless precipitate formed. The resulting suspension was stirred overnight. After filtration the colorless powder was dried in vacuum for 2 hours to give analytically pure 1-BCl₃. Yield: 95 mg, 71%. ¹H NMR (400.1 MHz, CDCl₃, 298 K): δ [ppm] = 4.49 (s, Si,H-satellites: ¹J(Si,H) = 165 Hz, 1 H, *Si-H*), 3.98 (s, 3H, N-CH₃), 3.81 (s, 3H, N-CH₃), 2.23 (d, *J* = 6.5 Hz, 6H, C-CH₃), 1.21 (s, 27H, C(CH₃)₃). ¹¹B NMR (128.4 MHz, CD₂Cl₂, 298 K): δ [ppm] = 5.45 (*h*_{1/2} = 90 Hz). ¹³C{¹H} NMR (100.6 MHz, CD₂Cl₂, 298 K): δ [ppm] = 155.5 (:CN₂), 129.6 (C-CH₃), 128.5 (C-CH₃), 37.6 (N-CH₃), 35.5 (N-CH₃), 31.9 (C(CH₃)₃), 24.4 (C(CH₃)₃), 10.0 (C-CH₃), 9.4 (C-CH₃). ²⁹Si{¹H} NMR (79.5 MHz, CD₂Cl₂, 298 K): δ [ppm] = 19.3 (*tBu₃Si*), n.o. (*Si-H*). Elemental analysis (%): calcd for C₁₉H₄₀BCl₃N₂Si₂: C, 48.57; H, 8.58; N, 5.96. Found: C, 48.28; H, 8.31; N, 5.61.

Synthesis of 1→BBr₃

To a solution of **1** (176 mg, 0.5 mmol) in 10 mL toluene, BBr₃ (0.05 mL, 0.5 mmol, d: 2.65 g mL⁻¹) was added dropwise. The yellow solution turned colorless after 15 min and a precipitate formed. The reaction mixture was stirred overnight. The suspension was filtered and the obtained off-white powder dried in vacuum for 2 hours to give analytically pure compound 1→BBr₃ (152 mg, 50%). Colorless crystals were grown from dichloromethane:hexane (1:1) at room temperature. (The same product could also be obtained by using the more convenient Me₂S→BBr₃ adduct instead of BBr₃ with 74% yield.) ¹H NMR (400.1 MHz, CD₂Cl₂, 298 K): δ [ppm] = 4.76 (s, Si,H-satellites: ¹J(Si,H) = 168 Hz, 1 H, *Si-H*), 4.00 (s, 3H, N-CH₃), 3.80 (s, 3H, N-CH₃), 2.23 (d, *J* = 3.2 Hz, 6H, C-CH₃), 1.22 (s, 27H, C(CH₃)₃). ¹¹B NMR (128.4 MHz, CD₂Cl₂, 298 K): δ [ppm] = -11.8 (*h*_{1/2}: 95 Hz). ¹³C{¹H} NMR (100.6 MHz, CDCl₃, 298 K): δ [ppm] = 156.3 (:CN₂), 128.9 (C-CH₃), 127.8 (C-CH₃), 37.9 (N-CH₃), 35.3 (N-CH₃), 31.9 (C(CH₃)₃), 24.3 (C(CH₃)₃), 9.9 (C-CH₃), 9.3 (C-CH₃). ²⁹Si{¹H} NMR (79.5 MHz, CDCl₃, 298 K): δ [ppm] = 22.0 (*tBu₃Si*), n.o. (*Si-H*). Elemental analysis (%): calcd for C₁₉H₄₀BBr₃N₂Si₂: C, 37.83; H, 6.68; N, 4.64. Found: C, 38.8; H, 6.66; N, 4.12.

Synthesis 1→BPhBr₂

PhBBr₂ (105 mg, 0.43 mmol) in 3 mL toluene was added dropwise to a solution of **1** (150 mg, 0.43 mmol) in 7 mL toluene. The yellow solution gradually decolorized, approximately 10 minutes later a white precipitate formed. For a complete conversion, the suspension was stirred overnight. It was filtered and the colorless solid was washed with 10 mL hexane and dried in vacuum to give analytically pure 1→BBr₂Ph.

Yield: 180 mg, 70%. ¹H NMR (400.1 MHz, CDCl₃, 298 K): δ [ppm] = 7.86–7.64 (m, 2H, Ph-H), 7.18–6.89 (m, 3H, Ph-H), 4.50 (s, Si,H-satellites: ¹J(Si,H) = 161 Hz, 1H, *Si-H*), 3.93 (s, 3H, N-CH₃), 3.66 (s, 3H, N-CH₃), 2.18 (s, 6H, C-CH₃), 1.06 (s, 27H, C(CH₃)₃). ¹¹B NMR (128.4 MHz, CDCl₃, 298 K): δ [ppm] = -0.77 (*h*_{1/2}: 550 Hz). ¹³C{¹H} NMR (75.5 MHz, CDCl₃, 298 K): δ [ppm] = 157.5 (:CN₂), 133.8 (PhCH), 128.4 (C-CH₃), 127.3 (C-CH₃), 126.6 (PhCH), 125.5 (PhCH), 37.7 (N-CH₃), 35.0 (N-CH₃), 31.7 (C(CH₃)₃), 24.0 (C(CH₃)₃), 9.8 (C-CH₃), 9.1 (C-CH₃). ²⁹Si{¹H} NMR (99.4 MHz, CDCl₃, 298 K): δ [ppm] = 20.2 (*tBu₃Si*), n.o. (*Si-H*). Elemental analysis (%): calcd for C₂₅H₄₅BBr₂N₂Si₂: C, 50.01; H, 7.55; N, 4.67. Found: C, 49.05; H, 7.27; N, 4.47 (the low value for C is reasoned by the formation of incombustible boron- and silicon carbides).

Conflicts of interest

The authors affirm that there are no conflicts to declare.

Acknowledgements

We gratefully acknowledge financial support from WACKER Chemie AG and the European Research Council (SILION 637394). We thank Lorenz J. Schiegerl (TUM) and Dr Maria Schlangen-Ahl (TU Berlin) for mass spectrometric analyses.

References

- Y. Cui, X. Duan, J. Hu and C. M. Lieber, *J. Phys. Chem. B*, 2000, **104**, 5213–5216.
- Y. Cui and C. M. Lieber, *Science*, 2001, **291**, 851–853.
- N. Fukata, *Adv. Mater.*, 2009, **21**, 2829–2832.
- M. Oestreich, E. Hartmann and M. Mewald, *Chem. Rev.*, 2013, **113**, 402–441.
- C. Kleeberg and C. Borner, *Eur. J. Inorg. Chem.*, 2013, **2013**, 2799–2806.
- E. Yamamoto, R. Shishido, T. Seki and H. Ito, *Organometallics*, 2017, **36**, 3019–3022.
- Y. Mizuhata, T. Sasamori and N. Tokitoh, *Chem. Rev.*, 2009, **109**, 3479–3511.
- M. Asay, C. Jones and M. Driess, *Chem. Rev.*, 2011, **111**, 354–396.
- B. Blom, M. Stoelzel and M. Driess, *Chem. – Eur. J.*, 2013, **19**, 40–62.
- Z. Benedek and T. Szilvási, *RSC Adv.*, 2015, **5**, 5077–5086.
- C. Marschner, *Eur. J. Inorg. Chem.*, 2015, **2015**, 3805–3820.
- T. Troadec, A. Prades, R. Rodriguez, R. Mirgalet, A. Baceiredo, N. Saffon-Merceron, V. Branchadell and T. Kato, *Inorg. Chem.*, 2016, **55**, 8234–8240.
- J. A. Cabeza, P. García-Álvarez and D. Polo, *Eur. J. Inorg. Chem.*, 2016, **2016**, 10–22.
- S. Raoufoghaddam, Y.-P. Zhou, Y. Wang and M. Driess, *J. Organomet. Chem.*, 2017, **829**, 2–10.

- 15 C. Weetman and S. Inoue, *ChemCatChem*, 2018, **10**, 4213–4228.
- 16 N. Metzler and M. Denk, *Chem. Commun.*, 1996, **1996**, 2657–2658.
- 17 D. Wendel, A. Porzelt, F. A. D. Herz, D. Sarkar, C. Jandl, S. Inoue and B. Rieger, *J. Am. Chem. Soc.*, 2017, **139**, 8134–8137.
- 18 H. Wang, L. Wu, Z. Lin and Z. Xie, *J. Am. Chem. Soc.*, 2017, **139**, 13680–13683.
- 19 Y. Suzuki, S. Ishida, S. Sato, H. Isobe and T. Iwamoto, *Angew. Chem., Int. Ed.*, 2017, **56**, 4593–4597.
- 20 Y. Li, R. K. Siwath, T. Mondal, Y. Li, R. Ganguly, D. Koley and C.-W. So, *Inorg. Chem.*, 2017, **56**, 4112–4120.
- 21 S. Kaufmann, S. Schäfer, M. T. Gamer and P. W. Roesky, *Dalton Trans.*, 2017, **46**, 8861–8867.
- 22 H. Braunschweig, T. Brückner, A. Deifsenberger, R. D. Dewhurst, A. Gackstatter, A. Gärtner, A. Hofmann, T. Kupfer, D. Prieschl, T. Thiess and S. R. Wang, *Chem. – Eur. J.*, 2017, **23**, 9491–9494.
- 23 F. M. Mück, J. A. Baus, R. Bertermann, C. Burschka and R. Tacke, *Organometallics*, 2016, **35**, 2583–2588.
- 24 A. Gackstatter, H. Braunschweig, T. Kupfer, C. Voigt and N. Arnold, *Chem. – Eur. J.*, 2016, **22**, 16415–16419.
- 25 H. Cui, M. Wu and P. Teng, *Eur. J. Inorg. Chem.*, 2016, **2016**, 4123–4127.
- 26 K. Junold, J. A. Baus, C. Burschka, C. Fonseca Guerra, F. M. Bickelhaupt and R. Tacke, *Chem. – Eur. J.*, 2014, **20**, 12411–12415.
- 27 R. Rodriguez, T. Troadec, T. Kato, N. Saffon-Merceron, J.-M. Sotiropoulos and A. Baccaredo, *Angew. Chem., Int. Ed.*, 2012, **51**, 7158–7161.
- 28 S. Inoue and K. Leszczyńska, *Angew. Chem., Int. Ed.*, 2012, **51**, 8589–8593.
- 29 S. M. I. Al-Rafia, R. McDonald, M. J. Ferguson and E. Rivard, *Chem. – Eur. J.*, 2012, **18**, 13810–13820.
- 30 S. M. I. Al-Rafia, A. C. Malcolm, R. McDonald, M. J. Ferguson and E. Rivard, *Chem. Commun.*, 2012, **48**, 1308–1310.
- 31 A. Jana, D. Leusser, I. Objartel, H. W. Roesky and D. Stalke, *Dalton Trans.*, 2011, **40**, 5458.
- 32 A. Jana, R. Azhakar, S. P. Sarish, P. P. Samuel, H. W. Roesky, C. Schulzke and D. Koley, *Eur. J. Inorg. Chem.*, 2011, **2011**, 5006–5013.
- 33 R. Azhakar, G. Tavčar, H. W. Roesky, J. Hey and D. Stalke, *Eur. J. Inorg. Chem.*, 2011, **2011**, 475–477.
- 34 M. Y. Abraham, Y. Wang, Y. Xie, P. Wei, H. F. Schaefer, P. v. R. Schleyer and G. H. Robinson, *J. Am. Chem. Soc.*, 2011, **133**, 8874–8876.
- 35 R. S. Ghadwal, H. W. Roesky, S. Merkel and D. Stalke, *Chem. – Eur. J.*, 2010, **16**, 85–88.
- 36 T. Kajiwara, N. Takeda, T. Sasamori and N. Tokitoh, *Organometallics*, 2004, **23**, 4723–4734.
- 37 T. Kajiwara, N. Takeda, T. Sasamori and N. Tokitoh, *Chem. Commun.*, 2004, **2004**, 2218–2219.
- 38 U. Holtmann, P. Jutzi, T. Kühler, B. Neumann and H.-G. Stammer, *Organometallics*, 1999, **18**, 5531–5538.
- 39 H.-C. Tsai, Y.-F. Lin, W.-C. Liu, G.-H. Lee, S.-M. Peng and C.-W. Chiu, *Organometallics*, 2017, **36**, 3879–3882.
- 40 B. Geng, C. Xu and Z. Chen, *J. Mol. Model.*, 2016, **22**, 134.
- 41 A. V. Protchenko, K. H. Birjkumar, D. Dange, A. D. Schwarz, D. Vidovic, C. Jones, N. Kaltsoyannis, P. Mountford and S. Aldridge, *J. Am. Chem. Soc.*, 2012, **134**, 6500–6503.
- 42 R. S. Alfredo, A. B. Isabel, B. Antoine, S. M. Nathalie, M. Stéphane, B. Vicenç and K. Tsuyoshi, *Angew. Chem., Int. Ed.*, 2017, **56**, 10549–10554.
- 43 S. Inoue, M. Ichinohe and A. Sekiguchi, *Chem. Lett.*, 2008, **37**, 1044–1045.
- 44 K. Takeuchi, M. Ichinohe and A. Sekiguchi, *Organometallics*, 2011, **30**, 2044–2050.
- 45 T. Kosai and T. Iwamoto, *J. Am. Chem. Soc.*, 2017, **139**, 18146–18149.
- 46 T. Kosai and T. Iwamoto, *Chem. – Eur. J.*, 2018, **24**, 7774–7780.
- 47 K. Takeuchi, M. Ikoshi, M. Ichinohe and A. Sekiguchi, *J. Am. Chem. Soc.*, 2010, **132**, 930–931.
- 48 S. Inoue and C. Eisenhut, *J. Am. Chem. Soc.*, 2013, **135**, 18315–18318.
- 49 C. Eisenhut, T. Szilvási, N. C. Breit and S. Inoue, *Chem. – Eur. J.*, 2015, **21**, 1949–1954.
- 50 C. Eisenhut, N. C. Breit, T. Szilvási, E. Irran and S. Inoue, *Eur. J. Inorg. Chem.*, 2016, **2016**, 2696–2703.
- 51 C. Eisenhut and S. Inoue, *Phosphorus, Sulfur Silicon Relat. Elem.*, 2016, **191**, 605–608.
- 52 C. Eisenhut, T. Szilvási, G. Dübek, N. C. Breit and S. Inoue, *Inorg. Chem.*, 2017, **56**, 10061–10069.
- 53 T. Kawamoto, S. J. Geib and D. P. Curran, *J. Am. Chem. Soc.*, 2015, **137**, 8617–8622.
- 54 T. R. McFadden, C. Fang, S. J. Geib, E. Merling, P. Liu and D. P. Curran, *J. Am. Chem. Soc.*, 2017, **139**, 1726–1729.
- 55 D. P. Curran, A. Solovyev, M. M. Brahmi, L. Fensterbank, M. Malacria and E. Lacôte, *Angew. Chem., Int. Ed.*, 2011, **50**, 10294–10317.
- 56 A. Prokofjevs, J. W. Kampf, A. Solovyev, D. P. Curran and E. Vedejs, *J. Am. Chem. Soc.*, 2013, **135**, 15686–15689.
- 57 A. Jana, C. Schulzke and H. W. Roesky, *J. Am. Chem. Soc.*, 2009, **131**, 4600–4601.
- 58 M. Stoelzel, C. Präsang, S. Inoue, S. Enthaler and M. Driess, *Angew. Chem., Int. Ed.*, 2012, **51**, 399–403.
- 59 K. J. Sabourin, A. C. Malcolm, R. McDonald, M. J. Ferguson and E. Rivard, *Dalton Trans.*, 2013, **42**, 4625–4632.
- 60 D. W. Stephan, S. Greenberg, T. W. Graham, P. Chase, J. J. Hastie, S. J. Geier, J. M. Farrell, C. C. Brown, Z. M. Heiden, G. C. Welch and M. Ullrich, *Inorg. Chem.*, 2011, **50**, 12338–12348.
- 61 D. W. Stephan, *Science*, 2016, **354**, aaf7229.
- 62 S. A. Weicker and D. W. Stephan, *Bull. Chem. Soc. Jpn.*, 2015, **88**, 1003–1016.
- 63 D. W. Stephan, *J. Am. Chem. Soc.*, 2015, **137**, 10018–10032.
- 64 D. W. Stephan, *Acc. Chem. Res.*, 2014, **48**, 306–316.

- 65 D. W. Stephan and G. Erker, *Angew. Chem., Int. Ed.*, 2015, **54**, 6400–6441.
- 66 A. C. Filippou, O. Chernov, K. W. Stumpf and G. Schnakenburg, *Angew. Chem., Int. Ed.*, 2010, **49**, 3296–3300.
- 67 H. Cui, J. Zhang and C. Cui, *Organometallics*, 2013, **32**, 1–4.
- 68 H. C. Brown and U. S. Racherla, *J. Org. Chem.*, 1986, **51**, 427–432.
- 69 K. V. Vasudevan, M. Findlater and A. H. Cowley, *Chem. Commun.*, 2008, **2008**, 1918–1919.
- 70 H. A. Jenkins, C. L. Dumaresque, D. Vidovic and J. A. C. Clyburne, *Can. J. Chem.*, 2002, **80**, 1398–1403.
- 71 L. Weber, J. Förster, H.-G. Stammer and B. Neumann, *Eur. J. Inorg. Chem.*, 2006, **2006**, 5048–5056.
- 72 M. Möhlen, K. Harms, K. Dehnicke, J. Magull, H. Goesmann and D. Fenske, *Z. Anorg. Allg. Chem.*, 1996, **622**, 1692–1700.
- 73 A. C. Neto, L. C. Ducati, R. Rittner, C. F. Tormena, R. H. Contreras and G. Frenking, *J. Chem. Theory Comput.*, 2009, **5**, 2222–2228.
- 74 C. K. Y. A. Okio, W. Levason, F. M. Monzittu and G. Reid, *J. Organomet. Chem.*, 2017, **848**, 232–238.
- 75 H. C. Brown and N. Ravindran, *Inorg. Chem.*, 1977, **16**, 2938–2940.
- 76 M. Schmidt and H. D. Block, *Chem. Ber.*, 1970, **103**, 3705–3710.
- 77 D. Kaufmann, *Chem. Ber.*, 1987, **120**, 853–854.

8 NHC-Stabilized Silyl-Substituted Chlorosilylene

Title: NHC-Stabilized Silyl-Substituted Chlorosilylene
Status: Communication, published online November 11, 2019
Journal: *Inorganic Chemistry*, 2019, 58, 23, 15700-15704.
Publisher: American Chemical Society
DOI: 10.1021/acs.inorgchem.9b02670
Authors: Gizem Dübek, Franziska Hanusch and Shigeyoshi Inoue*

Content: After the isolation of the first amidinato ligand stabilized monochlorosilylene by Roesky in 2006, several donor-stabilized silylenes with chloride functionality were reported. These subsequent reports utilized different ligands including phosphine, β -diketiminato, aryl or amino substituents yet silyl-substituted chlorosilylene remained missing. Silyl-groups are one of the excellent substituents in main group chemistry due to their tunable steric demand and high σ -donation properties. Therefore, we aimed to synthesize and isolate a novel monochlorosilylene that bears a silyl-substituent. This was achieved via the selective dehydrochlorination of a silyl-based Si(IV) precursor to afford the first NHC-stabilized (silyl)chlorosilylene. In addition, the reactivity of the title compound was explored and found to react through three distinct active sites. Firstly, (silyl)chlorosilylene can coordinate the iron carbonyl via its ylidenic site at the silicon center to form an iron chlorosilylene complex, with a relatively long Si-Fe bond length. Secondly, the title compound undergoes chloride/hydride metathesis to yield a stable NHC-silylene hydride borane adduct upon treatment with LiBH_4 which corroborates the Si-Cl functionality. Furthermore, due to the dative bond between the NHC and silicon atom, chlorosilylene can transform to a silyliumylidene ion upon treatment with excess less sterically demanding NHCs through ligand exchange reaction.

Reprinted with the permission from G. Dübek, F. Hanusch, S. Inoue, *Inorg. Chem.* **2019**, 58, 15700-15704. Copyright 2019 American Chemical Society.

* G. Dübek planned and executed all experiments including analysis and wrote the manuscript. F. Hanusch conducted all SC XRD measurements and managed the processing of the respective data. All work was performed under the supervision of S. Inoue.

NHC-Stabilized Silyl-Substituted Chlorosilylene

Gizem Dübek, Franziska Hanusch,[✉] and Shigeyoshi Inoue^{*✉}

Department of Chemistry, Catalysis Research Center and WACKER-Institute of Silicon Chemistry, Technical University of Munich, Lichtenbergstraße 4, D-85748 Garching, Germany

Supporting Information

ABSTRACT: The first N-heterocyclic carbene (NHC) stabilized silyl-substituted chlorosilylene (**1**) was isolated via selective dehydrochlorination by NHC from silyl-based Si(IV) precursor $t\text{Bu}_3\text{SiHCl}_2$. Compound **1** can form an iron chlorosilylene complex (**2**) with an iron carbonyl dimer and undergoes chloride/hydride metathesis to yield a stable NHC–silylene hydride borane adduct (**3**). Upon treatment with additional NHC, chlorosilylene **1** was converted into silyl-substituted silyliumylidene ions (**4**).

Silylenes, the heavier analogues of carbenes, are key intermediates in many thermal and photochemical reactions in organosilicon chemistry.¹ Prior to their discovery in 1994, silylenes were considered to be unstable species and could only be isolated at cryogenic temperatures.² Shortly after the initial report of the isolation of stable N-heterocyclic carbene by Arduengo et al., Denk and West et al. were able to isolate a stable dicoordinate N-heterocyclic silylene (NHSi).³ Since then a good number of room temperature stable silylenes were reported.⁴ Apart from the silylenes, the chemistry of functionalized silylenes has been given great attention. Among the α -substituted silylenes, divalent chlorosilylenes are an important group of compounds in organosilicon chemistry because of their industrial applications.⁵ Due to their high reactivity, organosilicon(II) halides can be isolated by either intramolecular donor–acceptor or Lewis-base stabilization.⁶ After the first isolation of monomeric amidinato chlorosilylene $[\text{PhC}(\text{N}t\text{Bu})_2]\text{SiCl}$ by Roesky and co-workers in 2006 (A, Chart 1), it led the way to the investigation of various novel divalent silicon halide compounds.⁷ Baceiredo, Kato, and co-

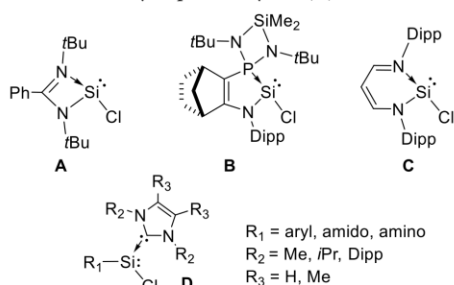
workers reported another intermolecular stabilized chlorosilylene B, by using phosphine as donor in 2010.⁸ Recently, Driess and co-workers have reported intramolecular Lewis-donor-stabilized silylenes by a well-known β -diketiminate ligand in 2018 (C).⁹ Aside from the intramolecular stabilization, electron donating N-heterocyclic carbenes (NHCs) can also be used to stabilize reactive main group species.¹⁰ The group of Filippou reported the first NHC adduct of an arylchlorosilylene in 2010, which was later successfully used as a precursor to isolate the first transition metal silylyne complex.¹¹ Not only aryl substituted but also amido- and amino-chloro silylenes were reported by external support via NHCs (D).^{11a,12} Apart from their electronic donation, bulky N-heterocyclic ligands can also provide steric hindrance to allow access to halosilylenes with a reactive Si(II) center like gaseous dichlorosilylene. In 2009, Roesky et al. showed the first room temperature stable base-stabilized silicon dichloride (LSiCl_2 ; L = 1,3-bis(2,6-diisopropylphenyl)imidazole-2-ylidene), and concurrently Filippou et al. reported the analogous SiX_2 (X = Br, I) employing the same NHC ligand.¹³

Although various different ligands have been employed as kinetic and thermodynamic stabilization of these highly reactive species so far, a silyl-substituted chlorosilylene has not yet been reported due to the lack of suitable synthetic methods. Since electropositive and sterically demanding silyl substituents (e.g. $t\text{Bu}_3\text{Si}$) can enhance the stability of low-valent silicon species and overcome the inherent high reactivity of chlorosilylenes, we embarked on introducing the bulky silyl substituent along with the NHC. Silyl-substituted chlorosilylene would be an excellent precursor for the synthesis of novel low-valent organosilicon compounds. Herein, we describe the preparation and characterization of the first isolable NHC-stabilized silyl-substituted chlorosilylene and its reactivity.

The treatment of a silyl-substituted dichlorosilane $t\text{Bu}_3\text{SiHCl}_2$ precursor with two equivalents of ImEt_2Me_2 (1,3-diethyl-4,5-dimethylimidazol-2-ylidene) in toluene at $-50\text{ }^\circ\text{C}$ (Scheme 1) furnished silicon(II) monochloride NHC adduct **1** in excellent yields (92%). Compound **1** is a deep orange, air- and moisture-sensitive solid and slowly decomposes at room temperature even under an inert atmosphere.

It is worthwhile to mention that the introduction of a smaller NHC (ImMe_4) did not yield the desired chlorosilylene. In the ^{29}Si NMR spectrum of **1**, the signal corresponding to the terminal Si(II)-Cl appears at 18.3 ppm, which is downfield shifted from previously reported NHC-stabilized arylchloro-

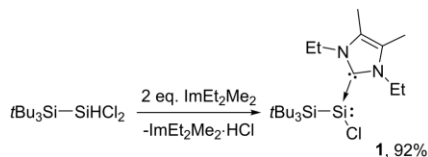
Chart 1. Previously Reported Silylene (II) Chlorides



Received: September 5, 2019

Published: November 11, 2019

Scheme 1. Synthesis of NHC-Adduct of Silyl-Substituted Chlorosilylene 1



osilylenes (0.77–1.34 ppm) probably due to the presence of an electropositive silyl substituent.^{11a} The ¹³C NMR signal for the NHC carbon atom of **1** (169.71 ppm) is consistent with other NHC→Si complexes.^{11a,13a} The ¹J(Si, C^{NHC}) coupling constant of 49 Hz is smaller than that of Si–C(sp²) single bonds in silanes (64–70 Hz) or Si–C(sp) bonds in silaallenes (84–142 Hz) and slightly larger than previously reported NHC-stabilized chlorosilylene (33–37 Hz), indicating a higher s character of **1**.^{11a,14}

The molecular structure of complex **1** was determined by X-ray crystallographic analysis and displays a trigonal pyramidal geometry, with the sum of bond angles at the silicon center being 309.25° (Figure 1). The Si–C^{NHC} bond length of

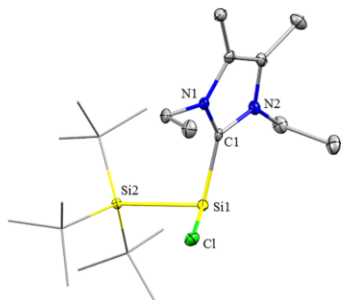
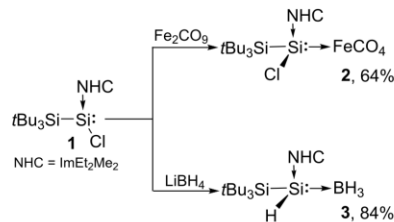


Figure 1. Ellipsoid plot (50% level) of the molecular structure of compound **1**. Hydrogen atoms are omitted for clarity, and *tert*-butyl groups are depicted in wireframe for simplicity. Selected bond lengths (Å) and angles (deg): Si1–C1, 1.9572(19); Si1–Si2, 2.4421(7); Si1–Cl, 2.1947(7); C1–Si1–Cl, 99.23(6); Cl–Si1–Si2, 103.51(3); C1–Si1–Si2, 106.51(6).

1.9572(19) Å suggests relatively stronger donor–acceptor interaction than known for NHC-stabilized silylene (II) chlorides (Si–C^{NHC} bond length = 1.963(2)–2.0023(19) Å).^{11a,12}

Considering the existence of a stereochemically active lone pair on the silicon, and a functional group attached to the α-position of the silicon center, it was apparent to study the fundamental reactivity of compound **1**. Treatment of **1** with half of an equivalent of Fe₂(CO)₉ afforded the silylene iron complex **2** as beige powder in 64% yield (Scheme 2). We observed no reaction between **1** and Fe(CO)₅. A significant downfield shift (**1**, δ 18.30; **2**, δ 64.94) in the ²⁹Si NMR was observed, which verifies the coordination of the iron center to the lone pair of the chlorosilylene and the presence of an active lone pair at the silicon center. Carbonyl groups were observed at δ 218.15 in the ¹³C NMR spectrum, which is comparable with previously reported silylene iron complexes.¹⁵

Scheme 2. Syntheses of Compounds **2** and **3** from Chlorosilylene **1**

The molecular structure of the complex **2** was also confirmed by single crystal X-ray diffraction analysis (Figure 2). The Si–Fe bond length (2.3620(5) Å) is longer than other

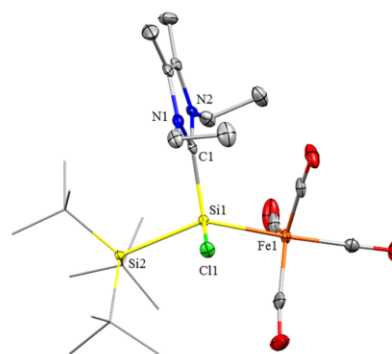
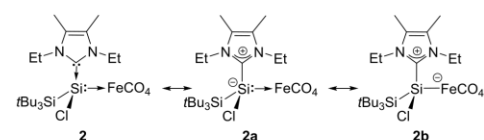


Figure 2. Ellipsoid plot (50% level) of the molecular structure of compound **2**. One out of two crystallographically independent molecules is shown. Hydrogen atoms are omitted for clarity, and *tert*-butyl groups are depicted in wireframe for simplicity. Selected bond lengths (Å): Si1–Fe1, 2.3620(5); Si1–Si2, 2.5185(6); Si1–Cl, 1.9927(16); Si1–Cl, 2.1440(6).

reported Si–Fe bonds (2.15–2.32 Å); however, it is slightly shorter than the recently reported *t*Bu₃Si(H)(ImMe₄)Si→Fe(CO)₄ (2.3717(16) Å).^{15a,b,16} Elongation of the silicon–iron bond length can be explained by the α-silyl effect. As also clarified by our recent report, introduction of the electron-donating bulky silyl-substituent in complex **2** compels more electron density on the silylene silicon, which stabilizes the zwitterionic resonance structures (Scheme 3).^{15b} As expected, the presence of a highly electronegative chlorine atom in complex **2**, instead of hydrogen, results in the shortening of the Si–Fe bond length compared to the hydrogen derivative.

Scheme 3. Resonance Structures of NHC-Stabilized Chlorosilylene Iron Complex **2a** and **2b**

Recently Rivard et al. reported that halide substituents on the tetrel(II) dihalides can undergo chloride/hydride metathesis.¹⁷ Encouraged by these studies, we aimed to functionalize the chlorine atom of complex **1**, by treating it with LiBH_4 . As expected formation of new silicon(II) hydride borane complex **3** was obtained and could be isolated in 84% yield (Scheme 2). Chloride/hydride metathesis was evident by inspection of ^1H NMR spectrum, with the Si–H bond assigned as a quartet at 4.31 ppm due to coupling with boron and silicon bonded hydrogens ($^3J_{\text{HH}} = 5.5$ Hz, ^{29}Si satellites $^1J_{\text{SiH}} = 150$ Hz). Ethyl and backbone hydrogens in the ImEt_2Me_2 exist in different magnetic environments giving rise to distinct shifts probably due to different orientation of the Et groups. The same behavior can be also observed in the ^{13}C NMR spectrum. The ^{11}B NMR spectrum gave a quartet at -40.31 ppm that was displayed as a singlet in the proton decoupled experiment, which also confirms coordination of the BH_3 group to the silicon. Due to the quadrupolar momentum of the ^{11}B nucleus, the signal for the coordinated silicon could not be observed in the 1D ^{29}Si NMR; however, we could assign the peak at -64.17 ppm in the $^{29}\text{Si}\{^1\text{H}\}$ heteronuclear correlation spectrum. The IR spectrum of compound **3** shows an absorption band for B–H stretching modes from 2233 to 2330 cm^{-1} and a sharp Si–H stretching mode at 2087 cm^{-1} which is in agreement with the reported values.^{12a,18}

The molecular structure of **3** was further determined by X-ray diffraction analysis (Figure 3), and the Si–B distance is

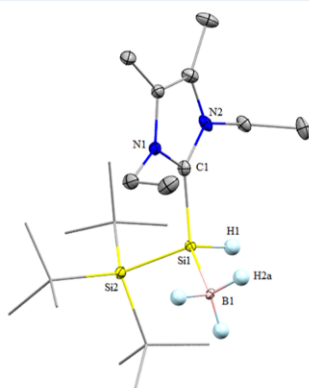


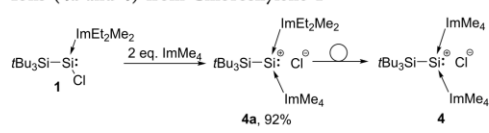
Figure 3. Ellipsoid plot (30% level) of the molecular structure of compound **3**. Hydrogen atoms except on B and Si are omitted for clarity, and *tert*-butyl groups are depicted in wireframe for simplicity. Selected bond lengths (Å) and angles (deg): Si1–B1, 1.999(7); Si1–Si2, 2.374(5); Si1–Cl1, 1.963(6); Si2–Si1–B1 = 121.0(2); Cl1–Si1–B1 = 112.0(2); Si2–Si1–Cl1 = 112.0(2).

found at 1.999(7) Å, which resembles previously reported silicon(II)–borane adducts (1.965(2)–2.009(5) Å).^{12a,18c,19} Very recently, we reported an isostructural complex with smaller NHC (ImMe_4), and as expected all spectral and structural data of the previously reported complex $t\text{Bu}_3\text{Si}(\text{H})(\text{ImMe}_4)\text{Si} \rightarrow \text{BH}_3$ are consistent with that observed for compound **3**.^{18c} Interestingly, we observed a second set of signals, which is consistent with the spectroscopic data of compound **3** in all multinuclear NMR spectra. Since in those analytics isolated crystals were used, it prohibits the presence

of a side product or impurity. The $^{13}\text{C}/^1\text{H}$ and $^{29}\text{Si}/^1\text{H}$ HMBC experiments reveal the formation of a minor product with a ratio of 1:6 in which we assume a symmetric (ethyl– CH_3 exist in same magnetic environments) isomer of compound **3**. Upon heating, we did not observe any changes in the ^1H spectrum of **3**, suggesting that the minor product does not form thermodynamically. Other reagents, like LiI and $(\text{dme})\text{-(TMS)}_2\text{PLi}$, were also used to exchange the chloride atom at the silicon center; however, compound **1** was relatively stable under these conditions, and we did not observe the formation of the desired product. Moreover, attempts to abstract chloride from the halide substituted compounds (**1** and **2**) by common reducing agents (e.g., KC_8 , lithium naphthalenide, $t\text{Bu}_3\text{SiNa}(\text{thf})_2$, etc.) were unsuccessful and yielded ill-defined mixtures.

In addition to the lone pair and halide functionality, complex **1** bears one more reactive site which is the coordinated NHC. Our first attempt was to exchange ImEt_2Me_2 with smaller NHC (ImMe_4), which was reported earlier by Scheschkewitz and co-workers.^{18b,20} Upon treatment of complex **1** with one equivalent of ImMe_4 in toluene, we observed immediate precipitation, which implies the formation of silyliumylidene. At this point, we aimed to treat chlorosilylene (**1**) directly with two equivalents of ImMe_4 to obtain the corresponding silylsilyliumylidene ion $[t\text{Bu}_3\text{SiSi}(\text{ImMe}_4)_2]\text{Cl}$ (**4**) as reported very recently by our group (Scheme 4).²¹ As expected upon

Scheme 4. Conversion into NHC-Stabilized Silyliumylidene Ions (**4a** and **4**) from Chlorosilylene **1**



treatment of **1** with NHC, immediate yellow precipitate was formed in toluene, which was isolated in good yield (92%). Although our presumption was to coordinate two ImMe_4 's to the silicon center by reaction with excess NHC, the ^1H NMR spectrum displayed the formation of mixed silyliumylidene ion **4a**. Two signals can be observed in the ^{13}C NMR at 163.28 and 162.97 ppm for the central carbons of the different NHCs. Complex **4a** has comparable ^1H and ^{13}C shifts with previously reported silyl-substituted silyliumylidene ion **4** and almost an exact ^{29}Si signal (**4a** = $\delta - 80.51$, **4** = $\delta - 82.0$).²¹ We conducted a time dependent ^1H NMR experiment of compound **4a** in CD_3CN at ambient temperature. Compound **4a** in solution showed no change at room temperature for 24 h but started to form compound **4** only after heating to 65 $^\circ\text{C}$ (see Supporting Information for full spectrum). Unfortunately, during crystallization, **4a** rearranged to **4**, hence **4a** could not be characterized crystallographically.

In conclusion, we described the synthesis, isolation, and reactivity of novel NHC-stabilized silyl-substituted chlorosilylene (**1**). Compound **1** reacts readily with $\text{Fe}_2(\text{CO})_9$ through its lone pair to yield the corresponding iron complex (**2**). Compound **2** has a relatively long Si–Fe bond length which can be attributed to the presence of an electron-donating bulky silyl substituent. Treatment of **1** with LiBH_4 afforded stable silylenehydride borane adduct (**3**) via the chloride-hydride salt metathesis reaction. Moreover, chlorosilylene **1** underwent a ligand exchange reaction with excess ImMe_4 , resulting in the formation of an asymmetric NHC silyliumylidene ion (**4a**),

which further transformed into more stable symmetric silyliumylidene ion **4**. We envisage that an electropositive silyl substituent on the low valent silicon(II) chloride is a promising building block since it is prone to metathesis reactions and can lead to various novel organosilicon compounds. Further reactivity investigations of compound **1** with transition metallates as well as other organic/inorganic small molecules are currently under investigation in our research group.

■ ASSOCIATED CONTENT

Supporting Information

The Supporting Information is available free of charge on the ACS Publications website at DOI: 10.1021/acs.inorgchem.9b02670.

Experimental details, including synthesis, and depiction of analysis spectra (PDF)

Accession Codes

CCDC 1950760–1950761 and 1961386 contain the supplementary crystallographic data for this paper. These data can be obtained free of charge via www.ccdc.cam.ac.uk/data_request/cif, or by emailing data_request@ccdc.cam.ac.uk, or by contacting The Cambridge Crystallographic Data Centre, 12 Union Road, Cambridge CB2 1EZ, UK; fax: +44 1223 336033.

■ AUTHOR INFORMATION

Corresponding Author

*E-mail: s.inoue@tum.de.

ORCID

Franziska Hanusch: 0000-0002-9509-194X

Shigeyoshi Inoue: 0000-0001-6685-6352

Notes

The authors declare no competing financial interest.

■ ACKNOWLEDGMENTS

We gratefully acknowledge financial support from WACKER Chemie AG and the European Research Council (SILION 637394). We thank Dr. Daniel Franz for measurement of structures **2** and **3** and Dr. Philipp Altmann for measurement and refinement of structure **1**.

■ REFERENCES

- (1) (a) Gaspar, P. P.; West, R. Silylenes. *The Chemistry of Organic Silicon Compounds*; Rappoport, Z., Apeloig, Y., Eds.; John Wiley & Sons, Ltd., 1998; pp 2463–2568. (b) Asay, M.; Jones, C.; Driess, M. N-Heterocyclic Carbene Analogues with Low-Valent Group 13 and Group 14 Elements: Syntheses, Structures, and Reactivities of a New Generation of Multitalented Ligands. *Chem. Rev.* **2011**, *111*, 354–396. (c) Gehrhuis, B.; Lappert, M. F. Chemistry of thermally stable bis(amino)silylenes. *J. Organomet. Chem.* **2001**, *617–618*, 209–223. (d) Mizuhata, Y.; Sasamori, T.; Tokitoh, N. Stable Heavier Carbene Analogues. *Chem. Rev.* **2009**, *109*, 3479–3511.
- (2) Drabnak, T. J.; Michl, J.; West, R. Dimethylsilylene, (CH₃)₂Si. *J. Am. Chem. Soc.* **1979**, *101*, 5427–5428.
- (3) (a) Arduengo, A. J.; Harlow, R. L.; Kline, M. A stable crystalline carbene. *J. Am. Chem. Soc.* **1991**, *113*, 361–363. (b) Denk, M.; Lennon, R.; Hayashi, R.; West, R.; Belyakov, A. V.; Verne, H. P.; Haaland, A.; Wagner, M.; Metzler, N. Synthesis and Structure of a Stable Silylene. *J. Am. Chem. Soc.* **1994**, *116*, 2691–2692.
- (4) (a) Gehrhuis, B.; Lappert, M. F.; Heinicke, J.; Boese, R.; Bläser, D. Synthesis, structures and reactions of new thermally stable silylenes. *J. Chem. Soc., Chem. Commun.* **1995**, 1931–1932. (b) Driess, M.; Yao, S.; Brym, M.; van Wüllen, C.; Lentz, D. A New Type of N-

Heterocyclic Silylene with Ambivalent Reactivity. *J. Am. Chem. Soc.* **2006**, *128*, 9628–9629. (c) Kira, M.; Ishida, S.; Iwamoto, T.; Kabuto, C. The First Isolable Dialkylsilylene. *J. Am. Chem. Soc.* **1999**, *121*, 9722–9723. (d) West, R.; Denk, M. Stable silylenes: synthesis, structure, reactions. *Pure Appl. Chem.* **1996**, *68*, 785.

(5) (a) Sirtl, E.; Reuschel, K. Über die Reduktion von Chlorsilanen mit Wasserstoff. *Z. Anorg. Allg. Chem.* **1964**, *332*, 113–123. (b) Bylander, E. G. Kinetics of Silicon Crystal Growth from SiCl₄ Decomposition. *J. Electrochem. Soc.* **1962**, *109*, 1171–1175. (c) Lorey, L.; Roewer, G. The direct synthesis of methylchlorosilanes: New aspects concerning its mechanism. *Silicon Chem.* **2002**, *1*, 299–308.

(6) Khan, S.; Roesky, H. W. Carbene-Stabilized Exceptional Silicon Halides. *Chem. - Eur. J.* **2019**, *25*, 1636–1648.

(7) So, C.-W.; Roesky, H. W.; Magull, J.; Oswald, R. B. Synthesis and Characterization of [PhC(NtBu)]₂SiCl: A Stable Monomeric Chlorosilylene. *Angew. Chem., Int. Ed.* **2006**, *45*, 3948–3950.

(8) Gau, D.; Kato, T.; Saffon-Merceron, N.; De Cózar, A.; Cossio, F. P.; Baceiredo, A. Synthesis and Structure of a Base-Stabilized C-Phosphino-Si-Amino Silyne. *Angew. Chem., Int. Ed.* **2010**, *49*, 6585–6588.

(9) Xiong, Y.; Yao, S.; Kostenko, A.; Driess, M. An isolable β-diketiminato chlorosilylene. *Dalton Trans* **2018**, *47*, 2152–2155.

(10) Nesterov, V.; Reiter, D.; Bag, P.; Frisch, P.; Holzner, R.; Porzelt, A.; Inoue, S. NHCs in Main Group Chemistry. *Chem. Rev.* **2018**, *118*, 9678–9842.

(11) (a) Filippou, A. C.; Chernov, O.; Blom, B.; Stumpf, K. W.; Schnakenburg, G. Stable N-Heterocyclic Carbene Adducts of Arylchlorosilylenes and Their Germanium Homologues. *Chem. - Eur. J.* **2010**, *16*, 2866–2872. (b) Filippou, A. C.; Chernov, O.; Stumpf, K. W.; Schnakenburg, G. Metal–Silicon Triple Bonds: The Molybdenum Silylidyne Complex [Cp(CO)₂Mo≡Si–R]. *Angew. Chem., Int. Ed.* **2010**, *49*, 3296–3300.

(12) (a) Al-Rafia, S. M. L.; McDonald, R.; Ferguson, M. J.; Rivard, E. Preparation of Stable Low-Oxidation-State Group 14 Element Amidohydrides and Hydride-Mediated Ring-Expansion Chemistry of N-Heterocyclic Carbenes. *Chem. - Eur. J.* **2012**, *18*, 13810–13820. (b) Cui, H.; Cui, C. Silylation of N-heterocyclic carbene with aminochlorosilane and -disilane: dehydrohalogenation vs. Si–Si bond cleavage. *Dalton Trans* **2011**, *40*, 11937–11940.

(13) (a) Ghadwal, R. S.; Roesky, H. W.; Merkel, S.; Henn, J.; Stalke, D. Lewis Base Stabilized Dichlorosilylene. *Angew. Chem., Int. Ed.* **2009**, *48*, 5683–5686. (b) Filippou, A. C.; Chernov, O.; Schnakenburg, G. SiBr₂(Idipp): A Stable N-Heterocyclic Carbene Adduct of Dibromosilylene. *Angew. Chem., Int. Ed.* **2009**, *48*, 5687–5690. (c) Filippou, A. C.; Lebedev, Y. N.; Chernov, O.; Straßmann, M.; Schnakenburg, G. Silicon(II) Coordination Chemistry: N-Heterocyclic Carbene Complexes of Si²⁺ and Si¹⁺. *Angew. Chem., Int. Ed.* **2013**, *52*, 6974–6978.

(14) (a) Brook, A. G.; Abdesaken, F.; Gutekunst, G.; Plavac, N. Carbon-13 and silicon-29 chemical shifts and coupling constants involving tris(trimethylsilyl)silyl systems. *Organometallics* **1982**, *1*, 994–998. (b) Trommer, M.; Miracle, G. E.; Eichler, B. E.; Powell, D. R.; West, R. Synthesis and Reactivity of Several Stable 1-Silaallenes. *Organometallics* **1997**, *16*, 5737–5747. (c) Spirk, S.; Belaj, F.; Albering, J. H.; Pietschnig, R. Formation of a Silylated 1-Silaallene via an Intermediate 1-Chloro-1-silaallene. *Organometallics* **2010**, *29*, 2981–2986.

(15) (a) Lutters, D.; Severin, C.; Schmidtman, M.; Müller, T. Activation of 7-Silanorbornadienes by N-Heterocyclic Carbenes: A Selective Way to N-Heterocyclic-Carbene-Stabilized Silylenes. *J. Am. Chem. Soc.* **2016**, *138*, 6061–6067. (b) Eisenhut, C.; Szilvási, T.; Dübek, G.; Breit, N. C.; Inoue, S. Systematic Study of N-Heterocyclic Carbene Coordinate Hydrosilylene Transition-Metal Complexes. *Inorg. Chem.* **2017**, *56*, 10061–10069. (c) Corriu, R. J. P.; Lanneau, G. F.; Chauhan, B. P. S. Photochemical reaction of 16-e metal species generated from Fe(CO)₅, Cr(CO)₆, or CrPm(CO)₃ (R = H, Me), with primary and secondary arylsilanes in the presence of internal or external electron donors: formation of functionally stabilized

- hydrosilanediy-transition metal complexes. *Organometallics* **1993**, *12*, 2001–2003.
- (16) (a) Pyykkö, P.; Atsumi, M. Molecular Double-Bond Covalent Radii for Elements Li–E112. *Chem. - Eur. J.* **2009**, *15*, 12770–12779. (b) Blom, B.; Enthaler, S.; Inoue, S.; Irran, E.; Driess, M. Electron-Rich N-Heterocyclic Silylene (NHSi)–Iron Complexes: Synthesis, Structures, and Catalytic Ability of an Isolable Hydridosilylene–Iron Complex. *J. Am. Chem. Soc.* **2013**, *135*, 6703–6713. (c) Braunstein, P.; Huch, V.; Stern, C.; Veith, M. Stannylene insertion into an amino-stabilized iron-silylene complex. Synthesis of $[(OC)_3\{(Me_2N)_2(RO)P\}Fe\{[NMe_2Si(OR)_2(SnNButSiMe_2NHBut)]\}](R = Me, Et)$. *Chem. Commun.* **1996**, 2041–2042. (d) Zybilla, C.; Wilkinson, D. L.; Leis, C.; Müller, G. Identification of $[(OC)_4FeSi(CH_3)_2\{(H_3C)_2N\}_3PO]$ as Intermediate in the Formation of Polysilanes from $(H_3C)_2SiCl_2$ and $[Na_2Fe(CO)_4]$. *Angew. Chem., Int. Ed. Engl.* **1989**, *28*, 203–205. (e) Simons, R. S.; Galat, K. J.; Bradshaw, J. D.; Youngs, W. J.; Tessier, C. A.; Aullón, G.; Alvarez, S. Reaction chemistry, NMR spectroscopy, and X-ray crystallography of $[Fe_2(\mu-SiMe_2)(CO)_4]$ and $[Fe_2(\mu-SiMeCl)_2(CO)_4]$. Electronic structure and bonding in Fe_2E_2 rings of $[Fe_2(\mu-ER)_2(CO)_4]$ binuclear complexes (E = C, Si, Ge, Sn, Pb). *J. Organomet. Chem.* **2001**, *628*, 241–254. (f) Schmedake, T. A.; Haaf, M.; Paradise, B. J.; Millevolte, A. J.; Powell, D. R.; West, R. Electronic and steric properties of stable silylene ligands in metal(0) carbonyl complexes. *J. Organomet. Chem.* **2001**, *636*, 17–25. (g) Leis, C.; Wilkinson, D. L.; Handwerker, H.; Zybilla, C.; Mueller, G. Structure and photochemistry of new base-stabilized silylene (silanediy) complexes $R_3(HMPA)Si:M(CO)_n$ of iron, chromium, and tungsten (R = tert-BuO, tert-BuS, MesO, 1-AdaO, 2-AdaO, NeopO, TritO, Me, Cl; M = Fe, n = 4; M = Cr, W, n = 5): silylene-Wittig reaction of the base-free reactive intermediate $[Me_2Si:Cr(CO)_5]$ with dimethyl carbonate. *Organometallics* **1992**, *11*, 514–529. (h) Kawamura, K.; Nakazawa, H.; Miyoshi, K. Selective Abstraction of an OR Group in the Reaction of $(C_2H_5)(CO)Fe\{SiMe_2(OR^1)\}\{PN(Me)-CH_2CH_2NMe(OR^2)\}$ with a Lewis Acid: Preferential Formation of a Silylene Complex over a Phosphenium Complex. *Organometallics* **1999**, *18*, 1517–1524. (i) Ueno, K.; Tobita, H.; Shimoi, M.; Ogino, H. Synthesis, characterization, and x-ray crystal structure of a donor-stabilized bis(silylene)iron complex. *J. Am. Chem. Soc.* **1988**, *110*, 4092–4093. (j) Zybilla, C.; Wilkinson, D. L.; Müller, G. Synthesis and Structure of $[(OC)_4Fe = Si = Fe(CO)_4 2(Me_2N)_3PO]$ —a Complex of Formally Zerovalent Silicon. *Angew. Chem., Int. Ed. Engl.* **1988**, *27*, 583–584. (k) Ghadwal, R. S.; Azhakar, R.; Pröpper, K.; Holstein, J. J.; Dittrich, B.; Roesky, H. W. N-Heterocyclic Carbene Stabilized Dichlorosilylene Transition-Metal Complexes of V(I), Co(I), and Fe(0). *Inorg. Chem.* **2011**, *50*, 8502–8508. (l) Blom, B.; Pohl, M.; Tan, G.; Gallego, D.; Driess, M. From Unsymmetrically Substituted Benzamidinato and Guanidinato Dichlorohydridosilanes to Novel Hydrido N-Heterocyclic Silylene Iron Complexes. *Organometallics* **2014**, *33*, 5272–5282.
- (17) (a) Ibrahim Al-Rafia, S. M.; Malcolm, A. C.; Liew, S. K.; Ferguson, M. J.; McDonald, R.; Rivard, E. Intercepting low oxidation state main group hydrides with a nucleophilic N-heterocyclic olefin. *Chem. Commun.* **2011**, *47*, 6987–6989. (b) Al-Rafia, S. M. L.; Malcolm, A. C.; Liew, S. K.; Ferguson, M. J.; Rivard, E. Stabilization of the Heavy Methylene Analogues, GeH_2 and SnH_2 , within the Coordination Sphere of a Transition Metal. *J. Am. Chem. Soc.* **2011**, *133*, 777–779. (c) Thimer, K. C.; Al-Rafia, S. M. L.; Ferguson, M. J.; McDonald, R.; Rivard, E. Donor/acceptor stabilization of Ge(II) dihydride. *Chem. Commun.* **2009**, 7119–7121. (d) Rivard, E. Group 14 inorganic hydrocarbon analogues. *Chem. Soc. Rev.* **2016**, *45*, 989–1003.
- (18) (a) Brown, H. C.; Singaram, B.; Mathew, C. P. Addition compounds of alkali metal hydrides. 20. Reaction of representative mono- and dialkylboranes with saline hydrides to form the corresponding alkylborohydrides. *J. Org. Chem.* **1981**, *46*, 2712–2717. (b) Cui, H.; Wu, M.; Teng, P. Reactivity of an NHC-Stabilized Silylene towards Lewis Acids and Lewis Bases. *Eur. J. Inorg. Chem.* **2016**, *2016*, 4123–4127. (c) Dübek, G.; Franz, D.; Eisenhut, C.; Altmann, P. J.; Inoue, S. Reactivity of an NHC-stabilized pyramidal hydrosilylene with electrophilic boron sources. *Dalton Trans* **2019**, *48*, 5756–5765.
- (19) (a) Jana, A.; Leusser, D.; Objartel, I.; Roesky, H. W.; Stalke, D. A stable silicon(II) monohydride. *Dalton Trans* **2011**, *40*, 5458–5463. (b) Leung, W.-P.; So, C.-W.; Chong, K.-H.; Kan, K.-W.; Chan, H.-S.; Mak, T. C. W. Reactivity of Pyridyl-1-azaallyl Germanium(II) Chloride: Synthesis of Novel Lithium Germinate $[(PhC\equiv C)_3Ge]_3GeLi(Et_2O)_3$ and Ge(II)–M(I) (M = Cu and Au) Adducts. *Organometallics* **2006**, *25*, 2851–2858. (c) Spikes, G. H.; Fettingler, J. C.; Power, P. P. Facile Activation of Dihydrogen by an Unsaturated Heavier Main Group Compound. *J. Am. Chem. Soc.* **2005**, *127*, 12232–12233. (d) Ding, Y.; Hao, H.; Roesky, H. W.; Noltemeyer, M.; Schmidt, H.-G. Synthesis and Structures of Germanium(II) Fluorides and Hydrides. *Organometallics* **2001**, *20*, 4806–4811. (e) Abraham, M. Y.; Wang, Y.; Xie, Y.; Wei, P.; Schaefer, H. F.; Schleyer, P. v. R.; Robinson, G. H. Cleavage of Carbene-Stabilized Disilicon. *J. Am. Chem. Soc.* **2011**, *133*, 8874–8876. (f) Azhakar, R.; Tavčar, G.; Roesky, H. W.; Hey, J.; Stalke, D. Facile Synthesis of a Rare Chlorosilylene–BH3 Adduct. *Eur. J. Inorg. Chem.* **2011**, *2011*, 475–477.
- (20) (a) Guddorf, B. J.; Hepp, A.; Lips, F. Efficient Synthesis of a NHC-Coordinated Trisilacyclopropylidene and Its Coordination Behavior. *Chem. - Eur. J.* **2018**, *24*, 10334–10338. (b) Maiti, A.; Mandal, D.; Omlor, I.; Dhara, D.; Klemmer, L.; Huch, V.; Zimmer, M.; Scheschke, D.; Jana, A. Equilibrium Coordination of NHCs to Si(IV) Species and Donor Exchange in Donor–Acceptor Stabilized Si(II) and Ge(II) Compounds. *Inorg. Chem.* **2019**, *58*, 4071–4075. (c) Jana, A.; Omlor, I.; Huch, V.; Rzepa, H. S.; Scheschke, D. N-Heterocyclic Carbene Coordinated Neutral and Cationic Heavier Cyclopropylidenes. *Angew. Chem., Int. Ed.* **2014**, *53*, 9953–9956.
- (21) Frisch, P.; Inoue, S. NHC-stabilized silyl-substituted silyliumylidene ions. *Dalton Trans* **2019**, *48*, 10403–10406.

9 An Air-stable Heterobimetallic Si₂M₂ Tetrahedral Cluster

Title: An Air-stable Heterobimetallic Si₂M₂ Tetrahedral Cluster
Status: Research Article, published online January 14, 2020
Journal: Angewandte Chemie International Edition, 2020, 59, 5823-5829.
Publisher: John Wiley & Sons, Inc.
DOI: 10.1002/anie.201916116 and 10.1002/ange.201916116
Authors: Gizem Dübek, Franziska Hanusch, Dominik Munz and Shigeyoshi Inoue*

Content: After the successful isolation of the first (silyl)silylene chloride, and the discovery that it contained a labile Si-Cl bond, it was hypothesized that this complex would be an ideal precursor for the formation of transition metal-silylene complexes. In this report, we demonstrated the synthesis and isolation of new NHC-stabilized transition-metal silylene (M = Mo, W) complexes which contain a metal-silicon double bond. In the next step, elimination of the coordinated NHC ligand from TM-silylene complexes was examined via addition of different Lewis acids. Treatment with strong Lewis acids such as B(C₆F₅)₃ or AlCl₃ led to the reversible coordination of the Lewis acid to one of the carbonyl ligands on metal center. The use of a milder Lewis acid like BPh₃, however, successfully removes the NHC from the TM-silylene complexes. Surprisingly, this affords the first examples of heterobimetallic tetrahedral Si₂M₂ clusters which were found to be air- and moisture stable and show no reaction with methanol even after prolonged heating at 70 °C. Computational investigations revealed the formation of tetrahedral cluster is based on the dimerization of the intermediate metal-silylyne (M≡Si) complex. This indicates that the steric bulk of the silyl-substituents on silylyne intermediate prevents the formation of planar four-membered ring and allows only tetrahedral structure due to perpendicular arrangement of the two silylyne groups.

* G. Dübek planned and executed all experiments including analysis and wrote the manuscript. F. Hanusch conducted all SC XRD measurements and managed the processing of the respective data. D. Munz designed and performed the theoretical analyses and contributed to manuscript. All work was performed under the supervision of S. Inoue.

Cluster Compounds

International Edition: DOI: 10.1002/anie.201916116
German Edition: DOI: 10.1002/ange.201916116An Air-Stable Heterobimetallic Si₂M₂ Tetrahedral Cluster

Gizem Dübek, Franziska Hanusch, Dominik Munz, and Shigeyoshi Inoue*

Dedicated to Professor Ytzhak Apeloig on the occasion of his 75th birthday

Abstract: Air- and moisture-stable heterobimetallic tetrahedral clusters [Cp(CO)₂MSiR]₂ (M = Mo or W; R = Si*t*Bu₃) were isolated from the reaction of *N*-heterocyclic carbene (NHC) stabilized silyl(silylidene) metal complexes Cp(CO)₂M=Si(Si*t*Bu₃)NHC with a mild Lewis acid (BPh₃). Alternatively, treatment of the NHC-stabilized silylidene complex Cp(CO)₂W=Si(Si*t*Bu₃)NHC with stronger Lewis acids such as AlCl₃ or B(C₆F₅)₃ resulted in the reversible coordination of the Lewis acid to one of the carbonyl ligands. Computational investigations revealed that the dimerization of the intermediate metal silylidyne (M=Si) complex to a tetrahedral cluster instead of a planar four-membered ring is due to steric bulk.

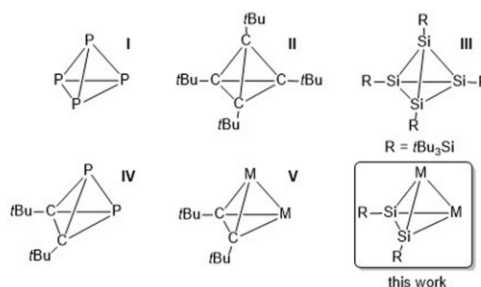


Figure 1. Selected examples of known neutral tetrahedranes.

Introduction

Tetrahedral clusters that consist of main-group elements are attractive synthetic targets because of their high ring strain and reactivity.^[1] Even white phosphorus (P₄), which has been known for centuries, has recently been the subject of intense research (I; Figure 1).^[2] The heavier homologue, As₄, is challenging to handle because of its thermal and photochemical instability. Nevertheless, Cummins and co-workers even managed to isolate As₃P, the first example of a heteroatomic tetrahedrane.^[3] The archetypical organic tetrahedrane (tBuC₄) (II) was isolated by Maier and co-workers in 1978,^[4] whereas Wiberg et al. reported the heavier analogue, tetrasilatetrahedrane (tBu₃SiSi)₄ (III), in 1993.^[5] One decade later, Sekiguchi and co-workers isolated a further tetrasilatetrahedrane (R₄Si₄, R = SiMe((CH(SiMe₂)₂)) while trying to isolate a disilyne with a Si=Si triple bond.^[6] Very recently, another neutral tetrahedron that contains two different heteroatoms, (tBuCP)₂ (IV), was reported to form upon dimerization of

phosphaalkynes (RC≡P).^[7] In addition to neutral tetrahedral complexes, anionic tetrahedral [E₄]⁴⁻ (E = Si, Ge, Sn) species, so-called Zintl-type polyanions, are known.^[8] Whilst binary combinations in Zintl tetrahedral clusters [E_nM_{4-n}] have been reported,^[9] there are no examples of neutral heterobimetallic tetrahedral clusters with heavier main-group elements and transition metals.

Numerous examples are known of M₂C₂-type bimetallic complexes (V) with bridging acetylene or acetylene derivatives that exhibit tetrahedral structures.^[10] Such complexes find application in the Pauson–Khand synthesis of cyclopentanone derivatives and are catalysts in hydroboration reactions,^[11] yet heavier congeners have remained unexplored to the best of our knowledge. Among heavier analogues of Group 14 element compounds M₂E₂ (E = Si, Ge, Sn), particular interest has been devoted to silicon as bimetallic clusters with bridging silicon atoms are indeed alleged key intermediates in various transition-metal-catalyzed transformations.^[12] Since the 1900s, various M₂Si₂ binuclear transition-metal complexes have been reported and their catalytic activities have been exploited in the dehydrocoupling of hydrosilanes and the metathesis of olefins.^[13] Thus far, however, all of these complexes feature a planar, diamond-shaped, or butterfly-type M₂Si₂ core, whereas tetrahedral structures remain elusive.^[13a,14] Generally, monoatomic tetrahedral derivatives R₄E₄ can be generated photochemically from the corresponding planar linear compounds by elimination or photoisomerization as reported for II.^[1,15] Accordingly, tetrahedranes can form by dimerization of disilynes or nickel-mediated dimerization of phosphaalkynes.^[7,16]

Herein, we report the first isolable heterobimetallic M₂Si₂ cluster with a tetrahedral structure. Inspired by the previous reports from the groups of Wiberg and Sekiguchi, we based our synthetic strategy on the elimination of an *N*-heterocyclic carbene (NHC) from a silylidene complex (Si=M) to generate

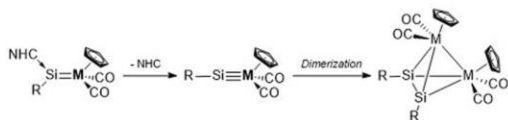
* G. Dübek, F. Hanusch, Prof. S. Inoue
Department of Chemistry, Catalysis Research Center and Institute of Silicon Chemistry, Technical University Munich
Lichtenbergstraße 4, 85748 Garching bei München (Germany)
E-mail: s.inoue@tum.de

Dr. D. Munz
Friedrich-Alexander-Universität Erlangen-Nürnberg (FAU)
Department of Chemistry and Pharmacy
General and Inorganic Chemistry
Egerlandstraße 1, 91058 Erlangen (Germany)

Supporting information and the ORCID identification number(s) for the author(s) of this article can be found under:
<https://doi.org/10.1002/anie.201916116>.

© 2020 The Authors. Published by Wiley-VCH Verlag GmbH & Co. KGaA. This is an open access article under the terms of the Creative Commons Attribution License, which permits use, distribution and reproduction in any medium, provided the original work is properly cited.

a silylydene complex (Si=M), which was hypothesized to dimerize subsequently to a tetrahedral M₂Si₂ cage cluster (Scheme 1).



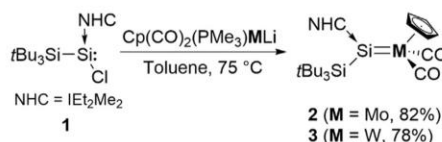
Scheme 1. Synthetic strategy to isolate a neutral M₂Si₂ tetrahedrane upon dimerization of a transient silylydene complex (Si=M).

The chemistry of transition-metal silylydene complexes has a short, yet spectacular history. The arguably first silylydene complex [Cp*(dmpe)(H)MoSiMes] (dmpe = PMe₂CH₂CH₂PMe₂) was reported by Tilley and Mork in 2003.^[17] Shortly after, when the role of the NHC in stabilizing low-valent silicon(II) species had been recognized, a genuine Mo=Si triple-bonded complex was isolated by the group of Filippou using this elegant synthetic approach.^[18] Following this achievement, a handful of transition-metal silylydene complexes and their reactivities were reported by further research groups.^[17–19] Characteristically, all room-temperature isolable transition-metal silylydene complexes bear very bulky ligands either on the silicon center (e.g., Ar^{Trip}, Eind) or on the metal center (e.g., Cp*, Tbb). We concluded that a M=Si complex with comparably reduced bulk on both the silicon atom and the transition-metal center should be an excellent choice for the targeted tetrahedral cluster.

Results and Discussion

Very recently, we reported the synthesis of the first silyl-substituted chlorosilylene (**1**) and studied the reactivity associated with its lone pair and chloride substituent.^[20] Compound **1** is prone to salt metathesis reactions because of the presence of the chloride atom. In fact, heating an orange toluene solution of chlorosilylene **1** with Cp(CO)₂(PMe₃)MLi (M = Mo, W) at 75 °C smoothly gave the IEt₂Me₂ (1,3-diethyl-4,5-dimethyl-imidazolin-2-ylidene) stabilized transition-metal silylydene complexes **2** and **3** as air- and moisture-sensitive, dark-green solids (**2**, M = Mo, 82%; **3**, M = W, 78%; Scheme 2).

The ²⁹Si NMR spectra of **2** and **3** show characteristic resonances, which are shifted strongly downfield to 278.8 ppm



Scheme 2. Synthesis of NHC-stabilized molybdenum (**2**) and tungsten (**3**) silylydene complexes.

and 229.7 ppm (¹J_{Si-W} = 261 Hz), respectively, in reference to those of **1** (δ = 18.3 ppm). Similar chemical shifts were observed for the previously reported transition-metal silylydene complexes.^[18,19m,21] The silicon-bonded NHC carbene atoms resonate at 168.3 ppm (**2**) and 172.6 ppm (**3**) in the ¹³C NMR spectroscopic analysis, which is similar to the chemical shift found for **1** (δ = 169.7 ppm).

The IR spectra of **2** and **3** each show two ν(CO) absorption bands at 1782 and 1864 cm⁻¹ (**2**), and at 1770 and 1849 cm⁻¹ (**3**). The positions of these bands agree well with previously reported metal arylsilylydene complexes and our predictions by density functional theory (DFT) calculations (**3**: 1837 and 1892 cm⁻¹).^[18,19l] Single crystals of **2** and **3** were obtained from a toluene/pentane (1:3) mixture at ambient temperature, and the structure in the solid state was determined by X-ray diffraction analysis (Figure 2). Complex **2** features a Mo=Si double bond (2.3499(10) Å), which is shorter than that found for the donor-free molybdenum silylydene complex Cp*(CO)₂(SiMe₂)Mo=Si(Mes)₂ (2.3872(7) Å) and lies in the range of previously reported molybdenum silylydene complexes (d(Mo–Si) = 2.288(2)–2.3872(7) Å).^[22] Similarly, **3** exhibits a W=Si (2.346(2) Å) bond that is considerably shorter than in [Cp*W(CO)₂(=SiMe₂)(SiMe₃)] (2.3850(12) Å) and in the neutral alkyl(sily-

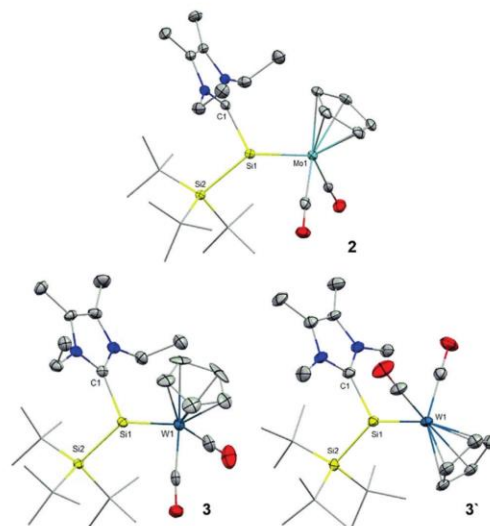
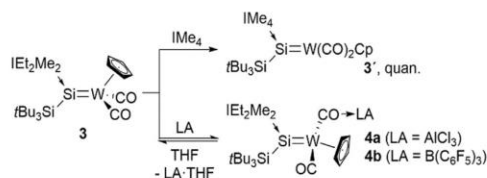


Figure 2. Ellipsoid plots (set at 50% probability) of the molecular structures of compounds **2** (one out of two independent molecules in the asymmetric unit is shown), **3** (one out of three independent molecules in the asymmetric unit is shown) and **3'**.^[19] Hydrogen atoms are omitted for clarity, and *tert*-butyl groups are depicted in wireframe for simplicity. Selected bond lengths [Å] and angles [°]: **2**: Si1–Mo1 2.3499(10), Si1–Si2 2.4418(11), Si1–C1 1.949(2), C1–Si1–Si2 102.64(6), Mo1–Si1–C1 116.33(6), Mo–Si1–Si2 141.03(3). **3**: Si1–W1 2.346(2), Si1–Si2 2.428(3), Si1–C1 1.935(7); C1–Si1–Si2 105.1(2), W1–Si1–C1 113.5(2), W1–Si1–Si2 141.38(10). **3'**: Si1–W1 2.3534(12), Si1–Si2 2.4402(16), Si1–C1 1.941(5); C1–Si1–Si2 104.15(14), W1–Si1–C1 115.67(14), W–Si1–Si2 140.15(6).

lidene)tungsten complex $[(\eta^5\text{-C}_5\text{Me}_4\text{Et})(\text{CO})_2(\text{H})\text{W}=\text{Si}[\text{C}(\text{SiMe}_3)_3]]$ (2.3703(11) Å), but slightly longer than that of the anionic complex $[\text{Cp}^*(\text{CO})_2\text{W}=\text{SiH}[\text{C}(\text{SiMe}_3)_3]][\text{H}^{\text{Me}}\text{I}^{\text{Pr}}]$ (2.3367(17) Å).^[21,23] UV/Vis analysis (Figure S6) revealed a characteristic absorption band at $\lambda^{\text{max}}=418$ nm for the Mo=Si complex **2**. For the W=Si complex **3**, a band at $\lambda^{\text{max}}=418$ nm and a very broad and weak band ranging from approximately $\lambda=500$ to 700 nm were found (Figure S12). Time-dependent DFT (TD-DFT) calculations reproduced these values very well (Figure S63). In addition, the Löwdin population analysis indicates that **3** has a d^1 electron configuration with considerable negative partial charge at the tungsten atom, which is consistent with an oxidation state of +II. Both complexes **2** and **3** feature trigonal-planar-coordinated silicon centers, with the sum of bond angles at the silicon center being 360°.

We investigated the replacement of the NHC moiety and treated the bulky IEt_2Me_2 compound with more nucleophilic IME_4 .^[24] Indeed, treatment of **3** with excess IME_4 resulted in quick conversion (60% in 30 min) and eventually, after 12 h, quantitative exchange of IEt_2Me_2 by IME_4 (**3'**; Scheme 3). As



Scheme 3. Synthesis of **3'** and **4a,b** from NHC-stabilized silyl(tungsten) complex **3**.

expected, only minor shifts in reference to the starting material were observed in all (^1H , ^{13}C , ^{29}Si) NMR experiments. Single crystals of **3'** were obtained at ambient temperature from a C_6D_6 /pentane (1:1) mixture, and the molecular structure was also confirmed by X-ray diffraction analysis (Figure 2). The W–Si bond is slightly elongated for **3'** (2.3534(12) Å) in comparison to **3** (2.346(2) Å); nevertheless, the structural parameters are very similar.

The ligand exchange ability of **3** encouraged us to abstract the NHC by treatment with Lewis acids. Indeed, treatment of **3** with the strong Lewis acid $\text{B}(\text{C}_6\text{F}_5)_3$ or more oxophilic AlCl_3 resulted in an immediate color change from dark green to dark red in toluene (Scheme 3). Significant downfield shifts of the ^{29}Si NMR resonances for **4a** ($\delta=322.0$ ppm) and **4b** ($\delta=323.2$ ppm) compared to that of **3** ($\delta=229.7$ ppm) were observed, whereas the ^{13}C NMR spectra of **4a** and **4b** displayed only a very small change in shift (166.9 ppm for **4a** and 167.3 ppm for **4b**) from **3** (^{13}C $\delta=172.6$ ppm). This suggests that the NHC remains coordinated to a silylidene unit. Intriguingly, the addition of coordinating THF to the red solutions of **4a** or **4b** resulted in the regeneration of the dark-green color, and the ^1H NMR spectroscopic analysis confirmed the regeneration of the initial starting material **3**. This reaction corroborated the formation of a peculiar Lewis acid–carbonyl adduct, and was likewise confirmed by X-ray crystal

structure analysis of **4a** (Figure 3). A comparable terminal carbonyl ligand activation was observed by Cummins and co-workers during preparation of a terminal molybdenum carbide upon acylation of a Mo^{II} carbonyl complex with pivaloyl chloride.^[25]

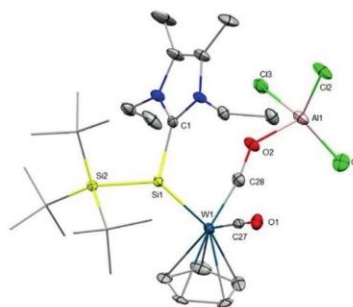
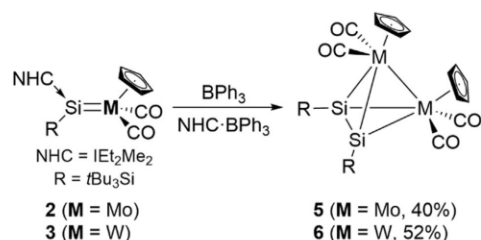


Figure 3. Ellipsoid plot (set at 30% probability) of the molecular structure of compound **4a**. Hydrogen atoms are omitted for clarity, and *tert*-butyl groups are depicted in wireframe for simplicity.^[39] Selected bond lengths [Å] and angles [°]: Si1–W1 2.3630(18), Si1–Si2 2.437(2), Si1–C1 1.940(10), Al1–O2 1.777(8), W1–C27 1.975(7), W1–C28 1.840(7); C1–Si1–Si2 106.4(6), W1–Si1–C1 114.6(6), W–Si1–Si2 138.89(9).

The W–Si bond in **4a** (2.3630(18) Å) is elongated in reference to **3** (2.346(2) Å) because of the reduced back-donation from tungsten to silicon and in line with the downfield-shifted resonance in the ^{29}Si spectrum ($\delta=322.0$ ppm). The W–C bond length for the AlCl_3 -coordinated CO ligand (1.840(7) Å) is significantly shortened in comparison with that of the terminal carbonyl ligand (1.975(7) Å) and even in the range of tungsten carbonyl complexes (1.82–1.87 Å).^[26] The Al–O bond length in **4a** (1.777(8) Å) is comparable with previously reported AlCl_3 coordinated to the oxygen atom of a carbonyl ligand without bond rupture (1.812(2) Å).^[27] Compound **4a** has a similar absorption band at 400 nm in the UV/Vis spectrum in toluene. Unfortunately, **4b** could only be isolated as a sticky solid and not in crystalline form. The IR spectrum of **4a** in the solid state shows two $\nu(\text{CO})$ bands that appear as broad bands at 1813 cm^{-1} for AlCl_3 -coordinated CO and at 1901 cm^{-1} for the terminal CO. Two peculiar carbonyl stretching frequencies are observed because of enhanced π -back-donation from tungsten to the carbonyl ligand and simultaneous weakening of the C–O bond (C27–O1 1.158(8) Å, C28–O2 1.255(9) Å) that is coordinated to AlCl_3 . Similarly, **4b** also shows two $\nu(\text{CO})$ bands at 1906 cm^{-1} and 1873 cm^{-1} . The latter can be assigned to $\text{CO}\cdots\text{B}(\text{C}_6\text{F}_5)_3$, which appears at a higher wavenumber than in $[\text{Cp}^*(\text{CO})\text{W}(\text{C}_6\text{F}_5)_3\text{B}\cdots\text{OC}]\text{W}=\text{Si}(\text{H})\text{Tsi}][\text{H}^{\text{Me}}\text{I}^{\text{Pr}}]$ ($\nu(\text{CO}\cdots\text{BCF})=1535\text{ cm}^{-1}$).^[19a] This observation indicates weaker coordination of the borane to the carbonyl group in comparison to that of the anionic silylidene complex.

In order to abstract the NHC from the silylidene complexes, we hence used a milder Lewis acid, namely triphenylboron (BPh_3 , Scheme 4). Indeed, heating toluene



Scheme 4. Formation of heterobimetallic tetrahedral compounds **5** and **6** by abstraction of the NHC from TM silylidene complexes **2** and **3** by BPh_3 .

solutions of **2** and **3** with one equivalent of BPh_3 for 30 min to 90 °C afforded the desired tetrahedral clusters **5** and **6** in 40% and 52% yield, respectively. These heterobimetallic compounds are well soluble in aromatic as well as aliphatic organic solvents. Surprisingly, the heterobimetallic tetrahedral Si_2M_2 clusters **5** and **6** are perfectly stable in moist air, as has been also reported for tetrasilatetrahedrane ($t\text{Bu}_3\text{SiSi}$)₄ (**III**). It is interesting to note that these complexes did not even react with methanol when heated to 70 °C for 24 h.

The single-crystal structure of **6** revealed the formation of a tetrahedral, bimetallic transition-metal silicon cluster (Figure 4). The W–Si (2.5507(15)–2.6913(15) Å) bonds in **6** are significantly longer than those in **3** (2.346(2) Å) and reported W=Si double bonds (2.34–2.47 Å), and fall in the range of W–Si single bonds (2.47–2.71 Å).^[21,23,28,29] The structural parameters of complex **6** are akin to the planar complexes W–Si–W–Si (W–W 3.183(1) Å, W–Si 2.586(5)–2.703(4) Å) and reported W–Si–W–H (W–Si 2.489(2)–2.487(2) Å).^[14c,30] The Si–Si bond (2.2221(19) Å) is significantly shorter than those in previously reported MSiSiM butterfly-shaped clusters ($d(\text{Si} \cdots \text{Si}) = 2.85$ –2.98 Å) and also those of tetrasilatetrahedranes, where the

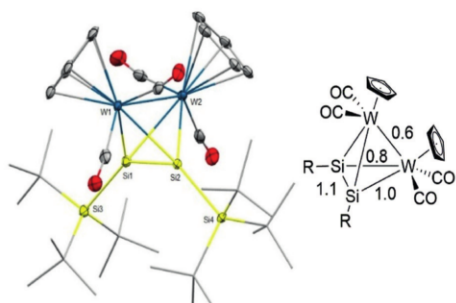


Figure 4. Ellipsoid plot (set at 30% probability) of the molecular structure of compound **6** (left; one of three independent molecules in the asymmetric unit is shown) and bond orders as predicted by the Löwdin population analysis (right). Hydrogen atoms are omitted for clarity, and *tert*-butyl groups are depicted in wireframe for simplicity. Selected bond lengths [Å] and angles [°]: Si1–W1 2.5507(15), Si1–W2 2.6913(15), Si2–W1 2.6790(14), Si2–W2 2.5593(14), W1–W2 3.0732(8), Si1–Si2 2.2221(19); W1–Si1–W2 71.73(4), W1–Si1–Si2 67.89(5), W2–Si1–Si2 61.92(5).

Si–Si bond lengths range from 2.315(2) to 2.3830(19) Å.^[5,6,14a,31] The short Si–Si separation is attributed to the partial multiple bond character (Figure 4, right) and reduced σ -donation from the silyl substituents due to the elongation of the exocyclic Si–Si bonds (Si1–Si3 2.437(2) Å, Si2–Si4 2.430(2) Å). The formation of bimetallic clusters for **5** and **6** was also confirmed by mass-spectrometric analysis (Figures S36–S46), which suggested that **5** is isostructural with **6**. The tetrahedral M_2Si_2 clusters melt below 70 °C (m.p. 64–65 °C for **5**; 67–69 °C for **6**), yet we did not observe any changes in the ¹H NMR spectra upon heating xylene solutions to 120 °C. This observation corroborates the high thermal stability and the absence of an equilibrium between the monomer $(\text{Cp}(\text{CO})_2\text{M}=\text{SiSi}t\text{Bu}_3)$ and the dimeric forms of **5** and **6**, and is consistent with diffusion NMR experiments (DOSY; Figures S28 and S40). The ²⁹Si NMR signals of skeletal silicon atoms shifted strongly to higher fields ($\delta = 3.65$ ppm for **5**, GIAO = 5 ppm; $\delta = -63.04$ ppm ($J_{\text{Si-W}} = 52$ Hz) for **6**; GIAO = -48 ppm), which corroborates strong silyl character due to a change in hybridization from sp^2 to sp^3 .^[19,32] In addition, such an upfield shift is also typically observed for ring C atoms of tetrahedranes.^[1,4,15a,33] The small $J_{\text{Si-W}}$ coupling constant of 52 Hz indicates a high degree of p-character at the Si atom and a relatively small contribution from the silicon's s-orbital. A significant low-field shift was observed for the supersilyl ligand ($\delta = 48.32$ ppm for **5**; 43.99 ppm for **6**). Similar shifts for *t*Bu₃Si were also reported for Wiberg's tetrasilatetrahedrane ($t\text{Bu}_3\text{SiSi}$)₄ (²⁹Si, $\delta = 53.07$ ppm; **III**, Figure 1).^[5] The IR spectra of **5** and **6** showed two $\nu(\text{CO})$ bands at higher wavenumbers than for the NHC–TM–silylidenes **2–4a,b** (1844 and 1918 cm^{-1} for **5**; 1860 and 1914 cm^{-1} for **6**; DFT: 1904 and 1916 cm^{-1}). This hypsochromic shift is due to reduced π -back-donation from the transition metal to the CO ligand. The UV/Vis spectra of **5** and **6** in toluene showed absorption bands at 543 nm and 530 nm, respectively. In excellent agreement, TD-DFT calculations for **6** predict the HOMO–LUMO transition to lie at 501 nm.

We performed detailed DFT calculations at the PBE0-D3BJ(SMD)/ZORA-def2-TZVPP//PBE0-D3BJ/def2-SVP level of theory in order to understand the electronic structures of **6** and **3** (Figures S57–S62).^[34,35] Indeed, Löwdin population analysis of the DFT-optimized structure of **6** also indicated a Si–Si bond order of 1.1, indicative of only very small multiple bond character (Figure 4, right), which is in line with the short Si–Si bond length in **6**. Interestingly, the calculations suggest a higher Si–Si multiple bond character of 1.3 for the molybdenum complex **5** (Figure S61), which is in line with the relative ²⁹Si NMR shifts of **5** and **6** (see above). Plotting the HOMO (highest occupied molecular orbital) and LUMO (lowest unoccupied molecular orbital) corroborates delocalization of both orbitals over the whole cluster (Figure S58). The intrinsic bond orbitals (IBOs)^[36] show two different, yet quite covalent, σ -interactions between Si1 and W1 or W2, respectively (Figure 5, top). The Si1–W1 σ -bond is polarized towards Si, whereas the longer Si1–W2 bond features additionally a π -back-bonding interaction with the CO π^* orbitals. Besides, we found a Si1–Si2 σ -bond as well as considerable bonding interactions between the W1 and W2 atoms (Fig-

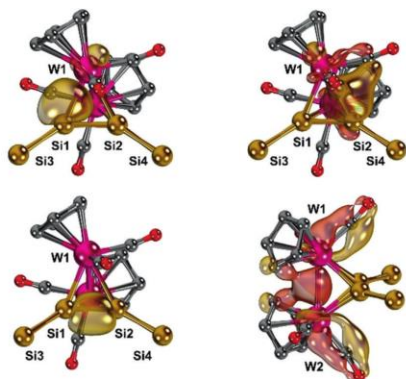


Figure 5. Intrinsic bond orbitals (IBOs) associated with the Si1–W1 (top, left), Si1–W2 (top, right), Si1–Si2 (bottom, left) and W1–W2 (bottom, right) bonds (*t*Bu groups and hydrogen atoms are omitted for clarity, but were included in the calculations).

ure 5, bottom). Overall, the calculations confirmed a tetrahedral structure with strong and covalent interactions between all silicon and tungsten atoms.

Furthermore, the reaction mechanism for the formation of **6** was modeled in order to understand the peculiar Si–Si dimerization (Figure 6).^[37] The restricted DFT calculations

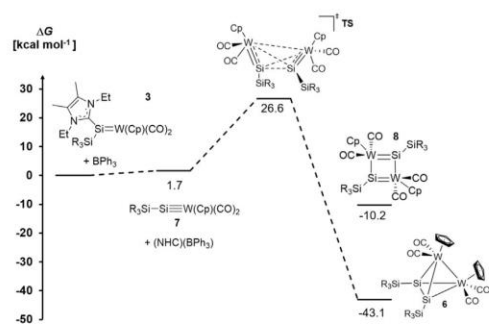


Figure 6. Proposed reaction profile for the formation of W₂Si₂ tetrahedral cluster **6**.

suggest that the formation of the intermediate silyldyne complex **7** proceeds essentially in isoergic fashion ($\Delta G = +1.7$ kcal mol⁻¹). The subsequent dimerization ($\Delta G = -43.1$ kcal mol⁻¹) features a barrier of $\Delta G^\ddagger = +26.6$ kcal mol⁻¹, which agrees well with a reaction occurring at elevated temperatures. The transition state (Figure 6) shows a very large separation of the two tungsten atoms (5.05 Å) and hence is indicative of only weak interactions between these two atoms. Nevertheless, a very small orbital overlap in HOMO-3 substantiates a very asynchronous, yet still concerted formation of the Si–Si and W–W bonds.^[38]

Most importantly, the transition state reveals that the steric bulk associated with the supersilyl groups and the Cp substituents allows only for a perpendicular arrangement of the two silyldyne groups. This orientation consequently determines the formation of the tetrahedral cluster instead of four-membered rings as would be expected by simplifying polarity considerations. Indeed, attempts to geometry-optimize four-membered rings with either Si–Si/W–W or alternating Si–W bonds led to isomeric tetrahedra ($\Delta G = -34.0$ kcal mol⁻¹; Figure S70), three-membered rings ($\Delta G = -15.8$ kcal mol⁻¹; Figure S70), or quadrangles of much higher energy (Si–W–Si–W quadrangle **8**: $\Delta G = -10.2$ kcal mol⁻¹). Attempts to model dimeric compounds with decoordination of only one NHC also did not meet with success. We conclude that the steric bulk in **6** prevents the formation of quadrangles or triangles and allows only for the formation of a tetrahedral cluster subsequent to abstraction of the NHC ligand.

Conclusion

We have reported the isolation of the heteroatomic, bimetallic M₂Si₂ tetrahedral clusters **5** and **6**. These compounds form after NHC abstraction from the respective NHC-stabilized silyldyne complexes **2** and **3** by dimerization of transient transition-metal silyldyne complexes. These tetrahedral clusters are air- and moisture-stable unlike many other main-group organometallic compounds. Furthermore, we have shown that the NHC (IEt₃Me₂) in complex **3** can be exchanged for a more nucleophilic NHC (IME₄). Contrarily, the addition of stronger Lewis acids such as AlCl₃ or B(C₆F₅)₃ resulted in reversible activation of the carbonyl ligands (**4a, b**). Calculations confirm the covalent bonding in the cluster and indicate that steric bulk is crucial for the formation of the tetrahedron-type structure.

Acknowledgements

We are grateful to WACKER Chemie AG and the European Research Council (SILION 637394) for financial support. We thank M. Muhr (Prof. R. A. Fischer, TUM) for the LIFDI-MS measurements, P. Frisch for measurement and refinement of the structure of **2**, and P. Nixdorf (TU Berlin) for measurement of the structure of **3**. D.M. thanks the RRZE Erlangen for computational resources, K. Meyer for continuous support, and the Fonds der chemischen Industrie for a Liebig fellowship.

Conflict of interest

The authors declare no conflict of interest.

Keywords: cluster compounds · silicon · silyldynes · tetrahedranes · silyldynes · tetrahedranes

How to cite: *Angew. Chem. Int. Ed.* **2020**, *59*, 5823–5829
Angew. Chem. **2020**, *132*, 5872–5878

- [1] G. Maier, *Angew. Chem. Int. Ed. Engl.* **1988**, *27*, 309–332; *Angew. Chem.* **1988**, *100*, 317–341.
- [2] a) A. Wiesner, S. Steinhauer, H. Beckers, C. Müller, S. Riedel, *Chem. Sci.* **2018**, *9*, 7169–7173; b) U. Lennert, P. B. Arockiam, V. Streitferdt, D. J. Scott, C. Rödl, R. M. Gschwind, R. Wolf, *Nat. Catal.* **2019**, *2*, 1101–1106.
- [3] B. M. Cossairt, M.-C. Diawara, C. C. Cummins, *Science* **2009**, *323*, 602–602.
- [4] G. Maier, S. Pfriem, U. Schäfer, R. Matusch, *Angew. Chem. Int. Ed. Engl.* **1978**, *17*, 520–521; *Angew. Chem.* **1978**, *90*, 552–553.
- [5] N. Wiberg, C. M. M. Finger, K. Polborn, *Angew. Chem. Int. Ed. Engl.* **1993**, *32*, 1054–1056; *Angew. Chem.* **1993**, *105*, 1140–1142.
- [6] M. Ichinohe, M. Toyoshima, R. Kinjo, A. Sekiguchi, *J. Am. Chem. Soc.* **2003**, *125*, 13328–13329.
- [7] G. Hierlmeier, P. Coburger, M. Bodensteiner, R. Wolf, *Angew. Chem. Int. Ed.* **2019**, *58*, 16918–16922; *Angew. Chem.* **2019**, *131*, 17074–17078.
- [8] a) M. Waibel, F. Kraus, S. Scharfe, B. Wahl, T. F. Fässler, *Angew. Chem. Int. Ed.* **2010**, *49*, 6611–6615; *Angew. Chem.* **2010**, *122*, 6761–6765; b) T. Henneberger, W. Klein, J. V. Dums, T. F. Fässler, *Chem. Commun.* **2018**, *54*, 12381–12384; c) C. Liu, Z.-M. Sun, *Coord. Chem. Rev.* **2019**, *382*, 32–56.
- [9] a) H. G. Von Schnering, M. Baitinger, U. Bolle, W. Carrillo-Cabrera, J. Curda, Y. Grin, F. Heinemann, J. Llanos, K. Peters, A. Schmedding, M. Somer, *Z. Anorg. Allg. Chem.* **1997**, *623*, 1037–1039; b) J. Witte, H. G. Schnering, W. Klemm, *Z. Anorg. Allg. Chem.* **1964**, *327*, 260–273; c) I. F. Hewaidy, E. Busmann, W. Klemm, *Z. Anorg. Allg. Chem.* **1964**, *328*, 283–293.
- [10] a) F. A. Cotton, J. D. Jamerson, B. R. Stults, *J. Am. Chem. Soc.* **1976**, *98*, 1774–1779; b) J. F. Halet, J. Y. Saillard, *J. Organomet. Chem.* **1987**, *327*, 365–377; c) A. S. Foust, C. F. Campana, J. D. Sinclair, L. F. Dahl, *Inorg. Chem.* **1979**, *18*, 3047–3054; d) S. Kahlal, J.-F. Halet, J.-Y. Saillard, K. H. Whitmire, *J. Organomet. Chem.* **1994**, *478*, 1–8; e) P. Bougeard, S. Peng, M. Mlekuz, M. J. McGlinchey, *J. Organomet. Chem.* **1985**, *296*, 383–391.
- [11] a) J. A. Casalanuovo, N. E. Schore, *Modern Acetylene Chemistry*, VCH, Weinheim, **1995**, pp. 139–172; b) R. Wilczynski, L. G. Sneddon, *J. Am. Chem. Soc.* **1980**, *102*, 2857–2858.
- [12] M. Sugimoto, Y. Ito, *Chem. Rev.* **2000**, *100*, 3221–3256.
- [13] a) E. A. Zarate, C. A. Tessier-Youngs, W. J. Youngs, *J. Am. Chem. Soc.* **1988**, *110*, 4068–4070; b) N. B. Bespalova, M. A. Bovina, A. V. Popov, J. C. Mol, *J. Mol. Catal. A* **2000**, *160*, 157–164.
- [14] a) S. Shimada, M. L. N. Rao, T. Hayashi, M. Tanaka, *Angew. Chem. Int. Ed.* **2001**, *40*, 213–216; *Angew. Chem.* **2001**, *113*, 219–222; b) M. H. Mobarok, R. McDonald, M. J. Ferguson, M. Cowie, *Inorg. Chem.* **2012**, *51*, 9249–9258; c) M. J. Bennett, K. A. Simpson, *J. Am. Chem. Soc.* **1971**, *93*, 7156–7160.
- [15] a) G. Maier, J. Neudert, O. Wolf, D. Pappusch, A. Sekiguchi, M. Tanaka, T. Matsuo, *J. Am. Chem. Soc.* **2002**, *124*, 13819–13826; b) M. Nakamoto, Y. Inagaki, T. Ochiai, M. Tanaka, A. Sekiguchi, *Heteroat. Chem.* **2011**, *22*, 412–416.
- [16] A. Sekiguchi, M. Ichinohe, R. Kinjo, *Bull. Chem. Soc. Jpn.* **2006**, *79*, 825–832.
- [17] B. V. Mork, T. D. Tilley, *Angew. Chem. Int. Ed.* **2003**, *42*, 357–360; *Angew. Chem.* **2003**, *115*, 371–374.
- [18] A. C. Filippou, O. Chernov, K. W. Stumpf, G. Schnakenburg, *Angew. Chem. Int. Ed.* **2010**, *49*, 3296–3300; *Angew. Chem.* **2010**, *122*, 3368–3372.
- [19] a) T. Fukuda, T. Yoshimoto, H. Hashimoto, H. Tobita, *Organometallics* **2016**, *35*, 921–924; b) T. Fukuda, H. Hashimoto, H. Tobita, *J. Am. Chem. Soc.* **2015**, *137*, 10906–10909; c) P. F. Engel, M. Pfeffer, *Chem. Rev.* **1995**, *95*, 2281–2309; d) H. Hashimoto, H. Tobita, *Coord. Chem. Rev.* **2018**, *355*, 362–379; e) A. C. Filippou, D. Hoffmann, G. Schnakenburg, *Chem. Sci.* **2017**, *8*, 6290–6299; f) P. Ghana, M. I. Arz, G. Schnakenburg, M. Straßmann, A. C. Filippou, *Organometallics* **2018**, *37*, 772–780; g) Z. Xu, M. B. Hall, *Inorg. Chim. Acta* **2014**, *422*, 40–46; h) P. G. Hayes, Z. Xu, C. Beddie, J. M. Keith, M. B. Hall, T. D. Tilley, *J. Am. Chem. Soc.* **2013**, *135*, 11780–11783; i) S. D. Grumbine, R. K. Chadha, T. D. Tilley, *J. Am. Chem. Soc.* **1992**, *114*, 1518–1520; j) A. C. Filippou, O. Chernov, G. Schnakenburg, *Angew. Chem. Int. Ed.* **2011**, *50*, 1122–1126; *Angew. Chem.* **2011**, *123*, 1154–1158; k) A. C. Filippou, O. Chernov, B. Blom, K. W. Stumpf, G. Schnakenburg, *Chem. Eur. J.* **2010**, *16*, 2866–2872; l) A. C. Filippou, O. Chernov, G. Schnakenburg, *Chem. Eur. J.* **2011**, *17*, 13574–13583; m) T. Yoshimoto, H. Hashimoto, N. Hayakawa, T. Matsuo, H. Tobita, *Organometallics* **2016**, *35*, 3444–3447.
- [20] G. Dübek, F. Hanusch, S. Inoue, *Inorg. Chem.* **2019**, *58*, 15700–15704.
- [21] a) K. Ueno, S. Asami, N. Watanabe, H. Ogino, *Organometallics* **2002**, *21*, 1326–1328; b) T. Watanabe, H. Hashimoto, H. Tobita, *Angew. Chem. Int. Ed.* **2004**, *43*, 218–221; *Angew. Chem.* **2004**, *116*, 220–223.
- [22] M. Hirotsu, T. Nunokawa, K. Ueno, *Organometallics* **2006**, *25*, 1554–1556.
- [23] T. Fukuda, H. Hashimoto, S. Sakaki, H. Tobita, *Angew. Chem. Int. Ed.* **2016**, *55*, 188–192; *Angew. Chem.* **2016**, *128*, 196–200.
- [24] a) B. J. Guddorf, A. Hepp, F. Lips, *Chem. Eur. J.* **2018**, *24*, 10334–10338; b) H. Cui, M. Wu, P. Teng, *Eur. J. Inorg. Chem.* **2016**, 4123–4127; c) A. Maiti, D. Mandal, I. Omlor, D. Dhara, L. Klemmer, V. Huch, M. Zimmer, D. Scheschkewitz, A. Jana, *Inorg. Chem.* **2019**, *58*, 4071–4075; d) A. Jana, I. Omlor, V. Huch, H. S. Rzepa, D. Scheschkewitz, *Angew. Chem. Int. Ed.* **2014**, *53*, 9953–9956; *Angew. Chem.* **2014**, *126*, 10112–10116; e) P. Frisch, S. Inoue, *Dalton Trans.* **2019**, *48*, 10403–10406.
- [25] J. C. Peters, A. L. Odum, C. C. Cummins, *Chem. Commun.* **1997**, 1995–1996.
- [26] a) E. O. Fischer, H. Hollfelder, P. Friedrich, F. R. Kreissl, G. Huttner, *Angew. Chem. Int. Ed. Engl.* **1977**, *16*, 401–402; *Angew. Chem.* **1977**, *89*, 416–417; b) W. W. Greaves, R. J. Angelici, B. J. Helland, R. Klima, R. A. Jacobson, *J. Am. Chem. Soc.* **1979**, *101*, 7618–7620; c) H. Huang, R. P. Hughes, A. L. Rheingold, *Dalton Trans.* **2011**, *40*, 47–55; d) J. D. Carter, K. B. Kingsbury, A. Wilde, T. K. Schoch, C. J. Leep, E. K. Pham, L. McElwee-White, *J. Am. Chem. Soc.* **1991**, *113*, 2947–2954; e) H. Sakaba, M. Yoshida, C. Kabuto, K. Kabuto, *J. Am. Chem. Soc.* **2005**, *127*, 7276–7277.
- [27] a) D. Vidovic, S. Aldridge, *Angew. Chem. Int. Ed.* **2009**, *48*, 3669–3672; *Angew. Chem.* **2009**, *121*, 3723–3726; b) A. Jayaraman, B. T. Sterenberg, *Organometallics* **2016**, *35*, 2367–2377.
- [28] a) T. Watanabe, H. Hashimoto, H. Tobita, *Chem. Asian J.* **2012**, *7*, 1408–1416; b) B. V. Mork, T. D. Tilley, *J. Am. Chem. Soc.* **2001**, *123*, 9702–9703; c) K. Takanashi, V. Y. Lee, T. Yokoyama, A. Sekiguchi, *J. Am. Chem. Soc.* **2009**, *131*, 916–917.
- [29] Based on a study of the Cambridge Structural Database (CSD).
- [30] a) H. Hashimoto, Y. Odagiri, Y. Yamada, N. Takagi, S. Sakaki, H. Tobita, *J. Am. Chem. Soc.* **2015**, *137*, 158–161; b) H. Hashimoto, K. Komura, T. Ishizaki, Y. Odagiri, H. Tobita, *Dalton Trans.* **2017**, *46*, 8701–8704.
- [31] W. D. Wang, R. Eisenberg, *J. Am. Chem. Soc.* **1990**, *112*, 1833–1841.
- [32] A. G. Brook, F. Abdesaken, G. Gutekunst, N. Plavac, *Organometallics* **1982**, *1*, 994–998.
- [33] G. Maier, D. Born, *Angew. Chem. Int. Ed. Engl.* **1989**, *28*, 1050–1052; *Angew. Chem.* **1989**, *101*, 1085–1087.
- [34] a) F. Neese, *Wiley Interdiscip. Rev.: Comput. Mol. Sci.* **2012**, *2*, 73–78; b) F. Neese, *Wiley Interdiscip. Rev.: Comput. Mol. Sci.* **2018**, *8*, e1327.

- [35] See the Supporting Information for a detailed benchmark analysis with experimental properties (CO stretching frequencies, structural parameters, NMR shifts, UV/Vis transitions) and a comparison with the functionals BP86, M06, and TPSSh.
- [36] G. Knizia, *J. Chem. Theory Comput.* **2013**, *9*, 4834–4843.
- [37] The dimerization of a tungsten alkylidene has also been reported in the literature; see: S. Arndt, R. R. Schrock, P. Muller, *Organometallics* **2007**, *26*, 1279–1290.
- [38] FOD analysis and CASSCF(12,12) calculations suggest small multireference character for the transition state. For details, see the Supporting Information.
- [39] CCDC 1970332 (**2**), 1970333 (**3**), 1970334 (**3'**), 1970335 (**4a**), and 1970336 (**6**) contain the supplementary crystallographic data for this paper. These data are provided free of charge by The Cambridge Crystallographic Data Centre.

Manuscript received: December 16, 2019
Accepted manuscript online: January 14, 2020
Version of record online: February 20, 2020

10 Summary and Outlook

This PhD project was started with initial focus to continuative reactivity studies of the (silyl)hydrosilylene **S4.26** (Figure 20), previously reported by our group.^[140] Beside the already reported reactivity of compound **S4.26** towards transition metals^[143] and unsaturated organic small molecules,^[141-142, 235] our target was the systematic investigation of the reactivity of **S4.26** towards different Lewis acidic borane sources.

The treatment of NHC-stabilized (silyl)silylene hydride **S4.26** with BR_3 ($\text{R} = \text{H}, \text{Ph}$) or $\text{H}_3\text{N} \rightarrow \text{BH}_3$ leads to formation of the silylene-hydride-borane complex **S10.1** or the product **S10.3** due to ammonia borane dehydrogenation, with concomitant insertion of the silicon (II) atom into an N-H bond (Figure 30).

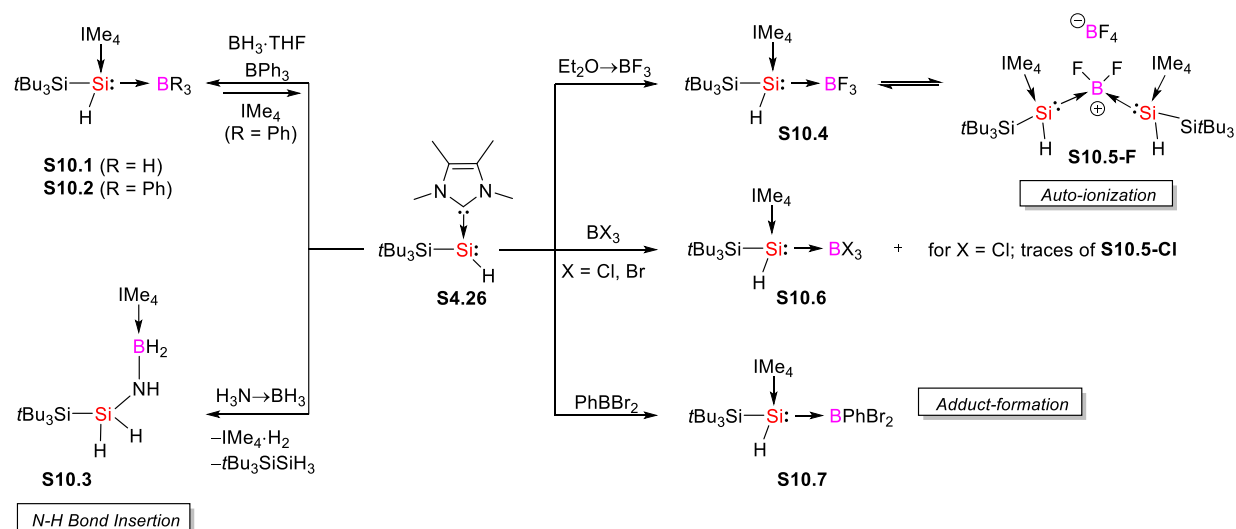


Figure 30. Reactivity of NHC-stabilized (silyl)silylene hydride (**S4.26**) towards electrophilic borane sources (e.g. hydro-, halo-, organo-boranes).

Different to the BH_3 -Adduct **S10.1**, the organoborane (BPh_3) adduct **S10.2** (Figure 30) is converted back to the free silylene upon treatment with excess IMe_4 with $\text{IMe}_4 \rightarrow \text{BPh}_3$ obtained as side product. The reaction of silylene hydride **S4.26** with haloboranes ($\text{Et}_2\text{O} \rightarrow \text{BF}_3$, BCl_3 , BBr_3) resulted in the formation of Lewis acid-base adducts **S10.4–6** which slowly equilibrated to the auto-ionization products **S10.5-X**, ($\text{X} = \text{F}, \text{Cl}$). The ratio of **S10.5-X** significantly depends on the atomic number of the halide. We conclude that the formation of auto-ionized products decreases with the rising atomic number of the halide. Hence, the stability of afforded Lewis acid-base adducts increases in the order $\text{Br} > \text{Cl} > \text{F}$. Although, the conversion of silylenes with haloboranes mostly occurs via insertion of the silicon atom into a boron-halide, with the hydrosilylene **S4.26** it successfully furnished the Lewis acid-

base adducts. Moreover, upon increasing stability of the counter anion $[BX_4]^-$, the system is more prone to auto-ionization. Accordingly, the treatment of **S4.26** with a mixed system BPh_2Br afforded the compound **S10.7** (Figure 30) as reminiscent of the related conversions described above.

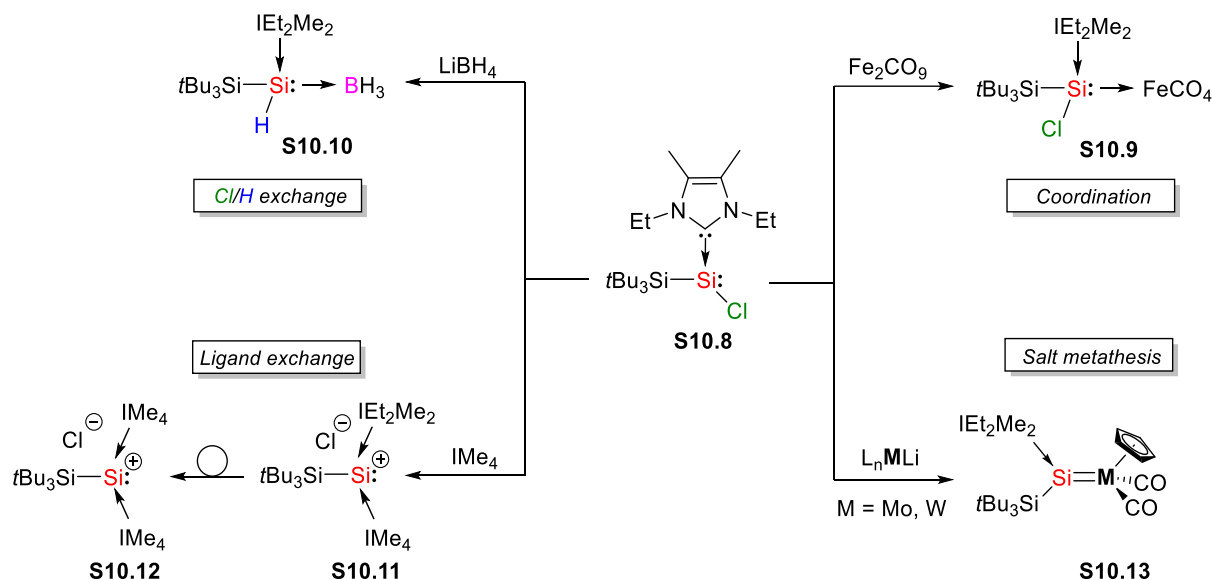


Figure 31. Reactivity products of NHC-stabilized (silyl)chlorosilylene **S10.8** via its corresponding active sites: (i) through active lone pair (**S10.9**), (ii) through labile Si–Cl bond (**S10.10**, **S10.13**), (iii) through its dative bond with NHC (**S10.11**, **S10.12**).

In an effort to expand the chemistry of functionalized low-valent silylenes, particular attention was paid to synthesis and isolation of silyl-substituted chlorosilylenes. As a major goal of this thesis, the aim was to exchange the hydride in **S4.26** and add a halide functionality to the (silyl)silylene, to afterwards take advantage of the silicon-halide bond being more labile than a silicon-hydride bond. Moreover, silyl-substituted halosilylenes had remained elusive due to the lack of suitable synthetic methods. Since (silyl)halosilylene, particularly chlorosilylene, would be prone to salt metathesis reactions, it should be an excellent precursor for the access of novel organosilicon compounds. The reaction of silyl-based Si(IV) precursor ($tBu_3SiSiHCl_2$) with two equivalents of IEt_2Me_2 in toluene at $-50\text{ }^\circ\text{C}$ successfully gave access to the silicon(II) monochloride NHC adduct **S10.8** (Figure 31) in excellent yields (92%) with a trigonal pyramidal geometry with the sum of bond angles at the silicon center being 309.25° . In the ^{29}Si NMR spectrum of **S10.8**, the signal corresponding to the terminal Si(II)–Cl appears at 18.3 ppm, that is downfield shifted to that of the NHC-stabilized arylchlorosilylenes **S4.15**^[105], due to the presence of an electropositive silyl substituent. Since compound **S10.8** has three potential active reactive sites, we investigated the reactivity of each of those active sites. Compound **S10.8** reacts readily with $Fe_2(CO)_9$ through its active lone pair to afford the corresponding silylene chloride-iron complex **S10.9** (Figure 31) with relatively long Si–Fe bond length due to the electron-

donating bulky silyl substituents. Treatment of (silyl)chlorosilylene **S10.8** with LiBH_4 leads to the formation of stable silylene hydride borane adduct **S10.10** (Figure 31) via Cl/H exchange, which is isostructural to **S10.1** (Figure 30). Moreover, chlorosilylene **S10.8** underwent a ligand exchange reaction with the less sterically demanding, but more σ -electron donating IME_4 ligand, resulting the formation of an asymmetric NHC-silyliumylidene ion **S10.11** which is confirmed by hetero-nuclear NMR analysis. Although compound **S10.11** found to be stable over time according to NMR experiments, it converted into more stable symmetric silyliumylidene ion **S10.12** (Figure 31).

We then continued by using the lability of Si–Cl bond stepwise to allow for accessibility to Si–M multiple bonds. As a starting point, salt metathesis reaction of (silyl)chlorosilylene (**S10.8**) towards transition metallates was investigated. Treatment of compound **S10.8** with $\text{Cp}(\text{CO})_2\text{PMe}_3\text{Li}$ ($M = \text{Mo}, \text{W}$) in hot toluene smoothly affords the NHC-stabilized $M=\text{Si}$ complexes **S10.13** (Figure 31) as dark green solids in good yields ($M = \text{Mo}$, 82%, $M = \text{W}$, 78%). The ^{29}Si NMR spectrum of compounds **S10.13** have characteristic resonances (**S10.13-Mo**, $\delta = 279$ ppm; **S10.13-W**, $\delta = 230$ ppm) similar to the reported transition metal-silylene complexes **S5.1-7**. Following this outcome, we studied whether or not NHC exchange is possible from compound **S10.13** with the smaller and more nucleophilic IME_4 . Treatment of compound **S10.13-W** with excess IME_4 resulted in a fast and quantitative exchange with the formerly coordinated IEt_2Me_2 by IME_4 to afford the compound **S10.14** (Figure 32). As expected, the structural parameters were very similar with **S10.13-W**. With the ability of ligand exchange proven in compounds **S10.13**, we tackled the next level to access increased bonding between silicon and the metal centers: abstraction of the NHC. As such, we introduced various Lewis acids in order to abstract the NHC as a Lewis acid-base adduct. The reaction of **S10.13-W** with strong Lewis acids like $\text{B}(\text{C}_6\text{F}_5)_3$ or more oxophilic AlCl_3 resulted in an immediate reaction to afford a peculiar Lewis-acid carbonyl adduct **S10.15A-B** (Figure 32) as confirmed by the single crystal X-ray crystallography. Interestingly, the addition of a coordinating solvent (i.e. THF) to the dark red solutions of **S10.15** spontaneously resulted in the regeneration of the initial starting material **S10.13**.

Thus clearly paving the way of milder Lewis acids, like triphenyl borane (BPh_3), being necessary in order to abstract the NHC from the TM-silylene complexes **S10.13**. Heating a toluene solution of **S10.13** to 90°C with one equivalent of BPh_3 yielded the desired NHC abstraction to afforded the air- and moisture-stable heterobimetallic tetrahedral complexes **S10.16** (Figure 32). The ^{29}Si NMR signals of the skeletal silicon atoms shifted strongly to the high field region (**S10.16-Mo**, $\delta = 4$ ppm; **S10.16-W**, $\delta = -63$ ppm) which corroborates strongly with the silyl characters change in hybridization from sp^2 to sp^3 . Moreover, such an upfield shift is also characteristic for the ring C atoms of tetrahedranes.^[236] According to DFT calculations, silicon and tungsten atoms in compound **S10.16-W** possesses two different yet quite covalent σ -interactions. In addition, a σ -bond between the two skeletal silicon atom as well as a considerable bonding interaction between the two tungsten atoms was found.

Overall, the DFT calculations confirm consequently a tetrahedral structure with strong and covalent interactions between all silicon and tungsten atoms in compound **S10.16**.

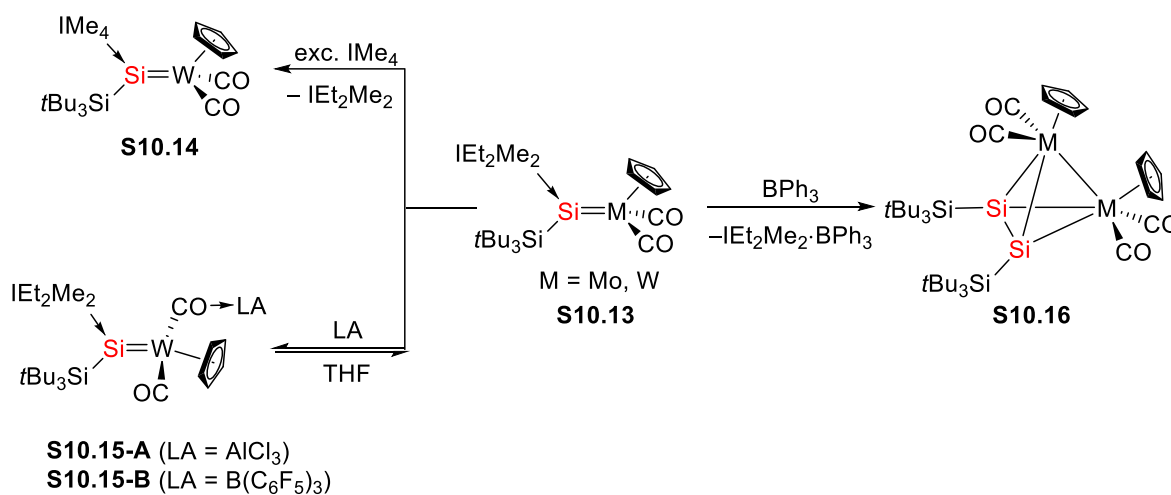


Figure 32. NHC exchange/abstraction products of TM-silylene complexes (**S10.13**) to afford compounds **S10.14-16**.

In order to understand the peculiar Si–Si dimerization for the formation of tetrahedral clusters, the reaction mechanism was modelled. The restricted DFT calculations suggest that compound **S10.16** forms via subsequent dimerization of linear transient TM-silylyne complex (Si≡M) ($\Delta G = +1.7$ kcal mol⁻¹). Most importantly, the transition state reveals that the steric bulk associated with the supersilyl group on the silicon atom and Cp ligands on the metal center allows only for a perpendicular arrangement of the two silylyne complexes and hence determines the formation of tetrahedral cluster instead of a four-membered ring, as would be expected by simplifying polarity considerations.

Future reactivity investigations of chlorosilylene, compound **S10.8** should build on the work highlighted within this thesis. In particular, towards accessing different anionic complexes through salt metathesis as it has been shown to be possible through the formation of **S10.10** and **S10.13**. For example, adapting a similar synthetic approach as for compound **S4.7** (Figure 15), treatment of compound **S10.8** with anionic diazo compound could give access to the formation of a silicon-carbon bond and subsequent elimination of N₂ and NHC may afford donor-free silynes (Si≡C), which is a long-sought target compound in silicon chemistry. An alternative approach would involve the NHC exchange reaction of **S10.8** with isocyanide (R–N≡C) which might yield a isocyanide stabilized chlorosilylene, that can be further reduced by alkali metals to afford triple bond between silicon and carbon.

This thesis also gives insight from a different perspective, as it was shown by DFT that the formation of the intermediate TM-silylyne complex is actually isoergic ($\Delta G = +1.7$ kcal mol⁻¹) with TM-silylene complex **S10.13**. This finding suggests that the employed *t*Bu₃Si substituent is not

sterically demanding enough to kinetically stabilize a silicon metal triple bond, hence subsequently dimerization occurs to yield tetrahedral heterobimetallic clusters **S10.16**. Moreover, this also implies that with increased steric bulk on either the silicon center and/or on metal center, first silyl-substituted TM-silylyne complex could be obtained. With this compound in hand, further investigated in terms of sila-alkyne type metathesis, akin to TM-carbyne complexes, would be great interest.

In conclusion, this doctoral work extends the scope of low-valent group 14 element chemistry especially in regard to low-valent functionalized silylene compounds. The work within this thesis has succeeded in the synthesis of first example of silyl-substituted chlorosilylene **S10.8** and formation of several novel low-valent silicon compounds **S10.9-15** via its three different reactive sites. With this achievement, the one of the missing spot for the class of functionalized low-valent silylenes was fulfilled. Strikingly, within this work the first neutral heterobimetallic tetrahedral cluster **S10.16** with Si_2M_2 core was discovered and thoroughly characterized from an experimental and theoretical point of view.

11 Bibliography

- [1] S. K. Mandal, H. W. Roesky, *Chem. Commun.* **2010**, 46, 6016-6041.
- [2] H. Jacobsen, T. Ziegler, *J. Am. Chem. Soc.* **1994**, 116, 3667-3679.
- [3] W. Kutzelnigg, *Angew. Chem. Int. Ed. Engl.* **1984**, 23, 272-295.
- [4] P. P. Power, *Nature* **2010**, 463, 171-177.
- [5] C. Weetman, S. Inoue, *ChemCatChem* **2018**, 10, 4213-4228.
- [6] A. H. Cowley, *J. Organomet. Chem.* **2004**, 689, 3866-3872.
- [7] T. Chu, G. I. Nikonov, *Chem. Rev.* **2018**, 118, 3608-3680.
- [8] A. V. Protchenko, K. H. Birj Kumar, D. Dange, A. D. Schwarz, D. Vidovic, C. Jones, N. Kaltsoyannis, P. Mountford, S. Aldridge, *J. Am. Chem. Soc.* **2012**, 134, 6500-6503.
- [9] J. Li, C. Schenk, C. Goedecke, G. Frenking, C. Jones, *J. Am. Chem. Soc.* **2011**, 133, 18622-18625.
- [10] G. H. Spikes, J. C. Fettinger, P. P. Power, *J. Am. Chem. Soc.* **2005**, 127, 12232-12233.
- [11] J. Li, M. Hermann, G. Frenking, C. Jones, *Angew. Chem. Int. Ed.* **2012**, 51, 8611-8614.
- [12] D. Gau, R. Rodriguez, T. Kato, N. Saffon-Merceron, A. de Cózar, F. P. Cossío, A. Baceiredo, *Angew. Chem.* **2011**, 123, 1124-1128.
- [13] X. Wang, Z. Zhu, Y. Peng, H. Lei, J. C. Fettinger, P. P. Power, *J. Am. Chem. Soc.* **2009**, 131, 6912-6913.
- [14] R. Rodriguez, D. Gau, T. Kato, N. Saffon-Merceron, A. De Cózar, F. P. Cossío, A. Baceiredo, *Angew. Chem. Int. Ed.* **2011**, 50, 10414-10416.
- [15] Y. Peng, B. D. Ellis, X. Wang, J. C. Fettinger, P. P. Power, *Science* **2009**, 325, 1668-1670.
- [16] J. B. Dumas, E. Peligot, *Ann. Chim. Phys.* **1835**, 58, 5-74.
- [17] A. Igau, H. Grutzmacher, A. Baceiredo, G. Bertrand, *J. Am. Chem. Soc.* **1988**, 110, 6463-6466.
- [18] A. J. Arduengo, R. L. Harlow, M. Kline, *J. Am. Chem. Soc.* **1991**, 113, 361-363.
- [19] W. A. Herrmann, *Angew. Chem. Int. Ed.* **2002**, 41, 1290-1309.
- [20] D. Bourissou, O. Guerret, F. P. Gabbaï, G. Bertrand, *Chem. Rev.* **2000**, 100, 39-92.
- [21] M. N. Hopkinson, C. Richter, M. Schedler, F. Glorius, *Nature* **2014**, 510, 485-496.
- [22] A. Doddi, M. Peters, M. Tamm, *Chem. Rev.* **2019**.
- [23] V. Nesterov, D. Reiter, P. Bag, P. Frisch, R. Holzner, A. Porzelt, S. Inoue, *Chem. Rev.* **2018**, 118, 9678-9842.
- [24] N. Marion, S. Díez-González, S. P. Nolan, *Angew. Chem. Int. Ed.* **2007**, 46, 2988-3000.
- [25] D. Enders, O. Niemeier, A. Henseler, *Chem. Rev.* **2007**, 107, 5606-5655.
- [26] R. Visbal, M. C. Gimeno, *Chem. Soc. Rev.* **2014**, 43, 3551-3574.
- [27] A. J. Boydston, K. A. Williams, C. W. Bielawski, *J. Am. Chem. Soc.* **2005**, 127, 12496-12497.
- [28] K. Oisaki, Q. Li, H. Furukawa, A. U. Czaja, O. M. Yaghi, *J. Am. Chem. Soc.* **2010**, 132, 9262-9264.
- [29] W. Liu, R. Gust, *Chem. Soc. Rev.* **2013**, 42, 755-773.
- [30] K. M. Hindi, M. J. Panzner, C. A. Tessier, C. L. Cannon, W. J. Youngs, *Chem. Rev.* **2009**, 109, 3859-3884.
- [31] T. M. Trmka, R. H. Grubbs, *Acc. Chem. Res.* **2001**, 34, 18-29.
- [32] M. Fèvre, J. Pinaud, Y. Gnanou, J. Vignolle, D. Taton, *Chem. Soc. Rev.* **2013**, 42, 2142-2172.
- [33] C. A. Dvorak, V. H. Rawal, *Tetrahedron Letters* **1998**, 39, 2925-2928.
- [34] J. C. Sheehan, D. H. Hunneman, *J. Am. Chem. Soc.* **1966**, 88, 3666-3667.
- [35] R. Singh, R. M. Kissling, M.-A. Letellier, S. P. Nolan, *The Journal of Organic Chemistry* **2004**, 69, 209-212.
- [36] N. E. Kamber, W. Jeong, S. Gonzalez, J. L. Hedrick, R. M. Waymouth, *Macromolecules* **2009**, 42, 1634-1639.
- [37] G. O. Jones, Y. A. Chang, H. W. Horn, A. K. Acharya, J. E. Rice, J. L. Hedrick, R. M. Waymouth, *J. Phys. Chem. B* **2015**, 119, 5728-5737.
- [38] V. Lavallo, Y. Canac, C. Präsang, B. Donnadiou, G. Bertrand, *Angew. Chem. Int. Ed.* **2005**, 44, 5705-5709.
- [39] S. Kundu, S. Sinhababu, V. Chandrasekhar, H. W. Roesky, *Chem. Sci.* **2019**, 10, 4727-4741.
- [40] M. Soleilhavoup, G. Bertrand, *Acc. Chem. Res.* **2015**, 48, 256-266.
- [41] M. Melaimi, R. Jazzar, M. Soleilhavoup, G. Bertrand, *Angew. Chem. Int. Ed.* **2017**, 56, 10046-10068.
- [42] G. D. Frey, V. Lavallo, B. Donnadiou, W. W. Schoeller, G. Bertrand, *Science* **2007**, 316, 439-441.
- [43] E. Aldeco-Perez, A. J. Rosenthal, B. Donnadiou, P. Parameswaran, G. Frenking, G. Bertrand, *Science* **2009**, 326, 556-559.
- [44] Á. Vivancos, C. Segarra, M. Albrecht, *Chem. Rev.* **2018**, 118, 9493-9586.
- [45] Q. Zhao, G. Meng, S. P. Nolan, M. Szostak, *Chem. Rev.* **2020**.
- [46] S. C. Sau, P. K. Hota, S. K. Mandal, M. Soleilhavoup, G. Bertrand, *Chem. Soc. Rev.* **2020**.
- [47] Y. Wang, Y. Xie, P. Wei, R. B. King, H. F. Schaefer, P. von R. Schleyer, G. H. Robinson, *Science* **2008**, 321, 1069-1071.
- [48] Y. Xiong, S. Yao, S. Inoue, J. D. Epping, M. Driess, *Angew. Chem. Int. Ed.* **2013**, 52, 7147-7150.
- [49] K. C. Mondal, H. W. Roesky, M. C. Schwarzer, G. Frenking, B. Niepötter, H. Wolf, R. Herbst-Irmer, D. Stalke, *Angew. Chem. Int. Ed.* **2013**, 52, 2963-2967.
- [50] N. Hayakawa, K. Sadamori, S. Mizutani, T. Agou, T. Sugahara, T. Sasamori, N. Tokitoh, D. Hashizume, T. Matsuo, *Inorganics* **2018**, 6, 30.
- [51] S. U. Ahmad, T. Szilvási, S. Inoue, *Chem. Commun.* **2014**, 50, 12619-12622.
- [52] S. L. Powley, S. Inoue, *Chem. Rec.* **2019**, 19, 2179-2188.
- [53] T. Agou, N. Hayakawa, T. Sasamori, T. Matsuo, D. Hashizume, N. Tokitoh, *Chem. Eur. J.* **2014**, 20, 9246-9249.
- [54] P. Frisch, S. Inoue, *Dalton Trans.* **2019**, 48, 10403-10406.
- [55] A. C. Filippou, Y. N. Lebedev, O. Chernov, M. Straßmann, G. Schnakenburg, *Angew. Chem. Int. Ed.* **2013**, 52, 6974-6978.
- [56] Y. Wang, B. Quillian, P. Wei, C. S. Wannere, Y. Xie, R. B. King, H. F. Schaefer, P. v. R. Schleyer, G. H. Robinson, *J. Am. Chem. Soc.* **2007**, 129, 12412-12413.
- [57] H. Braunschweig, R. D. Dewhurst, K. Hammond, J. Mies, K. Radacki, A. Vargás, *Science* **2012**, 336, 1420-1422.
- [58] S. J. Bonyhady, D. Collis, G. Frenking, N. Holzmann, C. Jones, A. Stasch, *Nature Chemistry* **2010**, 2, 865-869.
- [59] P. Bag, A. Porzelt, P. J. Altmann, S. Inoue, *J. Am. Chem. Soc.* **2017**, 139, 14384-14387.
- [60] C. Weetman, P. Bag, T. Szilvási, C. Jandl, S. Inoue, *Angew. Chem. Int. Ed.* **2019**, 58, 10961-10965.
- [61] Y. Wang, Y. Xie, P. Wei, R. B. King, H. F. Schaefer, P. v. R. Schleyer, G. H. Robinson, *J. Am. Chem. Soc.* **2008**, 130, 14970-14971.
- [62] S. Roy, K. C. Mondal, S. Kundu, B. Li, C. J. Schürmann, S. Dutta, D. Koley, R. Herbst-Irmer, D. Stalke, H. W. Roesky, *Chem. Eur. J.* **2017**, 23, 12153-12157.
- [63] T. Ochiai, D. Franz, S. Inoue, *Chem. Soc. Rev.* **2016**, 45, 6327-6344.
- [64] D. Franz, T. Szilvási, E. Irran, S. Inoue, *Nat. Commun.* **2015**, 6, 10037.
- [65] D. Wendel, D. Reiter, A. Porzelt, P. J. Altmann, S. Inoue, B. Rieger, *J. Am. Chem. Soc.* **2017**, 139, 17193-17198.

- [66] Y. Mizuhata, T. Sasamori, N. Tokitoh, *Chem. Rev.* **2009**, *109*, 3479-3511.
- [67] P. S. Skell, E. J. Goldstein, *J. Am. Chem. Soc.* **1964**, *86*, 1442-1443.
- [68] T. J. Drahnak, J. Michl, R. West, *J. Am. Chem. Soc.* **1979**, *101*, 5427-5428.
- [69] P. Jutzi, D. Kanne, C. Krüger, *Angew. Chem. Int. Ed. Engl.* **1986**, *25*, 164-164.
- [70] P. Ghana, M. I. Arz, G. Schnakenburg, M. Straßmann, A. C. Filippou, *Organometallics* **2018**, *37*, 772-780.
- [71] P. Jutzi, *Chem. Eur. J* **2014**, *20*, 9192-9207.
- [72] H. H. Karsch, U. Keller, S. Gamper, G. Müller, *Angew. Chem. Int. Ed. Engl.* **1990**, *29*, 295-296.
- [73] M. Veith, E. Werle, R. Lisowsky, R. Köppe, H. Schnöckel, *Chem. Ber.* **1992**, *125*, 1375-1377.
- [74] M. Denk, R. Lennon, R. Hayashi, R. West, A. V. Belyakov, H. P. Verne, A. Haaland, M. Wagner, N. Metzler, *J. Am. Chem. Soc.* **1994**, *116*, 2691-2692.
- [75] R. West, M. Denk, *Pure Appl. Chem.* **1996**, *68*, 785.
- [76] B. Gehrhus, M. F. Lappert, J. Heinicke, R. Boese, D. Bläser, *J. Chem. Soc., Chem. Commun.* **1995**, 1931-1932.
- [77] M. Driess, S. Yao, M. Brym, C. van Wüllen, D. Lentz, *J. Am. Chem. Soc.* **2006**, *128*, 9628-9629.
- [78] C.-W. So, H. W. Roesky, J. Magull, R. B. Oswald, *Angew. Chem. Int. Ed.* **2006**, *45*, 3948-3950.
- [79] M. Kira, S. Ishida, T. Iwamoto, C. Kabuto, *J. Am. Chem. Soc.* **1999**, *121*, 9722-9723.
- [80] T. Kosai, S. Ishida, T. Iwamoto, *Angew. Chem. Int. Ed.* **2016**, *55*, 15554-15558.
- [81] M. J. S. Gynane, D. H. Harris, M. F. Lappert, P. P. Power, P. Rivière, M. Rivière-Baudet, *J. Chem. Soc., Dalton Trans.* **1977**, 2004-2009.
- [82] D. H. Harris, M. F. Lappert, *J. Chem. Soc., Chem. Commun.* **1974**, 895-896.
- [83] G.-H. Lee, R. West, T. Müller, *J. Am. Chem. Soc.* **2003**, *125*, 8114-8115.
- [84] B. D. Recken, T. M. Brown, J. C. Fettingner, H. M. Tuononen, P. P. Power, *J. Am. Chem. Soc.* **2012**, *134*, 6504-6507.
- [85] A. V. Protchenko, A. D. Schwarz, M. P. Blake, C. Jones, N. Kaltsoyannis, P. Mountford, S. Aldridge, *Angew. Chem. Int. Ed.* **2013**, *52*, 568-571.
- [86] T. J. Hadlington, J. A. B. Abdalla, R. Tirfoin, S. Aldridge, C. Jones, *Chem. Commun.* **2016**, *52*, 1717-1720.
- [87] A. V. Protchenko, P. Vasko, D. C. H. Do, J. Hicks, M. A. Fuentes, C. Jones, S. Aldridge, *Angew. Chem. Int. Ed.* **2019**, *58*, 1808-1812.
- [88] D. Wendel, A. Porzelt, F. A. D. Herz, D. Sarkar, C. Jandl, S. Inoue, B. Rieger, *J. Am. Chem. Soc.* **2017**, *139*, 8134-8137.
- [89] H. Tanaka, M. Ichinohe, A. Sekiguchi, *J. Am. Chem. Soc.* **2012**, *134*, 5540-5543.
- [90] M. W. Stanford, J. I. Schweizer, M. Menche, G. S. Nichol, M. C. Holthausen, M. J. Cowley, *Angew. Chem. Int. Ed.* **2019**, *58*, 1329-1333.
- [91] D. Reiter, R. Holzner, A. Porzelt, P. J. Altmann, P. Frisch, S. Inoue, *J. Am. Chem. Soc.* **2019**, *141*, 13536-13546.
- [92] M. Haaf, T. A. Schmedake, R. West, *Acc. Chem. Res.* **2000**, *33*, 704-714.
- [93] A. Gackstatter, H. Braunschweig, T. Kupfer, C. Voigt, N. Arnold, *Chem. -Eur. J.* **2016**, *22*, 16415-16419.
- [94] S. Raoufoghaddam, Y.-P. Zhou, Y. Wang, M. Driess, *J. Organomet. Chem.* **2017**, *829*, 2-10.
- [95] N. J. Hill, R. West, *J. Organomet. Chem.* **2004**, *689*, 4165-4183.
- [96] S. S. Sen, H. W. Roesky, D. Stern, J. Henn, D. Stalke, *J. Am. Chem. Soc.* **2010**, *132*, 1123-1126.
- [97] S. S. Sen, J. Hey, M. Eckhardt, R. Herbst-Irmer, E. Maedl, R. A. Mata, H. W. Roesky, M. Scheer, D. Stalke, *Angew. Chem. Int. Ed.* **2011**, *50*, 12510-12513.
- [98] S. S. Sen, S. Khan, H. W. Roesky, D. Kratzert, K. Meindl, J. Henn, D. Stalke, J.-P. Demers, A. Lange, *Angew. Chem. Int. Ed.* **2011**, *50*, 2322-2325.
- [99] S. Inoue, W. Wang, C. Präsang, M. Asay, E. Irran, M. Driess, *J. Am. Chem. Soc.* **2011**, *133*, 2868-2871.
- [100] D. Gau, T. Kato, N. Saffon-Merceron, A. De Cózar, F. P. Cossío, A. Baceiredo, *Angew. Chem. Int. Ed.* **2010**, *49*, 6585-6588.
- [101] D. Gau, R. Nougaté, N. Saffon-Merceron, A. Baceiredo, A. De Cózar, F. P. Cossío, D. Hashizume, T. Kato, *Angew. Chem.* **2016**, *128*, 14893-14897.
- [102] T. Troadec, T. Wasano, R. Lenk, A. Baceiredo, N. Saffon-Merceron, D. Hashizume, Y. Saito, N. Nakata, V. Branchadell, T. Kato, *Angew. Chem. Int. Ed.* **2017**, *56*, 6891-6895.
- [103] Y. Xiong, S. Yao, A. Kostenko, M. Driess, *Dalton Trans.* **2018**, *47*, 2152-2155.
- [104] D. C. H. Do, A. V. Protchenko, M. Ángeles Fuentes, J. Hicks, E. L. Kolychev, P. Vasko, S. Aldridge, *Angew. Chem. Int. Ed.* **2018**, *57*, 13907-13911.
- [105] A. C. Filippou, C. Oleg, B. Blom, K. W. Stumpf, G. Schnakenburg, *Chem. Eur. J* **2010**, *16*, 2866-2872.
- [106] J. Li, B. Ma, C. Cui, *Organometallics* **2016**, *35*, 1358-1360.
- [107] H. Cui, B. Ma, C. Cui, *Organometallics* **2012**, *31*, 7339-7342.
- [108] H. Cui, C. Cui, *Dalton Trans.* **2015**, *44*, 20326-20329.
- [109] Y. Li, B. Ma, C. Cui, *Dalton Trans.* **2015**, *44*, 14085-14091.
- [110] S. M. I. Al-Rafia, R. McDonald, M. J. Ferguson, E. Rivard, *Chem. Eur. J* **2012**, *18*, 13810-13820.
- [111] D. Lutters, C. Severin, M. Schmidtman, T. Müller, *J. Am. Chem. Soc.* **2016**, *138*, 6061-6067.
- [112] J. M. Charig, B. A. Joyce, *J. Electrochem. Soc.* **1962**, *109*, 957.
- [113] M. Schmeisser, P. Voss, *Z. Anorg. Allg. Chem.* **1964**, *334*, 50-56.
- [114] J. L. Margrave, P. W. Wilson, *Acc. Chem. Res.* **1971**, *4*, 145-152.
- [115] P. W. Schenk, H. Bloching, *Z. Anorg. Allg. Chem.* **1964**, *334*, 57-65.
- [116] M. Schmeisser, M. Schwarzmann, *Z. Naturforsch., B* **1956**, *11*, 278.
- [117] S.-H. Kang, J. S. Han, M. E. Lee, B. R. Yoo, I. N. Jung, *Organometallics* **2003**, *22*, 2551-2553.
- [118] R. A. Benkeser, *Acc. Chem. Res.* **1971**, *4*, 94-100.
- [119] R. S. Ghadwal, H. W. Roesky, S. Merkel, J. Henn, D. Stalke, *Angew. Chem. Int. Ed.* **2009**, *48*, 5683-5686.
- [120] H. Cui, C. Cui, *Dalton Trans.* **2011**, *40*, 11937-11940.
- [121] D. C. H. Do, A. V. Protchenko, M. Ángeles Fuentes, J. Hicks, E. L. Kolychev, P. Vasko, S. Aldridge, *Angew. Chem.* **2018**, *130*, 14103-14107.
- [122] R. S. Ghadwal, K. Pröpper, B. Dittrich, P. G. Jones, H. W. Roesky, *Inorg. Chem.* **2011**, *50*, 358-364.
- [123] R. S. Ghadwal, H. W. Roesky, K. Pröpper, B. Dittrich, S. Klein, G. Frenking, *Angew. Chem. Int. Ed.* **2011**, *50*, 5374-5378.
- [124] A. C. Filippou, O. Chernov, G. Schnakenburg, *Angew. Chem. Int. Ed.* **2009**, *48*, 5687-5690.
- [125] M. I. Arz, D. Geiß, M. Straßmann, G. Schnakenburg, A. C. Filippou, *Chem. Sci.* **2015**, *6*, 6515-6524.
- [126] M. I. Arz, D. Hoffmann, G. Schnakenburg, A. C. Filippou, *Z. Anorg. Allg. Chem.* **2016**, *642*, 1287-1294.
- [127] K. C. Mondal, B. Dittrich, B. Maity, D. Koley, H. W. Roesky, *J. Am. Chem. Soc.* **2014**, *136*, 9568-9571.
- [128] K. C. Mondal, H. W. Roesky, M. C. Schwarzer, G. Frenking, I. Tkach, H. Wolf, D. Kratzert, R. Herbst-Irmer, B. Niepötter, D. Stalke, *Angew. Chem. Int. Ed.* **2013**, *52*, 1801-1805.
- [129] Y. Li, Y.-C. Chan, Y. Li, I. Purushothaman, S. De, P. Parameswaran, C.-W. So, *Inorg. Chem.* **2016**, *55*, 9091-9098.

- [130] J. M. Jasinski, F. K. LeGoues, *Chem. Mater.* **1991**, *3*, 989-992.
- [131] J. G. Ekerdt, Y. M. Sun, A. Szabo, G. J. Szulczewski, J. M. White, *Chem. Rev.* **1996**, *96*, 1499-1518.
- [132] M. Y. Abraham, Y. Wang, Y. Xie, P. Wei, H. F. Schaefer, P. v. R. Schleyer, G. H. Robinson, *J. Am. Chem. Soc.* **2011**, *133*, 8874-8876.
- [133] S. M. I. Al-Rafia, A. C. Malcolm, R. McDonald, M. J. Ferguson, E. Rivard, *Chem. Commun.* **2012**, *48*, 1308-1310.
- [134] A. Jana, D. Leusser, I. Objartel, H. W. Roesky, D. Stalke, *Dalton Trans.* **2011**, *40*, 5458-5463.
- [135] B. Blom, M. Driess, D. Gallego, S. Inoue, *Chem. Eur. J.* **2012**, *18*, 13355-13360.
- [136] B. Blom, S. Enthaler, S. Inoue, E. Irran, M. Driess, *J. Am. Chem. Soc.* **2013**, *135*, 6703-6713.
- [137] M. Stoelzel, C. Präsang, S. Inoue, S. Enthaler, M. Driess, *Angew. Chem. Int. Ed.* **2012**, *51*, 399-403.
- [138] A.-K. Jungton, A. Meltzer, C. Präsang, T. Braun, M. Driess, A. Penner, *Dalton Trans.* **2010**, *39*, 5436.
- [139] R. Rodriguez, D. Gau, Y. Contie, T. Kato, N. Saffon-Merceron, A. Baceiredo, *Angew. Chem. Int. Ed.* **2011**, *50*, 11492-11495.
- [140] S. Inoue, C. Eisenhut, *J. Am. Chem. Soc.* **2013**, *135*, 18315-18318.
- [141] C. Eisenhut, T. Szilvási, N. C. Breit, S. Inoue, *Chem. Eur. J.* **2015**, *21*, 1949-1954.
- [142] C. Eisenhut, N. C. Breit, T. Szilvási, E. Irran, S. Inoue, *Eur. J. Inorg. Chem.* **2016**, *2016*, 2696-2703.
- [143] C. Eisenhut, T. Szilvási, G. Dübek, N. C. Breit, S. Inoue, *Inorg. Chem.* **2017**, *56*, 10061-10069.
- [144] E. O. Fischer, *Angew. Chem.* **1974**, *86*, 651-663.
- [145] R. R. Schrock, *Angew. Chem. Int. Ed.* **2006**, *45*, 3748-3759.
- [146] D. J. Cardin, B. Cetinkaya, M. F. Lappert, *Chem. Rev.* **1972**, *72*, 545-574.
- [147] C. S. Higman, J. A. M. Lummiss, D. E. Fogg, *Angew. Chem. Int. Ed.* **2016**, *55*, 3552-3565.
- [148] J. C. Mol, *J. Mol. Catal. A: Chem.* **2004**, *213*, 39-45.
- [149] A. H. Hoveyda, A. R. Zhugralin, *Nature* **2007**, *450*, 243-251.
- [150] K. C. Nicolaou, P. G. Bulger, D. Sarlah, *Angew. Chem. Int. Ed.* **2005**, *44*, 4490-4527.
- [151] J. W. Herndon, *Coord. Chem. Rev.* **2002**, *227*, 1-58.
- [152] A. M. Lozano-Vila, S. Monsaert, A. Bajek, F. Verpoort, *Chem. Rev.* **2010**, *110*, 4865-4909.
- [153] S. Suthasupa, M. Shiotsuki, F. Sanda, *Polym. J.* **2010**, *42*, 905-915.
- [154] J. Chatt, L. A. Duncanson, *J. Chem. Soc.* **1953**, 2939-2947.
- [155] C. Zybilla, G. Müller, *Angew. Chem. Int. Ed. Engl.* **1987**, *26*, 669-670.
- [156] D. A. Straus, T. D. Tilley, A. L. Rheingold, S. J. Geib, *J. Am. Chem. Soc.* **1987**, *109*, 5872-5873.
- [157] D. A. Straus, S. D. Grumbine, T. D. Tilley, *J. Am. Chem. Soc.* **1990**, *112*, 7801-7802.
- [158] J. D. Feldman, G. P. Mitchell, J.-O. Nolte, T. D. Tilley, *J. Am. Chem. Soc.* **1998**, *120*, 11184-11185.
- [159] G. P. Mitchell, T. D. Tilley, *Angew. Chem. Int. Ed.* **1998**, *37*, 2524-2526.
- [160] M. Okazaki, H. Tobita, H. Ogino, *Dalton Trans.* **2003**, 493-506.
- [161] F. Gauvin, J. F. Harrod, H. G. Woo, in *Adv. Organomet. Chem.*, Vol. 42 (Eds.: F. G. A. Stone, R. West), Academic Press, **1998**, pp. 363-405.
- [162] M. D. Curtis, P. S. Epstein, in *Adv. Organomet. Chem.*, Vol. 19 (Eds.: F. G. A. Stone, R. West), Academic Press, **1981**, pp. 213-255.
- [163] H. K. Sharma, K. H. Pannell, *Chem. Rev.* **1995**, *95*, 1351-1374.
- [164] C. Zybilla, H. Handwerker, H. Friedrich, in *Adv. Organomet. Chem.*, Vol. 36 (Eds.: F. G. A. Stone, R. West), Academic Press, **1994**, pp. 229-281.
- [165] M. F. Lappert, R. S. Rowe, *Coord. Chem. Rev.* **1990**, *100*, 267-292.
- [166] P. B. Glaser, T. D. Tilley, *J. Am. Chem. Soc.* **2003**, *125*, 13640-13641.
- [167] T. Watanabe, H. Hashimoto, H. Tobita, *Chem. Asian J.* **2012**, *7*, 1408-1416.
- [168] H. Sakaba, M. Tsukamoto, T. Hirata, C. Kabuto, H. Horino, *J. Am. Chem. Soc.* **2000**, *122*, 11511-11512.
- [169] H. Sakaba, H. Oike, Y. Arai, E. Kwon, *Organometallics* **2012**, *31*, 8172-8177.
- [170] B. V. Mork, T. D. Tilley, *J. Am. Chem. Soc.* **2001**, *123*, 9702-9703.
- [171] T. Watanabe, H. Hashimoto, H. Tobita, *J. Am. Chem. Soc.* **2006**, *128*, 2176-2177.
- [172] T. Watanabe, H. Hashimoto, H. Tobita, *Angew. Chem. Int. Ed.* **2004**, *43*, 218-221.
- [173] K. Ueno, M. Sakai, H. Ogino, *Organometallics* **1998**, *17*, 2138-2140.
- [174] K. Ueno, S. Asami, N. Watanabe, H. Ogino, *Organometallics* **2002**, *21*, 1326-1328.
- [175] K. Takanashi, V. Y. Lee, T. Yokoyama, A. Sekiguchi, *J. Am. Chem. Soc.* **2009**, *131*, 916-917.
- [176] N. Nakata, T. Fujita, A. Sekiguchi, *J. Am. Chem. Soc.* **2006**, *128*, 16024-16025.
- [177] V. Y. Lee, O. A. Gapurenko, V. I. Minkin, S. Horiguchi, A. Sekiguchi, *Russ. Chem. Bull.* **2016**, *65*, 1139-1141.
- [178] V. Y. Lee, S. Aoki, T. Yokoyama, S. Horiguchi, A. Sekiguchi, H. Gornitzka, J.-D. Guo, S. Nagase, *J. Am. Chem. Soc.* **2013**, *135*, 2987-2990.
- [179] H. Ogino, *Chem. Rec.* **2002**, *2*, 291-306.
- [180] R. Waterman, P. G. Hayes, T. D. Tilley, *Acc. Chem. Res.* **2007**, *40*, 712-719.
- [181] B. V. Mork, T. D. Tilley, *Angew. Chem. Int. Ed.* **2003**, *42*, 357-360.
- [182] A. C. Filippou, O. Chernov, K. W. Stumpf, G. Schnakenburg, *Angew. Chem. Int. Ed.* **2010**, *49*, 3296-3300.
- [183] A. C. Filippou, D. Hoffmann, G. Schnakenburg, *Chem. Sci.* **2017**, *8*, 6290-6299.
- [184] P. Ghana, M. I. Arz, U. Chakraborty, G. Schnakenburg, A. C. Filippou, *J. Am. Chem. Soc.* **2018**, *140*, 7187-7198.
- [185] P. G. Hayes, Z. Xu, C. Beddie, J. M. Keith, M. B. Hall, T. D. Tilley, *J. Am. Chem. Soc.* **2013**, *135*, 11780-11783.
- [186] T. Fukuda, T. Yoshimoto, H. Hashimoto, H. Tobita, *Organometallics* **2016**, *35*, 921-924.
- [187] T. Yoshimoto, H. Hashimoto, N. Hayakawa, T. Matsuo, H. Tobita, *Organometallics* **2016**, *35*, 3444-3447.
- [188] R. R. Schrock, *Chem. Rev.* **2002**, *102*, 145-180.
- [189] E. O. Fischer, in *Adv. Organomet. Chem.*, Vol. 14 (Eds.: F. G. A. Stone, R. West), Academic Press, **1976**, pp. 1-32.
- [190] T. Yoshimoto, H. Hashimoto, N. Takagi, S. Sakaki, N. Hayakawa, T. Matsuo, H. Tobita, *Chem. Eur. J.* **2019**, *25*, 3795-3798.
- [191] A. C. Filippou, O. Chernov, G. Schnakenburg, *Angew. Chem. Int. Ed.* **2011**, *50*, 1122-1126.
- [192] A. C. Filippou, B. Baars, O. Chernov, Y. N. Lebedev, G. Schnakenburg, *Angew. Chem. Int. Ed.* **2014**, *53*, 565-570.
- [193] H. Hashimoto, H. Tobita, *Coord. Chem. Rev.* **2017**.
- [194] J. Y. Corey, *Chem. Rev.* **2011**, *111*, 863-1071.
- [195] J. Y. Corey, J. Braddock-Wilking, *Chem. Rev.* **1999**, *99*, 175-292.
- [196] M. Suginome, Y. Ito, *Chem. Rev.* **2000**, *100*, 3221-3256.
- [197] E. A. Zarate, C. A. Tessier-Youngs, W. J. Youngs, *J. Am. Chem. Soc.* **1988**, *110*, 4068-4070.
- [198] N. B. Bespalova, M. A. Bovina, A. V. Popov, J. C. Mol, *J. Mol. Catal. A: Chem.* **2000**, *160*, 157-164.
- [199] W. G. Sly, *J. Am. Chem. Soc.* **1959**, *81*, 18-20.
- [200] H. W. Sternberg, H. Greenfield, R. A. Friedel, J. Wotiz, R. Markby, I. Wender, *J. Am. Chem. Soc.* **1954**, *76*, 1457-1458.

- [201] W. I. Bailey, M. H. Chisholm, F. A. Cotton, L. A. Rankel, *J. Am. Chem. Soc.* **1978**, *100*, 5764-5773.
- [202] E. J. Forbes, N. Goodhand, T. A. Hamor, N. Iranpoor, *J. Fluorine Chem.* **1980**, *16*, 339-350.
- [203] P. M. Boorman, M. Wang, M. Parvez, *J. Chem. Soc., Dalton Trans.* **1996**, 4533-4542.
- [204] Q. Feng, M. L. H. Green, P. Mountford, *J. Chem. Soc., Dalton Trans.* **1992**, 2171-2181.
- [205] M. L. H. Green, P. C. McGowan, P. Mountford, *J. Chem. Soc., Dalton Trans.* **1995**, 1207-1214.
- [206] L. T. Byrne, C. S. Griffith, G. A. Koutsantonis, B. W. Skelton, A. H. White, *J. Chem. Soc., Dalton Trans.* **1998**, 1575-1580.
- [207] J. C. Stichbury, M. J. Mays, J. E. Davies, P. R. Raithby, G. P. Shields, *J. Chem. Soc., Dalton Trans.* **1997**, 2309-2314.
- [208] P. C. Dos Santos, D. R. Dean, Y. Hu, M. W. Ribbe, *Chem. Rev.* **2004**, *104*, 1159-1174.
- [209] E. Sappa, A. Tiripicchio, P. Braunstein, *Chem. Rev.* **1983**, *83*, 203-239.
- [210] I. Yuji, T. Fumihide, W. Hachiro, *Bull. Chem. Soc. Jpn.* **1970**, *43*, 1520-1523.
- [211] M. F. D'Agostino, M. J. McGlinchey, *Polyhedron* **1988**, *7*, 807-825.
- [212] R. Wilczynski, L. G. Sneddon, *J. Am. Chem. Soc.* **1980**, *102*, 2857-2858.
- [213] E. A. Zarate, C. A. Tessier-Youngs, W. J. Youngs, *J. Chem. Soc., Chem. Commun.* **1989**, 577-578.
- [214] L. Rosenberg, M. D. Fryzuk, S. J. Rettig, *Organometallics* **1999**, *18*, 958-969.
- [215] S. Shimada, Y.-H. Li, M. L. N. Rao, M. Tanaka, *Organometallics* **2006**, *25*, 3796-3798.
- [216] S. Bourg, B. Boury, F. Carré, R. J. P. Corriu, *Organometallics* **1997**, *16*, 3097-3099.
- [217] S. Bourg, B. Boury, F. H. Carré, R. J. P. Corriu, *Organometallics* **1998**, *17*, 167-172.
- [218] H. Arii, M. Takahashi, M. Nanjo, K. Mochida, *Organometallics* **2011**, *30*, 917-920.
- [219] R. S. Simons, K. J. Galat, J. D. Bradshaw, W. J. Youngs, C. A. Tessier, G. Aullón, S. Alvarez, *J. Organomet. Chem.* **2001**, *628*, 241-254.
- [220] H. Hashimoto, Y. Sekiguchi, T. Iwamoto, C. Kabuto, M. Kira, *Organometallics* **2002**, *21*, 454-456.
- [221] M. Auburn, M. Ciriano, J. A. K. Howard, M. Murray, N. J. Pugh, J. L. Spencer, F. G. A. Stone, P. Woodward, *J. Chem. Soc., Dalton Trans.* **1980**, 659-666.
- [222] G. L. Simon, L. F. Dahl, *J. Am. Chem. Soc.* **1973**, *95*, 783-789.
- [223] M. M. Crozat, S. F. Watkins, *J. Chem. Soc., Dalton Trans.* **1972**, 2512-2515.
- [224] M. Cowie, M. J. Bennett, *Inorg. Chem.* **1977**, *16*, 2325-2329.
- [225] M. Van Tiel, K. M. Mackay, B. K. Nicholson, *J. Organomet. Chem.* **1993**, *462*, 79-87.
- [226] W. D. Wang, S. I. Hommeltoft, R. Eisenberg, *Organometallics* **1988**, *7*, 2417-2419.
- [227] S. G. Anema, S. K. Lee, K. M. Mackay, B. K. Nicholson, *J. Organomet. Chem.* **1993**, *444*, 211-218.
- [228] G. Hencken, E. Weiss, *Chem. Ber.* **1973**, *106*, 1747-1751.
- [229] M. Stosur, A. Kochel, A. Keller, T. Szymańska-Buzar, *Organometallics* **2006**, *25*, 3791-3794.
- [230] M. Tanabe, K. Osakada, *Organometallics* **2010**, *29*, 4702-4710.
- [231] P. Jena, Q. Sun, *Chem. Rev.* **2018**, *118*, 5755-5870.
- [232] R. H. Heyn, T. D. Tilley, *J. Am. Chem. Soc.* **1992**, *114*, 1917-1919.
- [233] W. D. Wang, R. Eisenberg, *J. Am. Chem. Soc.* **1990**, *112*, 1833-1841.
- [234] S. Shimada, M. L. N. Rao, T. Hayashi, M. Tanaka, *Angew. Chem. Int. Ed.* **2001**, *40*, 213-216.
- [235] C. Eisenhut, S. Inoue, *Phosphorus Sulfur Silicon Rel. Elem.* **2016**, *191*, 605-608.
- [236] G. Maier, S. Pfruem, U. Schäfer, R. Matusch, *Angew. Chem. Int. Ed. Engl.* **1978**, *17*, 520-521.

12 Appendix

12.1 Supporting Information for Chapter 7

Electronic Supplementary Material (ESI) for Dalton Transactions.
This journal is © The Royal Society of Chemistry 2019

Electronic Supplementary Information ESI

**Reactivity of an NHC-stabilized Pyramidal Hydrosilylene with
Electrophilic Boron Sources**

Gizem Dübek, Daniel Franz, Carsten Eisenhut, Philipp J. Altmann, Shigeyoshi Inoue*

Department of Chemistry, WACKER-Institute of Silicon Chemistry and Catalysis Research Centre,
Technische Universität München, Lichtenbergstr. 4, 85748 Garching bei München, Germany

Table of Contents

I. NMR Spectra	2
II. Mass Spectra	21
III. IR Spectrum	23
IV. Single-Crystal X-ray structure determination	24

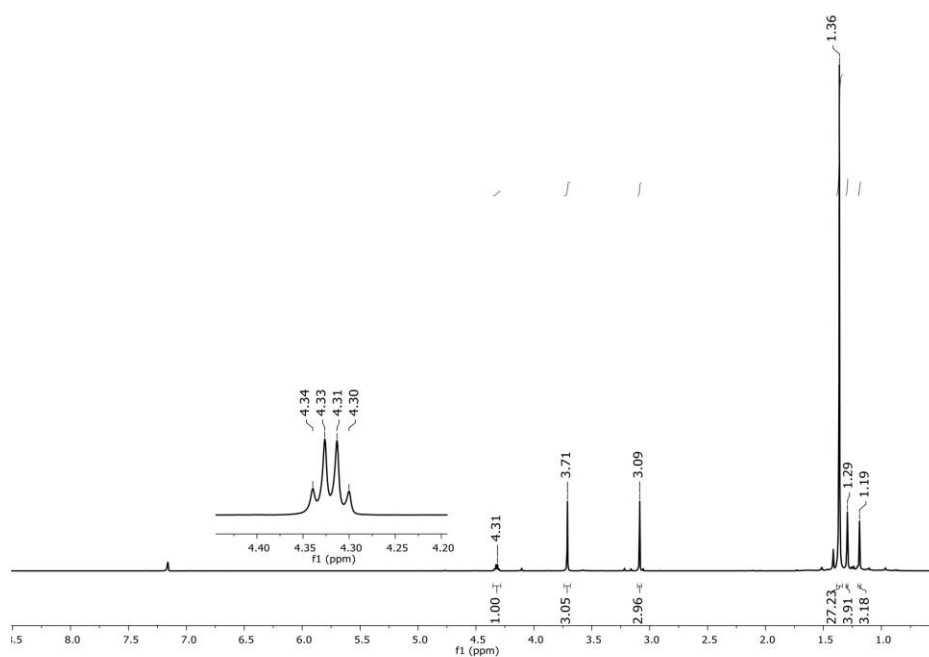
I. NMR Spectra

Figure S1. ^1H NMR of compound **1** \rightarrow BH_3 in C_6D_6 at $25\text{ }^\circ\text{C}$.

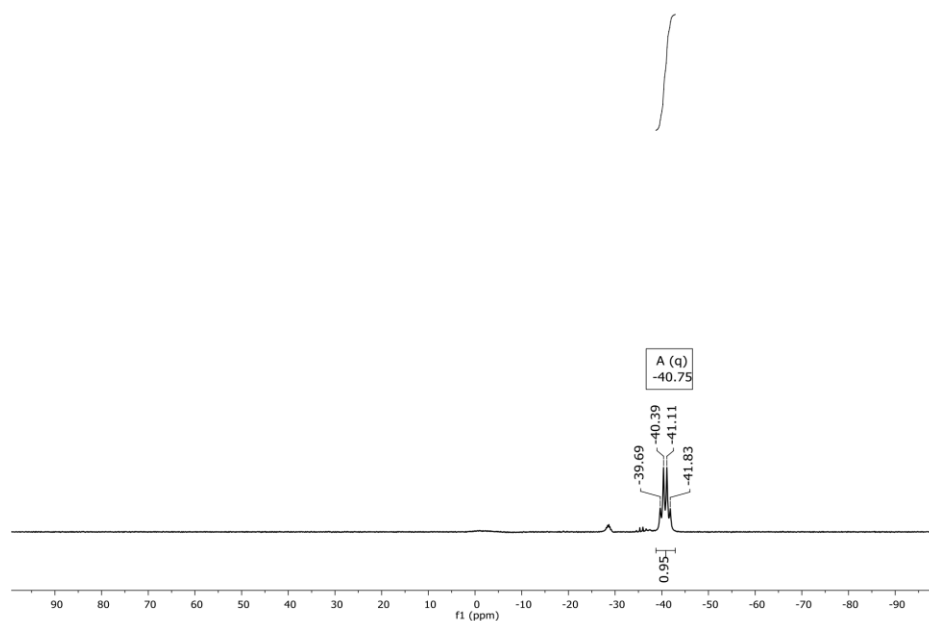


Figure S2. ^{11}B NMR spectrum of compound $1\rightarrow\text{BH}_3$ in C_6D_6 at 25 °C.

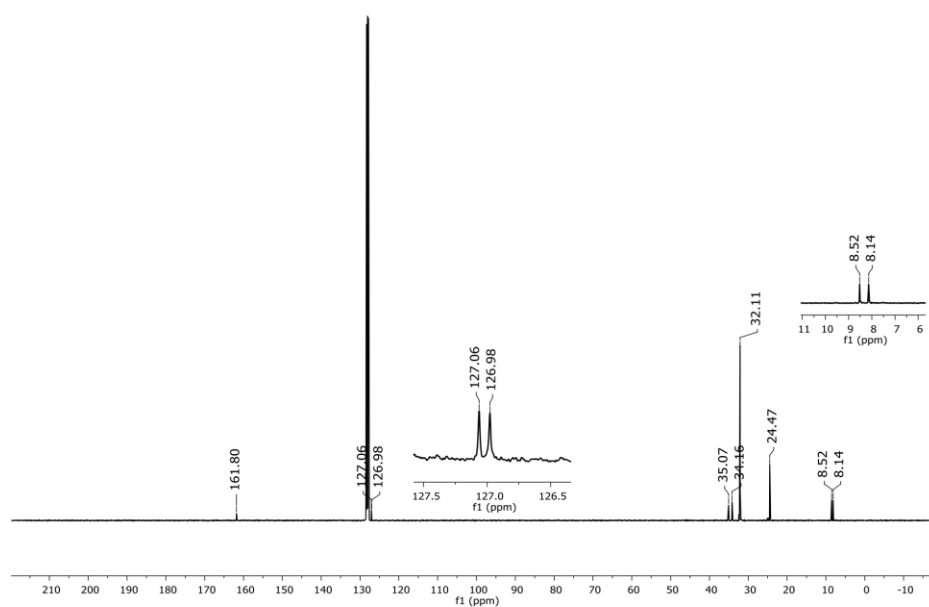


Figure S3. ^{13}C NMR spectrum of compound $1\rightarrow\text{BH}_3$ in C_6D_6 at 25 °C.

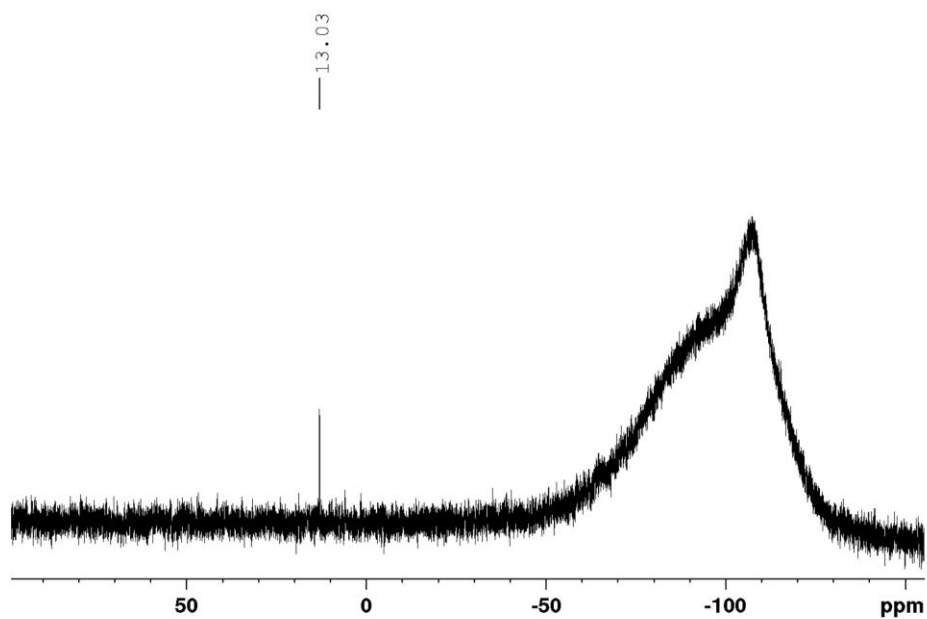


Figure S4. $^{29}\text{Si}\{^1\text{H}\}$ NMR spectrum of compound $\mathbf{1}\rightarrow\text{BH}_3$ in C_6D_6 at 25 °C.

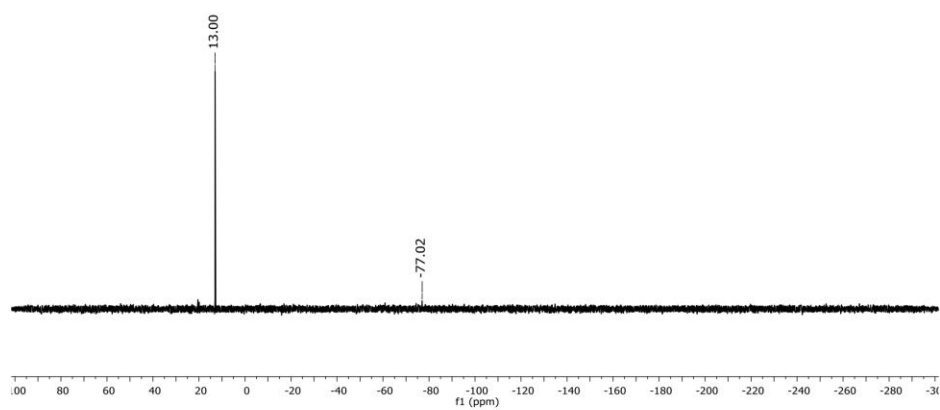


Figure S5. $^{29}\text{Si}\{^1\text{H}\}$ INEPT NMR spectrum of compound $\mathbf{1}\rightarrow\text{BH}_3$ in C_6D_6 at 25 °C.

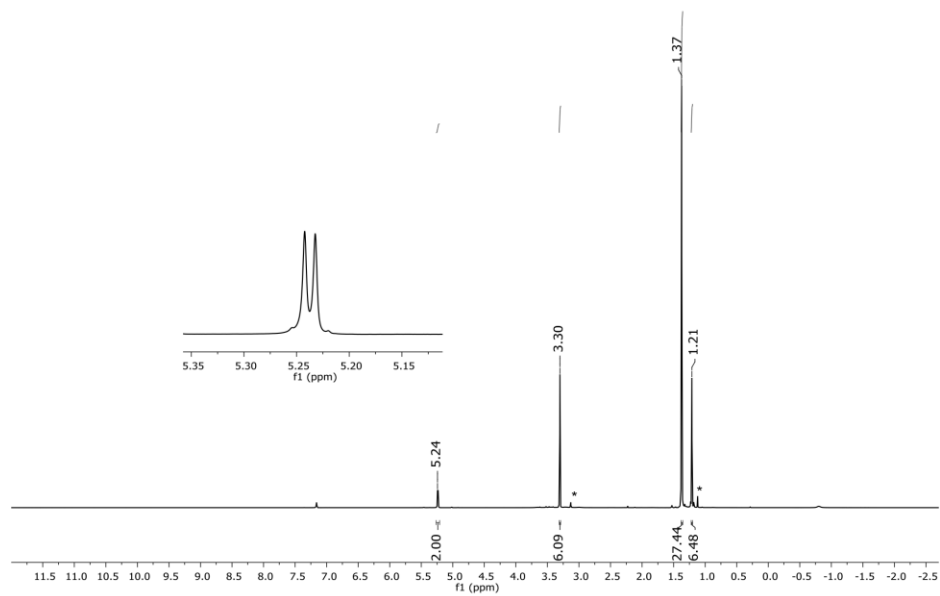


Figure S6. ^1H NMR spectrum of compound **2** in C_6D_6 at $25\text{ }^\circ\text{C}$. (*: $\text{tBu}_3\text{SiSiH}_3$, 2%)

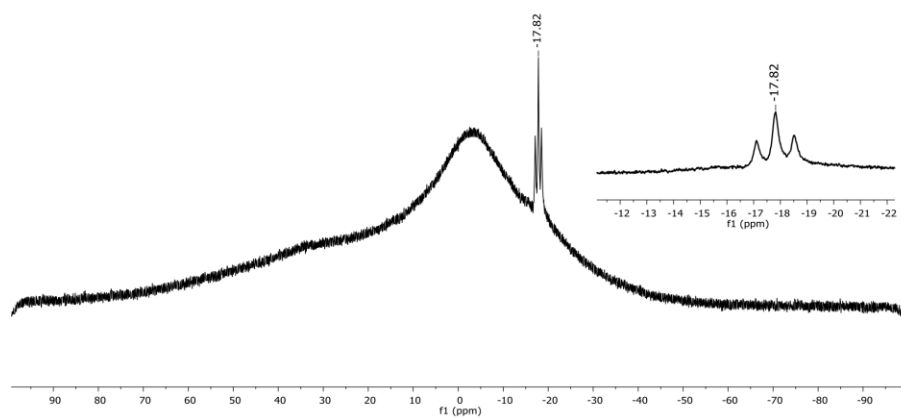


Figure S7. ^{11}B NMR spectrum of compound **2** in C_6D_6 at $25\text{ }^\circ\text{C}$.

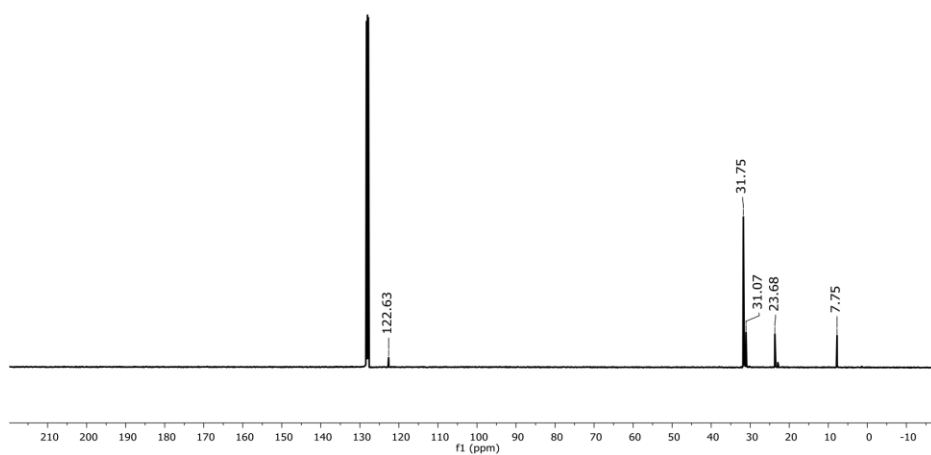


Figure S8. $^{13}\text{C}\{^1\text{H}\}$ NMR spectrum of compound **2** in C_6D_6 at 25 °C.

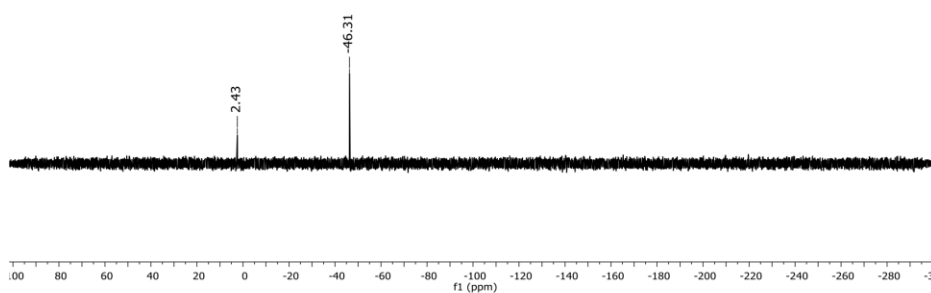


Figure S9. $^{29}\text{Si}\{^1\text{H}\}$ NMR spectrum of compound **2** in C_6D_6 at 25 °C.

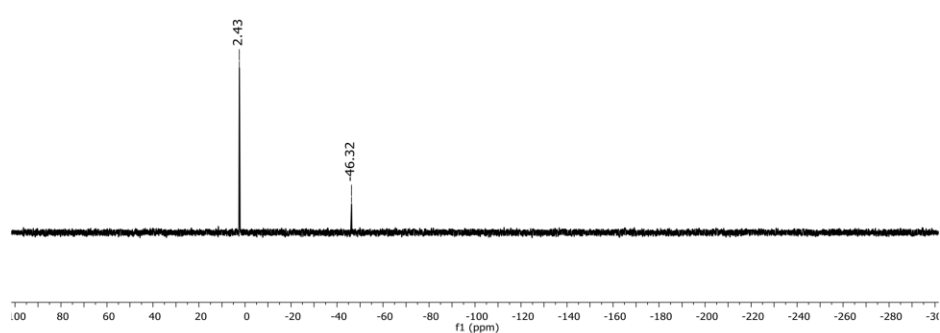


Figure S10. $^{29}\text{Si}\{^1\text{H}\}$ INEPT NMR spectrum of compound **2** in C_6D_6 at 25 °C.

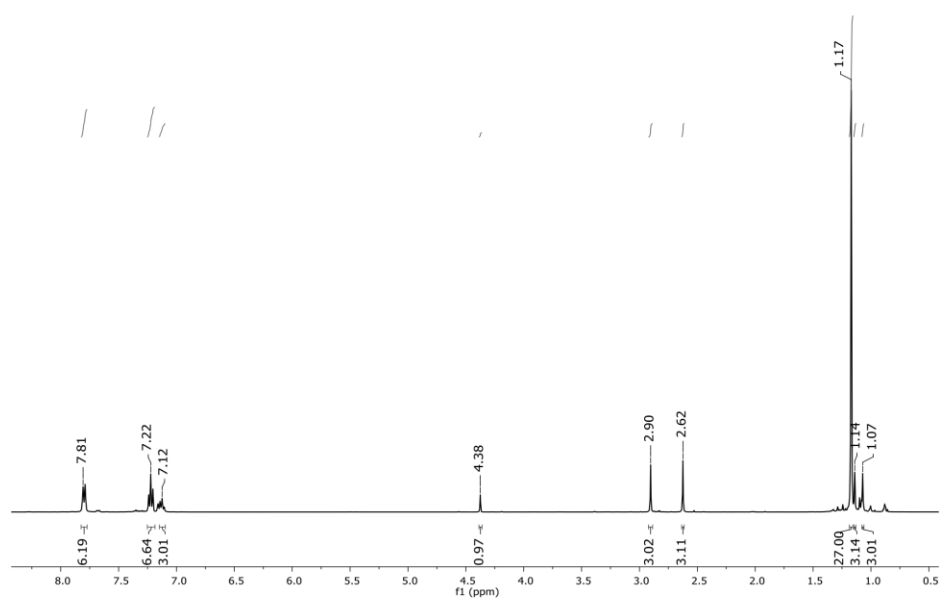


Figure S11. ^1H NMR spectrum of compound **1** $\rightarrow\text{BPh}_3$ in C_6D_6 at 25 °C.

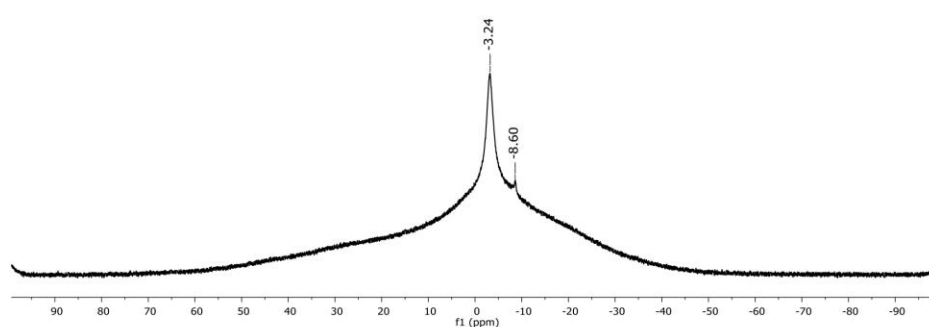


Figure S12. ^{11}B NMR spectrum of compound **1**- BPh_3 in C_6D_6 at 25 °C.

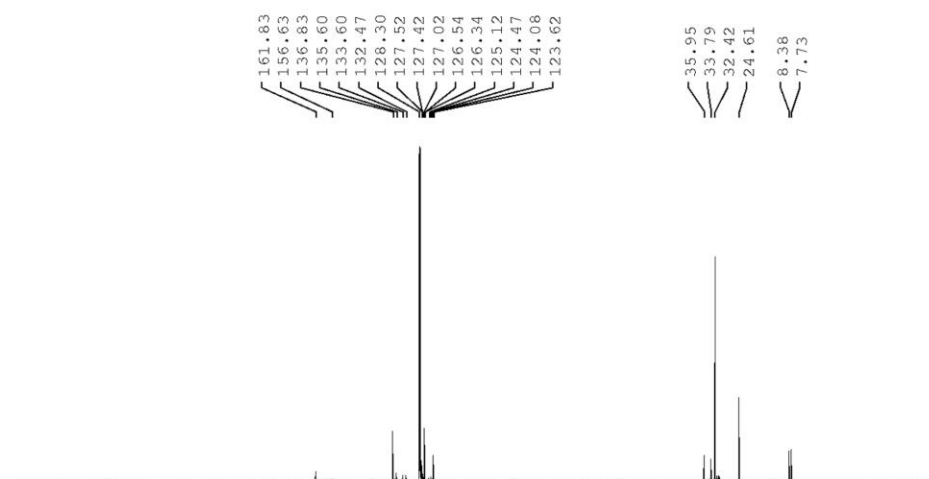


Figure S13. $^{13}\text{C}\{^1\text{H}\}$ NMR spectrum of compound **1**- BPh_3 in C_6D_6 at 25 °C.

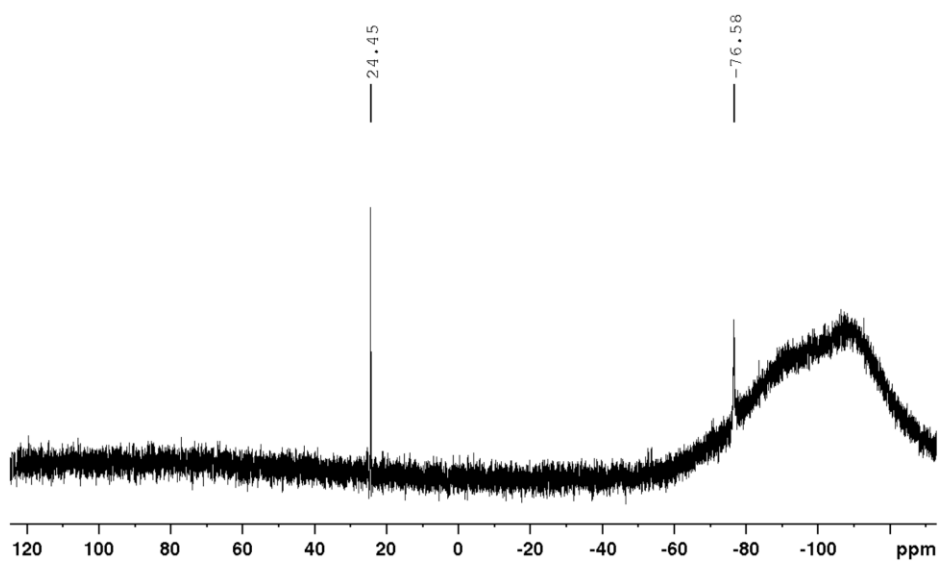


Figure S14. $^{29}\text{Si}\{^1\text{H}\}$ NMR spectrum of compound **1**- BPh_3 in C_6D_6 at 25 °C.

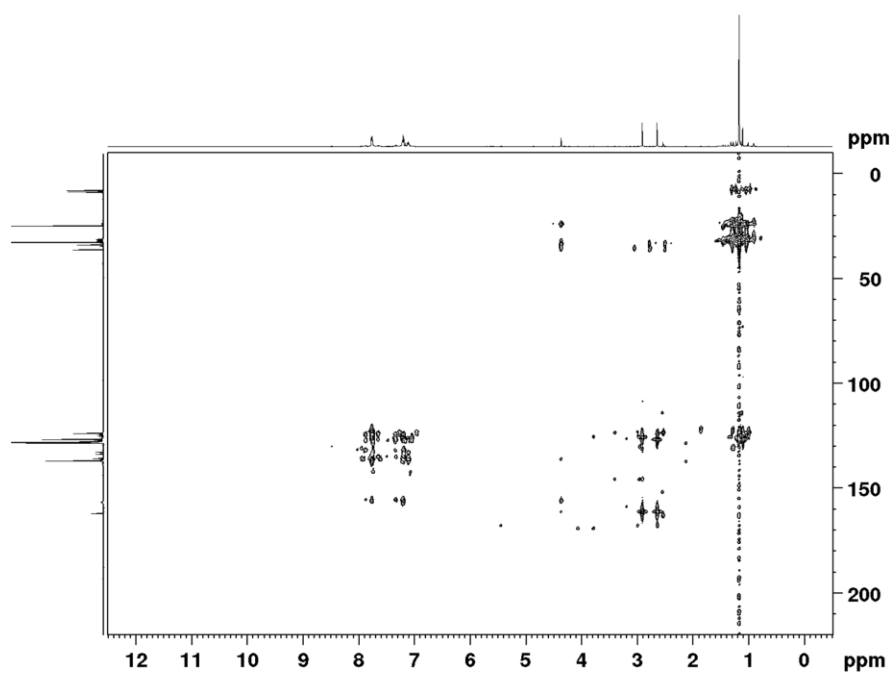


Figure S15. ^1H - ^{13}C -HMBC NMR spectrum of compound **1**- BPh_3 in C_6D_6 at 25 °C.

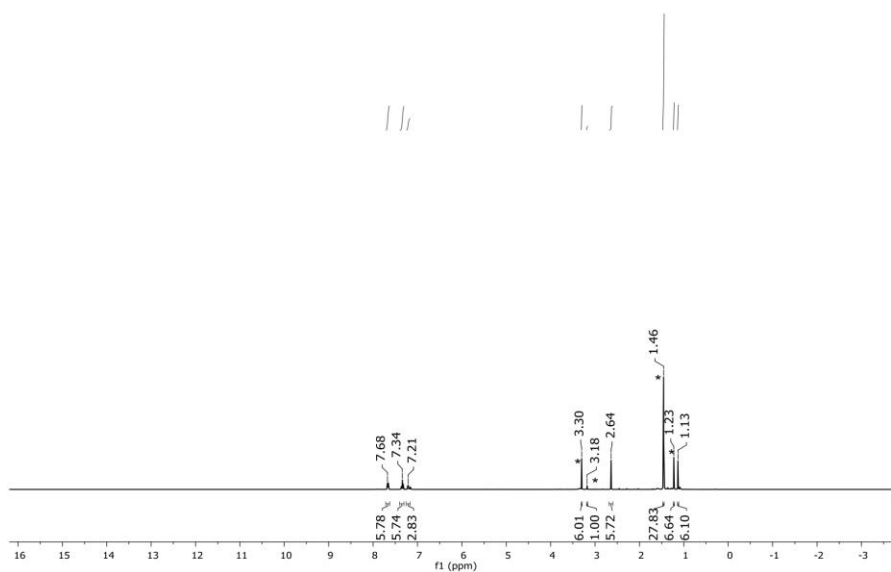


Figure S16. ^1H NMR spectrum of the reaction of compound $\mathbf{1} \rightarrow \text{BPh}_3$ with 1 equivalent of L^{Me_4} in C_6D_6 at 25°C . (*: $\text{tBu}_3\text{SiSi(H)L}^{\text{Me}_4}$, $\mathbf{1}$)

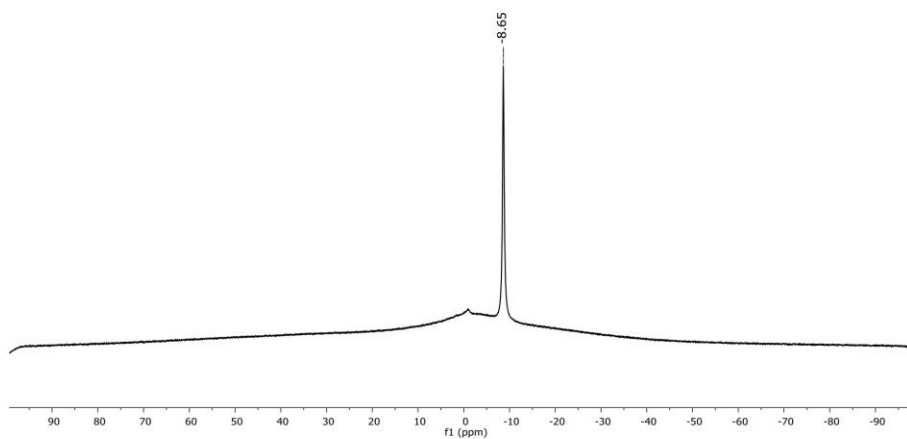


Figure S17. ^{11}B NMR spectrum of the reaction of compound $\mathbf{1} \rightarrow \text{BPh}_3$ with 1 equivalent of L^{Me_4} in C_6D_6 at 25°C .

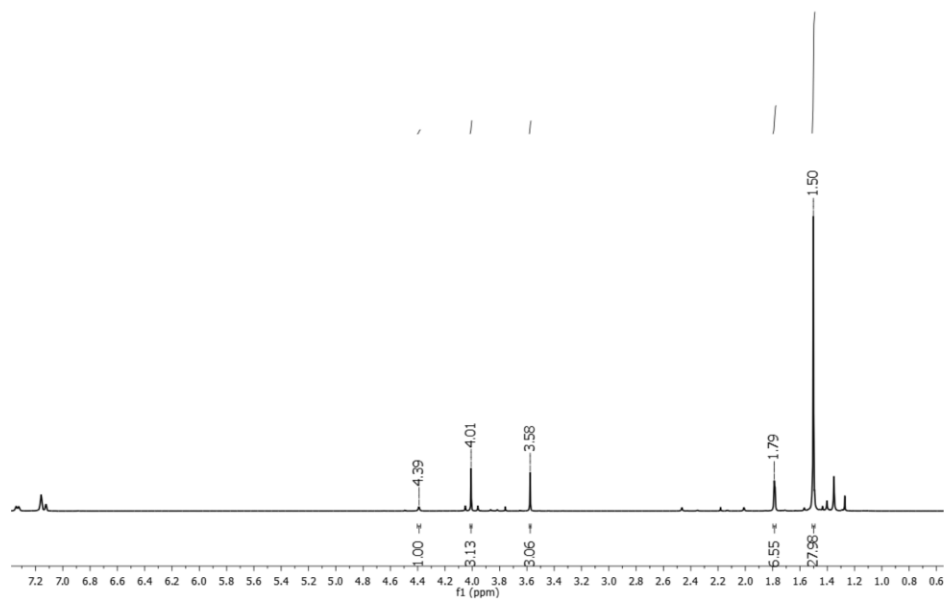


Figure S18. ^1H NMR spectrum of the compound $\mathbf{1}\cdot\text{BF}_3$ in $\text{C}_6\text{D}_5\text{F}$ at 25 °C.

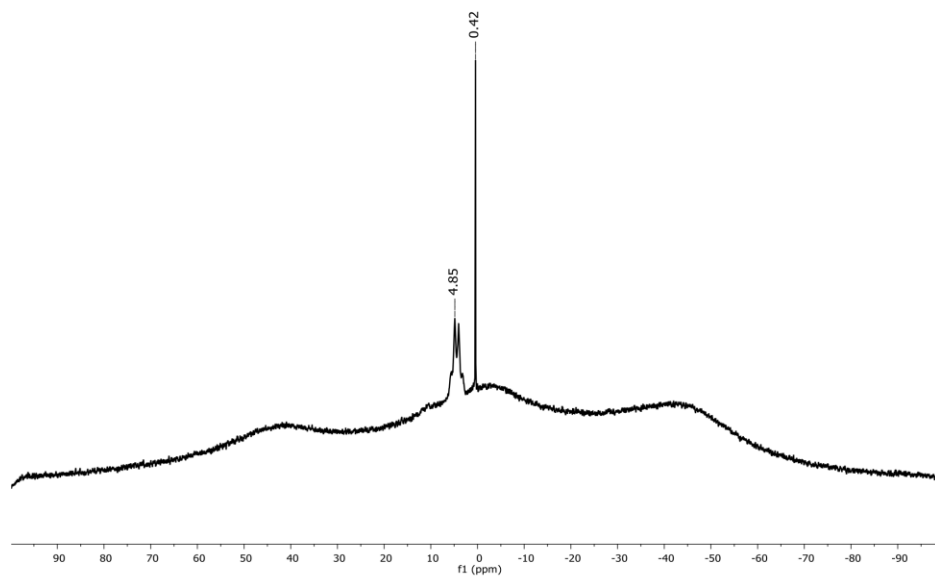


Figure S19. ^{11}B NMR spectrum of the compound $\mathbf{1}\cdot\text{BF}_3$ in $\text{C}_6\text{D}_5\text{F}$ at 25 °C.

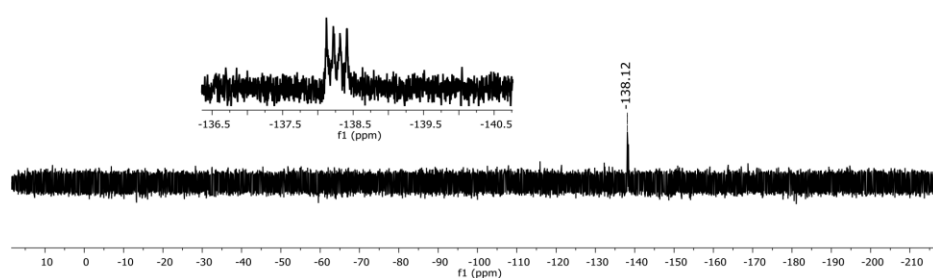


Figure S20. ^{19}F NMR spectrum of the compound $1\cdot\text{BF}_3$ in C_6D_6 at $25\text{ }^\circ\text{C}$. (RT 1 h)

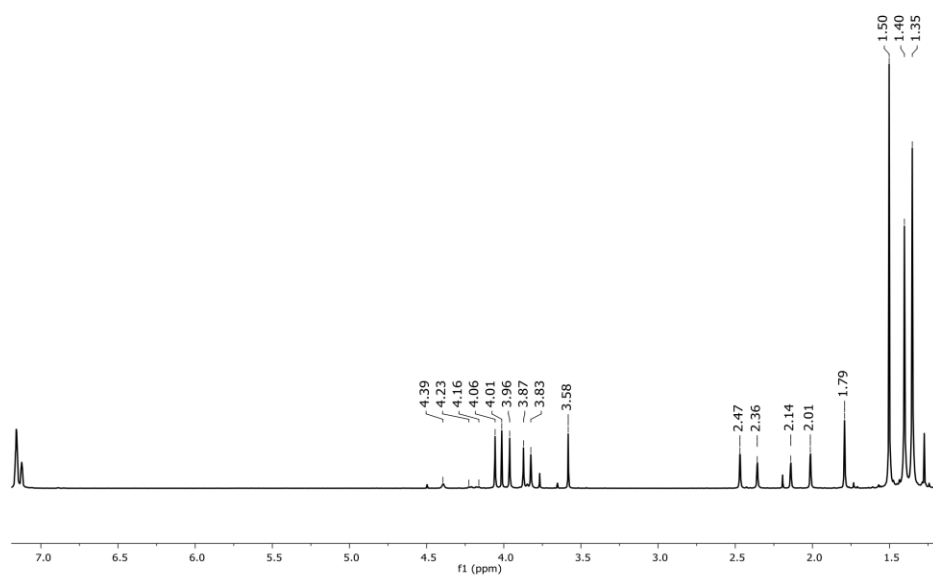


Figure S21. ^1H NMR spectrum of the compound $1\cdot\text{BF}_3$ in $\text{C}_6\text{D}_5\text{F}$ at $25\text{ }^\circ\text{C}$ after 20 hrs.

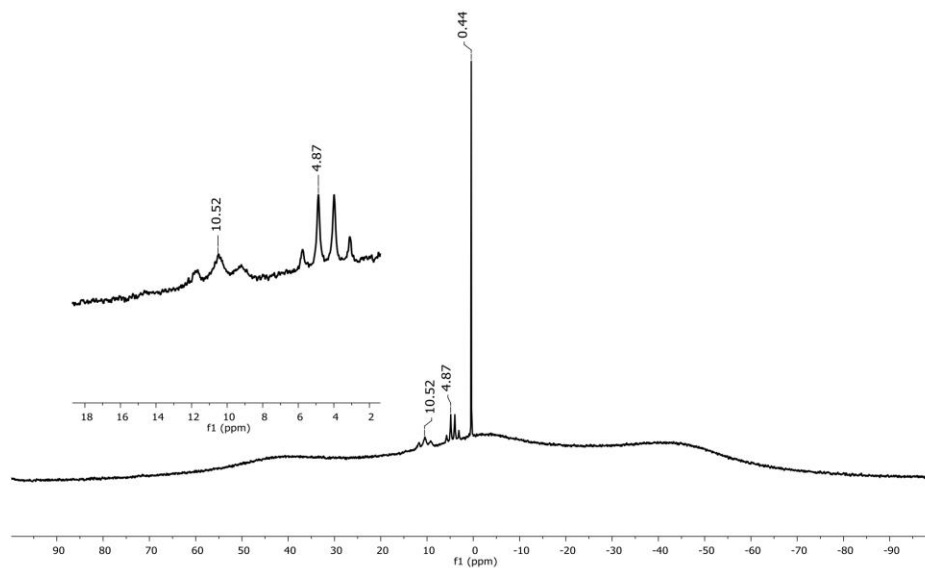


Figure S22. ^{11}B NMR spectrum of the compound $1\cdot\text{BF}_3$ in $\text{C}_6\text{D}_5\text{F}$ at 25 °C after 20 hrs.

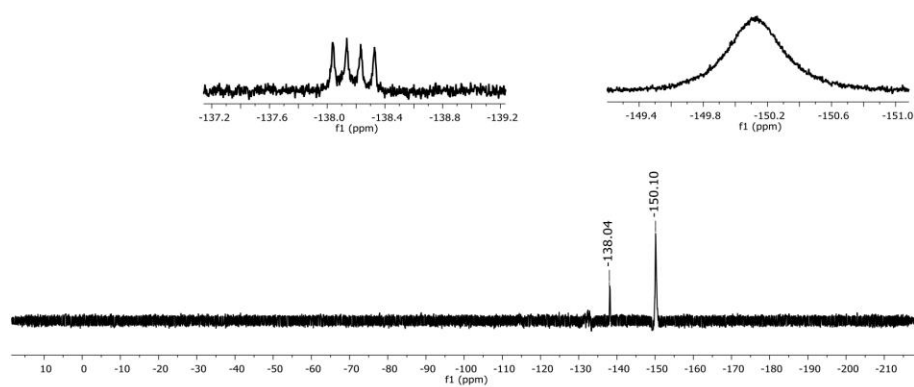


Figure S23. ^{19}F NMR spectrum of the compound $1\cdot\text{BF}_3$ in C_6D_6 at 25 °C after heating 70 °C 1h.

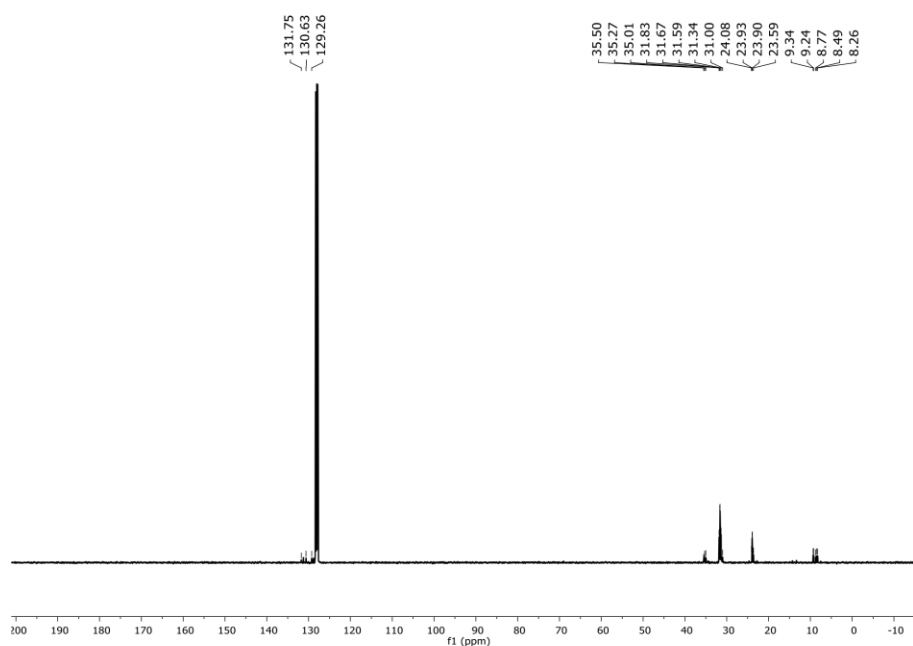


Figure S24. $^{13}\text{C}\{^1\text{H}\}$ NMR spectrum of the compound $1\cdot\text{BF}_3$ in C_6D_6 at 25 °C after heating 70 °C 1h.

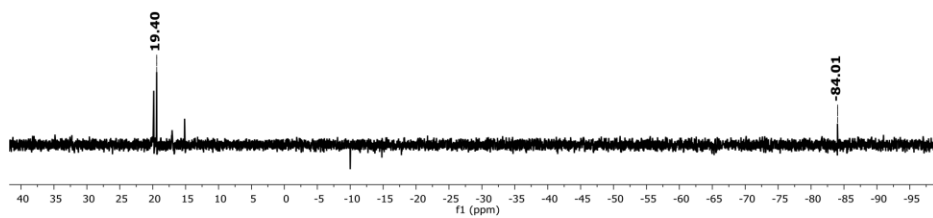


Figure S25. $^{29}\text{Si}\{^1\text{H}\}$ spectrum of the compound $1\cdot\text{BF}_3$ in $\text{C}_6\text{D}_5\text{F}$ at 25 °C after 20 hours.

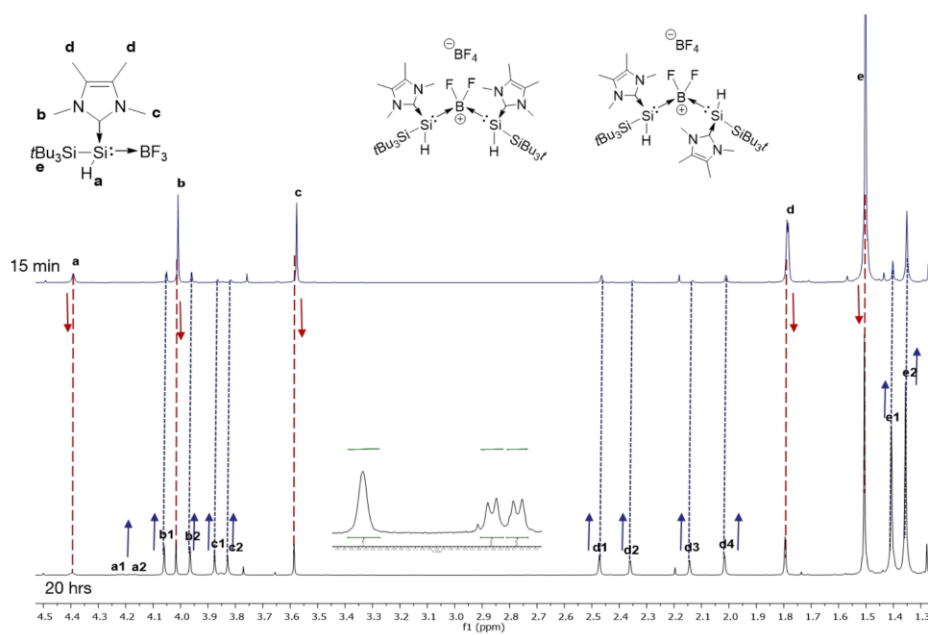


Figure S26. Comparison of ^1H NMR spectrum for $\mathbf{1}\cdot\text{BF}_3$ in $\text{C}_6\text{D}_5\text{F}$ at 25°C after 15 min and 20 hours.

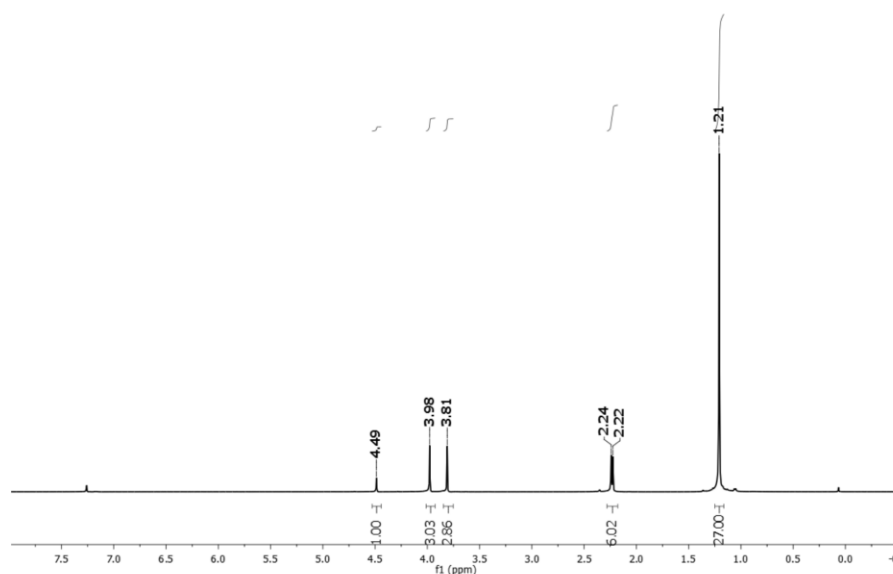


Figure S27. ^1H NMR spectrum of compound $\mathbf{1}\cdot\text{BCl}_3$ in CD_3Cl at 25°C .

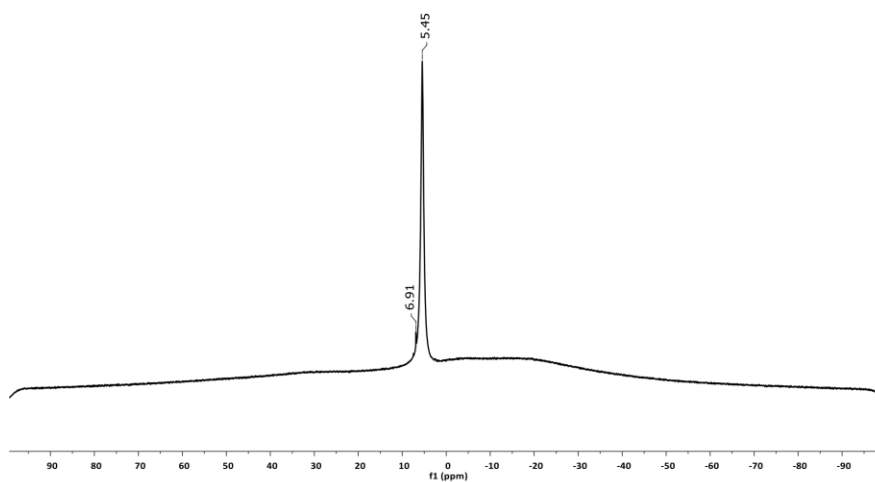


Figure S28. ^{11}B NMR spectrum of compound $1\cdot\text{BCl}_3$ in CD_2Cl_2 at 25 °C.

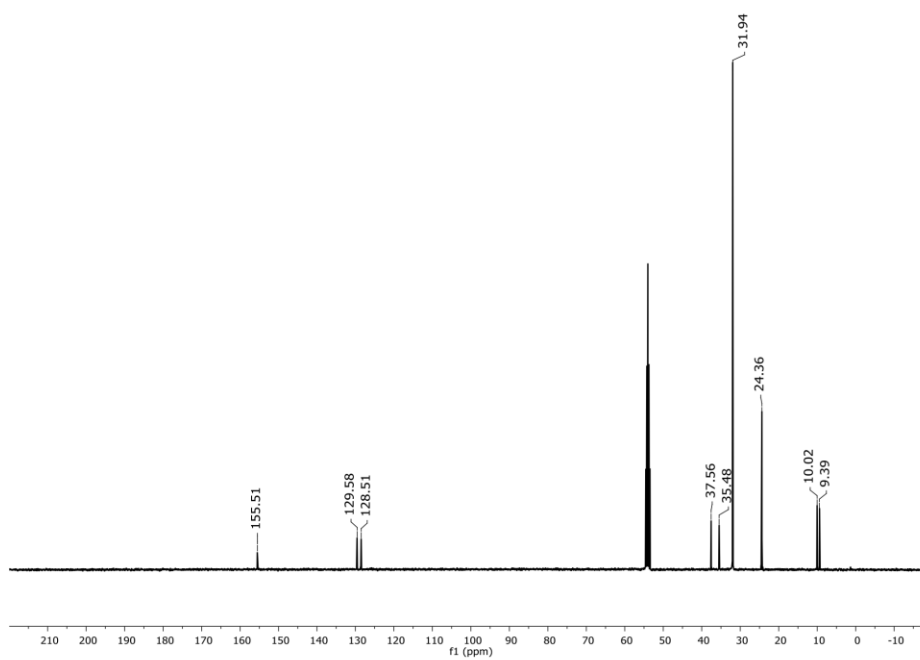


Figure S29. $^{13}\text{C}\{^1\text{H}\}$ NMR spectrum of compound $1\cdot\text{BCl}_3$ in CD_2Cl_2 at 25 °C.

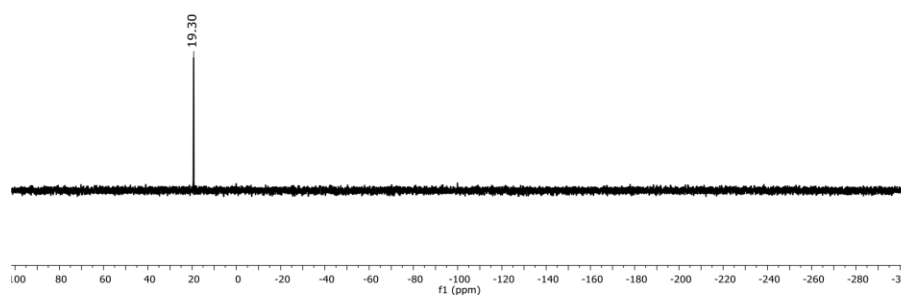


Figure S30. $^{29}\text{Si}\{^1\text{H}\}$ INEPT spectrum of compound $\mathbf{1}\cdot\text{BCl}_3$ in CD_2Cl_2 at 25 °C.

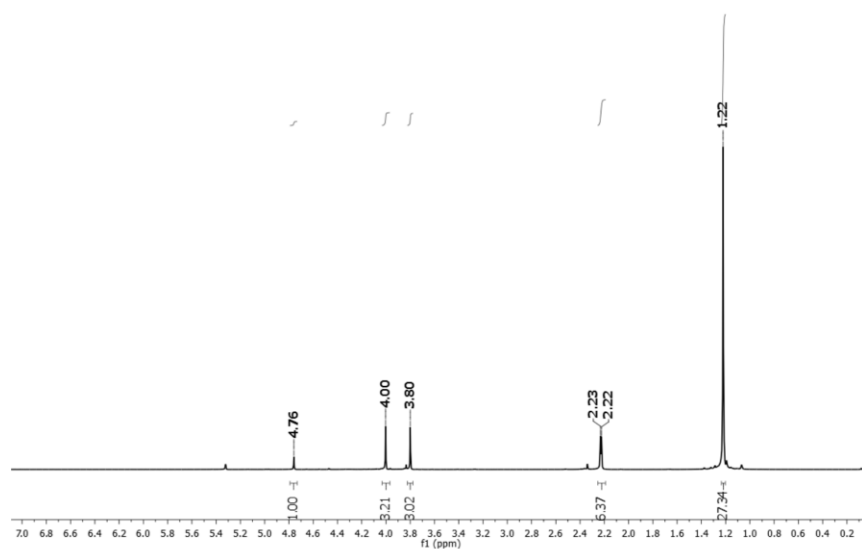


Figure S31. ^1H NMR spectrum of compound $\mathbf{1}\rightarrow\text{BBr}_3$ in CD_2Cl_2 at 25 °C.

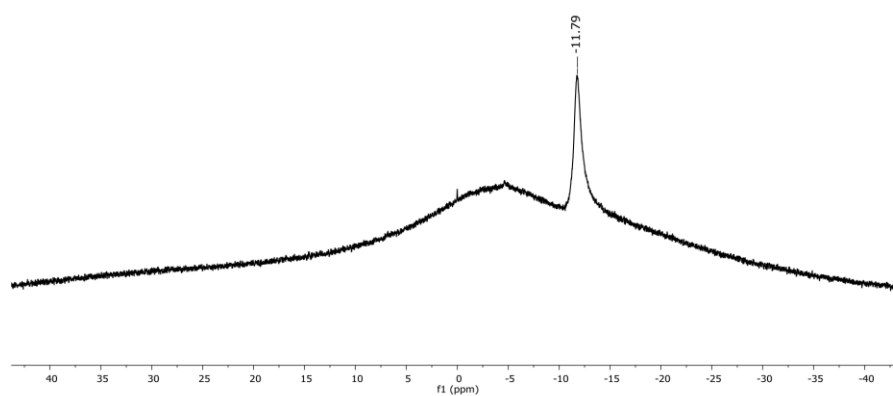


Figure S32. ^{11}B NMR spectrum of compound **1** \rightarrow BBr_3 in CD_2Cl_2 at 25 $^\circ\text{C}$.

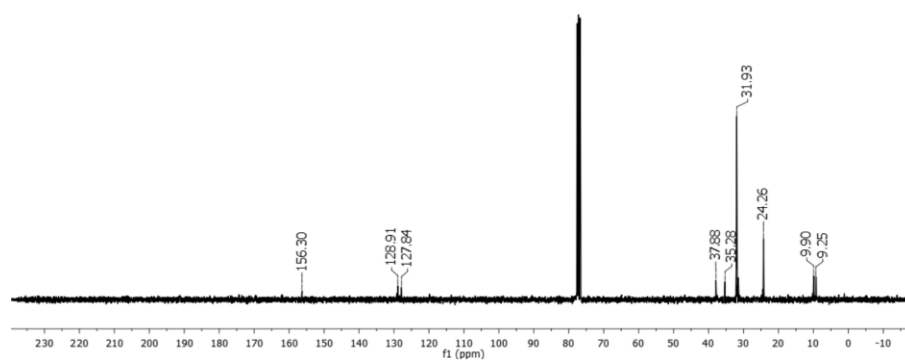


Figure S33. $^{13}\text{C}\{^1\text{H}\}$ NMR spectrum of **1** \rightarrow BBr_3 in CD_3Cl at 25 $^\circ\text{C}$.

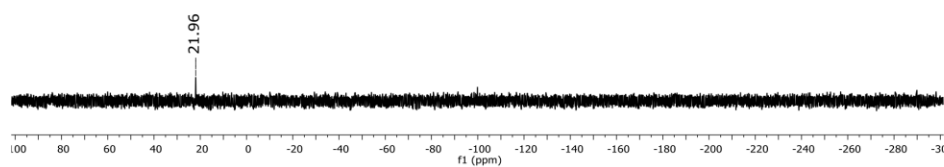


Figure S34. $^{29}\text{Si}\{^1\text{H}\}$ INEPT spectrum of compound $1 \rightarrow \text{BBr}_3$ in CD_3Cl at 25°C .

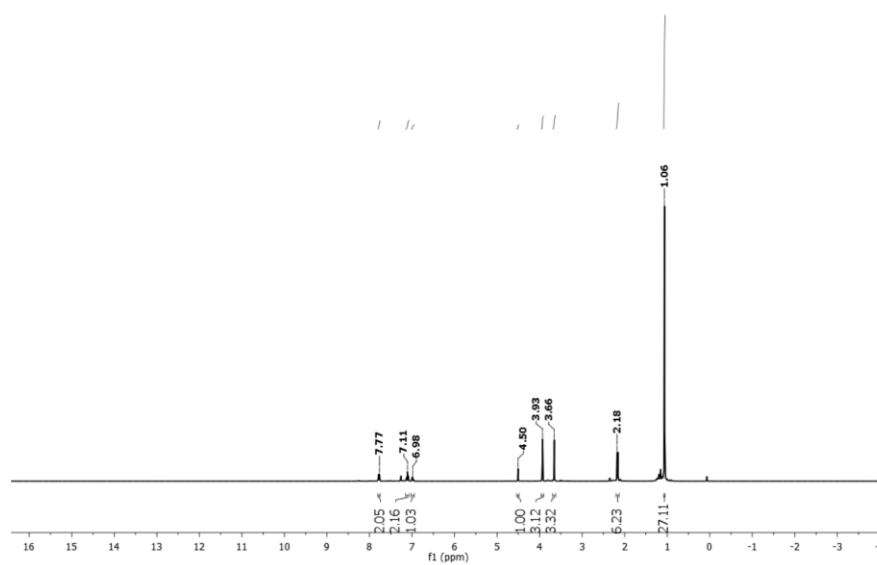


Figure S35. ^1H NMR spectrum of the compound $1 \rightarrow \text{BPhBr}_2$ in CD_3Cl at 25°C .

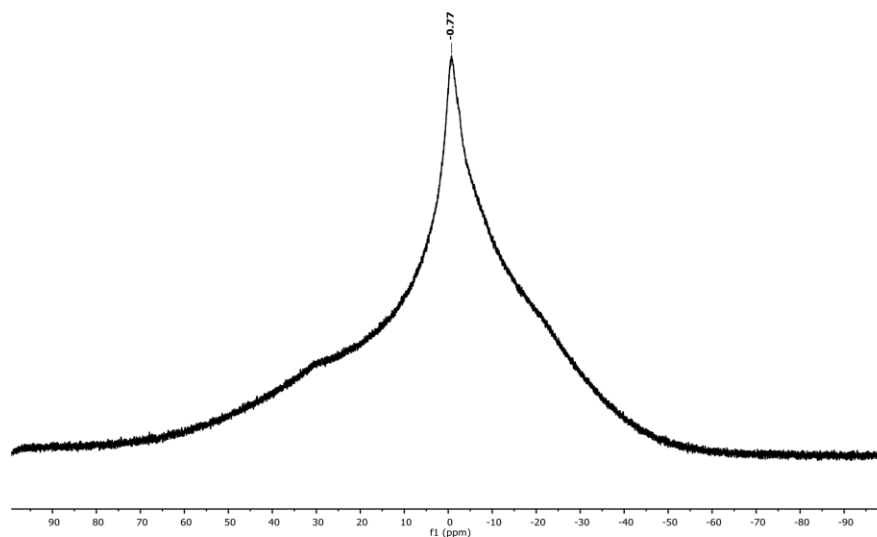


Figure S36. ^{11}B NMR spectrum of the compound $1\rightarrow\text{BPhBr}_2$ in CD_3Cl at $25\text{ }^\circ\text{C}$.

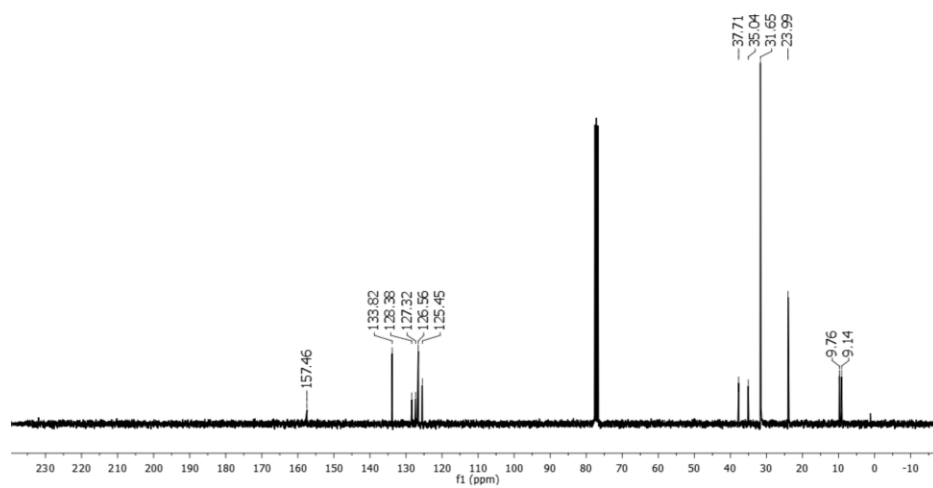


Figure S37. $^{13}\text{C}\{^1\text{H}\}$ NMR spectrum of the compound $1\rightarrow\text{BPhBr}_2$ in CD_3Cl at $25\text{ }^\circ\text{C}$.

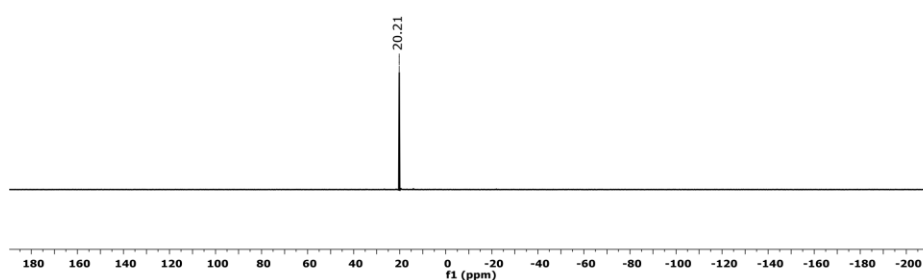


Figure S38. $^{29}\text{Si}\{^1\text{H}\}$ INEPT spectrum of the compound $1\rightarrow\text{BPhBr}_2$ in CD_3Cl at $25\text{ }^\circ\text{C}$.

II. Mass Spectra

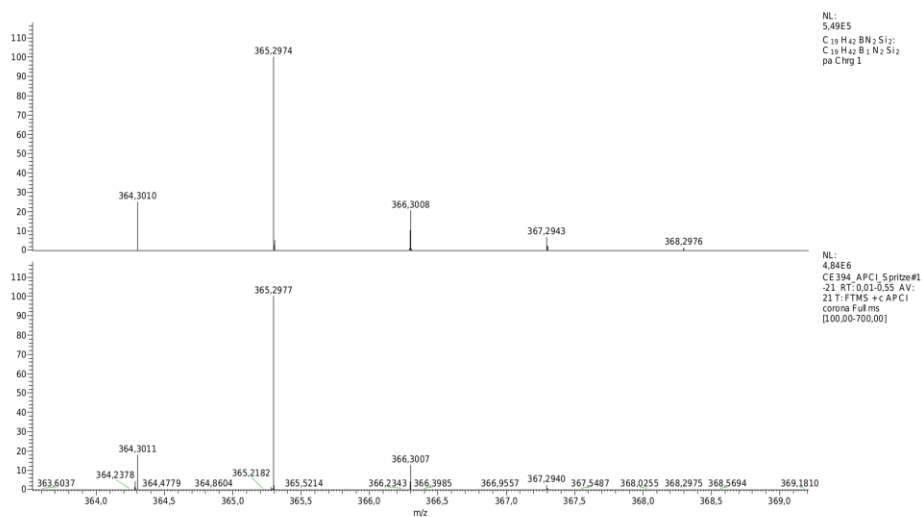


Figure S39. APCI-HRMS of $[\text{M} - \text{H}]^+$ signal of $1\rightarrow\text{BH}_3$. Top (theor.) Bottom (expt.)

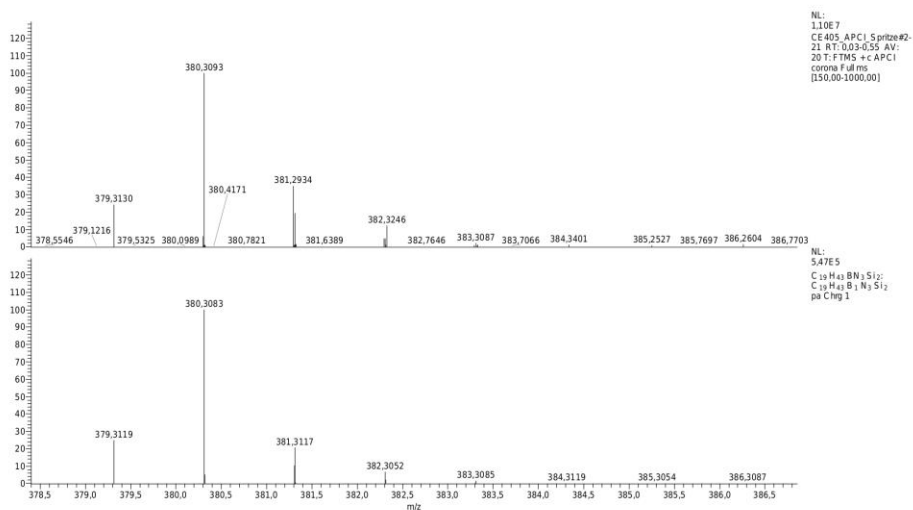


Figure S40. APCI-HRMS of $[M - H]^+$ Signal of **2**. Top (expt.) Bottom (theor.).

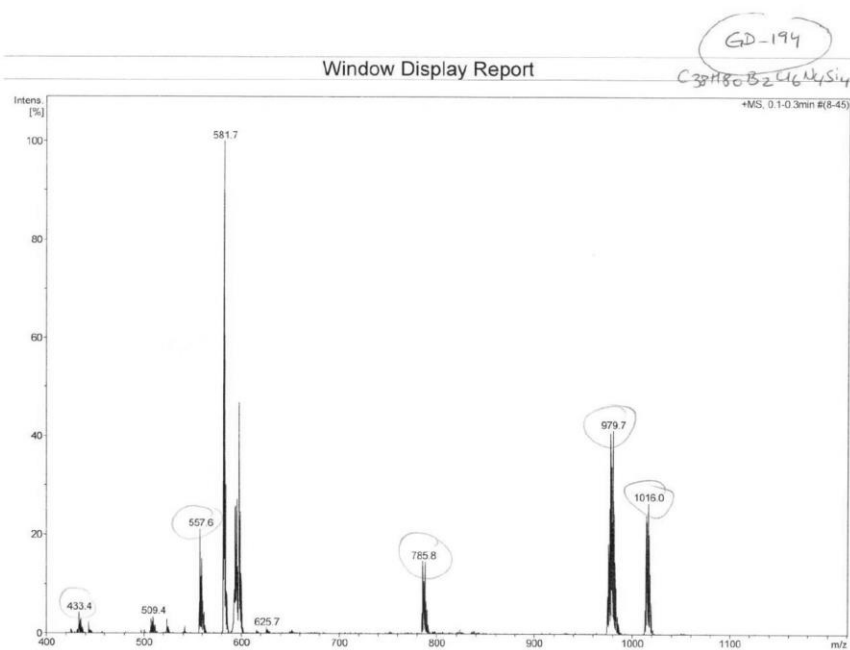


Figure S41. Scan of the original printout from the ESI measurement (positive mode) of **1-BCl₃** (sample provided in CH₃CN solution). See Figure S42 for signal assignment.

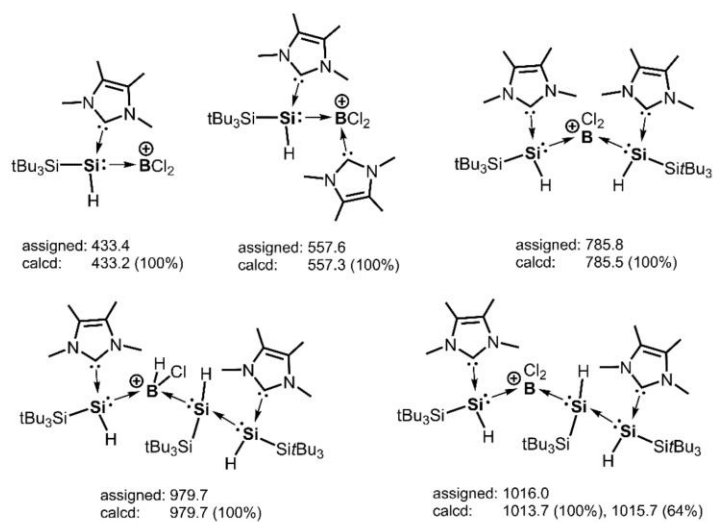


Figure S42. Suggested molecular structures derived from the stoichiometries assigned to the mass spectrum signals in Figure S41.

III. IR Spectrum

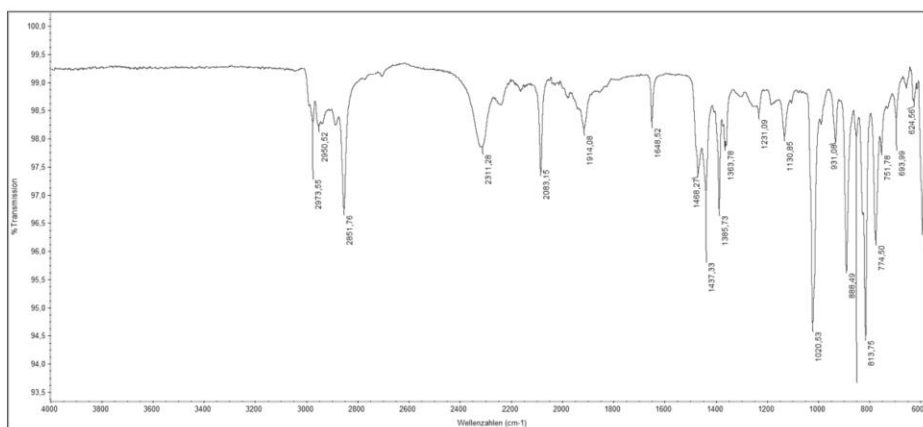


Figure S43. IR spectrum (no matrix) of compound $1 \rightarrow \text{BH}_3$

IV. Single-Crystal X-ray structure determination

Data for the Single Crystal XRD structure were collected on a Bruker D8 Venture Duo IMS system equipped with a Helios optic monochromator and a Mo IMS microsource ($\lambda = 0.71073 \text{ \AA}$). The individual crystals were mounted on a glass capillary or a MiTiGen MicroMount microsampling tool in per-fluoropolyether oil and measured in a cold N_2 flow. The data of the compound $\mathbf{1} \cdot \text{BH}_3$ were collected on an Oxford Diffraction SuperNova at 150 K (Cu-K α radiation, $\lambda = 1.5418 \text{ \AA}$). The structures were solved by direct methods and refined on F^2 with the SHELX-97[3] software package. The H atoms at the silicon and boron centers were found in the electron density map while all other hydrogen atoms were calculated and considered isotropically according to a riding model.

CCDC numbers: 1896328 ($\mathbf{1} \rightarrow \text{BH}_3$), 1896329 ($\mathbf{1} \rightarrow \text{BBr}_3$), 1896330 ($\mathbf{2}$), 1896331 ($\mathbf{1} \rightarrow \text{BPhBr}_2$)

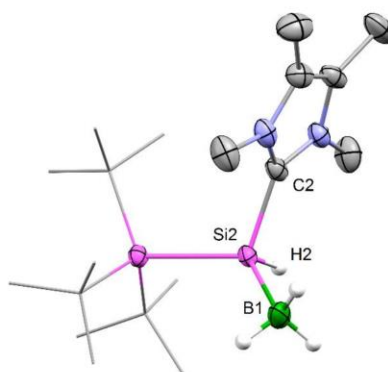


Figure S44. Molecular structure of compound $\mathbf{1} \rightarrow \text{BH}_3$. Thermal ellipsoids are drawn at the 30% probability level. H atoms except for the hydrogens at the silicon and at the boron have been omitted for clarity. Selected interatomic distances [\AA] and angles [$^\circ$]: Si1-Si2 2.401(1), Si2-C2 1.942(3), Si2-B1 2.009(5), Si1-Si2-B1 123.3(2), C2-Si2-B1 108.2(2), Si1-Si2-C2 111.3(2)

Table S1. Crystal data and structure refinement for compounds **1**→BH₃

Empirical formula	C ₁₉ H ₄₃ BN ₂ Si ₂	
Formula weight	366.54	
Temperature	150.00(10) K	
Wavelength	1.54184 Å	
Crystal system	Monoclinic	
Space group	I2/a	
Unit cell dimensions	a = 15.5684(6) Å	α = 90°.
	b = 8.9172(5) Å	β = 100.255(4)°
	c = 35.2491(17)	γ = 90°.
Volume	4815.3(4) Å ³	
Z	8	
Density (calculated)	1.011 Mg/m ³	
Absorption coefficient	1.340 mm ⁻¹	
F(000)	1632	
Crystal size	0.40 x 0.28 x 0.06 mm ³	
Theta range for data collection	2.55 to 67.49°.	
Index ranges	-18 ≤ h ≤ 18, -9 ≤ k ≤ 10, -37 ≤ l ≤ 42	
Reflections collected	8677	
Independent reflections	4347 [R(int) = 0.0413]	
Completeness to theta = 67.48°	99.9 %	
Absorption correction	Semi-empirical from equivalents	
Max. and min. transmission	0.9239 and 0.6136	
Refinement method	Full-matrix least-squares on F ²	
Data / restraints / parameters	4347 / 0 / 243	
Goodness-of-fit on F ²	1.052	
Final R indices [I > 2σ(I)]	R1 = 0.0714, wR2 = 0.1743	
R indices (all data)	R1 = 0.0844, wR2 = 0.1863	
Largest diff. peak and hole	0.712 and -0.332 e.Å ⁻³	

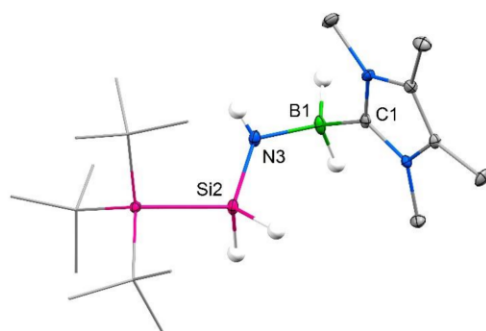


Figure S45. Molecular structure of compound **2**. Thermal ellipsoids are drawn at the 30% probability level. H atoms except for the hydrogens at the silicon, boron and nitrogen have been omitted for clarity. Selected interatomic distances [Å] and angles [°]: Si1-Si2 2.363(11), Si2-N3 1.703(3), B1-N3 1.542(4), B1-C1 1.635(4), Si1-Si2-N3 114.35(10), Si2-N3-B1 123.2(2), N3-B1-C1 110.2 (2).

Table S2. Crystal data and structure refinement for compound **2**.

Empirical formula	C ₁₉ H ₄₄ BN ₃ Si ₂	
Formula weight	381.56	
Temperature	100(2) K	
Wavelength	0.71073 Å	
Crystal system	triclinic	
Space group	P - 1	
Unit cell dimensions	a = 8.3084(7) Å	α = 81.990(3)°
	b = 8.5790(7) Å	β = 81.622(3)°
	c = 19.8196(16) Å	γ = 61.427(2)°
Volume	1223.45(18) Å ³	
Z	2	
Density (calculated)	1.036 g/cm ³	
Absorption coefficient	0.152 mm ⁻¹	
F(000)	424	
Crystal size	0.377 x 0.399 x 0.581 mm	
Theta range for data collection	2.71 to 25.03°	
Index ranges	-9 ≤ h ≤ 9, -10 ≤ k ≤ 10, -23 ≤ l ≤ 23	

Reflections collected	34475	
Independent reflections	4326 [R(int) = 0.0648]	
Completeness to theta	96.5%	
Absorption correction	Multi-Scan	
Max. and min. transmission	0.9450 and 0.9170	
Refinement method	Full-matrix least-squares on F ²	
Data / restraints / parameters	4326 / 0 / 255	
Goodness-of-fit on F ²	1.134	
Final R indices [I>2sigma(I)]	R1 = 0.0509, wR2 = 0.1179	
R indices (all data)	R1 = 0.0584, wR2 = 0.1258	
Largest diff. peak and hole	0.433 and -0.297 eÅ ⁻³	

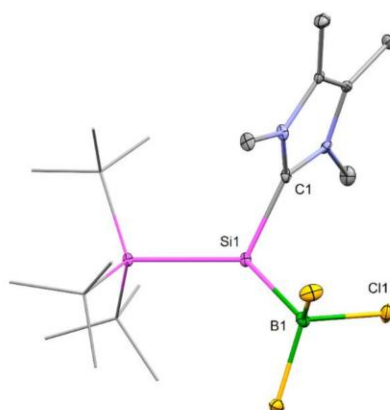


Figure S46. Molecular structure of compound **1**·BCl₃ in the solid state. Thermal ellipsoids are drawn at the 30% probability level. H atoms have been omitted for clarity. Data quality is insufficient for parameter discussion. Space Group: monoclinic, P2₁/n. Cell Parameters: a = 8.97 Å, b = 19.71 Å, c = 13.57 Å; $\alpha = 90^\circ$, $\beta = 91.9^\circ$, $\gamma = 90^\circ$.

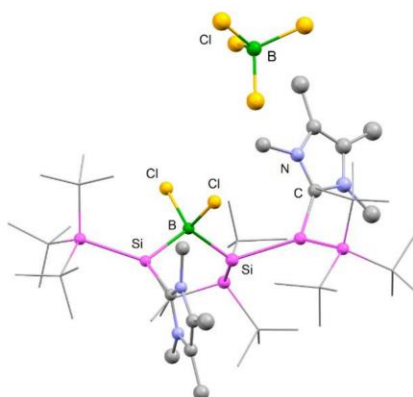


Figure S47. Molecular structure of compound $[(1)BCl_2(SiH(SitBu_3)1)]^+[BCl_4]^-$ in the solid state (Ball&Stick Model). H atoms have been omitted for clarity. Data quality is insufficient for parameter discussion. Space Group: monoclinic, $P2_1/n$. Cell Parameters: $a = 14.85 \text{ \AA}$, $b = 21.26 \text{ \AA}$, $c = 21.75 \text{ \AA}$; $\alpha = 90^\circ$, $\beta = 104.6^\circ$, $\gamma = 90^\circ$.

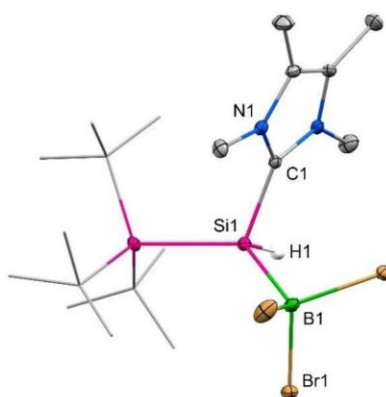


Figure S48. Molecular structure of compound $1 \rightarrow BBr_3$. Thermal ellipsoids are drawn at the 30% probability level. H atoms except for the hydrogens at the silicon have been omitted for clarity. Selected interatomic distances [\AA] and angles [$^\circ$]: Si1-Si2 2.428(2), Si1-C1 1.922(3), Si1-B1 2.045(3), Si2-Si1-B1 130.09(11), C1-Si1-B1 104.92(14), Si2-Si1-C1 113.56(10).

Table S3. Crystal data and structure refinement for compound **1**→BBr₃.

Empirical formula	C ₁₉ H ₄₀ BBr ₃ N ₂ Si ₂	
Formula weight	603.25	
Temperature	100(2) K	
Wavelength	0.71073 Å	
Crystal system	monoclinic	
Space group	P 1 21/n 1	
Unit cell dimensions	a = 9.131(5) Å	α = 90°
	b = 20.191(11) Å	β = 93.274(17)°
	c = 14.376(8) Å	γ = 90°
Volume	2646.(2) Å ³	
Z	4	
Density (calculated)	1.514 g/cm ³	
Absorption coefficient	4.672 mm ⁻¹	
F(000)	1224	
Crystal size	0.263 x 0.286 x 0.344 mm	
Theta range for data collection	2.45 to 29.65°	
Index ranges	-12 ≤ h ≤ 12, -27 ≤ k ≤ 21, -17 ≤ l ≤ 19	
Reflections collected	23398	
Independent reflections	7373 [R(int) = 0.0396]	
Absorption correction	Multi-Scan	
Max. and min. transmission	0.3730 and 0.2960	
Refinement method	Full-matrix least-squares on F ²	
Data / restraints / parameters	7373 / 331 / 380	
Goodness-of-fit on F ²	1.048	
Final R indices [I > 2σ(I)]	R1 = 0.0396, wR2 = 0.0784	
R indices (all data)	R1 = 0.0577, wR2 = 0.0837	
Largest diff. peak and hole	2.227 and -0.726 eÅ ⁻³	

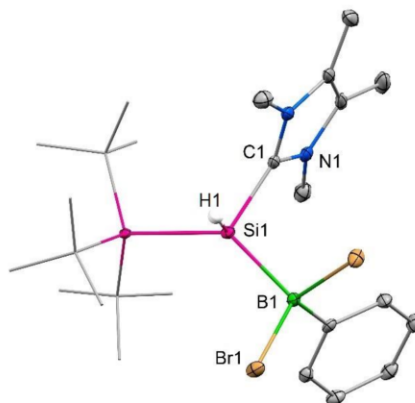


Figure S49. Molecular structure of compound **1**·BPhBr₂. Thermal ellipsoids are drawn at the 30% probability level. H atoms except for the hydrogen atom at the silicon atom have been omitted for clarity. Selected interatomic distances [Å] and angles [°]: Si1-Si2 2.421(1), Si1-C1 1.931(3), Si1-B1 2.074(3), Si2-Si1-B1 131.9(1), C1-Si1-B1 103.0(1), Si2-Si1-C1 113.1(1).

Table S4. Crystal data and structure refinement for compound **1**·BPhBr₂.

Empirical formula	C ₂₅ H ₄₅ BBr ₂ N ₂ Si ₂	
Formula weight	600.42	
Temperature	100(2) K	
Wavelength	0.71073 Å	
Crystal system	triclinic	
Space group	P - 1	
Unit cell dimensions	a = 8.6853(5) Å	α = 85.276(2)°
	b = 9.0560(5) Å	β = 89.604(2)°
	c = 20.7220(12) Å	γ = 63.638(2)°
Volume	1454.61(15) Å ³	
Z	2	
Density (calculated)	1.371 g/cm ³	
Absorption coefficient	2.885 mm ⁻¹	
F(000)	624.0	
Crystal size	0.263 x 0.286 x 0.344 mm	

Theta range for data collection	2.52 to 25.79°	
Index ranges	-10<=h<=10, -11<=k<=11, -25<=l<=25	
Reflections collected	61899	
Independent reflections	5567 [R(int) = 0.0338]	
Absorption correction	Multi-Scan	
Max. and min. transmission	0.7453 and 0.5649	
Refinement method	Full-matrix least-squares on F ²	
Data / restraints / parameters	5567 / 1 / 306	
Goodness-of-fit on F ²	1.169	
Final R indices [I>2sigma(I)]	R1 = 0.0378, wR2 = 0.0937	
R indices (all data)	R1 = 0.0395, wR2 = 0.0945	
Largest diff. peak and hole	2.222 and -0.745 eÅ ⁻³	

12.2 Supporting Information for Chapter 8

Supporting Information

NHC-stabilized Silyl-substituted Chlorosilylene

*Gizem Dübek, Franziska Hanusch and Shigeyoshi Inoue**

Department of Chemistry, Catalysis Research Center and WACKER-Institute of Silicon Chemistry, Technical University of Munich, Lichtenbergstraße 4, D-85747 Garching, Germany

Table of Contents

1. Experimental Section	S2
1.1 General Methods and Instrumentation	S2
NHC-stabilized silyl-chlorosilylene (1):	S2
Synthesis of compound 2	S5
Synthesis of compound 3	S8
Synthesis of compound 4a	S13
2. Single Crystal X-ray structure determination	S17
3. References	S22

1. Experimental Section

1.1 General Methods and Instrumentation

All experiments and manipulations were carried out under argon atmosphere using standard Schlenk techniques or in an MBraun inert-atmosphere glovebox. Glassware was heat dried under vacuum prior to use. Solvents were dried by standard methods. NMR spectra at ambient temperature (298 K) were recorded on a Bruker AV400US, DRX400, AVHD300, or AV500C device. $\delta(^1\text{H})$ and $\delta(^{13}\text{C})$ were referenced internally to the relevant residual solvent resonances. $\delta(^{29}\text{Si})$ was referenced to the signal of tetramethylsilane (TMS) ($\delta = 0$ ppm) as external standard. Some NMR spectra include resonances for silicone grease (C_6D_6 : $\delta(^1\text{H}) = 0.29$ ppm, $\delta(^{13}\text{C}) = 1.4$ ppm and $\delta(^{29}\text{Si}) = -21.8$ ppm) derived from B. Braun Melsungen AG Sterican® cannulas. Elemental analyses (EA) were conducted with a EURO EA (HEKA tech) instrument equipped with CHNS combustion analyzer by microanalytical laboratory of the Catalysis Research Center, Technische Universität München. IR spectra were recorded on a Perkin Elmer FT-IR spectrometer (diamond ATR) in a range of 400–4000 cm^{-1} at room temperature inside an argon-filled glovebox. The compounds 1,3,4,5-tetramethylimidazol-2-ylidene (ImMe_4)¹, 1,3-diethyl-4,5-dimethylimidazol-2-ylidene (ImEt_2Me_2)¹ and $t\text{Bu}_3\text{SiSiHCl}_2$ ² were prepared according to literature procedures.

Abbreviations: s = singlet, d = doublet, t = triplet, m = multiplet, br = broad, n.a. = not applicable/no answer, n.o. = not observed, SCXRD = Single Crystal X-ray diffraction, IG = Inverse-Gated, INEPT = Insensitive Nuclei Enhanced by Polarization Transfer, HMBC = Heteronuclear Multiple Bond Correlation.

NHC-stabilized silyl-chlorosilylene (1): A solution of ImEt_2Me_2 (4.32g, 28 mmol) in 30 mL toluene added dropwise to a cooled (-50°C) solution of $t\text{Bu}_3\text{SiSiHCl}_2$ (4.25g, 14 mmol) in 100 mL toluene. Upon addition, colorless precipitate formed while the color of the reaction mixture turned into red-orange. After 1 hour, cooling bath was removed and the suspension stirred overnight. Reaction mixture was filtered via frit, extracted with toluene (3 x 50 mL) and toluene removed by vacuum. The resulting orange powder was washed with pentane (2 x 25 mL) and dried under vacuum at 40°C for 3 hours. Suitable crystals for single X-ray diffraction analysis of **1** were obtained by slow diffusion of pentane to a concentrated toluene solution of **1** at room temperature. Yield: 5.4 g (92%).

^1H NMR (400 MHz, C_6D_6 , 298K): δ 4.47 (br, 2H, N- CH_2CH_3), 4.06 (br, 2H, N- CH_2CH_3), 1.51 (s, 27H, ((CH_3)₃C)), 1.34 (s, 6H, C- CH_3), 1.09 (t, 6H, N- CH_2CH_3).

^{13}C NMR (101 MHz, C_6D_6 , 298K): δ 169.71 (:CN₂, $^1J(\text{SiC}) = 49.32$ Hz), 126.19 ($\text{CH}_3\text{C}=\text{CCH}_3$), 43.48 (N- CH_2CH_3), 32.77 (C(CH_3)₃), 25.90 (C(CH_3)₃), 15.13 (N- CH_2CH_3), 8.19 ($\text{CH}_3\text{C}=\text{CCH}_3$).

$^{29}\text{Si}\{^1\text{H}\}$ NMR (79 MHz, C_6D_6 , 298K): δ 18.30 (ClSi), 9.44 ($t\text{Bu}_3\text{Si}$)

^{29}Si INEPT NMR (79 MHz, C_6D_6 , 298K): δ 9.44 ($t\text{Bu}_3\text{Si}$)

EA: $\text{C}_{21}\text{H}_{43}\text{ClN}_2\text{Si}_2$; Calculated [%]: C (60.75), H (10.44), N (6.75); Measured: C (59.94), H (10.48), N (6.06)

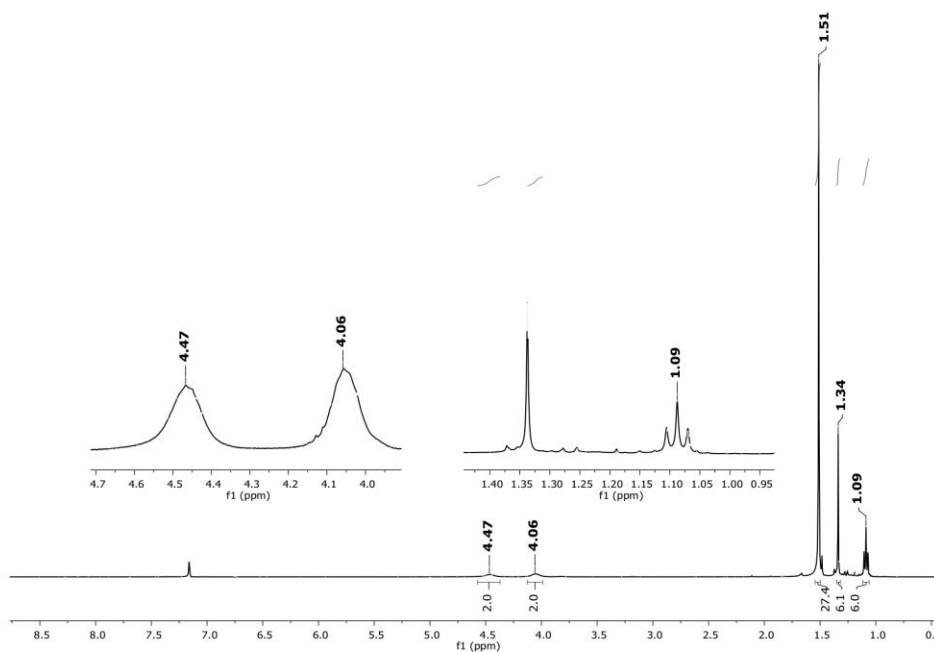


Figure S1. ^1H spectrum of compound **1** in C_6D_6 at 298 K.

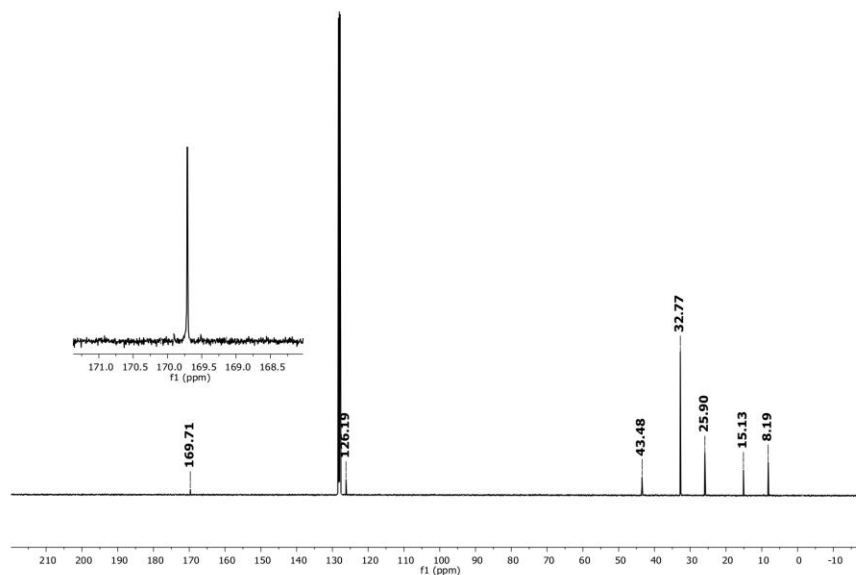


Figure S2. ^{13}C spectrum of compound **1** in C_6D_6 at 298 K.

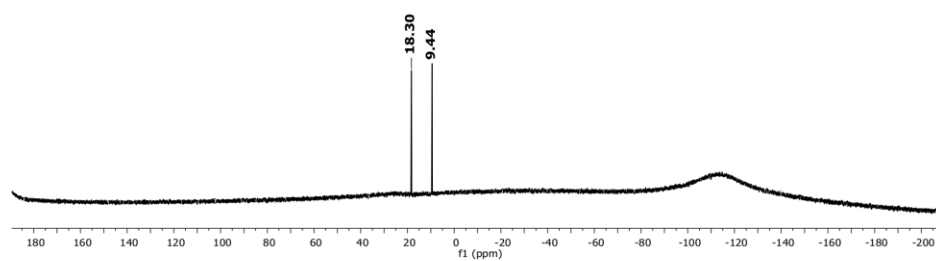


Figure S3. $^{29}\text{Si}\{^1\text{H}\}$ NMR spectrum of compound **1** in C_6D_6 at 298 K.

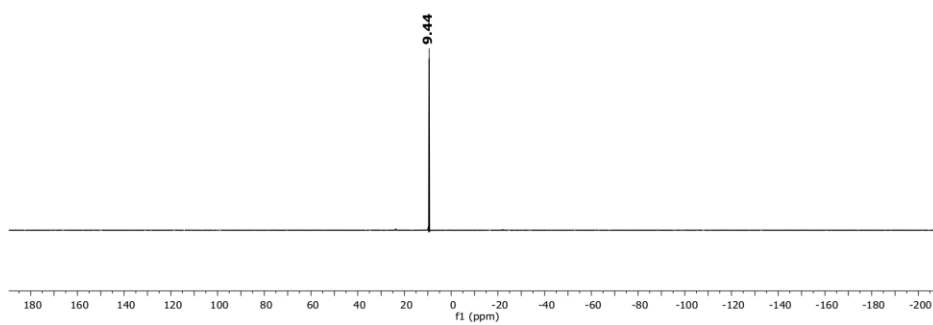


Figure S4. ^{29}Si -INEPT NMR spectrum of compound **1** in C_6D_6 at 298 K.

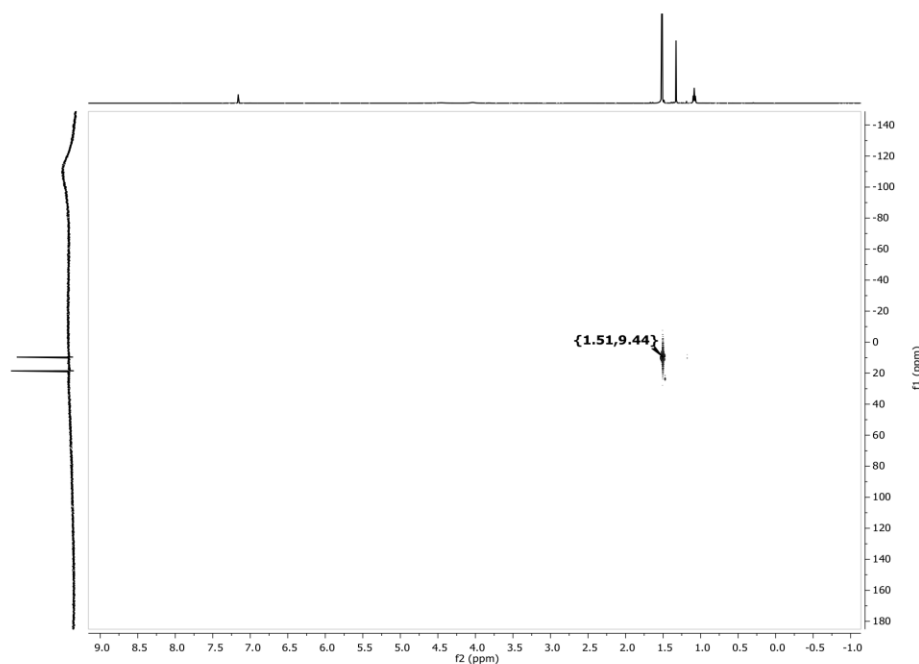


Figure S5. $^{29}\text{Si}\{^1\text{H}\}$ heteronuclear correlation spectrum of compound **1** in C_6D_6 at 298 K.

Synthesis of compound 2: Compound **1** (100 mg, 0.24 mmol) and $\text{Fe}_2(\text{CO})_9$ (45 mg, 0.12 mmol) were placed in a Schlenk flask and dissolved in 25 mL THF. The reaction mixture turned from red-orange to brownish purple after 30 minutes and was stirred overnight at ambient temperature. Solvent was removed and residue extracted with toluene (2 x 20 mL). Toluene was removed, the residue washed with hexane (2 x 10 mL) and dried. Suitable crystals for single X-ray diffraction analysis of **2** were obtained by layering of pentane onto concentrated toluene solution at room temperature. Compound **2** was isolated as a beige solid. (90 mg, 0.15 mmol, 64%)

^1H NMR (400 MHz, C_6D_6 , 298K): δ 5.34 (m, 1H, $\text{N}_1\text{-CH}_2\text{aCH}_3$), 5.02 (m, 1H, $\text{N}_2\text{-CH}_2\text{aCH}_3$), 3.28 (m, 1H, $\text{N}_1\text{-CH}_2\text{bCH}_3$), 3.14 (m, 1H, $\text{N}_2\text{-CH}_2\text{bCH}_3$), 1.39 (s, 27H, $((\text{CH}_3)_3\text{C})$), 1.25 (s, 3H, $\text{C-CH}_{3\text{a}}$), 1.19 (t, 3H, $\text{N-CH}_2\text{CH}_{3\text{a}}$), 1.16 (s, 3H, $\text{C-CH}_{3\text{b}}$), 1.09 (t, 3H, $\text{N-CH}_2\text{CH}_{3\text{b}}$).

^{13}C NMR (101 MHz, C_6D_6 , 298K): δ 218.15 (CO), 157.73 ($:\text{CN}_2$), 129.28 ($\text{CH}_3\text{C}=\text{CCH}_3$), 127.02 ($\text{CH}_3\text{C}=\text{CCH}_3$), 45.00 ($\text{N-C}_\alpha\text{H}_2\text{CH}_3$), 43.18 ($\text{N-C}_\beta\text{H}_2\text{CH}_3$), 32.74 ($\text{C}(\text{CH}_3)_3$), 26.07 ($\text{C}(\text{CH}_3)_3$), 16.37 ($\text{N-CH}_2\text{C}_\alpha\text{H}_3$), 14.06 ($\text{N-CH}_2\text{C}_\beta\text{H}_3$), 8.80 ($\text{CH}_3\text{C}=\text{CCH}_3$), 8.45 ($\text{CH}_3\text{C}=\text{CCH}_3$).

^{29}Si NMR (79 MHz, C_6D_6 , 298K): δ 64.94 ($\text{ClSi}:\rightarrow\text{Fe}$), 16.77 ($t\text{Bu}_3\text{Si}$).

IR (ATR, neat) [cm^{-1}]: $\nu(\text{CO}) = 2013, 1934, 1899, 1877$

EA: $\text{C}_{25}\text{H}_{43}\text{ClFeN}_2\text{O}_4\text{Si}_2$; Calculated [%]: C (51.50), H (7.43), N (4.80); Measured: C (51.53), H (7.53), N (4.87)

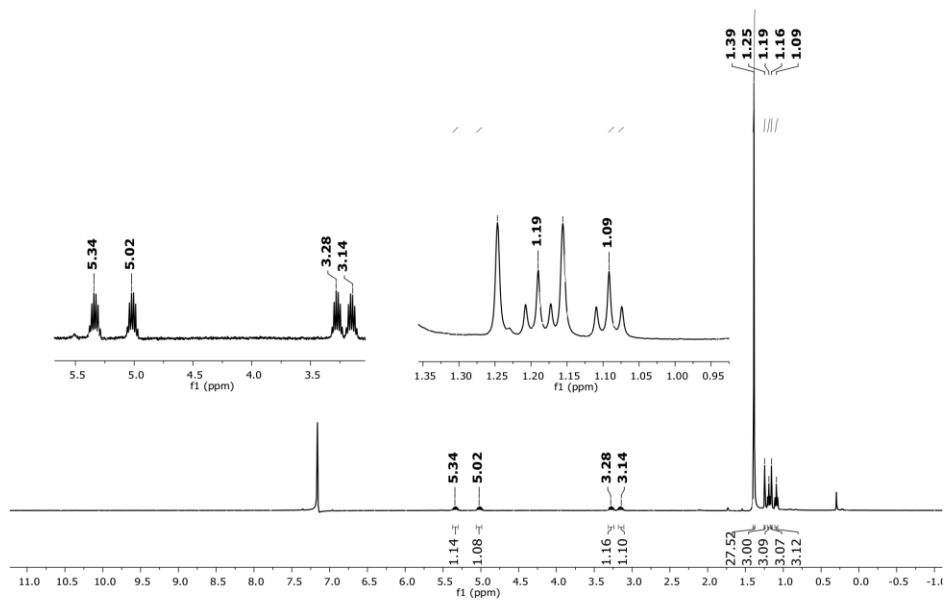


Figure S6. ^1H spectrum of compound **2** in C_6D_6 at 298 K.

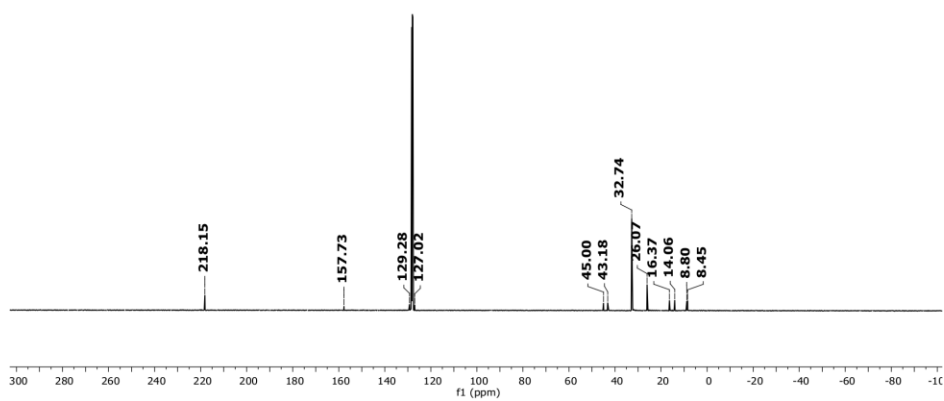


Figure S7. ^{13}C spectrum of compound **2** in C_6D_6 at 298 K.

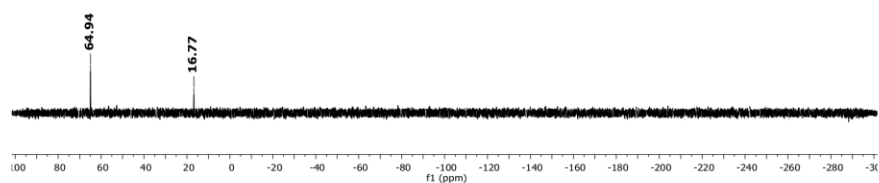


Figure S8. $^{29}\text{Si}\{^1\text{H}\}$ NMR spectrum of compound **2** in C_6D_6 at 298 K.

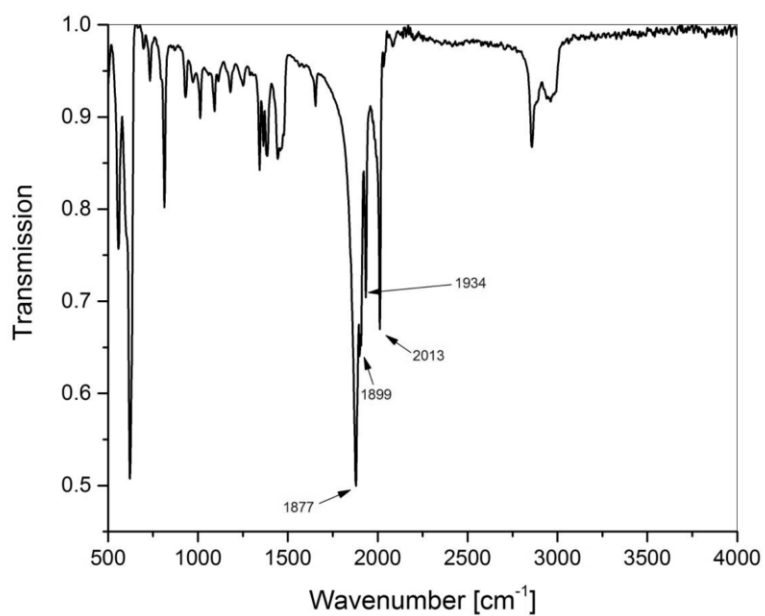


Figure S9. IR spectrum of compound **2** (ATR, neat).

S7

Synthesis of compound 3: To an orange solution of compound **1** (120 mg, 0.29 mmol) in 20 mL THF, LiBH₄ (8 mg, 0.35 mmol, 1.2 eq) in 5 mL THF was added via syringe at room temperature. The reaction mixture stirred overnight while the orange color disappeared to yield almost colorless, pale yellow cloudy solution. THF was removed by reduced pressure, toluene was added (20 mL + 5 mL) and filtered. Toluene was evaporated to afford colorless powder. Washing with 5 mL pentane followed by drying under reduced pressure yielded compound **3** in 84% yield (96 mg). Suitable crystals for single crystal X-ray diffraction analysis were obtained by layering pentane to a concentrated toluene solution of compound **3**.

¹H NMR (500 MHz, C₆D₆, 298K): δ 4.75 (m, 1H, N₁-CH_{2a}CH₃), 4.31 (q, ³J(H,H) = 5.5 Hz, Si,H satellites: ¹J(Si,H) = 150 Hz, 1H, Si-H), 4.25 (m, 1H, N₂-CH_{2a}CH₃), 3.48 (m, 1H, N₁-CH_{2b}CH₃), 3.17 (m, 1H, N₂-CH_{2b}CH₃), 1.39 (s, 27H, ((CH₃)₃C)), 1.31 (s, 3H, C-C_{H3a}), 1.27 (t, 3H, N-CH₂CH_{3a}), 1.26 (s, 3H, C-C_{H3b}), 0.88 (t, 3H, N-CH₂CH_{3b}), n.o (BH). Minor product; ¹H NMR (400 MHz, Benzene-*d*₆) δ 1.41 (s, 27H), 1.32 (s, 6H), 1.08 (t, *J* = 6.9 Hz, 6H) n.o. N-CH₂CH₃ and Si-H.

¹¹B NMR (128 MHz, C₆D₆, 298K): δ -40.31 (q, ¹J(B,H) = 92.9 Hz, BH₃, major product), -31.41 (q, ¹J(B,H) = 92.0 Hz, BH₃, minor product)

¹³C NMR (101 MHz, C₆D₆, 298K): δ 162.60 (:CN₂), 126.87 (CH₃C_a=CCH₃), 125.98 (CH₃C=C_bCH₃) 43.81 (N-C_aH₂CH₃), 42.40 (N-C_bH₂CH₃), 32.16 (C(CH₃)₃), 24.65 (C(CH₃)₃), 16.23 (N-CH₂C_aH₃), 15.60 (N-CH₂C_bH₃), 8.17 (CH₃C=CCH₃), 8.05 (CH₃C=CCH₃). Minor product: 43.99 (N-CH₂CH₃), 32.66 (C(CH₃)₃), 25.19 (C(CH₃)₃), 16.61 (N-CH₂CH₃), 8.28 (CH₃C=CCH₃), n.o :CN₂ and CH₃C=CCH₃.

²⁹Si NMR (79 MHz, C₆D₆, 298K): δ -64.17 (HSi:), 11.93 (*t*Bu₃Si). Minor product: 8.63 (*t*Bu₃Si).

IR (ATR, neat) [cm⁻¹]: ν(Si-H) = 2087, ν(B-H) = 2233 – 2330.

EA: C₂₁H₄₇BN₂Si₂; Calculated [%]: C (63.92), H (12.01), N (7.10); Measured: C (61.22), H (11.32), N (7.20)

Note: The low value for carbon explained by formation of incombustible boron and silicon carbides.

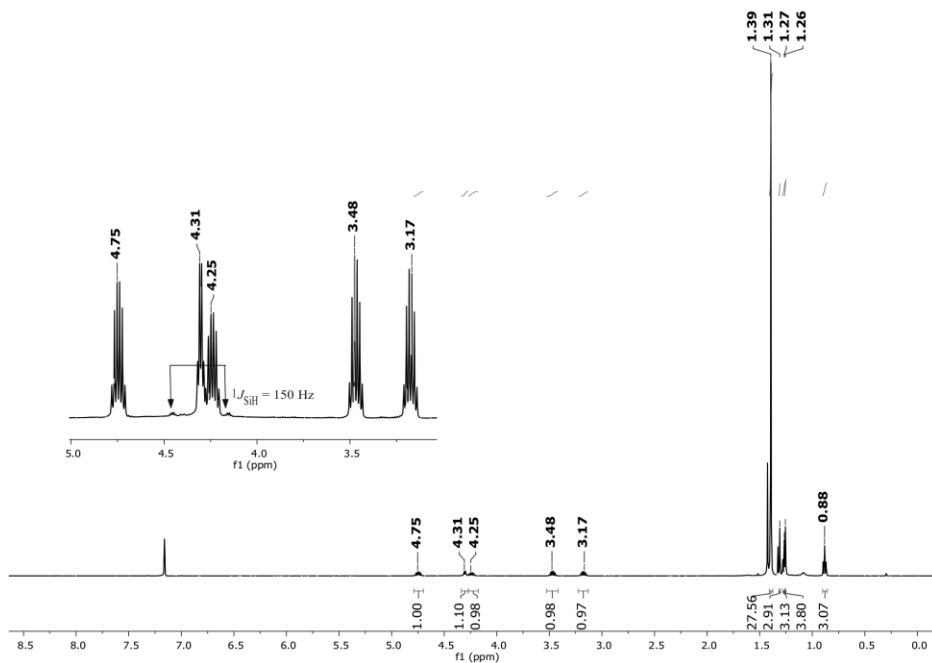


Figure S10. ^1H NMR spectrum of compound **3** in C_6D_6 at 298 K.

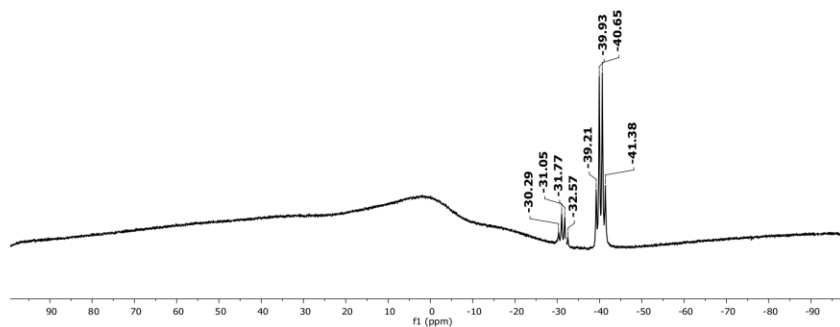


Figure S11. ^{11}B NMR spectrum of compound **3** in C_6D_6 at 298 K.

S9

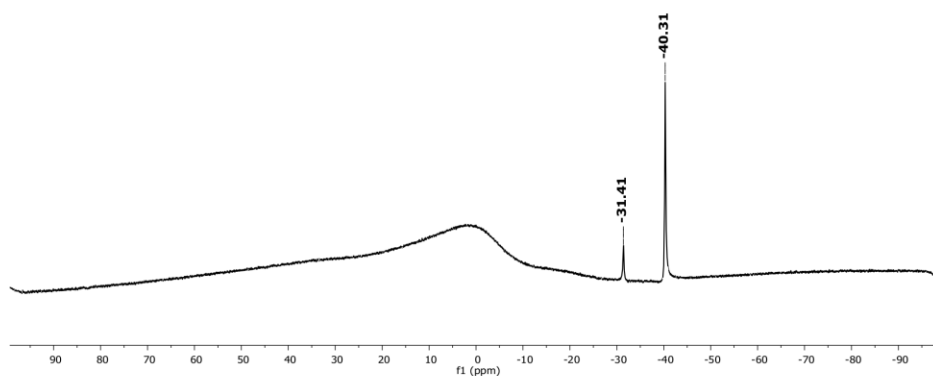


Figure S12. $^{11}\text{B}\{^1\text{H}\}$ NMR spectrum of compound **3** in C_6D_6 at 298 K.

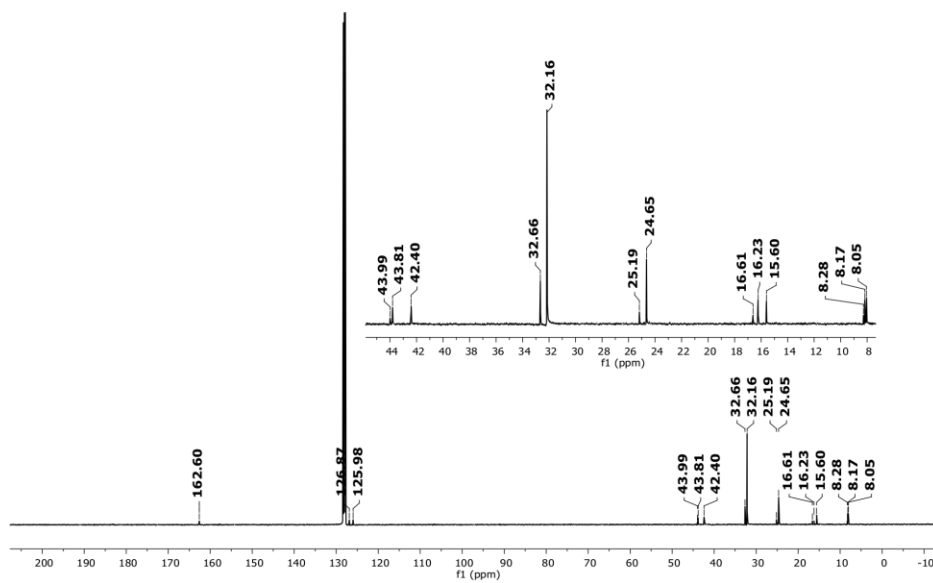


Figure S13. ^{13}C NMR spectrum of compound **3** in C_6D_6 at 298 K.

S10

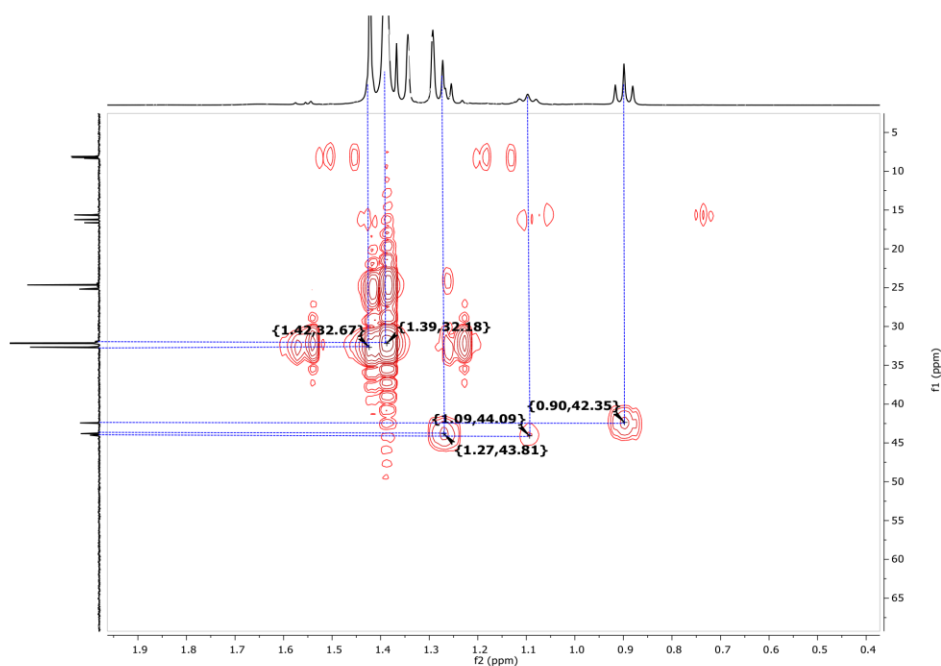


Figure S14. $^{13}\text{C}\{^1\text{H}\}$ heteronuclear correlation spectrum (2–0.4 ppm) of compound **3** in C_6D_6 at 298 K.

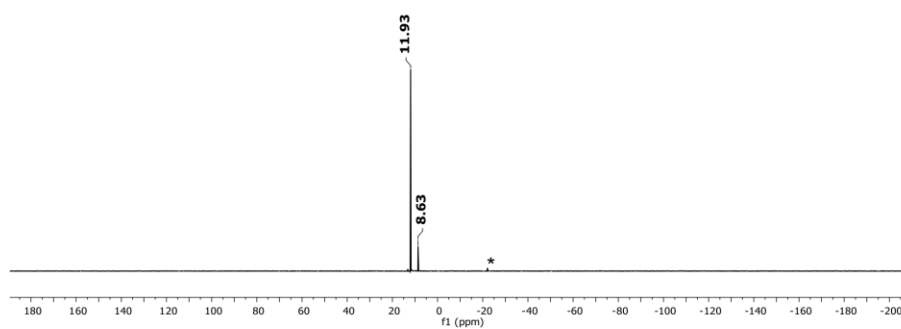


Figure S15. ^{29}Si -INEPT NMR spectrum of compound **3** in C_6D_6 at 298 K. (*: silicon grease)

S11

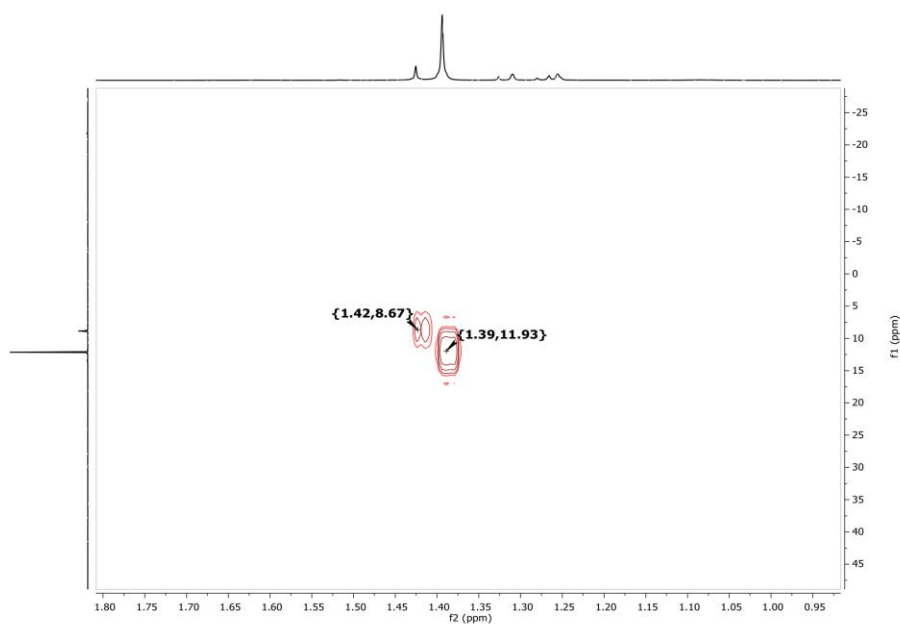


Figure S16. $^{29}\text{Si}\{^1\text{H}\}$ heteronuclear correlation spectrum (1.8–0.95 ppm) of compound **3** in C_6D_6 at 298 K.

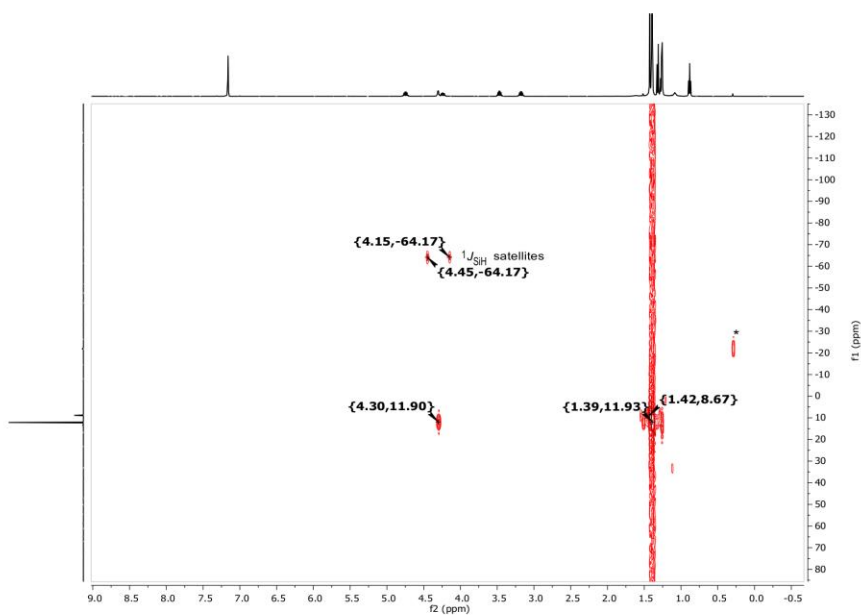


Figure S17. $^{29}\text{Si}\{^1\text{H}\}$ heteronuclear correlation spectrum (9.0–0 ppm) of compound **3** in C_6D_6 at 298 K. (*: silicon grease)

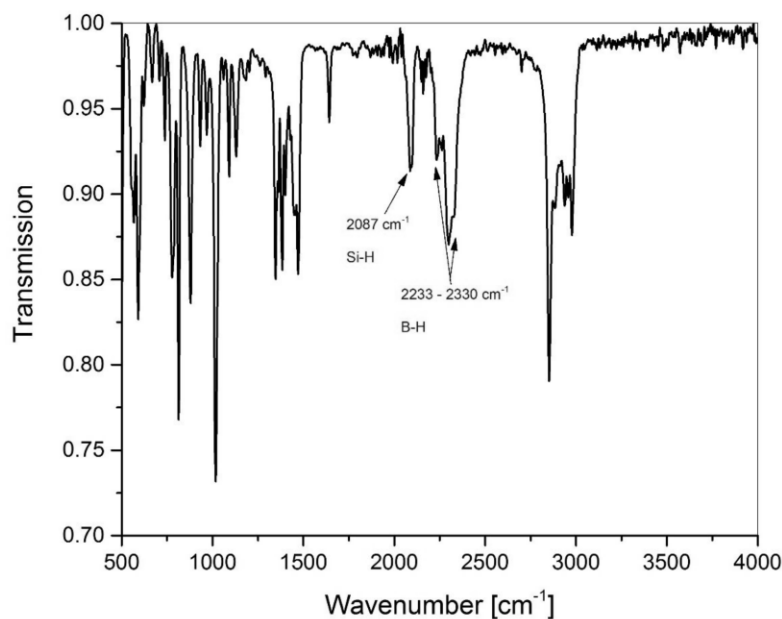


Figure S18. IR spectrum of compound **3** (ATR, neat).

Synthesis of compound 4a: Pale yellow solution of ImMe₄ (61 mg, 0.48 mmol, 2 equiv.) in 2 mL toluene was added dropwise to a deep orange solution of compound **1** (100 mg, 0.24 mmol) in 4 mL toluene. Approximately 5 minutes after addition, yellow solid dropped out of the solution. The suspension stirred additional 1 h, during this time more precipitate formed while the color of supernatant became pale yellow. Suspension filtered, yellow solid washed two times with toluene (2x3 mL), then with pentane (2x4 mL) and dried under vacuum. Compound **4a** afforded as a yellow solid (120 mg, 92%). During the crystallization process (slow diffusion of pentane into concentrated difluorobenzene solution of compound **4a**), compound **4a** rearranged itself to compound **4** as the measured crystal showed the already reported structure of [tBu₃SiSi(ImMe₄)₂]Cl.³

¹H NMR (400 MHz, CD₃CN, 298K): δ 4.40 (q, 4H, N-CH₂CH₃), 3.88 (s, 6H, N-CH₃), 2.20 (s, 6H, NHC-CH₃), 2.18 (s, 6H, NHC-CH₃), 1.20 (s, 27H, (CH₃)₃C), 0.95 (t, 6H, N-CH₂CH₃).

¹³C NMR (101 MHz, CD₃CN, 298K): δ 163.28 (:CN₂), 162.97 (:CN₂), 129.88 (CH₃C=CCH₃), 129.18 (CH₃C=CCH₃), 45.27 (N-CH₂CH₃), 37.21 (N-CH₃), 33.06 (C(CH₃)₃), 26.17 (C(CH₃)₃), 14.84 (N-CH₂CH₃), 9.58 (CH₃C=CCH₃), 9.39 (CH₃C=CCH₃).

²⁹Si NMR (79 MHz, CD₃CN, 298K): δ 21.79 (tBu₃Si), -80.51 (Si:⁺)

EA: C₂₈H₅₅ClN₄Si₂ Calculated [%]: C (62.35), H(10.28), N(10.39); Measured: C(63.59), H(9.83), N(9.29)

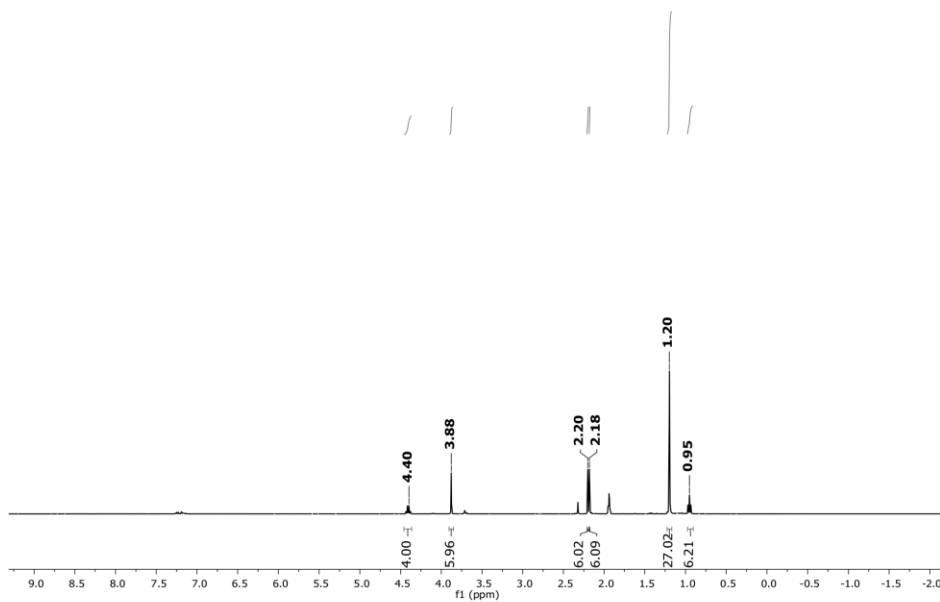


Figure S19. ¹H NMR spectrum of compound **4a** in CD₃CN at 298 K.

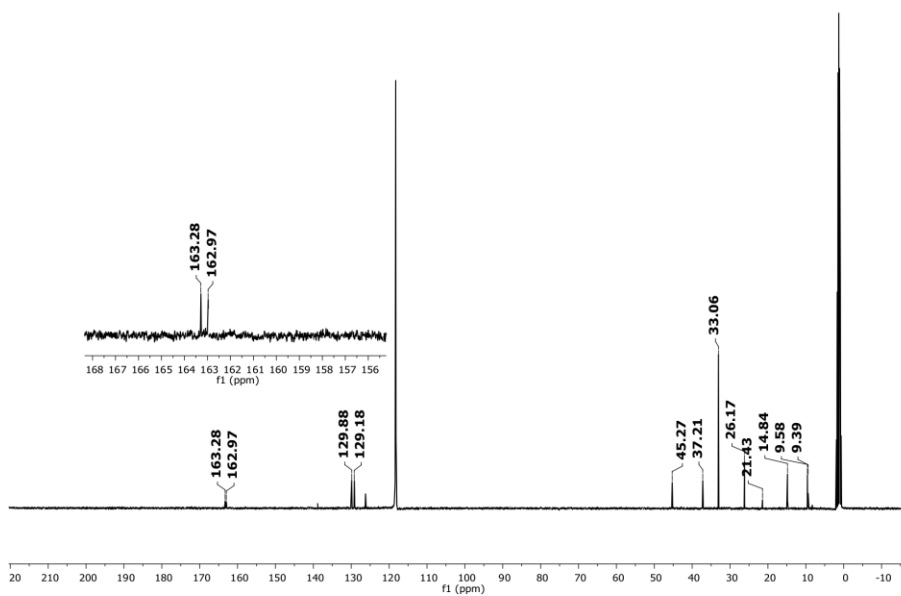


Figure S20. ¹³C NMR spectrum of compound **4a** in CD₃CN at 298 K.

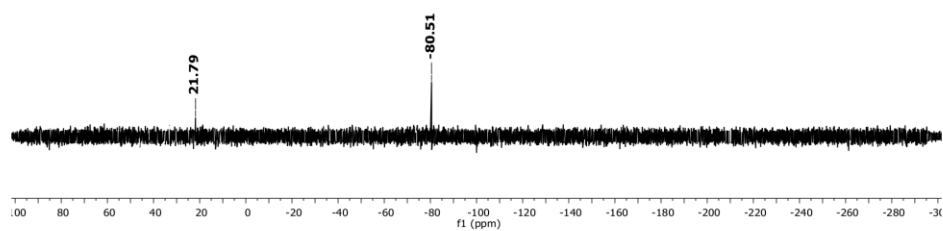


Figure S21. ^{29}Si NMR spectrum of compound **4a** in CD_3CN at 298 K.

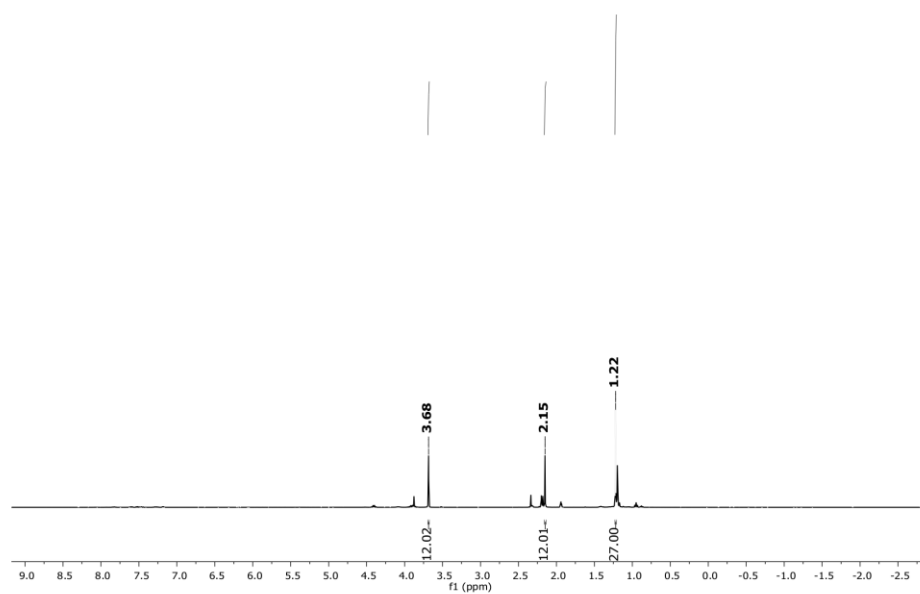


Figure S22. ^1H NMR spectrum of compound **4** in CD_3CN at 298 K (obtained crystals from slow diffusion of pentane to the concentrated solution of **4a** in DFB).

S15

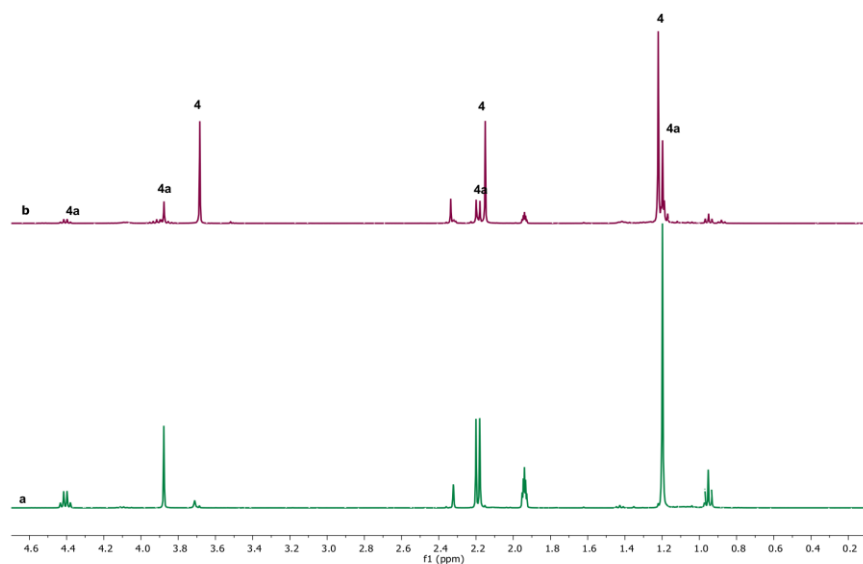


Figure S23. Comparison of ^1H NMR spectra of compounds **4** (b) and **4a** (a) in CD_3CN at 298 K.

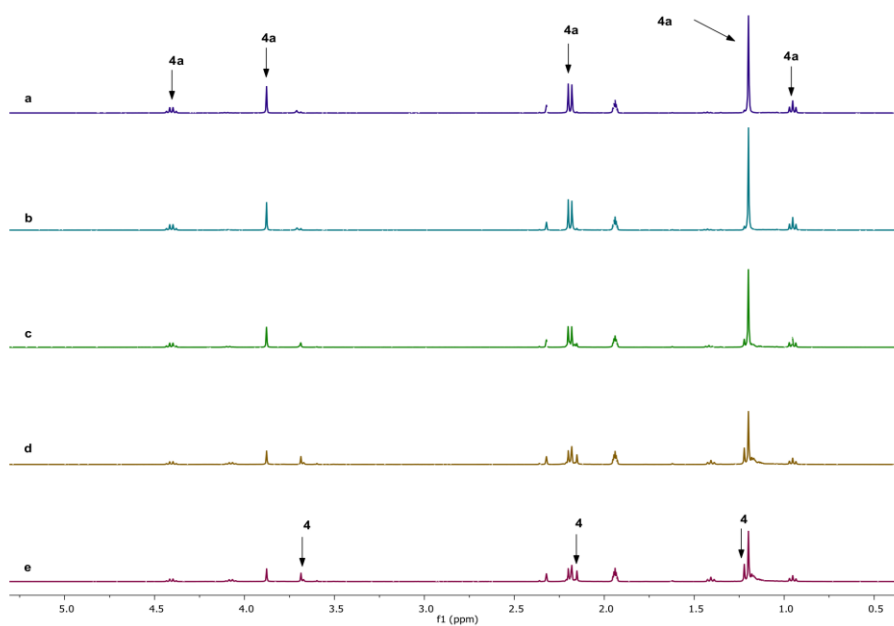


Figure S24. Stacked ^1H NMR spectra of the NHC exchange of compound **4a** to the compound **4** upon heating in CD_3CN . (a) t: 12 hrs, (b) t: 24 hrs, (c) Heating 2 hours at 65°C . (d) Heating 3 hours at 70°C . (e) Storing the heated solution (d) at room temperature for 2 days.

S16

2. Single Crystal X-ray structure determination

Single crystal diffraction data were recorded on a Bruker D8 Venture system equipped with a Helios optic monochromator and a Mo TXS rotating anode ($\lambda = 0.71073 \text{ \AA}$). The data collection was performed, using the APEX III software package⁴ on single crystals coated with Fomblin® Y as perfluorinated ether. The single crystal was picked on a micro sampler, transferred to the diffractometer and measured frozen under a stream of cold nitrogen. A matrix scan was used to determine the initial lattice parameters. Reflections were merged and corrected for Lorenz and polarization effects, scan speed, and background using SAINT.⁵ Absorption corrections, including odd and even ordered spherical harmonics were performed using SADABS.⁵ Space group assignments were based upon systematic absences, E statistics, and successful refinement of the structures. Structures were solved by direct methods with the aid of successive difference Fourier maps, and were refined against all data using the APEX III software in conjunction with SHELXL-2014⁶ and SHELXLE.⁷ H atoms were placed in calculated positions and refined using a riding model, with methylene and aromatic C–H distances of 0.99 and 0.95 Å, respectively, and $U_{iso}(H) = 1.2 \cdot U_{eq}(C)$. Non-hydrogen atoms were refined with anisotropic displacement parameters. Full-matrix least-squares refinements were carried out by minimizing $\sum w(F_o - F_c)^2$ with the SHELXL weighting scheme.⁸ Neutral atom scattering factors for all atoms and anomalous dispersion corrections for the non-hydrogen atoms were taken from International Tables for Crystallography.⁹ The images of the crystal structures were generated by Mercury.¹⁰ The CCDC numbers CCDC-(1950760), CCDC-(1950761) and CCDC-(1961386) contain the supplementary crystallographic data for the structures **1**, **2** and **3**, respectively. These data can be obtained free of charge from the Cambridge Crystallographic Data Centre via <https://www.ccdc.cam.ac.uk/structures/>.

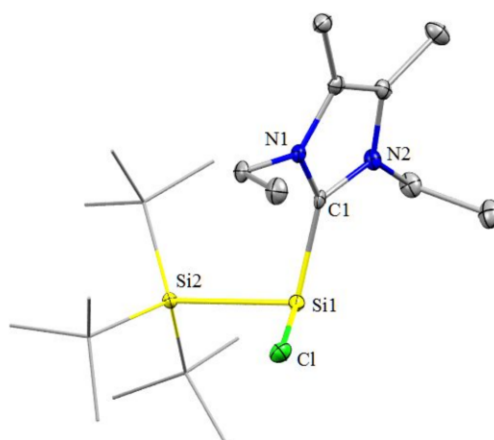


Figure S25. Ellipsoid plot (50% level) of the molecular structure of compound **1**. Hydrogen atoms are omitted for clarity and *tert*-butyl groups are depicted in wireframe for simplicity. Selected bond lengths (Å) and angles (°): Si1–C1: 1.9572(19), Si1–Si2: 2.4421(7), Si1–Cl: 2.1947(7); C1–Si1–Cl: 99.23(6), Cl–Si1–Si2: 103.51(3), C1–Si1–Si2: 106.51(6)

Table S1. Crystal data and structure refinement for compound 1.

Empirical formula	C ₂₁ H ₄₃ ClN ₂ Si ₂	
Formula weight	415.20	
Temperature	100 K	
Wavelength	0.71073 Å	
Crystal system	Monoclinic	
Space group	P 21/n	
Unit cell dimensions	a = 8.7189(8) Å	α = 90
	b = 12.8975(13) Å	β = 99.928(4)
	c = 21.868(2) Å	γ = 90
Volume	2422.3(4) Å ³	
Z	4	
Density (calculated)	1.138 g/cm ³	
Absorption coefficient	0.265 mm ⁻¹	
F(000)	912	
Crystal size	0.108 x 0.133 x 0.176 mm	
Theta range for data collection	2.40 to 25.03°	
Index ranges	-10 ≤ h ≤ 10, -15 ≤ k ≤ 15, - 26 ≤ l ≤ 26	
Reflections collected	73528	
Independent reflections	4283 [R(int) = 0.0875]	
Completeness	100.0%	
Absorption correction	Multi-Scan	
Max. and min. transmission	0.7452 and 0.7152	
Refinement method	Full-matrix least-squares on F ²	
Data / restraints / parameters	4283 / 0 / 248	
Goodness-of-fit on F ²	1.070	
Final R indices [I > 2σ(I)]	R1 = 0.0374, wR2 = 0.0739	
R indices (all data)	R1 = 0.0509, wR2 = 0.0780	
Largest diff. peak and hole	0.394 and -0.213 eÅ ⁻³	

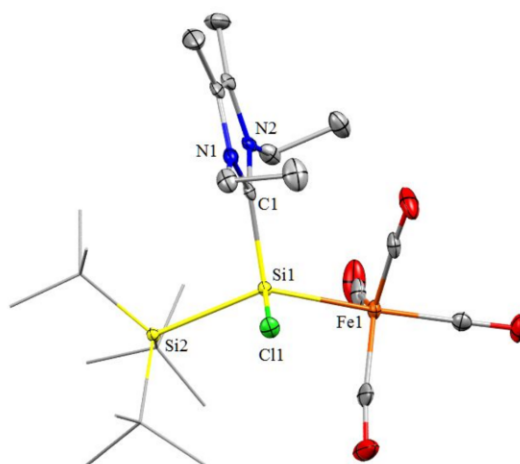


Figure S26. Ellipsoid plot (50% level) of the molecular structure of compound **2**. One out of two crystallographically independent molecules is shown. Hydrogen atoms are omitted for clarity and *tert*-butyl groups are depicted in wireframe for simplicity. Selected bond lengths (Å): Si1–Fe1: 2.3620(5), Si1–Si2: 2.5185(6), Si1–C1:1.9927(16) Si1–Cl: 2.1440(6).

Table S2. Crystal data and structure refinement for compound 2.

Empirical formula	C ₂₅ H ₄₃ ClFeN ₂ O ₄ Si ₂	
Formula weight	583.09	
Temperature	100K	
Wavelength	0.71073	
Crystal system	Triclinic	
Space group	P -1	
Unit cell dimensions	a = 13.2797(6)	α = 96.182(2)
	b = 15.4976(8)	β = 107.635(2)
	c = 16.8010(8)	γ = 110.024(2)
Volume	3008.5(3)	
Z	4	
Density (calculated)	1.287	
Absorption coefficient	0.701	
F(000)	1240	
Crystal size	0.135 x 0.220 x 0.275 mm	
Theta range for data collection	2.38 to 25.35°	
Index ranges	-15<=h<=15, -18<=k<=18, -	

	20<= <=20	
Reflections collected	126810	
Independent reflections	10980	
Completeness	0.999	
Absorption correction	Multi-Scan	
Max. and min. transmission	0.7015 and 0.7452	
Refinement method	Full-matrix least-squares on F ²	
Data / restraints / parameters	10980 / 0 / 657	
Goodness-of-fit on F ²	1.050	
Final R indices [I>2sigma(I)]	R1 = 0.0242, wR2 = 0.0541	
R indices (all data)	R1 = 0.0294, wR2 = 0.0565	
Largest diff. peak and hole	0.308 and -0.273 eÅ ⁻³	

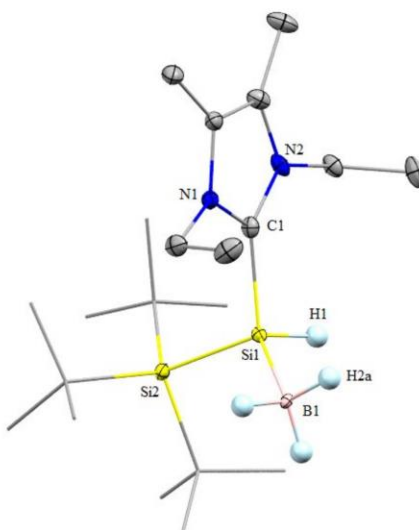


Figure S27. Ellipsoid plot (30% level) of the molecular structure of compound **3**. *Tert*-butyl groups are depicted in wireframe for simplicity. H atoms except B-H₃ and Si-H have been omitted for clarity. Selected bond lengths (Å) and angles (°): Si1–B1: 1.999(7), Si1–Si2: 2.374(5), Si1–C1: 1.963(6); Si2–Si1–B1 = 121.0(2), C1–Si1–B1 = 112.0(2), Si2–Si1–C1 = 112.0(2)

Table S3. Crystal data and structure refinement for compound 3.

Empirical formula	C ₂₁ H ₄₇ BN ₂ Si ₂	
Formula weight	394.60	
Temperature	100K	
Wavelength	0.71073	
Crystal system	Monoclinic	
Space group	P 21	
Unit cell dimensions	a = 8.757(9)	$\alpha = 90$
	b = 12.714(17)	$\beta = 103.51(4)$
	c = 11.610(14)	$\gamma = 90$
Volume	1257(3)	
Z	2	
Density (calculated)	1.043	
Absorption coefficient	0.149	
F(000)	440	
Crystal size	0.148 x 0.231 x 0.245 mm	
Theta range for data collection	2.39 to 25.91°	
Index ranges	-10 ≤ h ≤ 9, -15 ≤ k ≤ 15, -14 ≤ l ≤ 14	
Reflections collected	9833	
Independent reflections	4738	
Completeness	0.998	
Absorption correction	Multi-Scan	
Max. and min. transmission	0.6162 and 0.7453	
Refinement method	Full-matrix least-squares on F ²	
Data / restraints / parameters	4738 / 86 / 294	
Goodness-of-fit on F ²	1.077	
Final R indices [I > 2σ(I)]	R1 = 0.0450, wR2 = 0.1205	
R indices (all data)	R1 = 0.0483, wR2 = 0.1244	
Largest diff. peak and hole	0.571 and -0.618 eÅ ⁻³	

3. References

- (1) Kuhn, N.; Kratz, T., Synthesis of Imidazol-2-ylidenes by Reduction of Imidazole-2-(3H)-thiones. *Synthesis* **1993**, 1993, 561-562.
- (2) Wiberg, N.; Niedermayer, W.; Nöth, H.; Knizek, J.; Ponikvar, W.; Polbom, K., Supersilylsilane R*SiX₃: Darstellung, Charakterisierung und Strukturen; sterische und van-der-Waals Effekte der Substituenten X [1] / Supersilylsilanes R*SiX₃: Syntheses, Characterization and Structures; Steric and van-der-Waals Effects of Substituents X [1]. *Zeitschrift für Naturforschung B* **2000**, 55.
- (3) Frisch, P.; Inoue, S., NHC-stabilized Silyl-substituted Silyliumylidene Ions. *Dalton Trans.* **2019**.
- (4) APEX suite of crystallographic software, APEX 3 version 2015.5-2; Bruker AXS Inc.: Madison, Wisconsin, USA, 2015.
- (5) SAINT, Version 7.56a and SADABS Version 2008/1; Bruker AXS Inc.: Madison, Wisconsin, USA, 2008.
- (6) Sheldrick, G. M. SHELXL-2014, University of Göttingen, Göttingen, Germany, 2014.
- (7) Hübschle, C. B.; Sheldrick, G. M.; Dittrich, B. *J. Appl. Cryst.* 2011, 44, 1281-1284.
- (8) Sheldrick, G. M. SHELXL-97, University of Göttingen, Göttingen, Germany, 1998.
- (9) Wilson, A. J. C. *International Tables for Crystallography*, Vol. C, Tables 6.1.1.4 (pp. 500-502), 4.2.6.8 (pp. 219-222), and 4.2.4.2 (pp. 193-199); Kluwer Academic Publishers: Dordrecht, The Netherlands, 1992.
- (10) Macrae, C. F.; Bruno, I. J.; Chisholm, J. A.; Edgington, P. R.; McCabe, P.; Pidcock, E.; Rodriguez-Monge, L.; Taylor, R.; van de Streek, J.; Wood, P. A. *J. Appl. Cryst.* 2008, 41, 466-470.

12.3 Supporting Information for Chapter 9



Supporting Information

An Air-Stable Heterobimetallic Si₂M₂ Tetrahedral Cluster

*Gizem Dübek, Franziska Hanusch, Dominik Munz, and Shigeyoshi Inoue**

anie_201916116_sm_miscellaneous_information.pdf

Supporting Information

Contents

1. Experimental Section	S2
General Methods and Instrumentation	S2
Synthesis of $\text{Cp}(\text{CO})_2\text{Mo}=\text{Si}(\text{Si}t\text{Bu}_3)(\text{IE}t_2\text{Me}_2)$ (2)	S3
Synthesis of $\text{Cp}(\text{CO})_2\text{W}=\text{Si}(\text{Si}t\text{Bu}_3)(\text{IE}t_2\text{Me}_2)$ (3):	S6
Synthesis of $\text{Cp}(\text{CO})_2\text{W}=\text{Si}(\text{Si}t\text{Bu}_3)(\text{IMe}_4)$ (3'):	S11
$[\text{Cp}(\text{CO})(\text{Cl}_3\text{Al}\cdots\text{OC})\text{W}=\text{Si}(\text{Si}t\text{Bu}_3)(\text{IE}t_2\text{Me}_2)$ (4a)	S13
$[\text{Cp}(\text{CO})((\text{C}_6\text{F}_5)_3\text{B}\cdots\text{OC})\text{W}=\text{Si}(\text{Si}t\text{Bu}_3)(\text{IE}t_2\text{Me}_2)$ (4b):	S13
$[\text{Cp}(\text{CO})_2\text{MoSi}(\text{Si}t\text{Bu}_3)]_2$ (5):	S18
$[\text{Cp}(\text{CO})_2\text{WSi}(\text{Si}t\text{Bu}_3)]_2$ (6):	S25
Isolation of $\text{IE}t_2\text{Me}_2 \cdot \text{BPh}_3$	S32
2. Single Crystal X-ray structure determination.....	S35
3. Computational Data.....	S40
General.....	S40
4. References.....	S63

1. Experimental Section

General Methods and Instrumentation

All experiments and manipulations were carried out under argon atmosphere using standard Schlenk techniques or in an MBraun inert-atmosphere glovebox unless otherwise stated. Glassware was heat dried under vacuum prior to use. Solvents were dried by standard methods. NMR spectra at ambient temperature (298 K) were recorded on a Bruker AV400US, DRX400, AVHD300, or AV500C device. $\delta(^1\text{H})$ and $\delta(^{13}\text{C})$ were referenced internally to the relevant residual solvent resonances. $\delta(^{29}\text{Si})$ was referenced to the signal of tetramethylsilane (TMS) ($\delta = 0$ ppm) as external standard. Some NMR spectra include resonances for silicone grease (C_6D_6 : $\delta(^1\text{H}) = 0.29$ ppm, $\delta(^{13}\text{C}) = 1.4$ ppm and $\delta(^{29}\text{Si}) = -21.8$ ppm) derived from B. Braun Melsungen AG Sterican® cannulas. Elemental analyses (EA) were conducted with a EURO EA (HEKA tech) instrument equipped with CHNS combustion analyzer and melting points (m.p.) were determined in small glass capillaries under air by a Büchi M-565 melting point apparatus by microanalytical laboratory of the Catalysis Research Center, Technische Universität München. IR spectra were recorded on a Perkin Elmer FT-IR spectrometer (diamond ATR) in a range of 400–4000 cm^{-1} at room temperature inside an argon-filled glovebox. Mass spectrometry data were acquired using an Exactive Plus Orbitrap system (ionization method: LIFDI) by Thermo Fisher Scientific. The compounds 1,3,4,5-tetramethylimidazol-2-ylidene (IME_4)^[1], $\text{Cp}(\text{CO})_2(\text{PMe}_3)\text{MLi}$ ^[2] and $\text{tBu}_3\text{SiSi}(\text{Cl})(\text{IEt}_2\text{Me}_2)$ ^[3] were prepared according to literature procedures. Commercially available chemicals (BPh_3 , AlCl_3 and $\text{B}(\text{C}_6\text{F}_5)_3$) were purchased from abcr GmbH or Tokyo Chemical Industry Co., Ltd and used without further purification. Abbreviations: s = singlet, d = doublet, t = triplet, m = multiplet, br = broad, n.a. = not applicable/no answer, n.o. = not observed, SCXRD = Single Crystal X-ray diffraction, IG = Inverse-Gated, INEPT = Inensitive Nuclei Enhanced by Polarization Transfer, HMBC = Heteronuclear Multiple Bond Correlation.

Synthesis of Cp(CO)₂Mo=Si(Si^tBu₃)(IEt₂Me₂) (2) : tBu₃Si(Cl)Si: ←IEt₂Me₂ (**1**) (500 mg, 1.2 mmol) and CpMo(CO)₂PMe₃Li (380 mg, 1.26 mmol, 1.05 equiv.) were mixed in 15 mL toluene and the suspension heated to 75 °C overnight. During this time almost all solids were dissolved and color of reaction changed from orange to dark green. Suspension filtered from colorless precipitate (LiCl) and toluene was removed under vacuum to yield dark green residue. Residue filtered by toluene:pentane mixture (10 mL:30 mL) from insoluble brown material. Suitable crystals for single X-ray diffraction analysis were obtained by toluene:pentane (1:3) mixture of compound **2** at room temperature. Yield: 590 mg (82%)

¹H NMR (400 MHz, C₆D₆, 298K): δ 5.44 (s, 5H, C₅H₅), 4.32 (m, 2H, N-CH₂CH₃), 3.62 (m, 2H, N-CH₂CH₃), 1.42 (s, 6H, C-CH₃), 1.35 (s, 27H, ((CH₃)₃C)), 1.25 (t, 6H, N-CH₂CH₃).

¹³C NMR (101 MHz, C₆D₆, 298K): δ 241.51 (CO), 168.26 (:CN₂), 125.79 (CH₃C=CCH₃), 90.14 (C₅H₅), 42.59 (N-CH₂CH₃), 32.57 (C(CH₃)₃), 24.96 (C(CH₃)₃), 14.58 (N-CH₂CH₃), 8.33 (CH₃C=CCH₃).

²⁹Si{¹H} NMR (80 MHz, C₆D₆, 298K): δ 278.76 (Si=Mo), 6.36 (tBu₃Si)

²⁹Si INEPT NMR (80 MHz, C₆D₆, 298K): δ 6.36 (tBu₃Si)

IR (ATR, neat) [cm⁻¹]: ν(CO) = 1782, 1864

EA: C₂₈H₄₈MoN₂O₂Si₂; Calculated [%]: C (56.35), H (8.11), N (4.69); Measured: C (56.34), H (8.12), N (4.46)

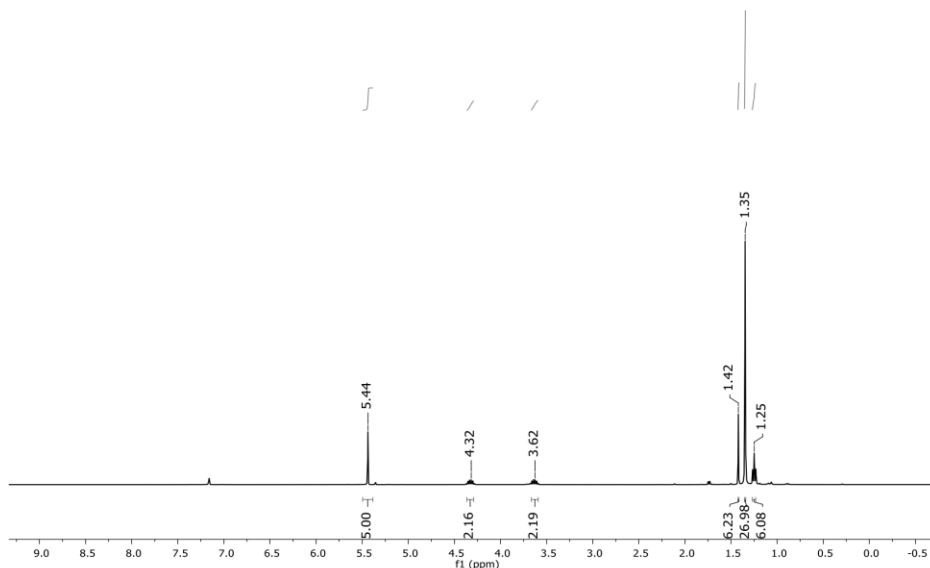


Figure S1. ¹H spectrum of compound **2** in C₆D₆ at 298 K.

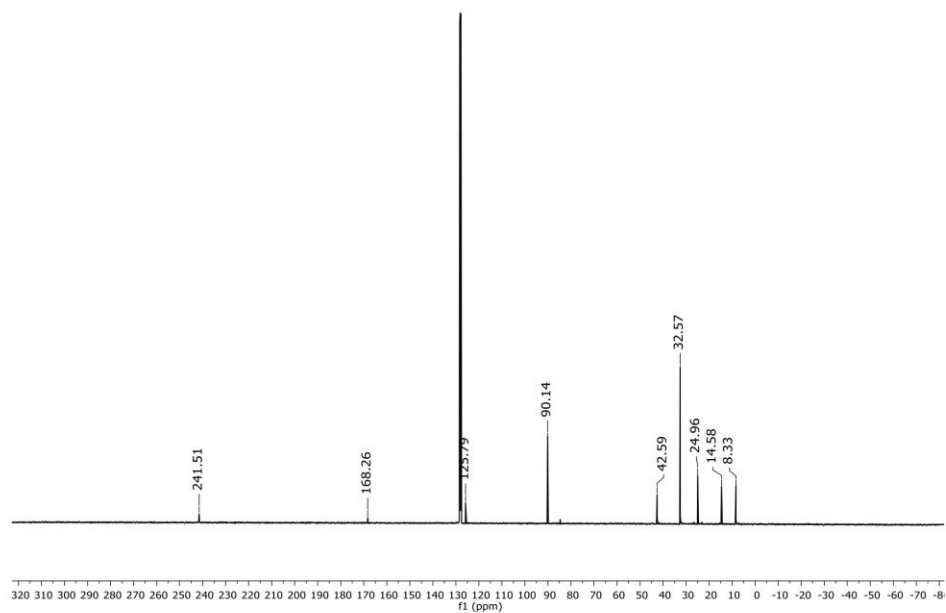


Figure S2. ^{13}C spectrum of compound **2** in C_6D_6 at 298 K.

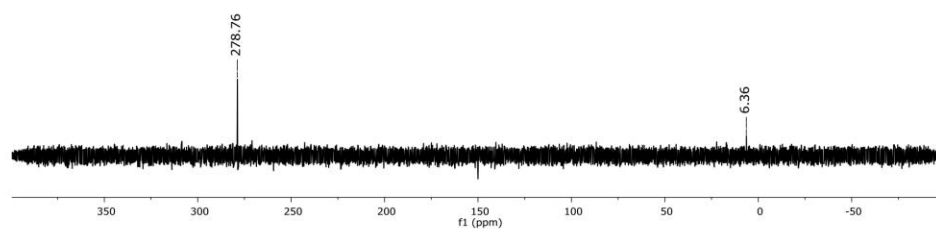


Figure S3. $^{29}\text{Si}\{^1\text{H}\}$ spectrum of compound **2** in C_6D_6 at 298 K.

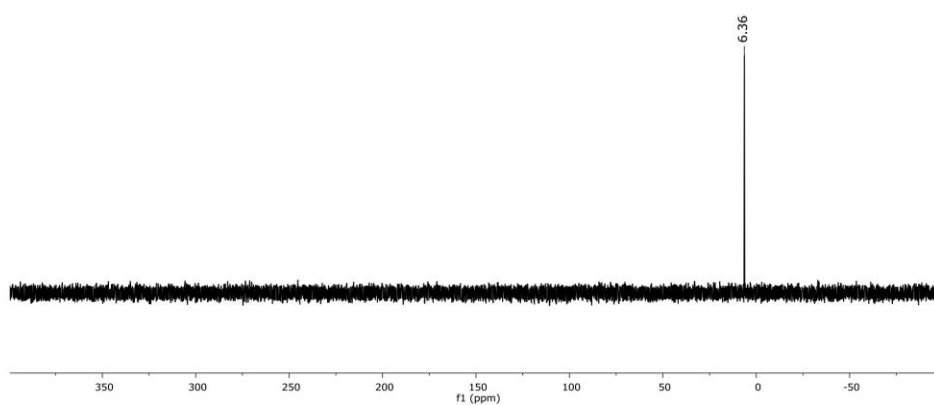


Figure S4. ^{29}Si -INEPT spectrum of compound **2** in C_6D_6 at 298 K.

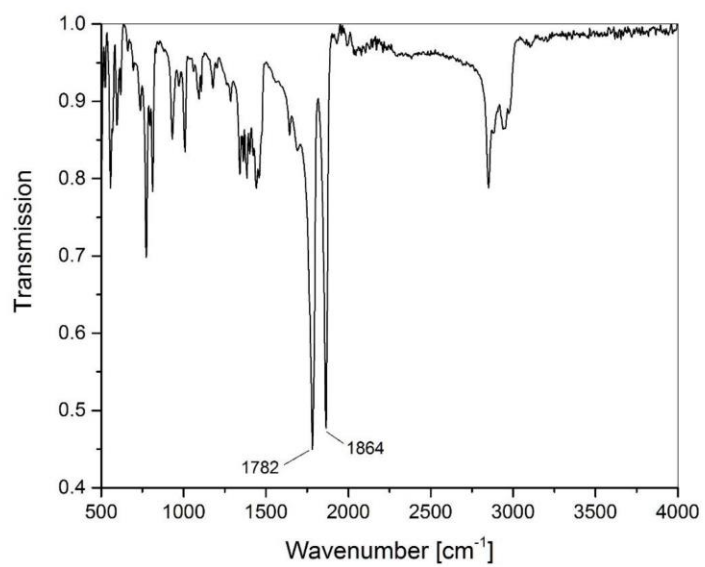


Figure S5. IR Spectrum of compound **2**. (ATR, neat)

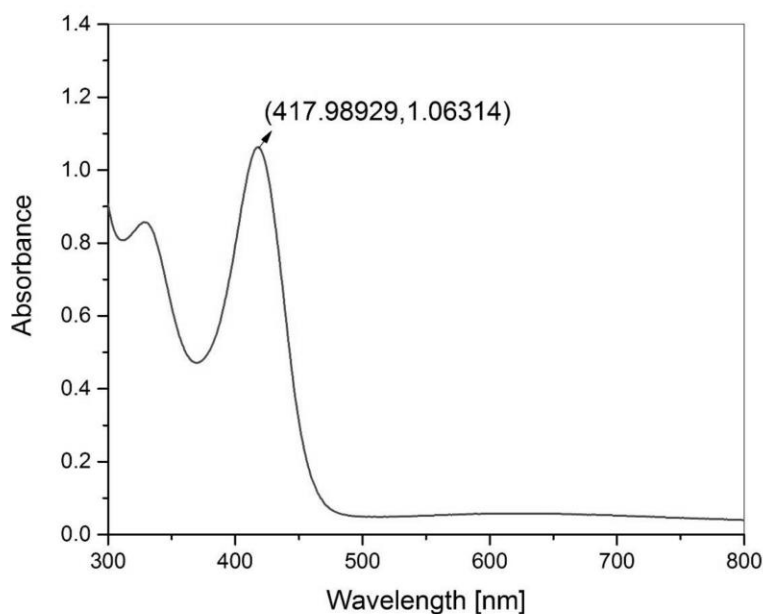


Figure S6. UV-Vis spectra of compound **2** in toluene. (Conc. 1.173×10^{-4} M; $\epsilon = 9063 \text{ L mol}^{-1}\text{cm}^{-1}$)

Synthesis of $\text{Cp}(\text{CO})_2\text{W}=\text{Si}(\text{Si}t\text{Bu}_3)(\text{IEt}_2\text{Me}_2)$ (3**):** $t\text{Bu}_3\text{Si}(\text{Cl})\text{Si} \leftarrow \text{IEt}_2\text{Me}_2$ (**1**) (500 mg, 1.2 mmol) and $\text{CpW}(\text{CO})_2\text{PMe}_3\text{Li}$ (490 mg, 1.26 mmol, 1.05 equiv.) were mixed in 15 mL toluene and the suspension heated to 75°C overnight. During this time almost all solids were dissolved and color of reaction changed from orange to dark-brown green. Suspension filtered from colorless precipitate (LiCl) and toluene was removed under vacuum to yields dark green residue. Residue filtered by toluene:pentane mixture (15 mL:20mL) from insoluble brown material. Suitable crystals for single X-ray diffraction analysis were obtained by toluene:pentane (1:1) mixture of compound **3** at 4°C . Yield: 640 mg (78%).

^1H NMR (400 MHz, C_6D_6 , 298K): δ 5.38 (s, 5H, C_5H_5), 4.54 (m, 2H, N- CH_2CH_3), 3.80 (m, 2H, N- CH_2CH_3), 1.43 (s, 6H, C- CH_3), 1.34 (s, 27H, $((\text{CH}_3)_3\text{C})$), 1.21 (t, 6H, N- CH_2CH_3).

^{13}C NMR (101 MHz, C_6D_6 , 298K): δ 232.77 (CO), 172.62 ($:\text{CN}_2$), 125.60 ($\text{CH}_3\text{C}=\text{CCH}_3$), 88.68 (C_5H_5), 40.95 (N- CH_2CH_3), 32.51 (C(CH_3) $_3$), 24.45 (C(CH_3) $_3$), 14.63 (N- CH_2CH_3), 8.28 ($\text{CH}_3\text{C}=\text{CCH}_3$).

$^{29}\text{Si}\{^1\text{H}\}$ NMR (99 MHz, C_6D_6 , 298K): δ 229.71 (Si=W, $^1J_{\text{WSi}} = 261 \text{ Hz}$), 12.32 ($t\text{Bu}_3\text{Si}$)

^{29}Si INEPT NMR (80 MHz, C_6D_6 , 298K): δ 12.38 ($t\text{Bu}_3\text{Si}$)

IR (ATR, neat) [cm⁻¹]: $\nu(\text{CO}) = 1770, 1849$

EA: C₂₈H₄₈WN₂O₂Si₂; Calculated [%]: C (49.12), H (7.07), N (4.09); Measured: C (51.38), H (7.79), N (3.90)

LIFDI-MS [m/z]: calculated (for C₂₈H₄₈N₂O₂Si₂W): 684.2765, observed: 684.2765

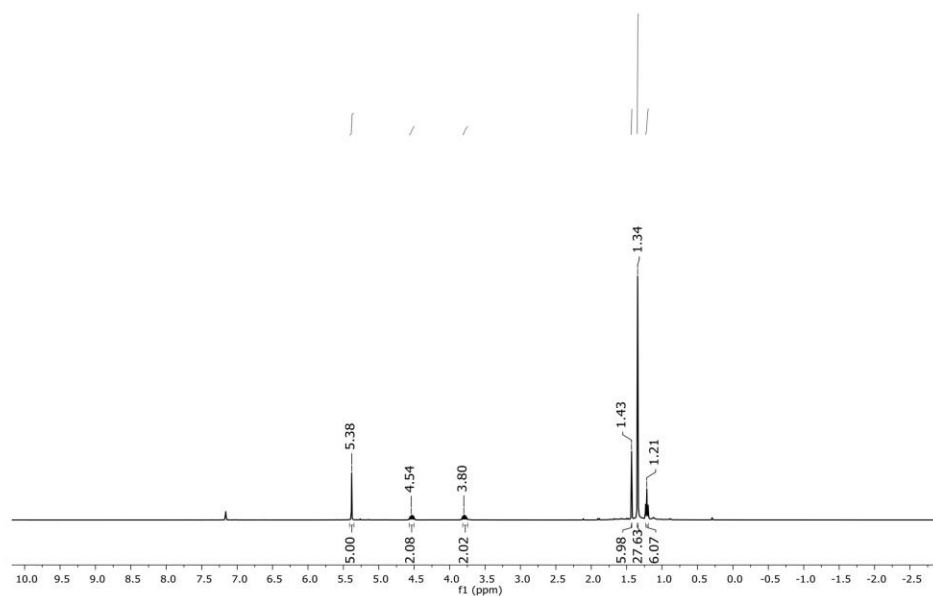


Figure S7. ¹H spectrum of compound **3** in C₆D₆ at 298 K.

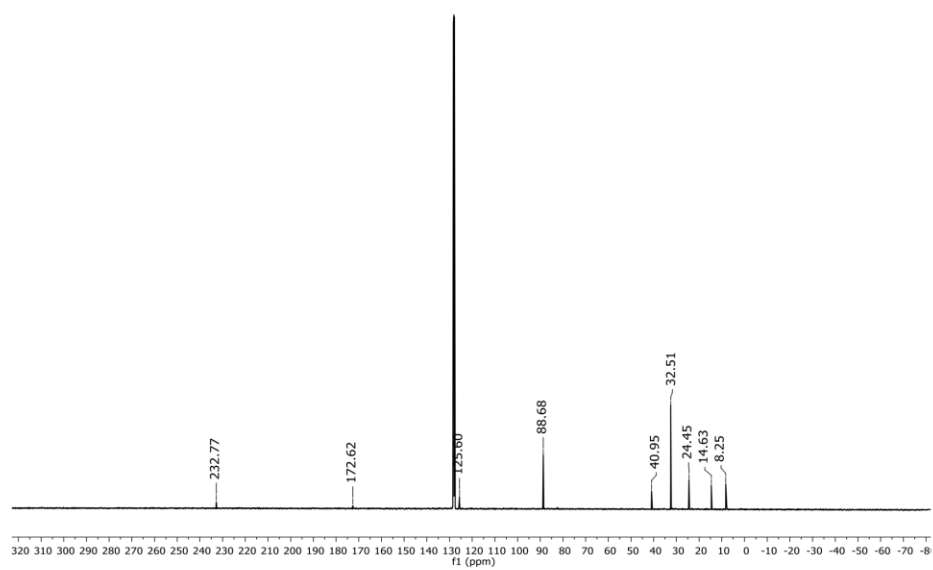


Figure S8. ^{13}C spectrum of compound **3** in C_6D_6 at 298 K.

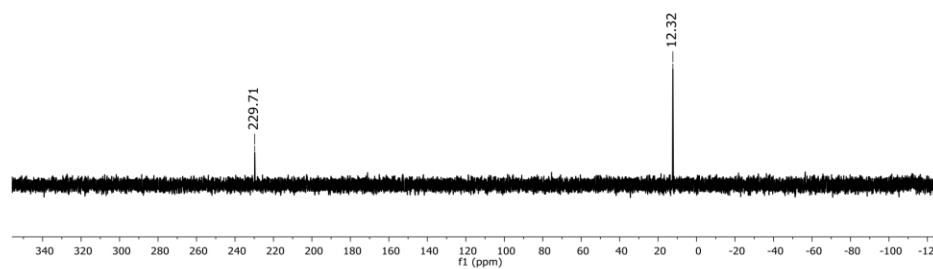


Figure S9. $^{29}\text{Si}\{^1\text{H}\}$ spectrum of compound **3** in C_6D_6 at 298 K.

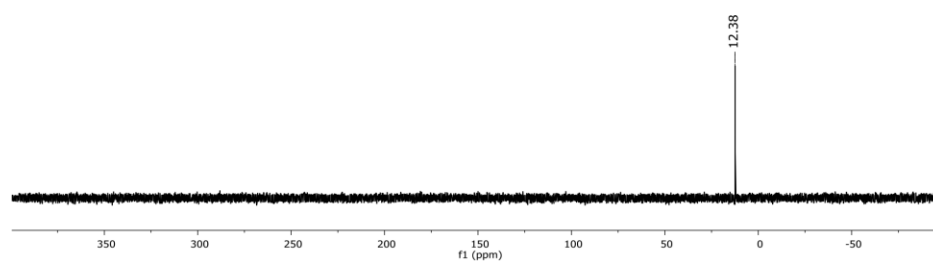


Figure S10. ^{29}Si -INEPT spectrum of compound **3** in C_6D_6 at 298 K.

S8

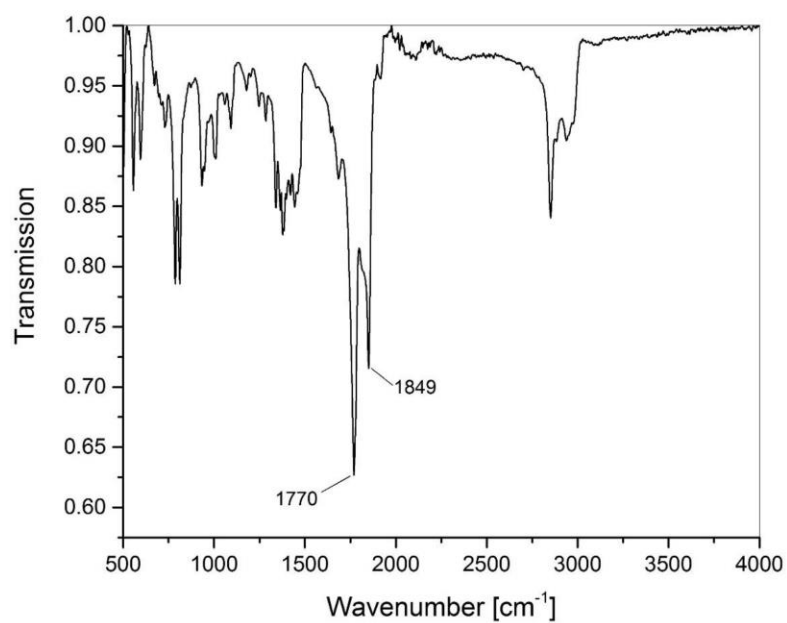


Figure S11. IR Spectrum of compound **3**. (ATR, neat)

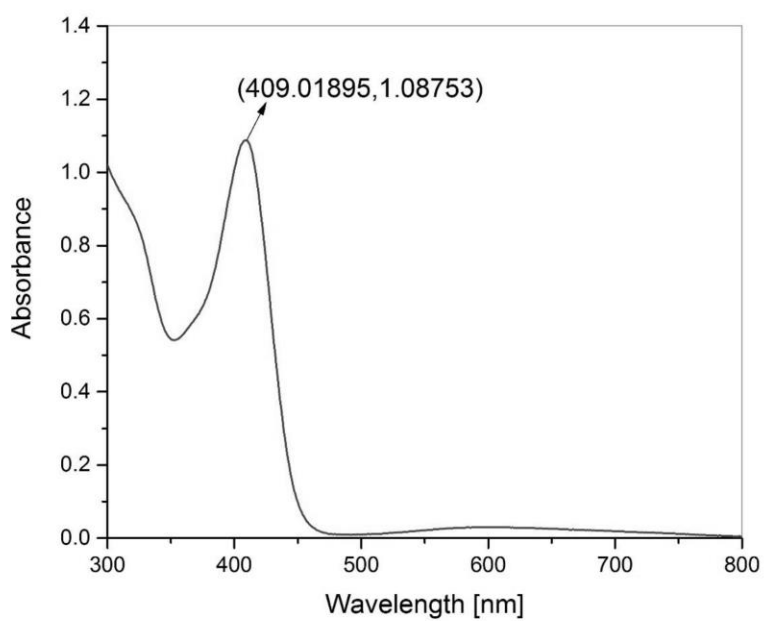


Figure S12. UV-Vis spectra of compound **3** in toluene. (Conc. 1.168×10^{-4} M; $\epsilon = 9311 \text{ L mol}^{-1}\text{cm}^{-1}$)

S9

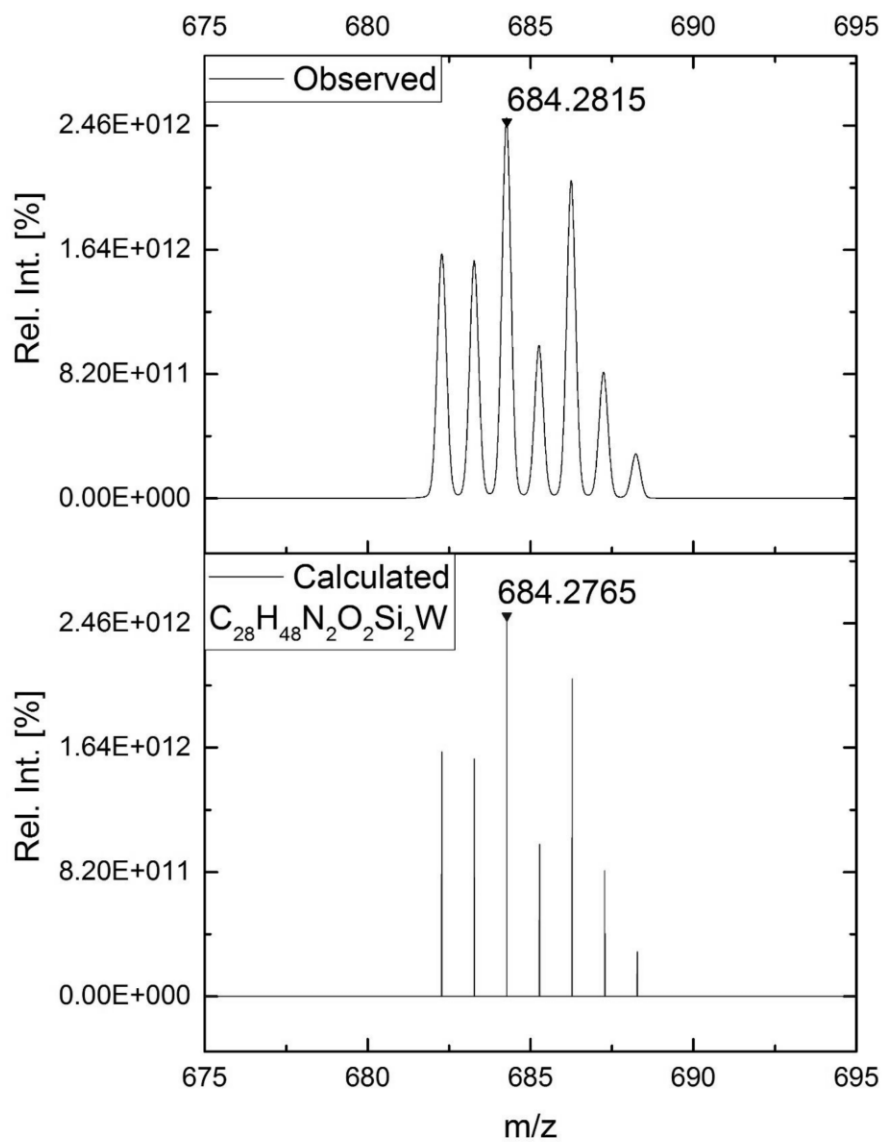


Figure S13. LIFDI-MS Spectrum: Expanded region of the compound signal showing the isotopic pattern of compound **3**. Observed (top) and calculated (bottom).

Synthesis of Cp(CO)₂W=Si(SiEt₃)(IMe₄) (3⁺): To an NMR solution of compound **3** (25mg, 0.036 mmol) in 0.4 mL C₆D₆, IMe₄ (5 mg, 0.04 mmol, 1.1 equiv.) added. The ¹H NMR spectra of reaction mixture was measured at room temperature after 30 minutes in which signals of **3** and **3⁺** were observed in an approximately 40:60 ratio. After 12 hours a quantitative exchange was observed in ¹H NMR spectrum. Suitable crystals for single X-ray diffraction analysis were obtained by C₆D₆:pentane (1:1) mixture of compound **3⁺** at ambient temperature.

¹H NMR (400 MHz, C₆D₆, 298K): δ 5.48 (s, 5H, C₅H₅), 3.64 (s, 6H, N-CH₃), 1.34 (s, 6H, C-CH₃), 1.28 (s, 27H, ((CH₃)₃C)).

¹³C NMR (101 MHz, C₆D₆, 298K): δ 235.48 (CO), 172.73 (:CN₂), 125.69 (CH₃C=CCH₃), 89.88 (C₅H₅), 32.27 (C(CH₃)₃), 31.68 (N-CH₃), 24.01 (C(CH₃)₃), 7.84 (CH₃C=CCH₃).

²⁹Si{¹H} NMR (80 MHz, C₆D₆, 298K): δ 231.14 (Si=W, ¹J_{WSi} = n.a.), 13.49 (tBu₃Si)

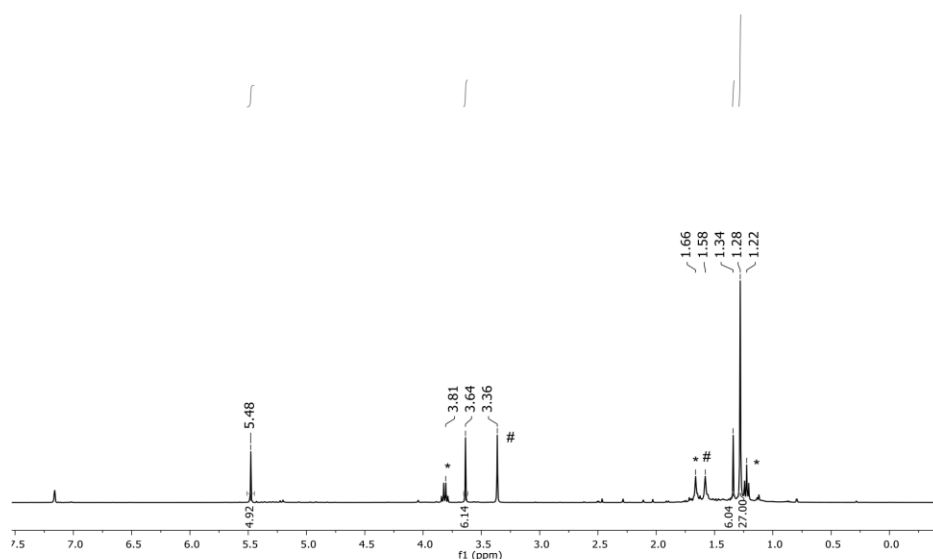


Figure S14. ¹H spectrum of compound **3⁺** in C₆D₆ at 298 K. (* = free IEt₂Me₂, # = Excess IMe₄)

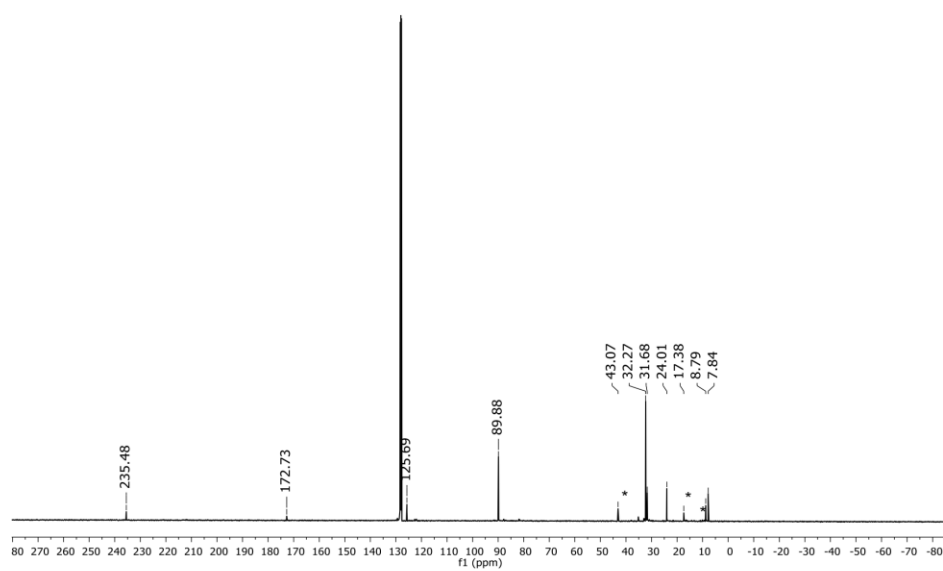


Figure S15. ^{13}C spectrum of compound **3** in C_6D_6 at 298 K. (* = Free IEt_2Me_2)

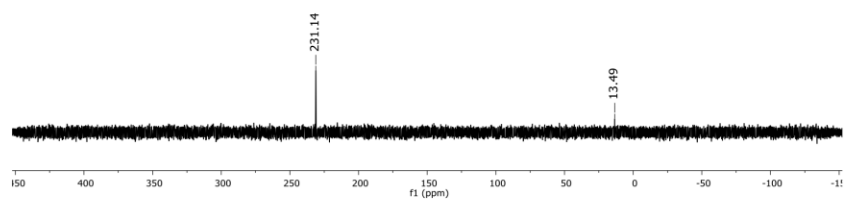


Figure S16. $^{29}\text{Si}\{^1\text{H}\}$ spectrum of compound **3** in C_6D_6 at 298 K.

[Cp(CO)(Cl₃Al···OC)W=Si(SitBu₃)(IEt₂Me₂) (4a) : To a toluene solution of **3** (50 mg, 0.073 mmol), AlCl₃ (10 mg, 0.073 mmol) added. Dark green solution turned immediately to dark red which was filtered from insoluble oily residue. Toluene was removed and **4a** was obtained as sticky dark red solid in 64% yield. Suitable crystals for single X-ray diffraction analysis were obtained by concentrated toluene solution of **4a** at 3 °C.

¹H NMR (400 MHz, C₆D₆, 298K): δ 5.28 (s, 5H, C₅H₅), 3.97 (m, 1H, N-CH₂CH₃), 3.88 (m, 1H, N-CH₂CH₃), 3.49 (m, 1H, N-CH₂CH₃), 3.32 (m, 1H, N-CH₂CH₃), 1.76 (s, 3H, C-CH₃), 1.74 (s, 3H, C-CH₃), 1.14 (s, 27H, ((CH₃)₃C)), 1.36 (t, 6H, N-CH₂CH₃).

¹³C NMR (101 MHz, C₆D₆, 298K): δ 220.22 (CO), 166.86 (:CN₂), 126.82 (CH₃C=CCH₃), 91.51 (C₅H₅), 43.55 (N_a-CH₂CH₃), 41.85 (N_b-CH₂CH₃), 32.14 (C(CH₃)₃), 24.80 (C(CH₃)₃), 15.15 (N_a-CH₂CH₃), 13.21 (N_b-CH₂CH₃), 8.75 (CH₃C=CCH₃), 8.40 (CH₃C=CCH₃).

²⁹Si{¹H} NMR (80 MHz, C₆D₆, 298K): δ 322.03 (Si=W, ¹J_{WSi} = n.a.), 15.59 (tBu₃Si)

²⁹Si INEPT NMR (80 MHz, C₆D₆, 298K): δ 15.57 (tBu₃Si)

IR (ATR, neat) [cm⁻¹]: ν(CO) = 1813, 1901

EA: Due to presence of undefined oily impurities, satisfactory elemental analysis results were not obtained.

[Cp(CO)((C₆F₅)₃B···OC)W=Si(SitBu₃)(IEt₂Me₂) (4b): Compound **4b** was synthesized in similar manner as **4a**. Unfortunately, we could not isolate **4b** due to its oily nature hence we could not obtain pure NMR spectra except ¹¹B and ²⁹Si.

¹¹B NMR (128 MHz, C₆D₆, 298K): δ – 14.53

²⁹Si{¹H} NMR (80 MHz, C₆D₆, 298K): δ 323.15 (Si=W, ¹J_{WSi} = n.a.), 17.06 (tBu₃Si).

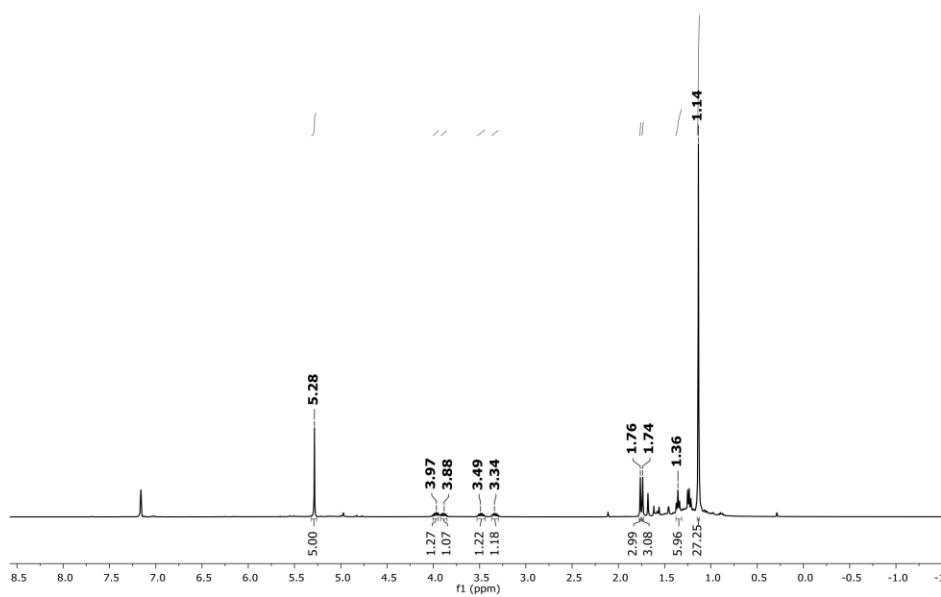


Figure S17. ^1H spectrum of compound **4a** in C_6D_6 at 298 K.

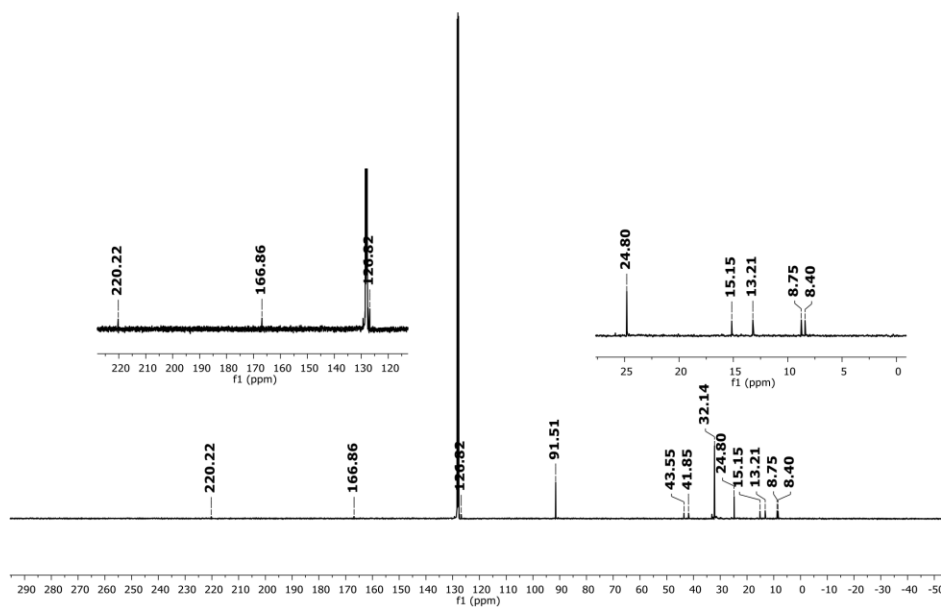


Figure S18. ^{13}C spectrum of compound **4a** in C_6D_6 at 298 K.

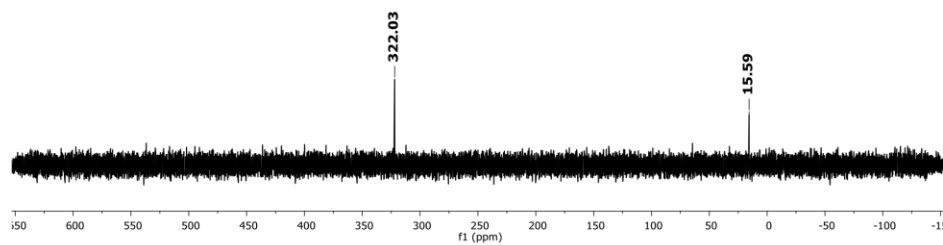


Figure S19. $^{29}\text{Si}\{^1\text{H}\}$ spectrum of compound **4a** in C_6D_6 at 298 K.

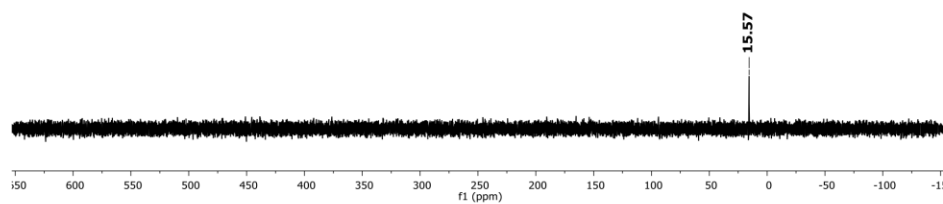


Figure S20. ^{29}Si -INEPT spectrum of compound **4a** in C_6D_6 at 298 K.

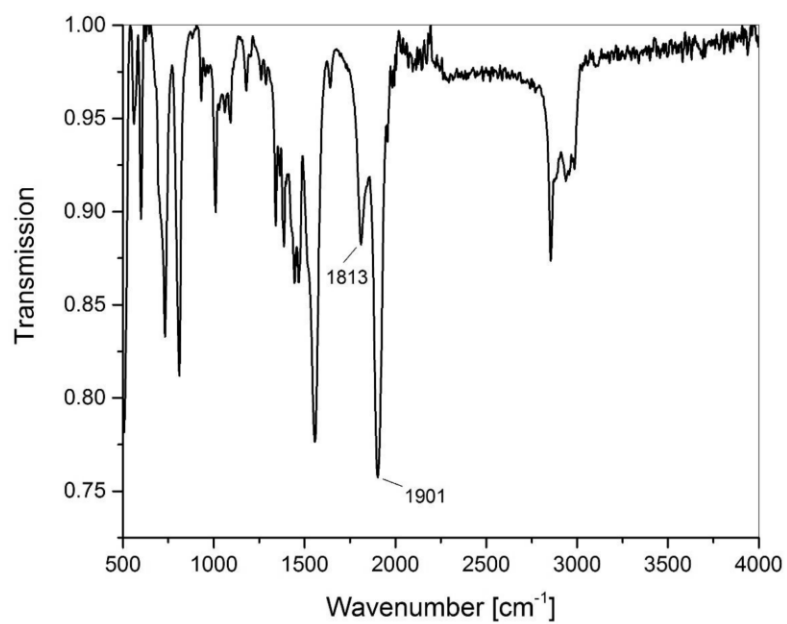


Figure S21. IR Spectrum of compound **4a**. (ATR, neat)

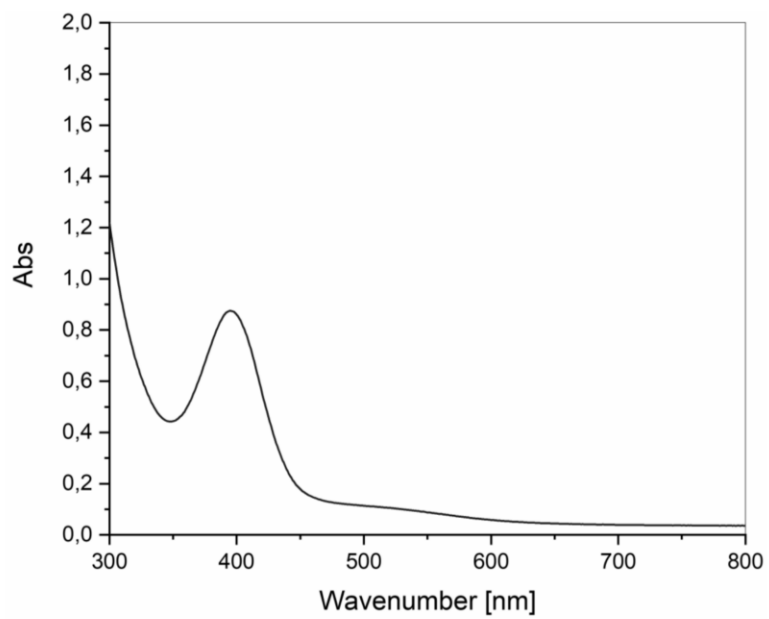


Figure S22. UV-Vis spectra of compound **4a** in toluene. (Conc. 1.17×10^{-4} M; $\epsilon_{395} = 7474 \text{ L mol}^{-1} \text{ cm}^{-1}$)

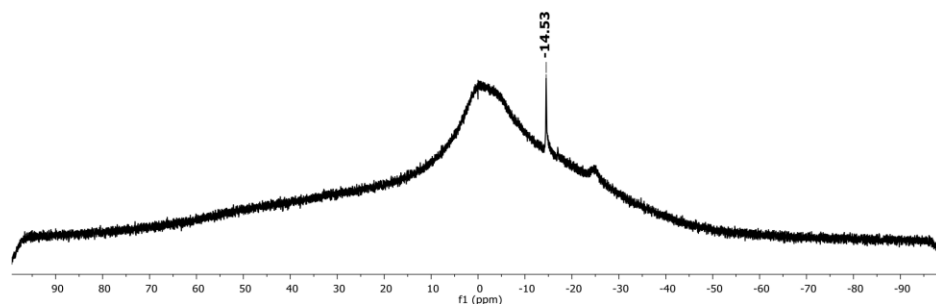


Figure S23. ^{11}B spectrum of compound **4b** in C_6D_6 at 298 K.

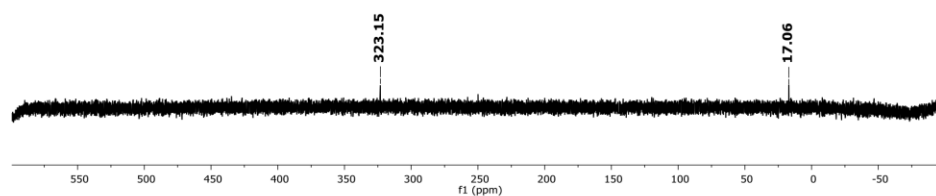


Figure S24. $^{29}\text{Si}\{^1\text{H}\}$ spectrum of compound **4b** in C_6D_6 at 298 K.

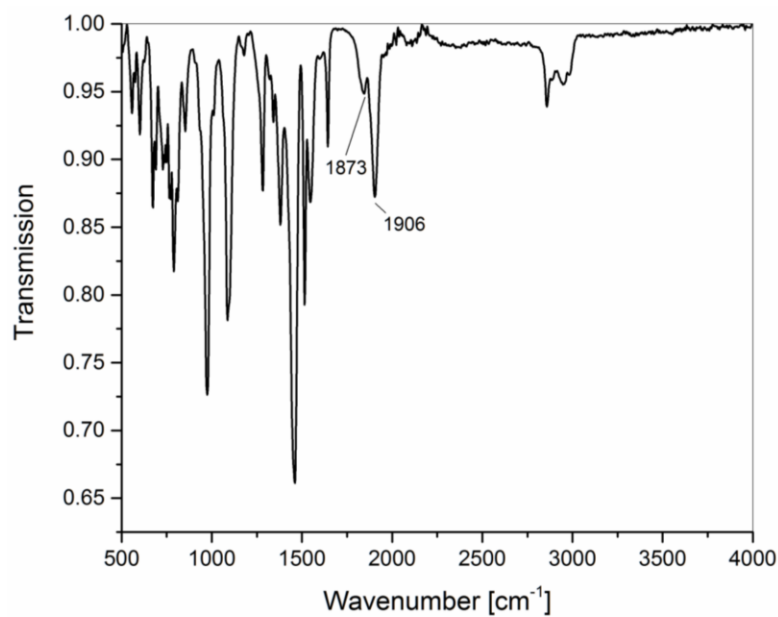


Figure S25. IR Spectrum of compound **4b**. (ATR, neat)

[Cp(CO)₂MoSi(tBu₃)₂] (5): Compound **2** (250 mg, 0.42 mmol) and BPh₃ (102 mg, 0.42 mmol) were dissolved in 10 mL toluene and heated to 90 °C. After 30 minutes the dark green solution turned into purple-brown solution. Toluene was removed to yield purple waxy residue and 15 mL pentane was added (upon pentane addition, beige solid precipitated, which was later characterized as BPh₃·IEt₂Me₂). Suspension placed at -80 °C cold bath for 30 minutes and purple solution was filtered at cold. Added 5 mL pentane to the beige solid, stirred 10 minutes, placed in cold bath again for 40 minutes and filtered again. Pentane was evaporated to yield compound **5** as a purple solid. (75 mg, 40%)

¹H NMR (400 MHz, C₆D₆, 298K): δ 4.72 (s, 5H, C₅H₅), 1.43 (s, 27H, ((CH₃)₃C)).

¹³C NMR (101 MHz, C₆D₆, 298K): δ 238.09 (CO), 230.37 (CO), 86.50 (C₅H₅), 32.77 (C(CH₃)₃), 25.96 (C(CH₃)₃).

²⁹Si{¹H} NMR (79 MHz, C₆D₆, 298K): δ 3.65 (SiMo), 48.32 (tBu₃Si)

²⁹Si INEPT NMR (79 MHz, C₆D₆, 298K): δ 48.52 (tBu₃Si)

IR (ATR, neat) [cm⁻¹]: ν(CO) = 1844, 1918

LIFDI-MS [m/z]: calculated (for C₃₈H₆₄O₄Si₄Mo₂): 889.2004, observed: 889.1627

M.P.: 64–65 °C

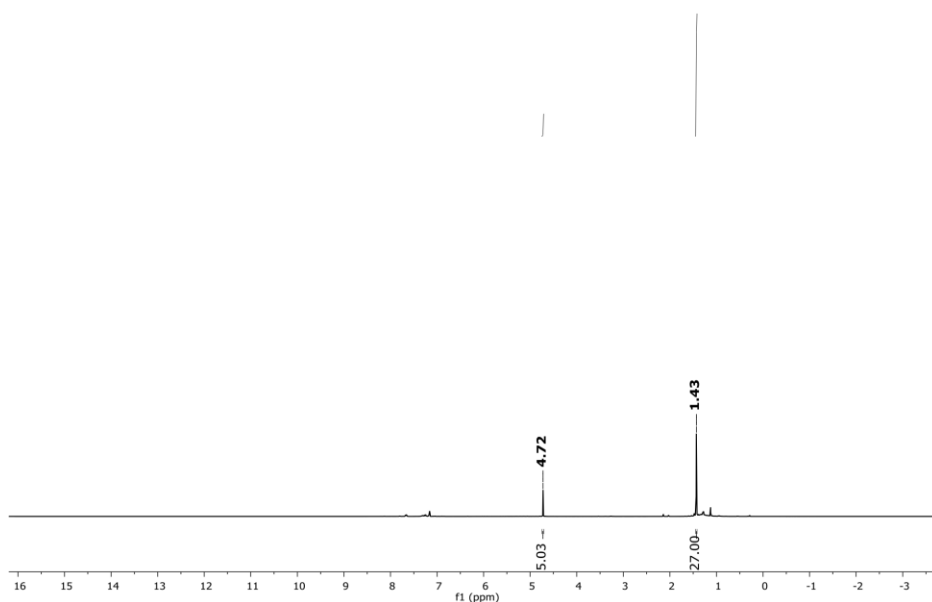


Figure S26. ^1H spectrum of compound 5 in C_6D_6 at 298 K.

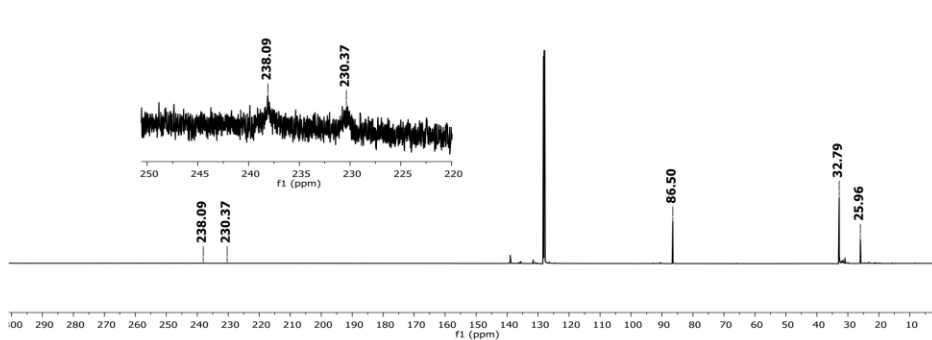


Figure S27. ^{13}C spectrum of compound 5 in C_6D_6 at 298 K.

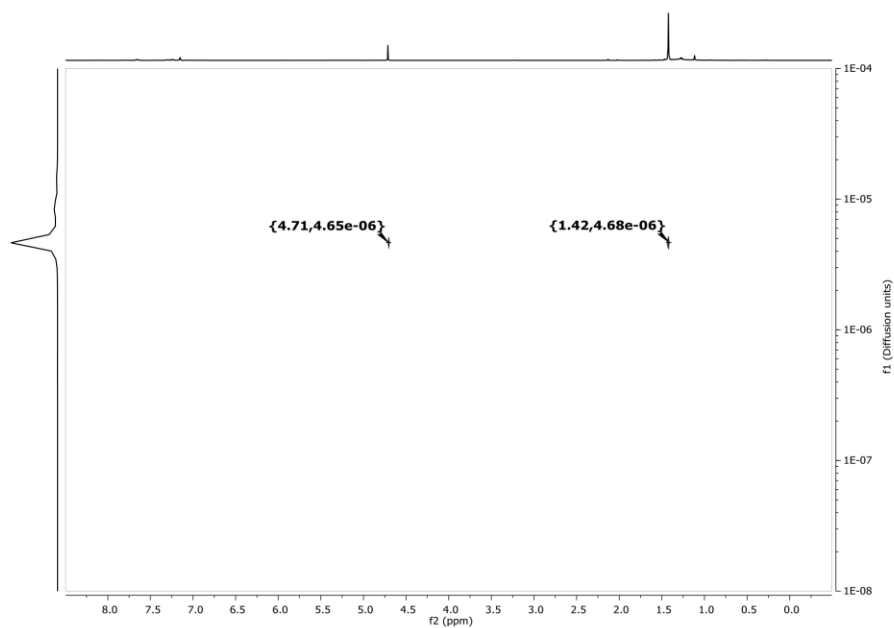


Figure S28. ^1H -2D DOSY NMR spectrum of compound **5** in C_6D_6 at 298 K.

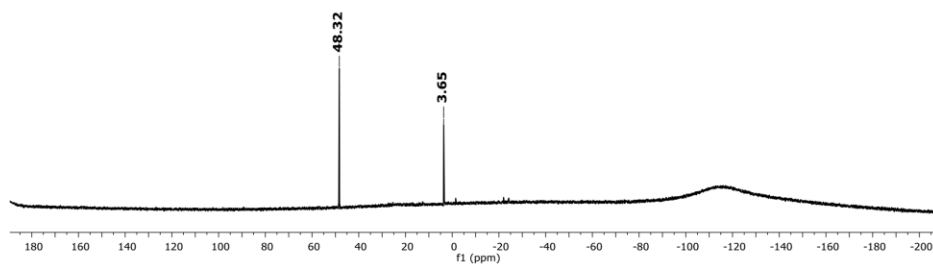


Figure S29. $^{29}\text{Si}\{^1\text{H}\}$ NMR spectrum of compound **5** in C_6D_6 at 298 K.

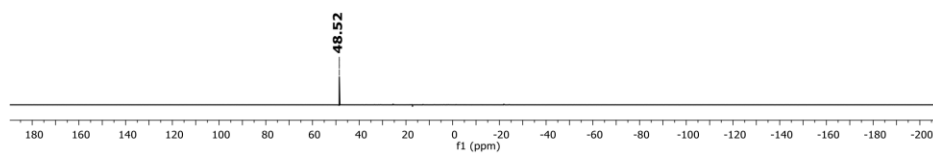


Figure S30. ^{29}Si -INEPT NMR spectrum of compound **5** in C_6D_6 at 298 K.

S20

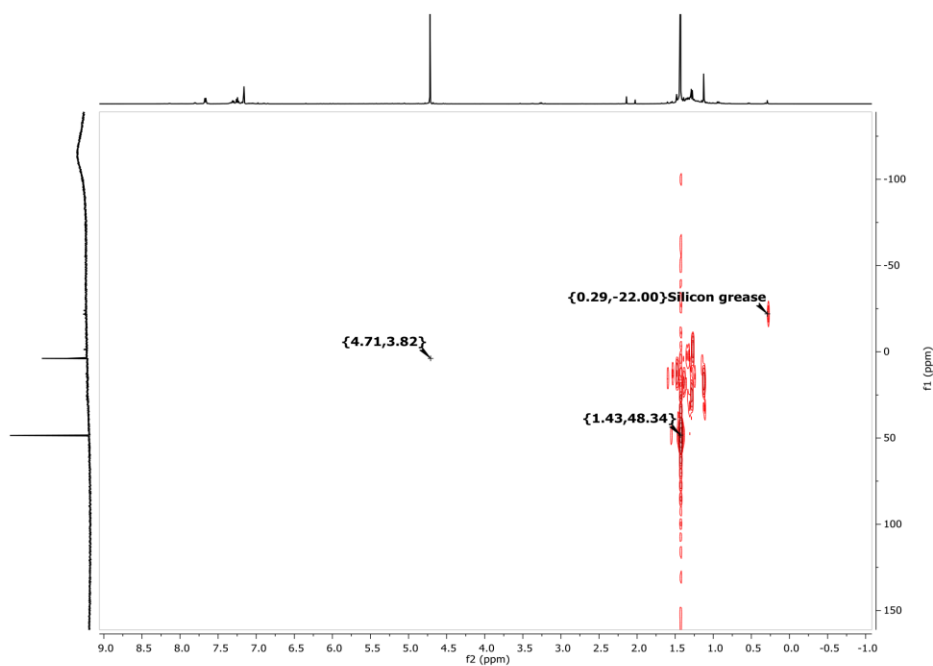


Figure S31. ^1H - ^{29}Si HMBC NMR spectrum of compound **5** in C_6D_6 at 298 K.

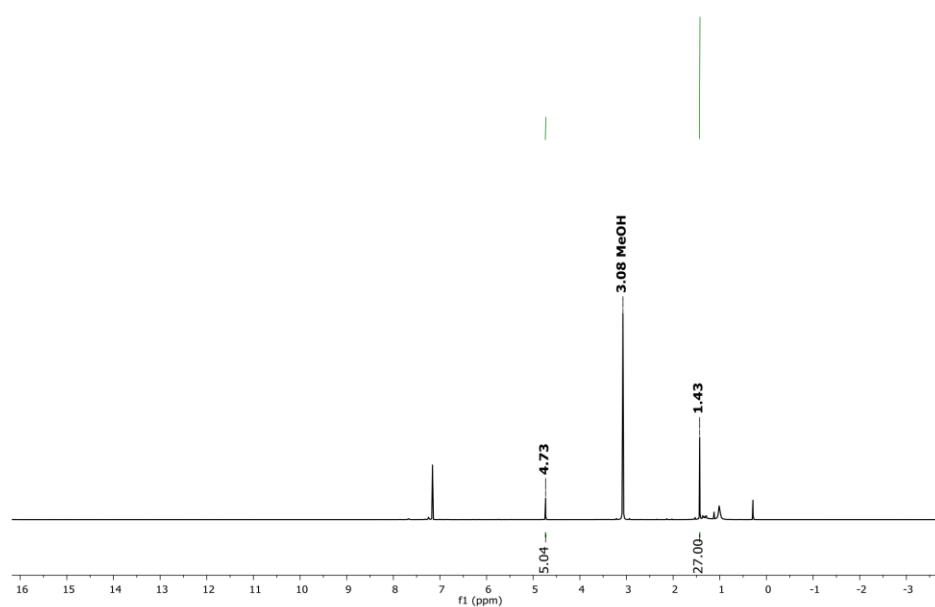


Figure S32. ^1H NMR spectrum of compound **5** upon treatment of excess MeOH in C_6D_6 at 298 K.

S21

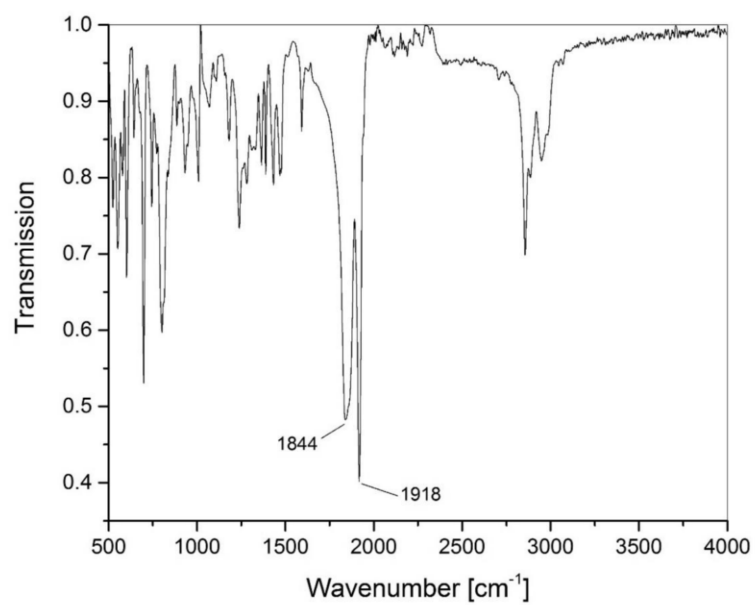


Figure S33. IR Spectrum of compound **5**. (ATR, neat)

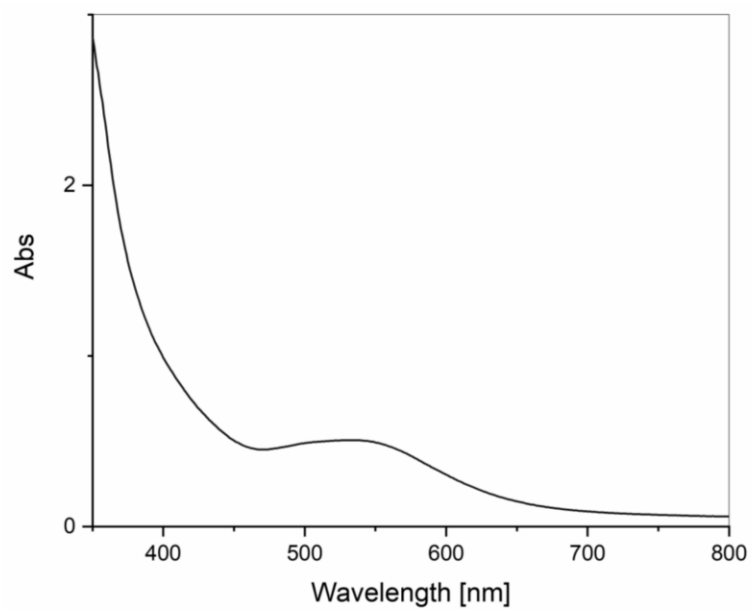


Figure S34. UV-Vis Spectra of compound **5** in toluene at 298 K. (Conc. 5.625×10^{-4} M; $\epsilon_{543} = 894 \text{ L mol}^{-1} \text{cm}^{-1}$)

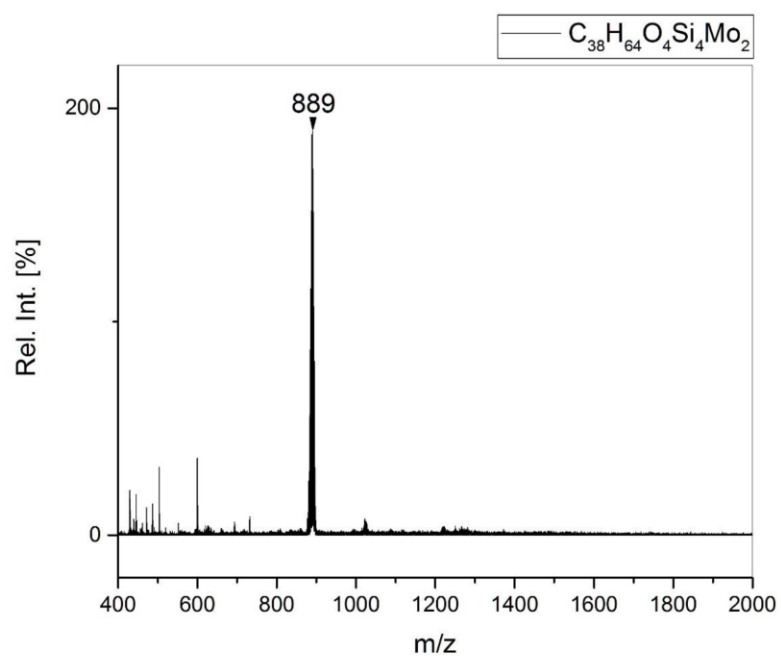


Figure S35. LIFDI-MS spectrum of compound **5** (in toluene solution). Compound observed at $m/z = 889$.

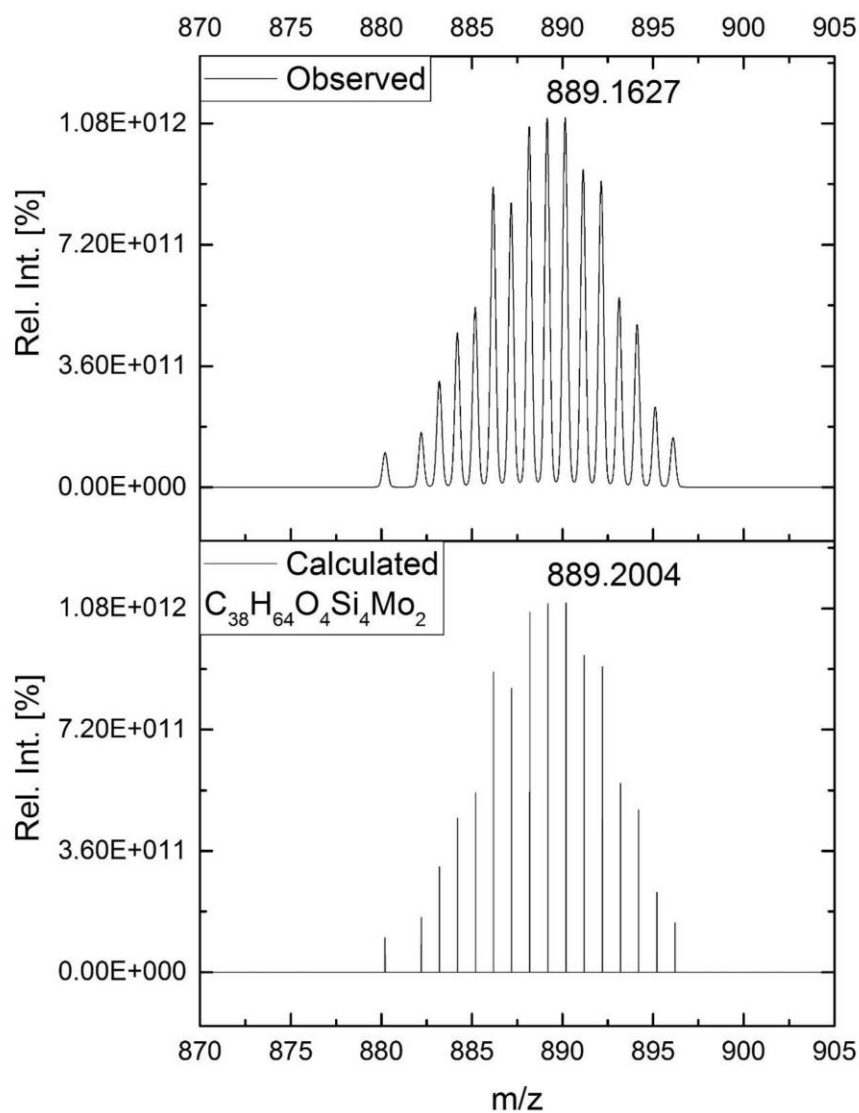


Figure S36. LIFDI-MS Spectrum: expanded region of the product signal illustrating the isotopic pattern of compound **5**. Observed (top) and calculated (bottom).

[Cp(CO)₂WSi(Si^tBu₃)]₂ (6): Compound **3** (99 mg, 0.14 mmol) and BPh₃ (35 mg, 0.14 mmol) were dissolved in 8 mL toluene and heated to 90 °C. After 30 minutes the dark green solution turned into dark red. Toluene was removed to yield red waxy residue and 15 mL pentane was added (upon pentane addition, beige solid precipitated, which was later characterized as BPh₃·IEt₂Me₂). Suspension placed at -80 °C cold bath for 30 minutes and red solution was filtered. Added 5 mL pentane to the beige solid, stirred 10 minutes, placed in cold bath again for 40 minutes and filtered again. Pentane was evaporated to yield compound **6** as a red solid. (40 mg, 52%). Suitable crystals for single X-ray diffraction analysis were obtained by concentrated hexane solution of **6** at ambient temperature.

¹H NMR (400 MHz, C₆D₆, 298K): δ 4.70 (s, 5H, C₅H₅), 1.44 (s, 27H, ((CH₃)₃C)).

¹³C NMR (101 MHz, C₆D₆, 298K): δ 225.38 (CO), 215.11 (CO), 83.99 (C₅H₅), 32.85 (C(CH₃)₃), 25.82 (C(CH₃)₃).

²⁹Si{¹H} NMR (79 MHz, C₆D₆, 298K): δ -63.04 (SiW, ¹J_{W_{Si}} = 52.07 Hz), 43.99 (tBu₃Si)

²⁹Si INEPT NMR (79 MHz, C₆D₆, 298K): δ 44.10 (tBu₃Si)

IR (ATR, neat) [cm⁻¹]: ν(CO) = 1860, 1914

LIFDI-MS [m/z]: calculated (for C₃₈H₆₄O₄Si₄W₂): 1064.2903, observed: 1064.3159

M.P.: 67–69 °C

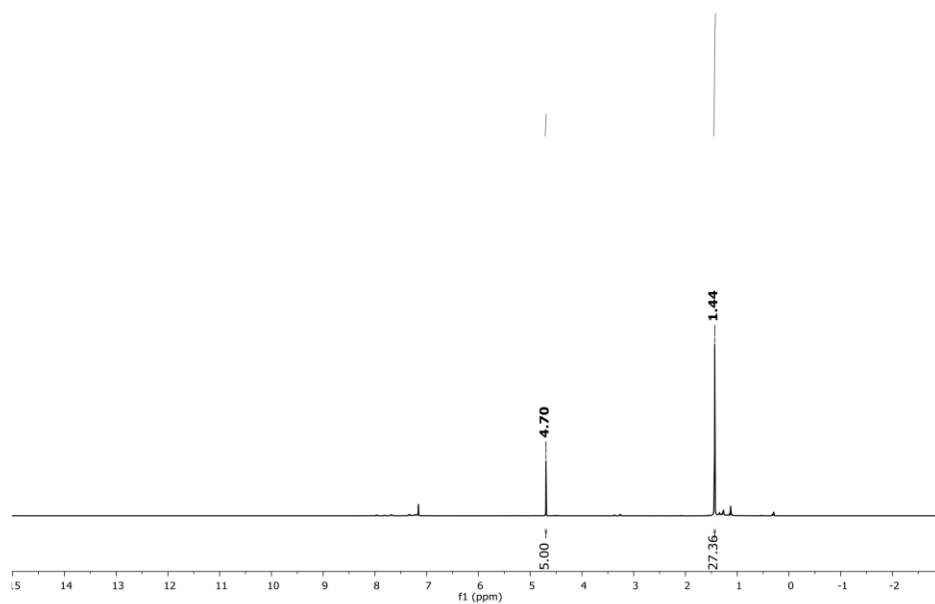


Figure S37. ¹H NMR spectrum of compound **6** in C₆D₆ at 298 K.

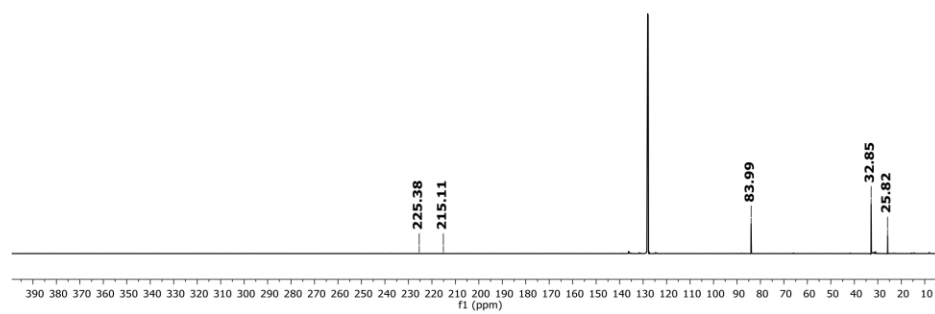


Figure S38. ¹³C NMR spectrum of compound **6** in C₆D₆ at 298 K.

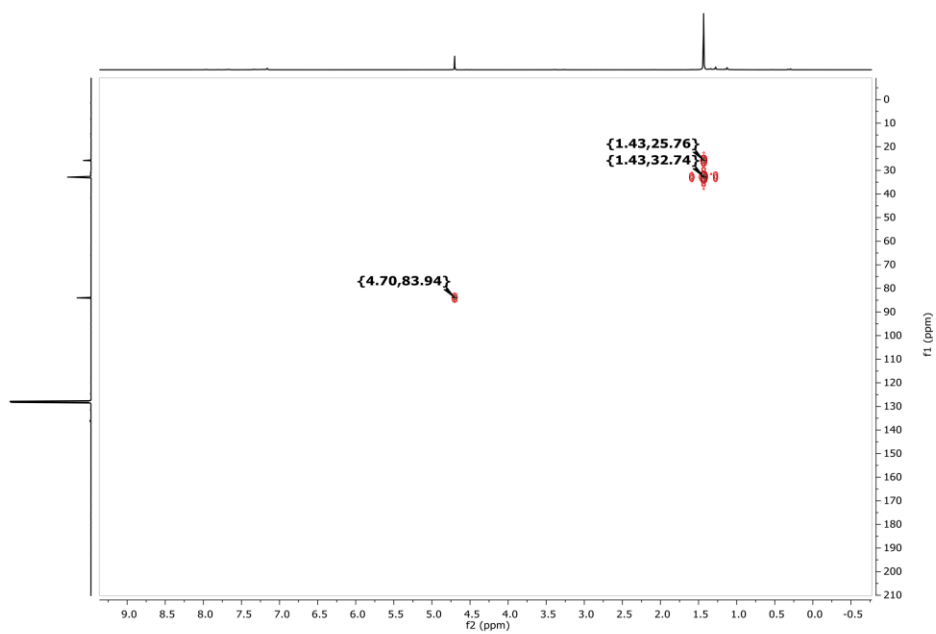


Figure S39. ^1H - ^{13}C HMBC NMR spectrum of compound **6** in C_6D_6 at 298 K.

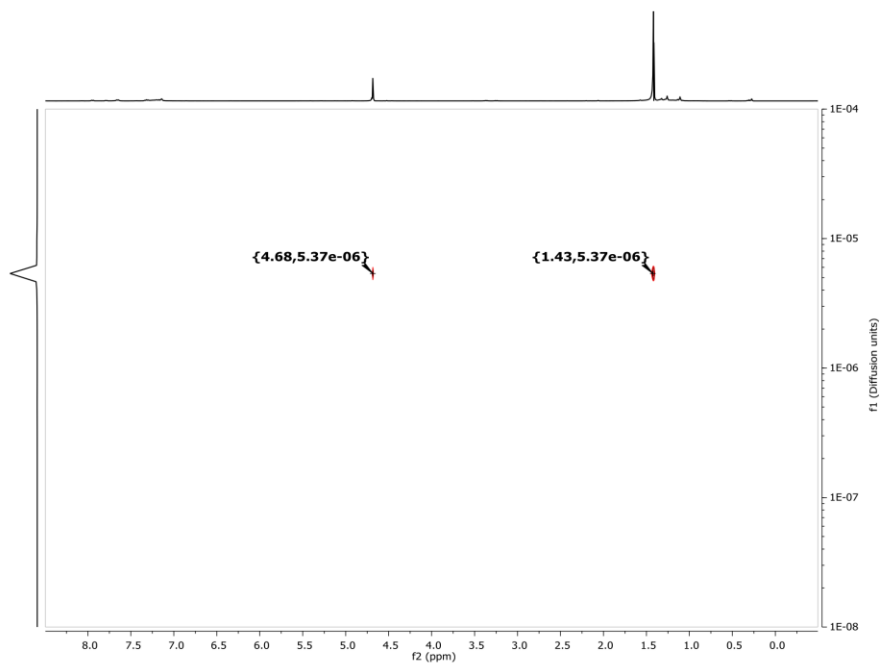


Figure S40. ^1H -2D DOSY NMR spectrum of compound **6** in C_6D_6 at 298 K.

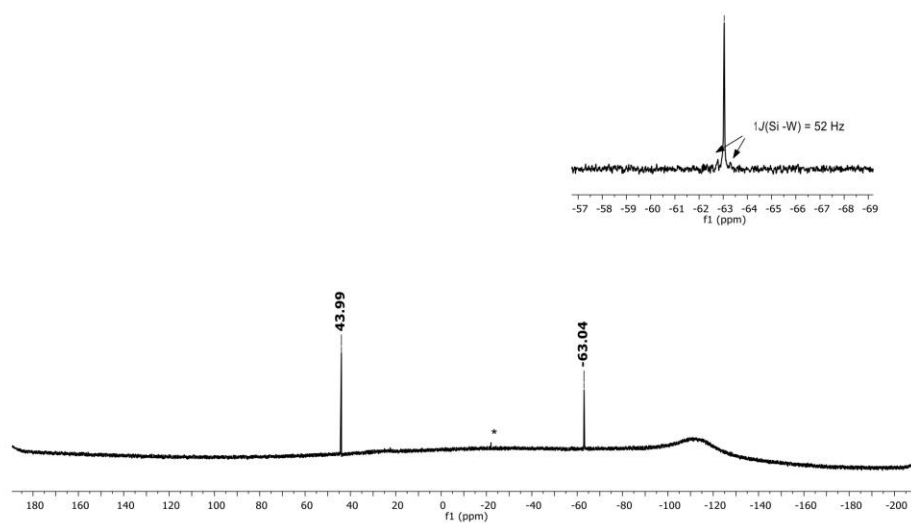


Figure S41. $^{29}\text{Si}\{^1\text{H}\}$ NMR spectrum of compound **6** in C_6D_6 at 298 K. (* = silicon grease)

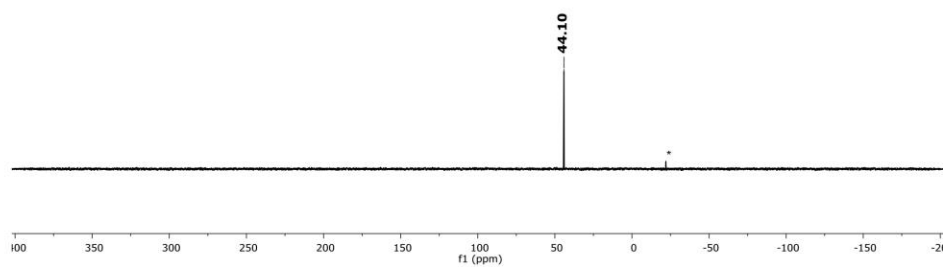


Figure S42. ^{29}Si -INEPT NMR spectrum of compound **6** in C_6D_6 at 298 K. (* = silicon grease)

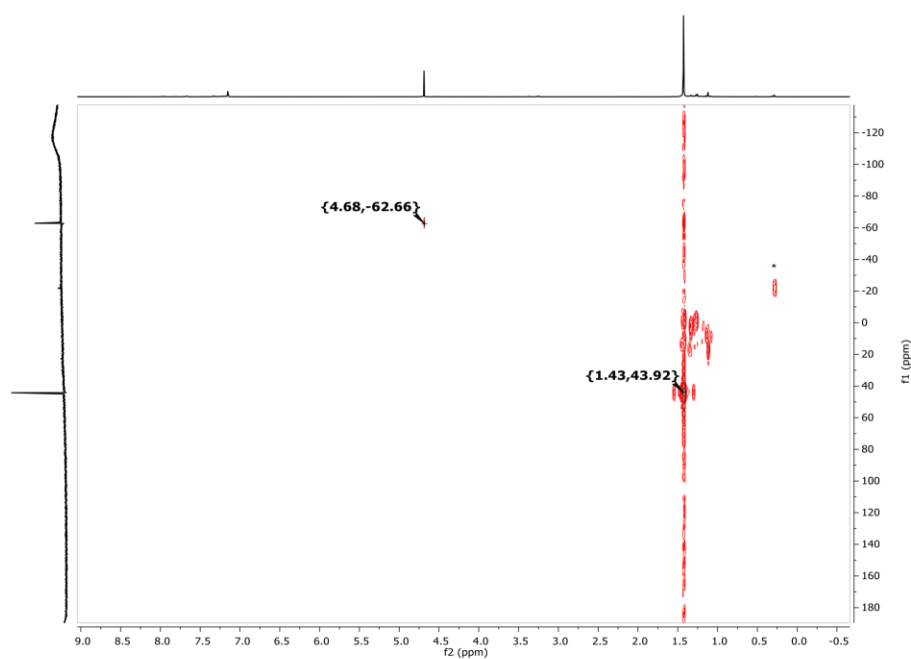


Figure S43. ^{29}Si - ^1H HMBC NMR spectrum of compound **6** in C_6D_6 at 298 K.

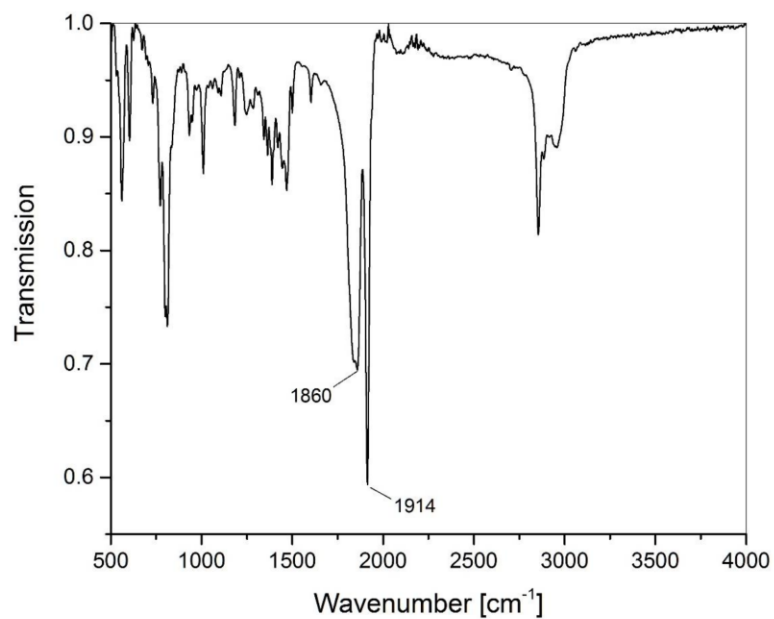


Figure S44. IR Spectrum of compound **6**. (ATR, neat)

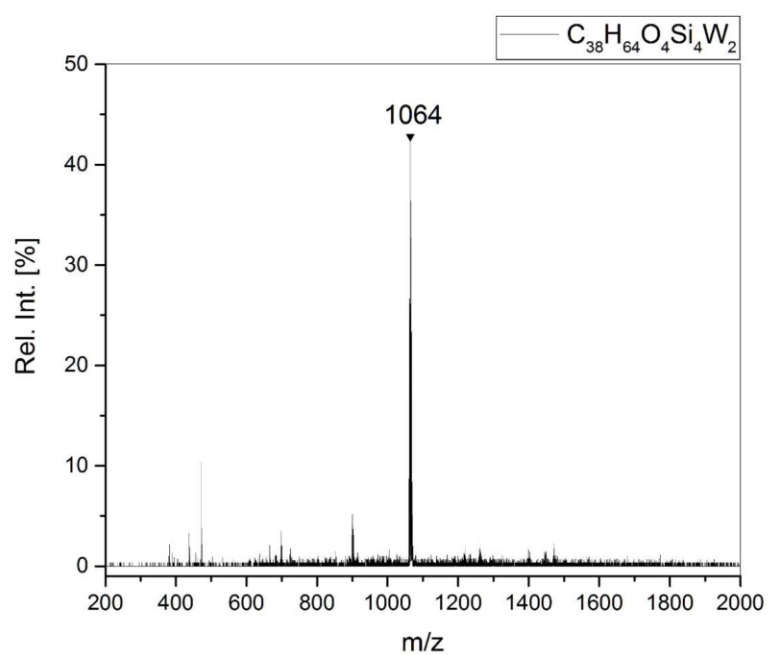


Figure S45. LIFDI-MS spectrum of compound **6** (in toluene solution). Compound observed at $m/z = 1064$.

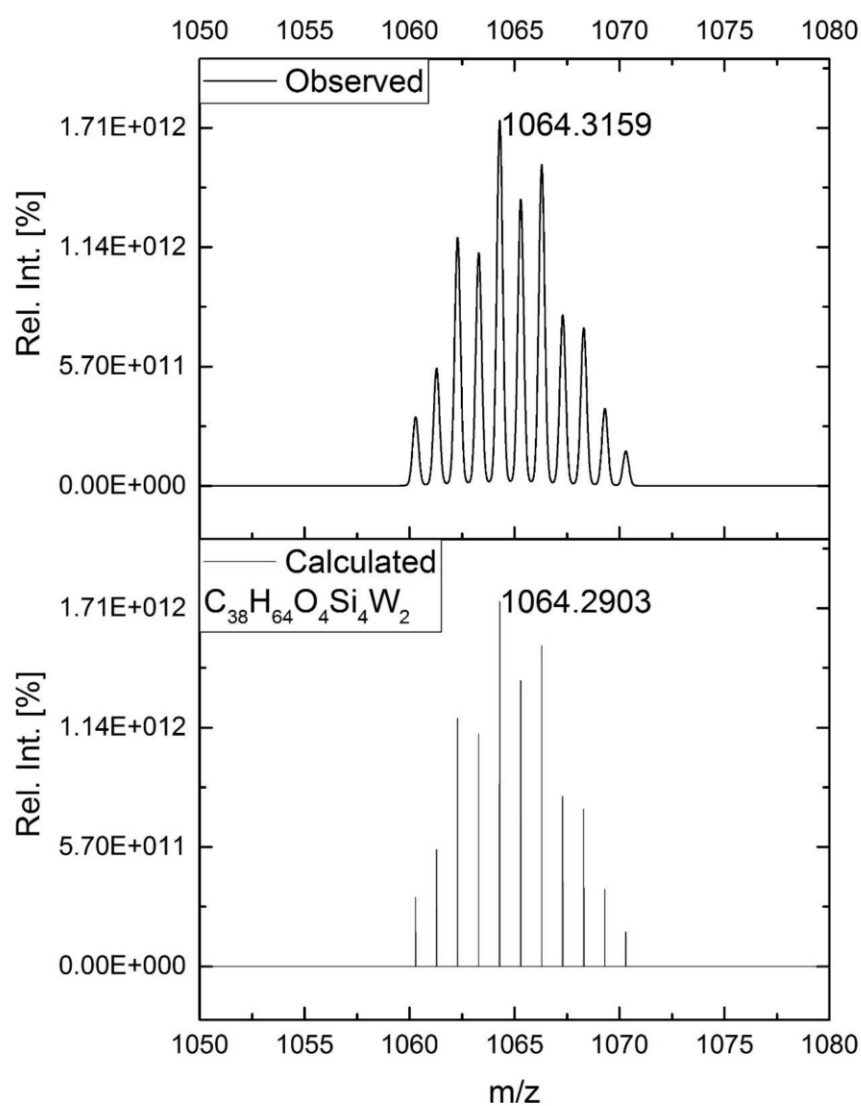


Figure S46. LIFDI-MS Spectrum: expanded region of the product signal illustrating the isotopic pattern of compound **6**. Observed (top) and calculated (bottom).

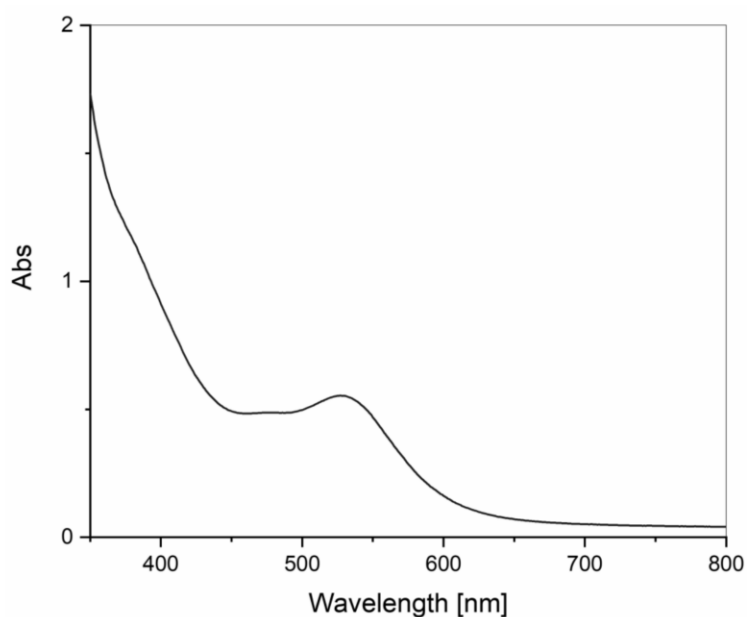


Figure S47. UV-Vis Spectra of compound **6** in toluene at 298 K. (Conc. $4.695 \times 10^{-4} \text{M}$; $\epsilon_{530} = 1178 \text{ L mol}^{-1} \text{cm}^{-1}$)

Isolation of $\text{IEt}_2\text{Me}_2\cdot\text{BPh}_3$ (beige precipitate that collected from synthesis of compound **6**)

^1H NMR (400 MHz, C_6D_6 , 298K): δ 7.69 (d, 6H, o- C_6H_5), 7.34 (t, 6H, m- C_6H_5), 7.21 (t, 3H, p- C_6H_5), 3.38 (q, 4H, N- CH_2CH_3), 1.28 (s, 6H, $\text{CH}_3\text{C}=\text{CCH}_3$), 0.33 (t, 6H, N- CH_2CH_3).

^{11}B NMR (128 MHz, C_6D_6 , 298K): -8.53 (br, $w_{1/2} = 46.8$ Hz)

^{13}C NMR (101 MHz, C_6D_6 , 298K): 169.25^a (N₂C:BPh₃, IEt₂Me₂), 157.71^a (B- C_6H_5), 136.2 (o- C_6H_5), 127.33 (m- C_6H_5), 124.70 (p- C_6H_5), 124.29 ($\text{CH}_3\text{C}=\text{CCH}_3$), 41.77 (N- CH_2CH_3), 14.59 (N- CH_2CH_3), 8.21 ($\text{CH}_3\text{C}=\text{CCH}_3$).

a: The signals were not observed in ^{13}C -1D NMR spectra but found in the 2D $^1\text{H}^{13}\text{C}$ HMBC experiment.

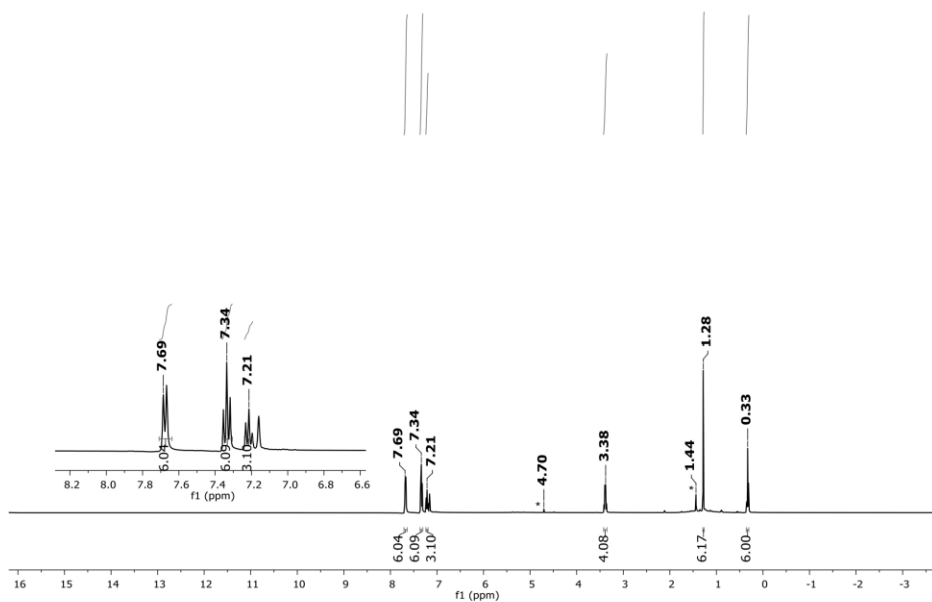


Figure S48. ^1H NMR spectrum of $\text{BPh}_3 \cdot \text{IEt}_2\text{Me}_2$ in C_6D_6 at 298 K. (* = compound **6**)

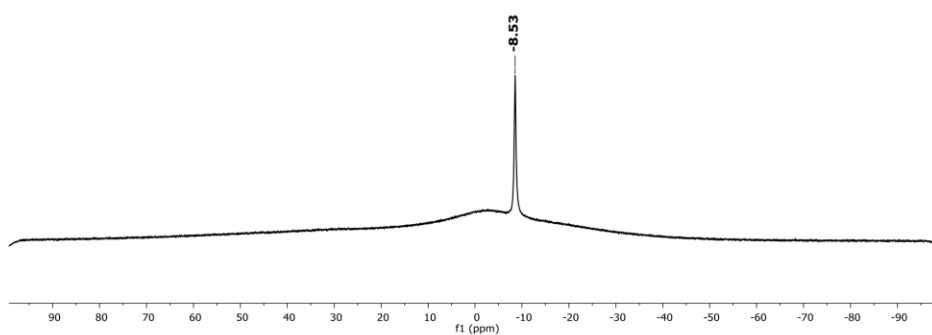


Figure S49. ^{11}B NMR spectrum of $\text{BPh}_3 \cdot \text{IEt}_2\text{Me}_2$ in C_6D_6 at 298 K.

S33

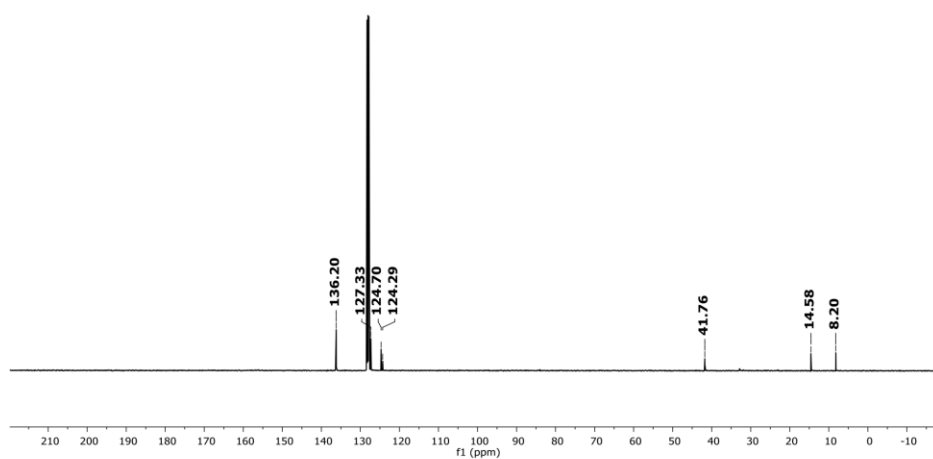


Figure S50. ^{13}C NMR spectrum of $\text{BPh}_3 \cdot \text{IEt}_2\text{Me}_2$ in C_6D_6 at 298 K.

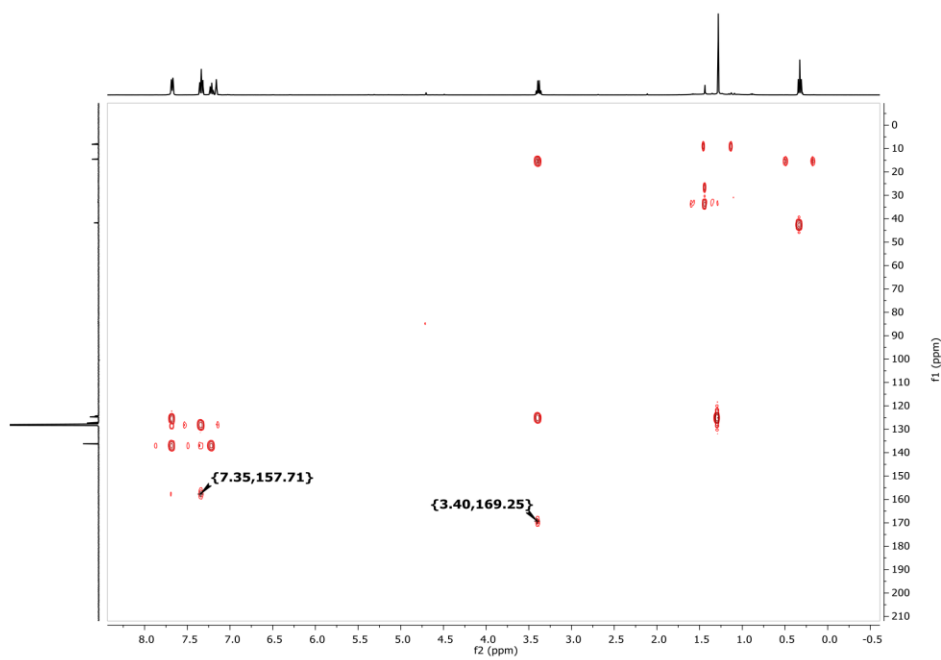


Figure S51. ^1H - ^{13}C HMBC of $\text{BPh}_3 \cdot \text{IEt}_2\text{Me}_2$ in C_6D_6 at 298 K.

S34

2. Single Crystal X-ray structure determination

Single crystal diffraction data were recorded on a Bruker Photon CMOS system equipped with a Helios optic monochromator and a Mo IMS microsource ($\lambda = 0.71073 \text{ \AA}$) and an Atlas SuperNova system equipped with a mirror monochromator and a Cu micro-focus sealed X-ray tube ($\lambda = 1.54178 \text{ \AA}$). The data collection was performed, using the APEX III software package^[4] and CrysAlisPro on single crystals coated with Fomblin ® Y as perfluorinated ether. The single crystal was picked on a micro sampler, transferred to the diffractometer and measured frozen under a stream of cold nitrogen. A matrix scan was used to determine the initial lattice parameters. Reflections were merged and corrected for Lorentz and polarization effects, scan speed, and background using SAINT.^[5] Absorption corrections, including odd and even ordered spherical harmonics were performed using SADABS.^[5] Space group assignments were based upon systematic absences, E statistics, and successful refinement of the structures. Structures were solved by direct methods with the aid of successive difference Fourier maps, and were refined against all data using the APEX III software in conjunction with SHELXL-2014^[6] and SHELXLE.^[7] H atoms were placed in calculated positions and refined using a riding model, with methylene and aromatic C–H distances of 0.99 and 0.95 Å, respectively, and $U_{iso}(H) = 1.2 \cdot U_{eq}(C)$. Non-hydrogen atoms were refined with anisotropic displacement parameters. Full-matrix least-squares refinements were carried out by minimizing $\sum w(F_o - F_c)^2$ with the SHELXL weighting scheme.^[8] Neutral atom scattering factors for all atoms and anomalous dispersion corrections for the non-hydrogen atoms were taken from International Tables for Crystallography.^[9] The images of the crystal structures were generated by Mercury.^[10] The CCDC numbers CCDC-1970332 (**2**), 1970333 (**3**), 1970334 (**3'**), 1970335 (**4a**), 1970336 (**6**) contain the supplementary crystallographic data for the structures **2** - **6**. These data can be obtained free of charge from the Cambridge Crystallographic Data Centre via <https://www.ccdc.cam.ac.uk/structures/>.

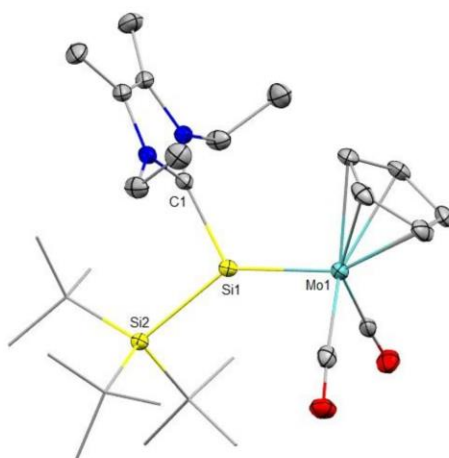


Figure S52. Ellipsoid plot (50% level) of the molecular structure of compound **2** (one out of two independent molecules in the asymmetric unit is shown). Hydrogen atoms are omitted for clarity and tert-butyl groups are depicted in wireframe for simplicity. Selected bond lengths (Å) and angles (°): Si1–Mo1 2.3499(8), Si1–Si2 2.4418(9), Si1–C1 1.949(2), C1–Si1–Si2 102.64(6), Mo1–Si1–C1 116.33(6), Mo–Si1–Si2 141.03(3)

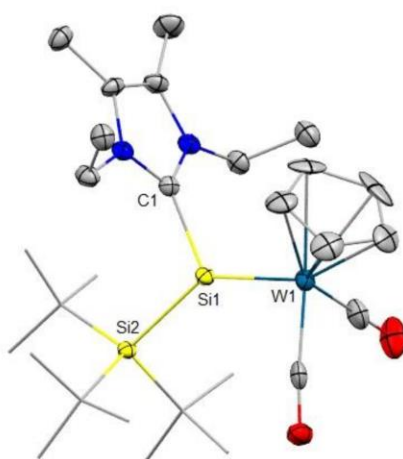


Figure S53. Ellipsoid plot (50% level) of the molecular structure of compound **3** (one out of three independent molecules in the asymmetric unit is shown). Hydrogen atoms are omitted for clarity and tert-butyl groups are depicted in wireframe for simplicity. Selected bond lengths (Å) and angles (°): Si1–W1 2.346(2), Si1–Si2 2.428(3), Si1–C1 1.935(7), C1–Si1–Si2 105.1(2), W1–Si1–C1 113.5(2); W1–Si1–Si2 141.38(10).

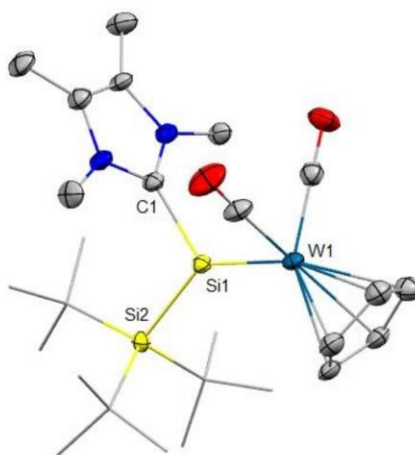


Figure S54. Ellipsoid plot (50% level) of the molecular structure of compound **3**. Hydrogen atoms are omitted for clarity and tert-butyl groups are depicted in wireframe for simplicity. Selected bond lengths (Å) and angles (°): Si1–W1 2.3534(12), Si1–Si2 2.4402(16), Si1–C1 1.941(5), C1–Si1–Si2 104.15(14), W1–Si1–C1 115.67(1); W–Si1–Si2 140.15(6).

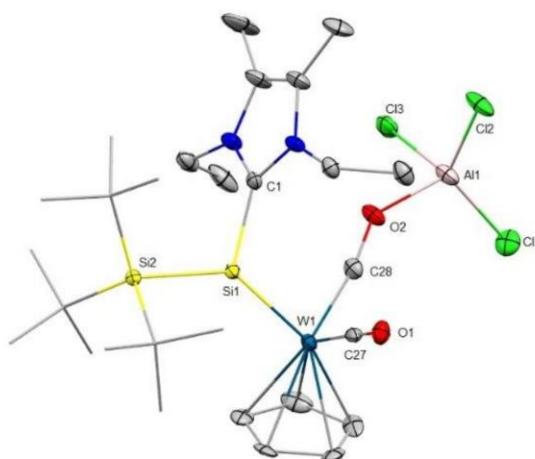


Figure S55. Ellipsoid plot (30% level) of the molecular structure of compound **4a**. Hydrogen atoms are omitted for clarity and tert-butyl groups are depicted in wireframe for simplicity. Selected bond lengths (Å) and angles (°): Si1–W1 2.3630(18), Si1–Si2 2.437(2), Si1–C1 1.940(10), Al1–O2 1.777(8), W1–C27 1.975(7), W1–C28 1.840(7), C1–Si1–Si2 106.4(6), W1–Si1–C1 114.6(6), W–Si1–Si2 138.89(9).

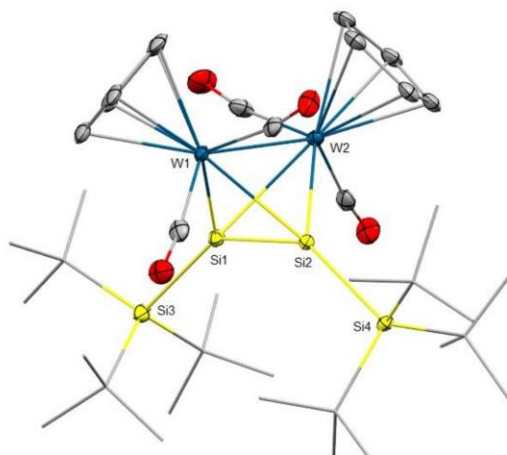


Figure S56. Ellipsoid plot (30% level) of the molecular structure of compound **6** (one out of three independent molecules in the asymmetric unit is shown). Hydrogen atoms are omitted for clarity and tert-butyl groups are depicted in wireframe for simplicity. Selected bond lengths [Å] and angles [°]: Si1–W1 2.5507(15), Si1–W2 2.6913(15), Si2–W1 2.6790(14), Si2–W2 2.5593(14), W1–W2 3.0732(8), Si1–Si2 2.2221(19); W1–Si1–W2 71.73(4), W1–Si1–Si2 67.89(5), W2–Si1–Si2 61.92(5).

Table S1. Crystal data and structure refinement for compound **2**, **3**, **3'**, **4a** and **6**.

Compound #	2	3	3'	4a	6
Chemical formula	C28 H48 Mo N2 O2 Si2	C28 H48 N2 O2 Si2 W	C26 H44 N2 O2 Si2 W	C28 H48 Al Cl3 N2 O2 Si2 W	C38 H64 O4 Si4 W2
Formula weight	596.80 g/mol	684.70 g/mol	656.65 g/mol	818.03 g/mol	1064.93 g/mol
Temperature	100 K	100 K	150.00(10) K	100 K	100 K
Wavelength	0.71073 Å	0.71073 Å	1.54178 Å	0.71073 Å	0.71073 Å
Crystal size	0.142 x 0.109 x 0.104 mm	0.253 x 0.161 x 0.146 mm	0.187 x 0.165 x 0.144 mm	0.208 x 0.099 x 0.096 mm	0.265 x 0.231 x 0.189 mm
Crystal habit	clear green-blue fragment	clear blue fragment	clear dark green fragment	clear orange fragment	clear red fragment
Crystal system	triclinic	monoclinic	triclinic	monoclinic	triclinic
Space group	P -1	P 21/n	P -1	C 2/c	P -1
Unit cell dimensions	a = 11.022(3) Å; α = 87.215(12) ^o b = 16.013(5) Å; β = 74.756(11) ^o c = 17.938(6) Å; γ = 85.153(12) ^o	a = 17.245(4) Å; α = 90 ^o b = 16.554(4) Å; β = 96.375(8) ^o c = 32.197(8) Å; γ = 90 ^o	a = 8.4517(2) Å; α = 88.492(2) ^o b = 11.0751(3) Å; β = 88.555(2) ^o c = 16.9012(5) Å; γ = 83.191(2) ^o	a = 43.864(4) Å; α = 90 ^o b = 10.3745(9) Å; β = 103.431(3) ^o c = 17.2634(16) Å; γ = 90 ^o	a = 14.4964(17) Å; α = 86.770(4) ^o b = 17.691(2) Å; β = 87.223(4) ^o c = 24.954(3) Å; γ = 79.443(4) ^o
Volume	3042.5(16) Å ³	9135(4) Å ³	1569.92(7) Å ³	7641.2(12) Å ³	6276.5(13) Å ³
Z	4	12	2	8	6
Density (calculated)	1.303 g/cm ³	1.494 g/cm ³	1.389 g/cm ³	1.422 g/cm ³	1.691 g/cm ³
Radiation source	IMS microsource	IMS microsource	SuperNova (Cu) X-ray Source	IMS microsource	IMS microsource
Theta range for data collection	1.92 to 25.68 ^o	2.05 to 25.37 ^o	2.62 to 73.81 ^o	2.02 to 25.35 ^o	1.91 to 25.35 ^o
Index ranges	-13<h<13, -19<k<19, -21<l<21	-20<h<20, -19<k<19, -38<l<38	-9<h<10, -9<k<13, -20<l<20	-52<h<52, -12<k<12, -20<l<20	-17<h<17, -21<k<21, -30<l<30
Reflections collected	66492	16712	10942	64728	22936
Independent reflections	11544	13102	6143	7002	18819
Completeness	0.999	0.999	0.963	0.998	0.998
Absorption correction	Multi-Scan	Multi-Scan	Multi-Scan	Multi-Scan	Multi-Scan
Max. and min. transmission	0.7217 and 0.7467	0.6520 and 0.7452	0.54903 and 1.00000	0.6167 and 0.7452	0.6388 and 0.7416
Refinement method	Full-matrix least-squares on F ²	Full-matrix least-squares on F ²	Full-matrix least-squares on F ²	Full-matrix least-squares on F ²	Full-matrix least-squares on F ²
Function minimized	$\sum w(F_o^2 - F_c^2)^2$	$\sum w(F_o^2 - F_c^2)^2$	$\sum w(F_o^2 - F_c^2)^2$	$\sum w(F_o^2 - F_c^2)^2$	$\sum w(F_o^2 - F_c^2)^2$
Data / restraints / parameters	11544 / 0 / 657	16712 / 658 / 1151	6143 / 252 / 358	7002 / 566 / 506	22936 / 672 / 1443
Goodness-of-fit on F ²	1.036	1.147	1.064	1.074	1.140
Final R indices [I>2sigma(I)]	R1 = 0.0238, wR2 = 0.0533	R1 = 0.0430, wR2 = 0.0992	R1 = 0.0388, wR2 = 0.1152	R1 = 0.0457, wR2 = 0.1231	R1 = 0.0281, wR2 = 0.0585
R indices (all data)	R1 = 0.0288, wR2 = 0.0566	R1 = 0.0693, wR2 = 0.1247	R1 = 0.0404, wR2 = 0.1168	R1 = 0.0584, wR2 = 0.1313	R1 = 0.0453, wR2 = 0.0687
Largest diff. peak and hole	0.338 and -0.391 eÅ ⁻³	6.273 and -3.373 eÅ ⁻³	1.698 and -2.626 eÅ ⁻³	3.499 and -2.028 eÅ ⁻³	1.311 and -1.409 eÅ ⁻³

3. Computational Data

General

All calculations were performed with ORCA v. 4.0.1.^[11] The geometric parameters were optimized using the PBE0 functional,^[12] with dispersion correction D3(BJ)^[13] and the def2-SVP basis set.^[14] For Si and W, the def2-TZVP basis set and the def2-ECP for W were used.^[15] Tighter than default scf ("*tightscf*") and optimization criteria ("*tightopt*") were chosen in conjunction with finer than default grid values ("*grid6*"; "*nofinalgrid*"; "*gridx6*"). The RIJ COSX approximation with the related auxiliary basis sets (def2/J) was used.^[16] The optimized geometric parameters were verified as true minima by the absence of negative eigenvalues in the harmonic vibrational frequency analysis (one for the transition states, respectively); calculated frequencies were scaled by 0.95 according to the Database of Frequency Scale Factors for Electronic Model Chemistries by D. Truhlar.^[17] For the analysis of the electronic structure and final energies, single point calculations with either the def2/TZVPP basis set or scalar relativistic calculations with the Zeroth Order Regular Approximation (ZORA)^[18] and the all-electron ZORA-def2-TZVPP basis set ("SARC-ZORA-TZVPP" for W; "old-ZORA-TZVPP" for Mo) were subsequently performed with even tighter grid settings ("*grid7*", "*nofinalgrid*"). The latter method was also used to calculate the NMR shifts^[19] and the TD-DFT transitions. For the TD-DFT calculations, 50 roots were calculated WITHOUT application of the Tamm-Dancoff approximation and with inclusion of solvation effects through the SMD model (solvent: TOLUENE).^[20] The reported energies for the mechanism relate to the PBE0-D3BJ (SMD=TOLUENE)/ZORA-def2-TZVPP//PBE0-D3BJ/def2-SVP level of theory. Localized orbitals were generated using Knizia's Intrinsic Bond Orbitals at the PBE0-D3BJ/def2-TZVPP//PBE0-D3BJ/def2-SVP level of theory.^[21] Single point calculations with the hybrid meta-GGA functionals M06^[22] (ZORA-def2-TZVPP) with D3ZERO^[23] dispersion correction and TPSSH^[24] (ZORA-def2-TZVPP) with D3BJ dispersion correction gave consistent results (vide infra).

For compound **3**, three conformers (NHC-Si-W-Cp torsion) were calculated. The most stable isomer **3** is not the one obtained in the solid-state **3**^{XRAY} ($\Delta\Delta G = +2.3$ kcal mol⁻¹ vs. the most stable conformer), but corresponds to the conformation found in **3'**. The energy of the third investigated isomer **3^{rot}** is even higher ($\Delta\Delta G = +3.0$ kcal mol⁻¹ vs. the most stable conformer). The most stable conformer **3** was used for the calculation of the dimerization mechanism.



Figure S57. The lowest-energy isomer **3** (left), the solid-state structure conformer **3^{XRAY}** (middle) and the third investigated isomer **3^{rot}** (right).

The calculated carbonyl stretching frequencies of the most stable isomer fit best to the experimental values.

Table S2. Comparison of experimental and calculated IR stretching frequencies for the CO ligands. Values are given in cm^{-1} .

	Compound 3		Compound 3^{XRAY}		Compound 3^{rot}		Compound 6	
	1	2	1	2	1	2	1	2
Exp.	1770	1849	1770	1849	1770	1849	1860	1914
Calc.	1837	1892	1878	1921	1838	1912	1904	1916

Table S3. Comparison of experimental and calculated ^{29}Si NMR shifts for tungsten complexes. Values are given in ppm vs. SiMe_4 ; values are averaged for the two Si atoms for compound **6**.

	Compound 3		Compound 3^{XRAY}		Compound 3^{rot}		Compound 6	
	Si1 (Si=W)	Si2 (tBu₃Si)	Si1 (Si=W)	Si2 (tBu₃Si)	Si1 (Si=W)	Si2 (tBu₃Si)	Si1 (Si-W)	Si2 (tBu₃Si)
Exp.	+230	+12	+230	+12	+230	+12	-63	+44
Calc.	+267	+10	+229	+3	+255	+1	-48	+22

Table S4. Comparison of experimental and calculated ^{29}Si NMR shifts for molybdenum complexes. Values are given in ppm vs. SiMe_4 ; values are averaged for the two Si atoms for compound **5**.

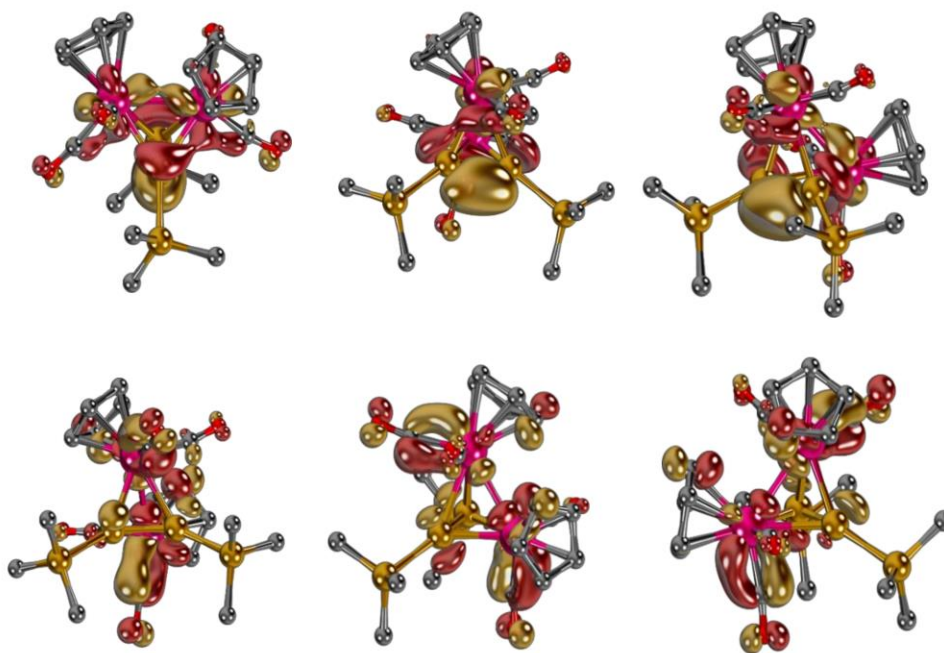
	Compound 2		Compound 2^{XRAY}		Compound 2^{rot}		Compound 5	
	Si1 (Si=Mo)	Si2 (tBu₃Si)	Si1 (Si=Mo)	Si2 (tBu₃Si)	Si1 (Si=Mo)	Si2 (tBu₃Si)	Si1 (Si-Mo)	Si2 (tBu₃Mo)
Exp.	+279	+6	+279	+6	+279	+6	+4	+48
Calc.	+265	-2	+292	-10	+309	+1	+5	+51

Table S5. Comparison of bond lengths (in Å) and angles (in °) for compound **3^{XRAY}**.

Compd. 3^{XRAY}	Si1-Si2	W1-Si1	Si1-C1^{NHC}	Si2-Si1-W1	Si2-Si1-C1^{NHC}
X-Ray	2.428(3)	2.346(2)	1.949(2)	141.38(10)	105.1(2)
Calc.	2.412	2.349	1.952	140.5	105.0

Table S6. Comparison of bond lengths (in Å) and angles (in °) for compound **6**.

Compd. 6	X-Ray	Calc.
W1-W2	3.073	3.065
W1-Si1	2.551	2.564
W2-Si2	2.559	2.559
W2-Si1	2.691	2.726
W1-Si2	2.679	2.706
Si1-Si2	2.222	2.235
Si1-Si3	2.437	2.423
Si2-Si4	2.429	2.416
Si1-W1-Si2	50.2	50.1
Si1-W2-Si2	50.0	49.9
Si3-Si1-Si2-Si4	3.5	2.7

**Figure S58.** Canonical HOMO (top) and LUMO (bottom) molecular orbitals of **6** from different view angles.

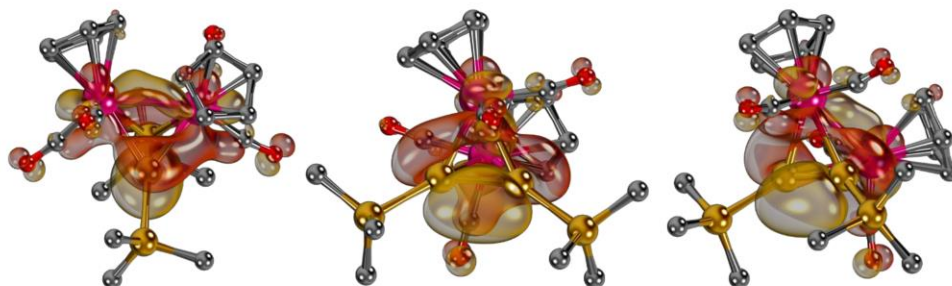


Figure S59. The canonical HOMO of molybdenum complex **5** (shown from three different perspectives) is delocalized, yet shows significant Si-Si π -character indicative of considerable multiple bond character.

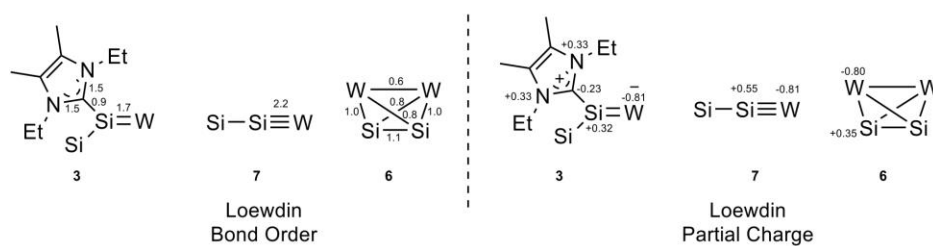


Figure S60. Löwdin bond orders and partial charges of compounds **3**, **6** and **7**.

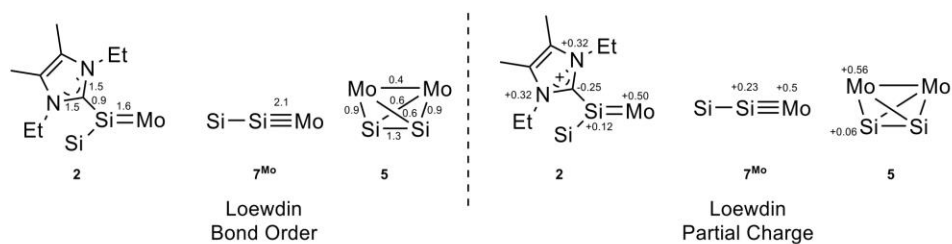


Figure S61. Löwdin bond orders and partial charges of compounds **2**, **5** and **7^{Mo}**.

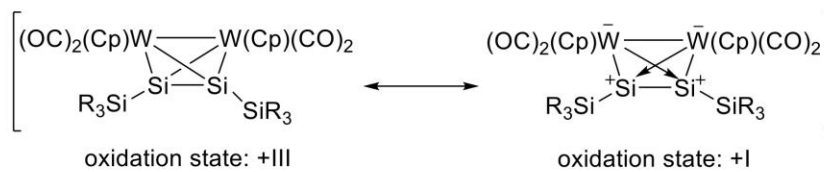


Figure S62. Important resonance structures of compound **6**.

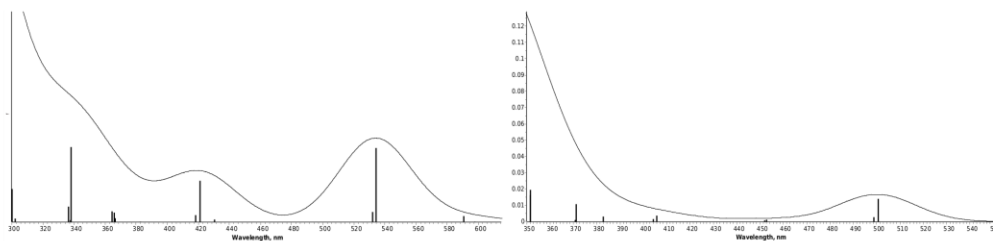
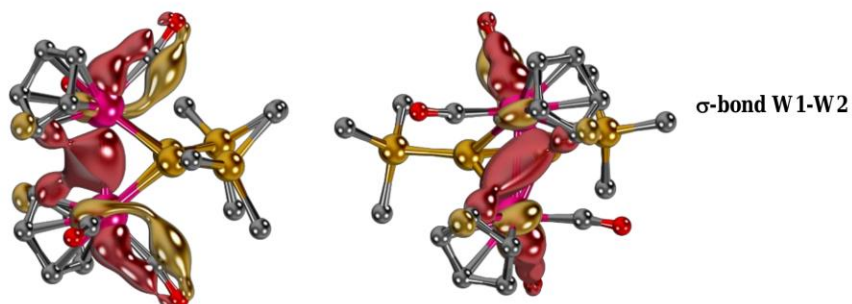
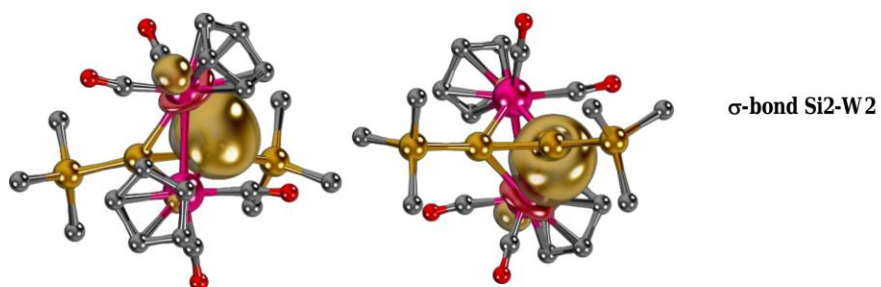
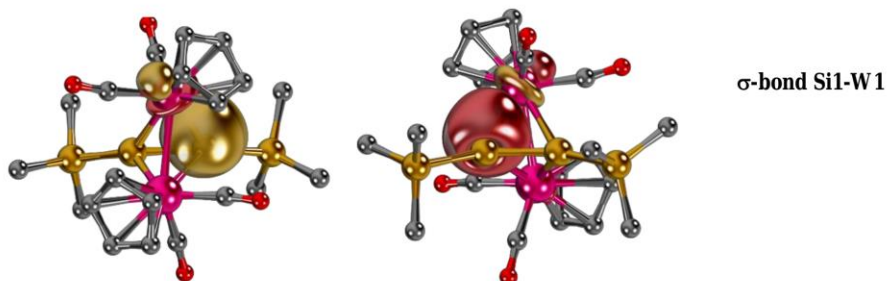


Figure S63. Calculated UV-Vis spectrum of compound **3** (left) and compound **6** (right).

Table S4. Excerpt of the TD-DFT calculations of the compounds **3** and **6** with approximate assignment of transitions.

3		6	
Wavelength [nm]	MO Contributions	Wavelength[nm]	MO Contributions
658	HOMO → LUMO	501	HOMO → LUMO
663	HOMO-1 → LUMO	499	HOMO-1 → LUMO
534	HOMO-2 → LUMO	452	HOMO → LUMO+1
411	HOMO-3 → LUMO	453	HOMO → LUMO+2
397	HOMO → LUMO+2	404	HOMO → LUMO
399	HOMO → LUMO+3		



S45

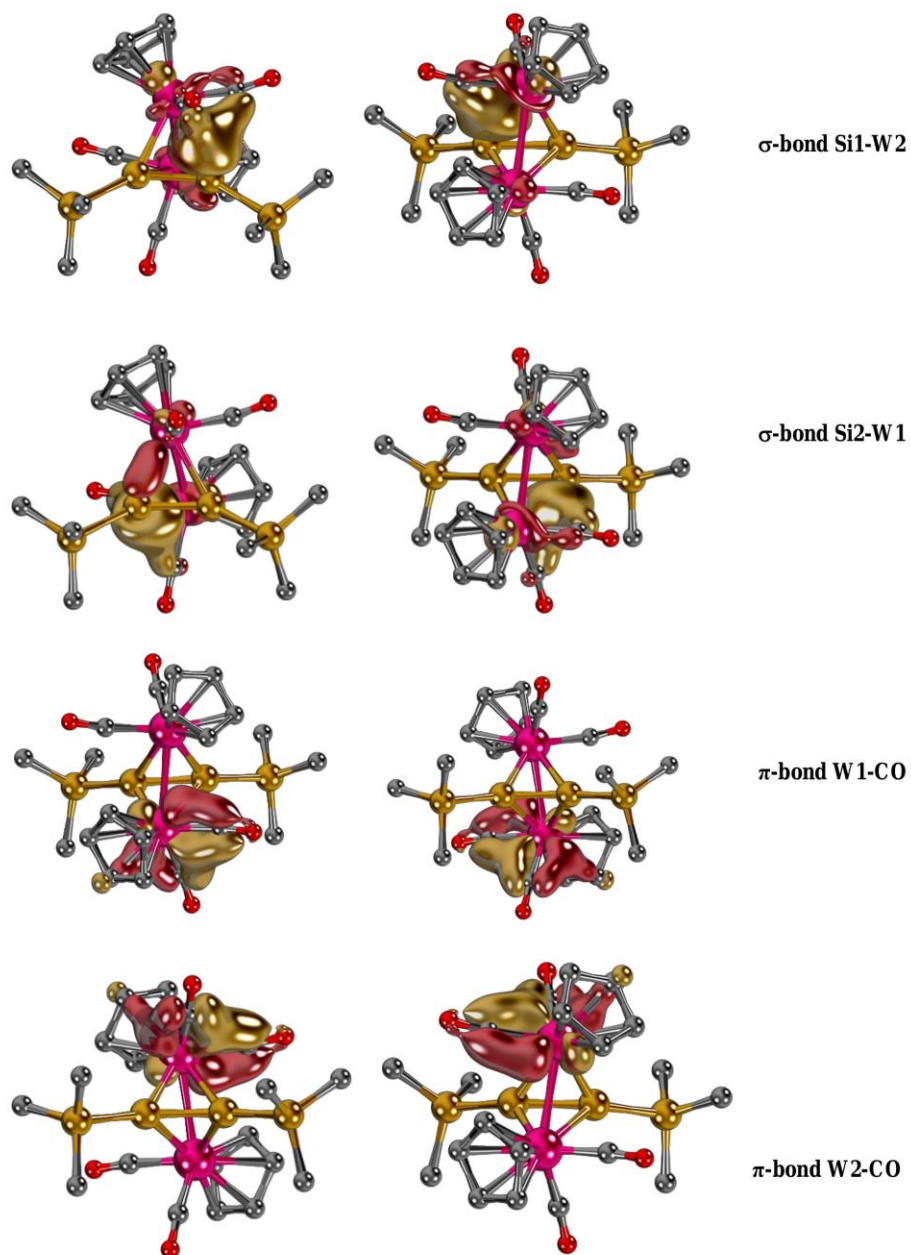


Figure S64. Intrinsic Bond Orbitals (IBOs) of compound 6.

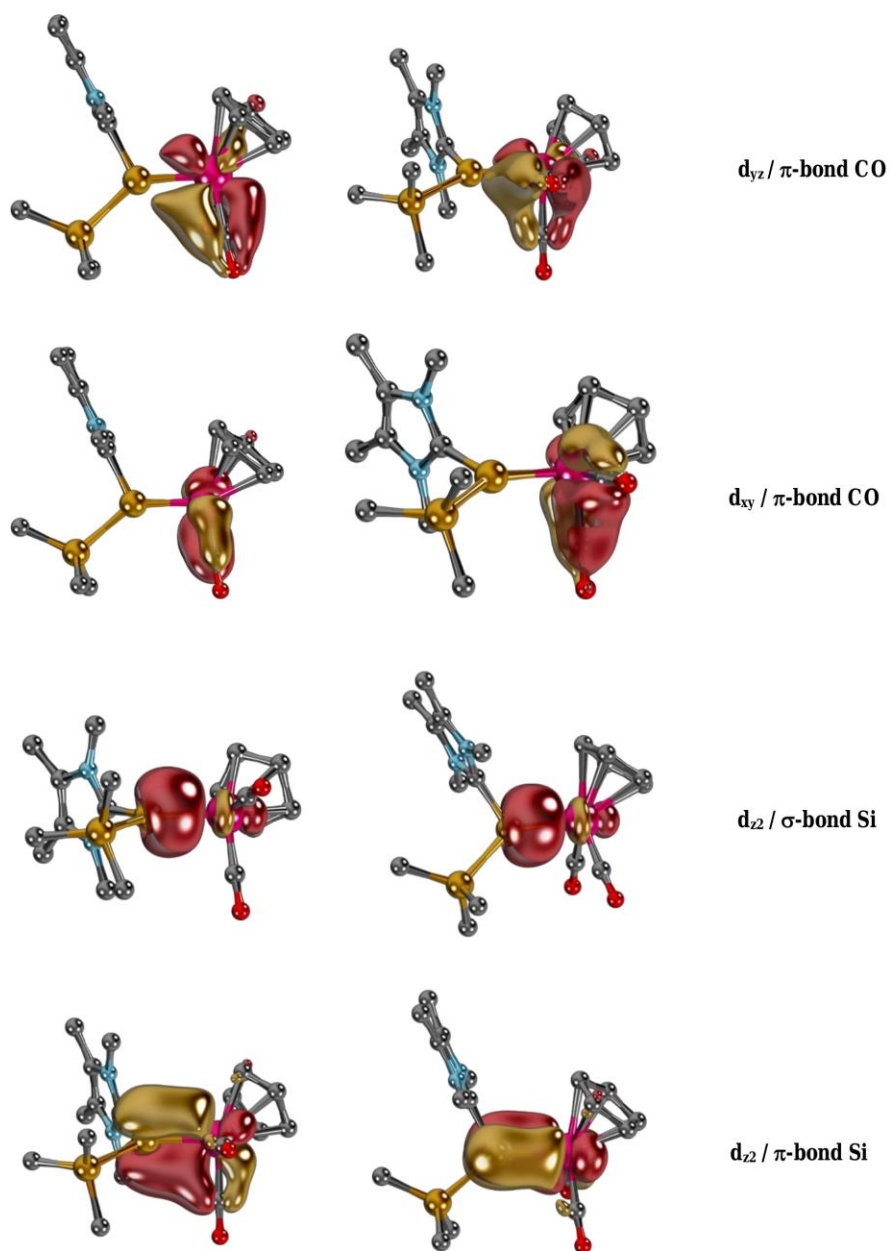


Figure S65. Intrinsic Bond Orbitals (IBOs) of compound 3^{XRAY} .

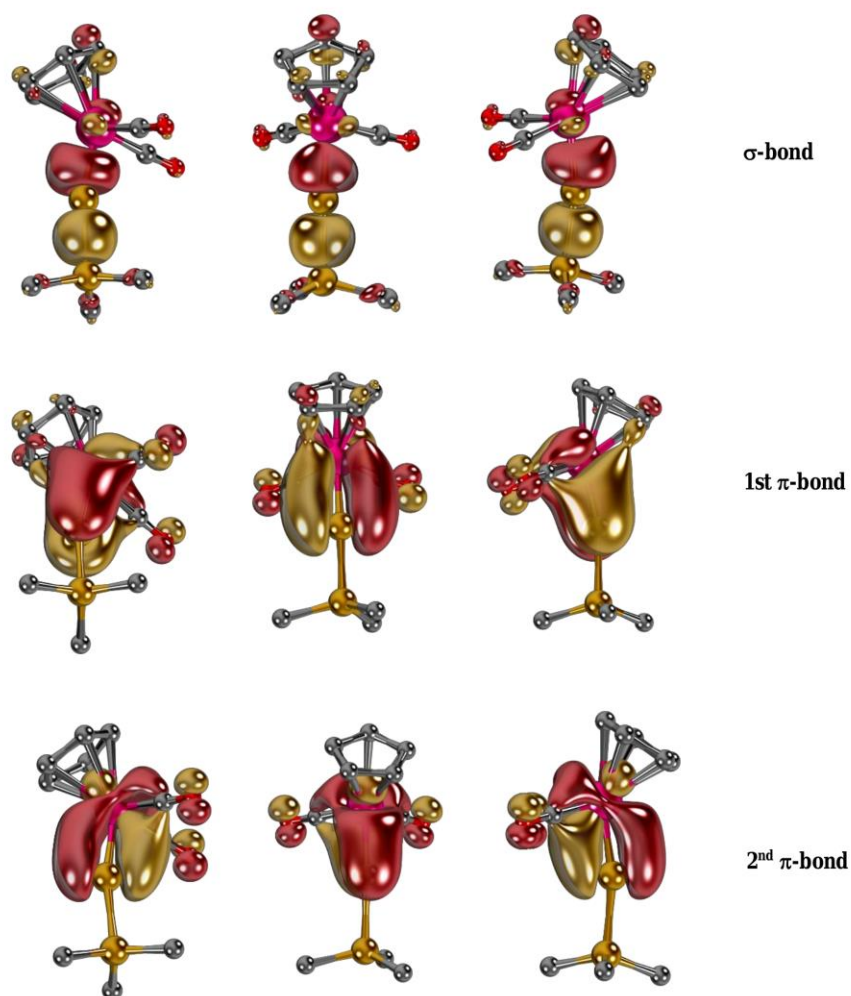


Figure S66. Intrinsic Bond Orbitals (IBOs) of calculated silylydyne **7**.

Multireference Character

Table S8. Vertical singlet/triplet gaps and Fractional occupation densities (FODs) of compounds **3**, **6**, **7** and transition state.

	s/t gap [kcal mol ⁻¹]	FOD
Compd. 3	22	0.63
Compd. 7	25	0.44
Transition State	12.5	1.69
Compd. 6	27	0.53

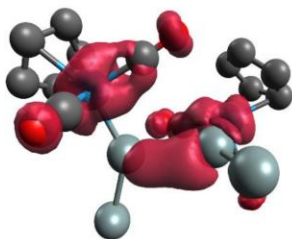


Figure S67. FOD plot of transition state (tBu groups and H atoms omitted for clarity)

NEVPT2/CASSCF(12,12) calculations

State averaged (triplet, singlet) NEVPT2/CASSCF(12,12) calculations were performed on top of the DFT optimized transition state structure using the scalar relativistic ZORA method, the def2-TZVPP basis set and without using the frozencore approximation (“*nofrozenscore*”). The calculations suggest a vertical singlet/triplet gap of 0.9 eV and indicate moderate multireference character. The active space relates to the metal valence d-orbitals, viz. the molecular orbitals associated with the π -/ π^* -interaction with the silyldiyne / carbonyl ligands (antibonding and bonding interaction).

```

0.79876 [ 0]: 222222000000
0.03449 [ 7]: 222220200000
0.01441 [111]: 222202020000
0.00985 [ 35]: 222211100000
0.00834 [ 781]: 222022002000
0.00817 [1563]: 221221100100
0.00771 [15133]: 2022220000020
0.00726 [49741]: 022222000002
0.00386 [ 772]: 222022101000
0.00379 [2070]: 221122001100
0.00378 [ 7282]: 212122001010
0.00362 [ 777]: 222022011000
0.00344 [ 112]: 222202011000
0.00314 [1560]: 221221200000
0.00274 [2060]: 221122101000
0.00262 [1632]: 221212110000
0.00251 [ 275]: 222121100100

```

Figure S68. Weight of configuration state functions.

Energies

Table S9. Calculated Energies and imaginary frequencies.

	Imag [cm ⁻¹]	PBE0/def2- SVP	PBE0/def2- SVP	PBE0/ZORA- def2- TZVPP// PBE0-def2- SVP	PBE0(SMD)/ ZORA-def2- TZVPP// PBE0/def2- SVP	PBE0/def2- TZVPP//PBE0/ def2-SVP	M06/ZORA- def2- TZVPP//PBE0- def2-SVP	TPSSH/ZORA- def2-TZVPP// PBE0/def2- SVP
		E in [H]	G in [H]	E in [H]	E in [H]	E in [H]	E in [H]	E in [H]
2XRAY	-	-2000.24248	-1999.59267	-6024.41583	-6024.44417	-2001.91944	-6025.45827	-6026.65264
2	-	-2000.24781	-1999.59851	-6024.42144	-6024.44748	-2001.92503	-6025.46426	-6026.65807
2rot	-	-2000.24426	-1999.59508	-6024.41727	-6024.44238	-2001.9209	-6025.4602	-6026.65445
3XRAY	-	-1999.13023	-1998.48144	-18567.2136	-18567.2423	-2000.80334	-18568.4797	-18569.0821
3	-	-1999.13547	-1998.48713	-18567.2189	-18567.245	-2000.80866	-18568.4855	-18569.0874
3rot	-	-1999.13221	-1998.48407	-18567.2154	-18567.2407	-2000.80497	-18568.482	-18569.0843
Dimerization_ W_Silyidyne TS	-52	-3075.69875	-3074.83416	-36212.383	-36210.2539	-3078.06816	-36212.383	-36212.7819
5	-	-3078.03052	-3077.15966	-11124.7358	-11124.76226	-3080.40433	-11126.43	-11128.0232
6	-	-3075.81128	-3074.94228	-36210.3398	-36210.3663	-3078.17885	-36212.4837	-36212.8895
6isomer	-	-3075.79762	-3074.92756	-36210.326	-36210.3528	-3078.16608	-36212.4696	-36212.8754
6triangle	-	-3075.76715	-3074.89987	-36210.2928	-36210.3211	-3078.13349	-36212.4354	-36212.8446
6quadrangle	-	-3075.70572	-3074.84306	-36210.2796	-36210.3076	-3078.07667	-36212.3835	-36212.8315
7	-	-1537.84152	-1537.42475	-18105.1121	-18105.1297	-1539.0311	-18106.1871	-18106.3843
7Mo	-	-1538.95499	-1538.53815	-5562.31354	-5562.33075	-1540.14716	-5563.16436	-5563.95395
NHC	-	-461.211612	-461.007568	-462.03349	-462.054493	-461.702762	-461.902537	-462.628445
NHC_BPh ₃	-	-1179.77885	-1179.30746	-1181.81734	-1181.84028	-1181.01074	-1182.29374	-1183.35556
NHC_BPh ₃ isomer	-	-1179.77938	-1179.30768	-1181.81802	-1181.84713	-1181.01139	-1182.29501	-1183.35628
BPh ₃	-	-718.48888	-718.249696	-719.714015	-719.733555	-719.237788	-720.001761	-720.658419
Add NHC BPh ₃ TS	-51	-1179.71819	-1179.25024	-1182.25217	-1181.79097	-1180.95401	-1182.25217	-1183.30158
3_minusCO	-	-1885.91415	-1885.27032	-18453.7465	-18453.7701	-1887.45371	-18454.9503	-18455.4873
CO	-	-113.096482	-113.109772	-113.345053	-113.340665	-113.231974	-113.417016	-113.4731

Mechanism

The potential energy surface is very flat, complicating the search for transition states (cf. imaginary frequencies for transition states). Accordingly, no transition states could be found for model systems with truncated ligands and barrierless dimerization was obtained instead. Furthermore, no transition state could be found for the dimerization of the silyidyne on the triplet hypersurface and instead also barrierless dimerization was predicted. Equally, no transition state could be found for the abstraction of the NHC from **3** by BPh₃. A scan of the NHC–Si bond distance indicates also here barrierless dissociation without interaction between the NHC and the silyidyne at a distance of 3.7 Å.

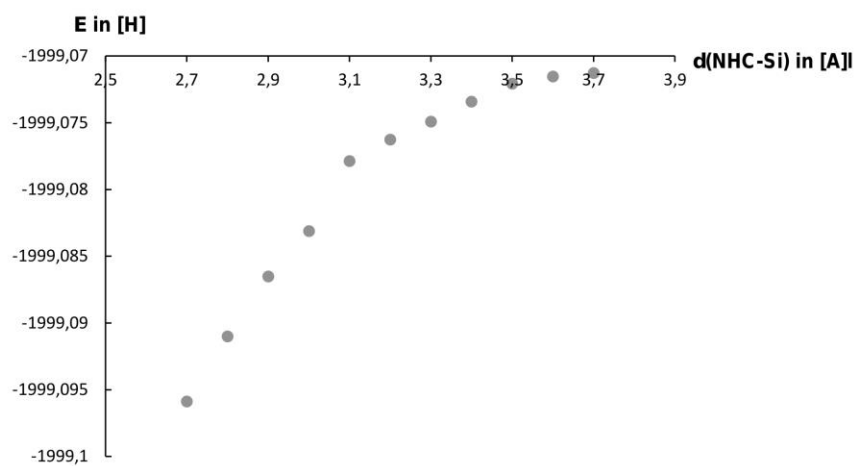


Figure S69. Scan of the NHC–Si distance in **3**.

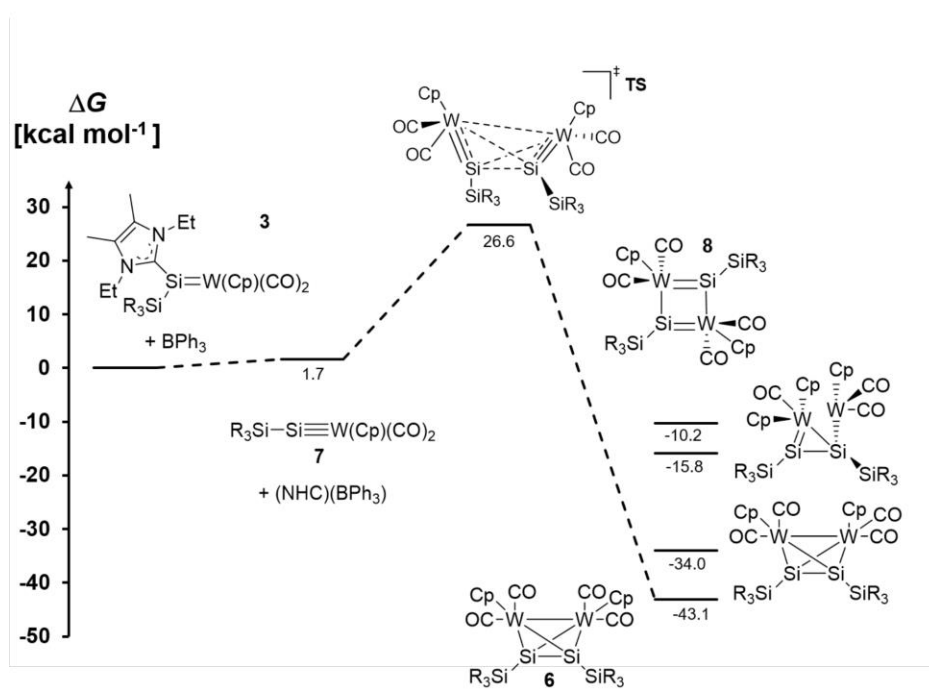


Figure S70. Calculated reaction profile for the formation of W₂Si₂ tetrahedral cluster (**6**).

The reaction of the free NHC with BPh_3 (Addition NHC BPh_3 TS) proceeds with a low barrier of $13.7 \text{ kcal mol}^{-1}$ (imaginary frequency: 51 cm^{-1}).

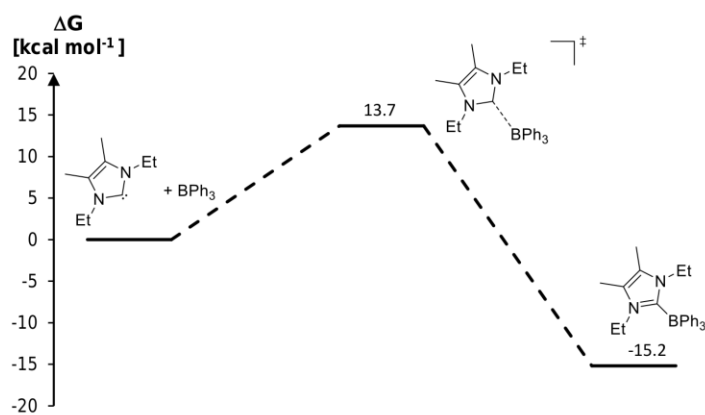


Figure S71. Calculated reaction profile for the reaction of the NHC with BPh_3 .

XYZ Coordinates

Silylidene 3

W	5.80079	1.14558	8.94433
C	7.04750	1.33319	10.44622
O	7.73023	1.34996	11.39590
C	6.95458	2.28164	7.87700
O	7.64277	2.96573	7.21403
C	4.92286	-0.34194	7.33002
H	4.77398	-0.03554	6.29597
C	6.09525	-0.95130	7.87247
H	7.00959	-1.18668	7.33212
C	5.84027	-1.21476	9.24511
H	6.53865	-1.66979	9.94586
C	4.51127	-0.80585	9.55273
H	4.01927	-0.90067	10.51870
C	3.95276	-0.25381	8.37066
H	2.94725	0.15053	8.26423
Si	4.91555	3.09497	9.88313
Si	3.28507	3.68162	11.55707
C	5.83784	4.74317	9.41157
C	7.35150	6.39311	9.21159
C	6.40191	6.58265	8.24615
C	7.77023	4.62749	10.95877
H	7.13962	3.84309	11.39839
H	7.94785	5.38098	11.74265
C	9.06277	4.02417	10.44417
H	8.84854	3.29032	9.65654
H	9.57739	3.50377	11.26297
H	9.73909	4.78673	10.03302
C	8.55869	7.20057	9.51595
H	9.45780	6.79892	9.02287
H	8.75937	7.24214	10.59611
H	8.41737	8.23142	9.16426
C	6.33416	7.60876	7.17837
H	6.69979	7.21242	6.21711
H	6.96202	8.46934	7.44266
H	5.31028	7.97782	7.02133
C	4.34323	5.32709	7.52005
H	3.84324	6.29341	7.35474
H	3.63956	4.69453	8.08021
C	4.72002	4.65935	6.21206
H	3.84161	4.62472	5.55143
H	5.07235	3.63447	6.39821
H	5.51922	5.20380	5.69042
N	6.98740	5.24666	9.89990
N	5.48380	5.55580	8.39387
C	3.80987	2.67498	13.16705
C	5.03686	3.34469	13.79868
H	5.87545	3.40709	13.08693
H	5.38949	2.73753	14.65094
H	4.83064	4.35345	14.18451
C	4.23230	1.23693	12.83223
H	4.97513	1.19316	12.02362
H	3.38393	0.60613	12.53912
H	4.68788	0.77787	13.72843

C	2.68808	2.60193	14.21008
H	1.81600	2.04600	13.83541
H	2.33777	3.58732	14.54534
H	3.05015	2.06134	15.10347
C	1.58183	3.03804	10.81587
C	1.57891	1.50746	10.86764
H	0.73025	1.11610	10.27840
H	1.46656	1.12515	11.89185
H	2.50125	1.08469	10.44289
C	0.33314	3.54235	11.54846
H	0.18861	4.62773	11.44638
H	0.34683	3.30585	12.62317
H	-0.56164	3.05577	11.11837
C	1.46741	3.42444	9.33492
H	2.28929	2.98441	8.74652
H	1.46605	4.50990	9.16609
H	0.52200	3.02896	8.92070
C	3.18730	5.61004	11.93348
C	4.57089	6.25955	12.06690
H	5.06658	6.35333	11.09260
H	5.24745	5.71637	12.73800
H	4.45924	7.28237	12.47148
C	2.41504	5.87502	13.23310
H	2.26116	6.96246	13.35811
H	2.97017	5.52537	14.11526
H	1.42451	5.39906	13.25054
C	2.48014	6.33829	10.78580
H	2.99640	6.18055	9.82638
H	2.48097	7.42665	10.97889
H	1.43166	6.03440	10.66371

Silylidene 3^{rot}

W	5.29667	1.17904	8.69639
C	5.73132	2.38735	7.25758
O	6.04227	3.10727	6.38065
C	3.42414	1.20774	8.08258
O	2.31326	1.12552	7.74076
C	5.48044	-0.84096	10.00825
H	4.81360	-1.06099	10.83945
C	5.27211	-1.20676	8.64668
H	4.41049	-1.74943	8.25910
C	6.38524	-0.76852	7.88121
H	6.54215	-0.92909	6.81616
C	7.27292	-0.08581	8.76426
H	8.22796	0.35688	8.48521
C	6.71153	-0.13665	10.07714
H	7.16672	0.27241	10.97729
Si	4.78101	3.08651	9.96159
Si	4.23998	3.68525	12.24542
C	4.84944	4.72340	8.89889
C	5.69382	6.45279	7.72967
C	4.38369	6.30918	7.37004
C	7.26542	5.22035	9.24734
H	7.10483	4.61781	10.14829

S53

C	4.39885	1.44604	13.10959	C	3.64406	9.10574	19.76039
H	5.27419	1.45457	12.44436	H	4.56318	8.82065	20.26204
H	3.66884	0.75653	12.67194	C	3.26551	8.75976	18.43197
H	4.72054	1.01701	14.07638	H	3.84576	8.14823	17.74273
C	2.66652	2.74916	14.31428	C	2.01927	9.39515	18.14378
H	1.86625	2.10747	13.91957	H	1.48546	9.36949	17.19558
H	2.22476	3.72182	14.57213	C	1.62393	10.11321	19.31434
H	3.01131	2.28373	15.25581	H	0.72650	10.72026	19.42031
C	1.66032	2.95529	10.91849	C	2.63138	9.94565	20.29859
C	1.68124	1.42944	11.06614	H	2.64996	10.40407	21.28210
H	0.84461	0.99206	10.49458	Si	0.58905	5.78884	21.25788
H	1.56871	1.10866	12.11144	Si	-0.94319	3.91714	21.12540
H	2.60411	0.98347	10.67081	C	-0.61245	2.70713	22.62512
C	0.39733	3.48771	11.60767	C	-0.34643	3.47924	23.92237
H	0.23742	4.56203	11.43111	H	0.56111	4.09040	23.85090
H	0.39926	3.32147	12.69507	H	-0.18506	2.76263	24.74753
H	-0.48346	2.96038	11.19810	H	-1.16956	4.14058	24.21774
C	1.54681	3.26193	9.41873	C	0.61989	1.84155	22.36838
H	2.38202	2.82529	8.85257	H	0.48730	1.14744	21.52752
H	1.49827	4.33736	9.20021	H	0.82960	1.22939	23.26298
H	0.62474	2.80409	9.01864	H	1.50842	2.45170	22.17389
C	3.20657	5.63312	11.84142	C	-1.80385	1.76576	22.84126
C	4.57644	6.30964	11.97844	H	-2.06642	1.19610	21.93769
H	5.09050	6.36711	11.01043	H	-2.70449	2.29206	23.18540
H	5.24435	5.80846	12.68947	H	-1.54376	1.03227	23.62455
H	4.44218	7.34864	12.33250	C	-0.57873	3.08004	19.39879
C	2.38689	5.96709	13.09548	C	0.93436	2.92014	19.19832
H	2.21824	7.05826	13.14967	H	1.13302	2.55813	18.17391
H	2.91101	5.67574	14.01640	H	1.37619	2.19399	19.89197
H	1.40139	5.48181	13.10550	H	1.47594	3.86768	19.32233
C	2.52749	6.27863	10.62946	C	-1.22871	1.69628	19.27113
H	3.06480	6.05079	9.69680	H	-2.32142	1.72488	19.39204
H	2.52356	7.37817	10.74419	H	-0.82806	0.97301	19.99511
H	1.48253	5.96385	10.50471	H	-1.02186	1.28995	18.26475
6				C	-1.11737	3.96176	18.26586
W	0.95300	7.82770	22.76892	H	-0.77658	3.55931	17.29618
C	1.42549	6.54499	24.18628	H	-0.75801	4.99909	18.32814
O	1.64348	5.90094	25.12143	H	-2.21614	3.98316	18.24433
C	2.71772	8.60767	23.10396	C	-2.75544	4.64398	21.27016
O	3.64859	9.22986	23.41587	C	-3.83812	3.65161	20.83035
C	-1.38523	8.34948	22.79252	H	-3.75709	3.39213	19.76479
H	-2.16475	7.72713	22.36470	H	-4.82906	4.11938	20.97366
C	-0.72850	9.43042	22.14386	H	-3.83227	2.71716	21.40607
H	-0.92387	9.77052	21.13130	C	-2.87683	5.89576	20.40209
C	0.18061	10.01368	23.06372	H	-2.73704	5.69900	19.33264
H	0.81254	10.87940	22.87055	H	-2.13454	6.64928	20.68529
C	0.08155	9.30327	24.30096	H	-3.87682	6.35028	20.52497
H	0.61672	9.53590	25.21968	C	-3.04002	5.07105	22.71706
C	-0.88148	8.26468	24.12090	H	-2.23804	5.70552	23.12438
H	-1.20691	7.55574	24.88061	H	-3.16645	4.21882	23.39771
W	1.63645	7.82696	19.78073	H	-3.97897	5.65302	22.75141
C	1.62757	6.42061	18.39725	Si	2.75905	6.27817	21.48054
O	1.64264	5.74536	17.45812	Si	4.92560	5.25611	21.79793
C	-0.29735	7.94424	19.42648	C	6.07512	6.45581	22.82579
O	-1.38071	8.19973	19.10201	C	7.52940	5.96584	22.87954
				H	7.99970	5.95962	21.88515

S55

C	-1.96018	4.91533	22.87208	H	4.64103	5.83485	23.20760
H	-2.39503	5.17504	23.85263	W	1.57227	8.81040	19.15827
H	-2.00751	3.82156	22.77243	C	-0.26124	8.92708	19.80312
H	-0.90179	5.21303	22.90348	O	-1.34230	9.21819	20.12176
C	1.57011	3.22695	15.72992	C	1.91392	9.97972	20.69259
H	0.86494	2.94025	14.93119	O	2.01957	10.89609	21.41025
H	2.32799	2.43484	15.78577	C	0.79648	9.44774	17.06777
H	1.00896	3.22666	16.66903	H	-0.19797	9.16096	16.73129
C	1.00652	5.54341	15.09394	C	1.12928	10.63322	17.79533
H	1.34157	6.53982	14.77276	H	0.43237	11.40365	18.12053
H	0.38168	5.12983	14.28222	C	2.54030	10.64764	17.98323
H	0.35246	5.66785	15.97114	H	3.10358	11.42013	18.50484
C	3.00829	4.39917	14.11759	C	3.07976	9.47908	17.40659
H	3.86816	3.73329	14.28321	H	4.13327	9.21979	17.37032
H	2.37787	3.92452	13.34472	C	1.99744	8.72574	16.84255
H	3.38401	5.34002	13.69362	H	2.08029	7.78527	16.30310
C	3.80008	7.63331	15.29410	Si	0.64293	6.50318	20.01129
H	4.46228	8.48578	15.06035	Si	-1.45514	5.27469	19.81751
H	3.53329	7.15866	14.34055	C	-0.86971	3.43103	19.52818
H	2.88378	8.03879	15.74301	C	-2.40467	5.93919	18.23151
C	5.73477	6.08006	15.56774	C	-2.51932	5.44992	21.44146
H	6.35389	5.49223	16.26052	Si	2.79611	6.52810	19.42957
H	5.47549	5.43649	14.71523	Si	4.45857	5.12977	18.36381
H	6.37205	6.89497	15.18041	C	5.80587	6.33433	17.60098
C	4.99082	7.54421	17.43666	C	3.58896	4.07940	16.96351
H	4.15430	8.03011	17.96030	C	5.23285	3.95842	19.72895
H	5.58099	6.97941	18.16966	C	-1.40720	6.28704	17.11799
H	5.64162	8.34966	17.05382	H	-0.63390	6.99028	17.46540
C	4.86019	2.92816	16.89872	H	-0.89264	5.40593	16.71430
H	5.40814	2.17636	17.49428	H	-1.94510	6.76686	16.28022
H	4.17469	2.37817	16.24068	C	-3.22438	7.19736	18.53720
H	5.59969	3.43814	16.26484	H	-3.66835	7.56990	17.59643
C	3.13141	3.11250	18.70178	H	-4.06046	6.98857	19.21937
H	2.39874	2.56081	18.10035	H	-2.63164	8.00854	18.97051
H	3.66423	2.37699	19.32971	C	-3.40557	4.89952	17.70278
H	2.56100	3.77581	19.36843	H	-3.95035	5.33815	16.84773
C	5.19471	4.46869	18.79817	H	-2.93597	3.97499	17.34348
H	4.77671	5.20329	19.49587	H	-4.15725	4.62482	18.45643
H	5.62536	3.65301	19.40565	C	-1.96369	2.39300	19.80296
H	6.02525	4.94553	18.26002	H	-2.87867	2.56525	19.21756
				H	-1.58059	1.39395	19.52670
				H	-2.24396	2.34691	20.86460
6 isomer				C	-0.40565	3.24761	18.08194
W	2.43224	7.39341	21.84786	H	0.33631	4.00238	17.79085
C	0.72339	8.04323	22.61734	H	0.06821	2.25734	17.97282
O	-0.17202	8.49848	23.18264	H	-1.23106	3.28706	17.36075
C	1.91253	5.59321	22.46020	C	0.32093	3.12993	20.44056
O	1.70850	4.56892	22.95902	H	0.08229	3.23213	21.50655
C	3.46243	7.62666	23.87545	H	0.66920	2.09430	20.27338
H	2.99029	7.27759	24.79227	H	1.16893	3.79949	20.23100
C	3.35984	8.93486	23.30953	C	-2.72789	6.91692	21.82649
H	2.77264	9.76636	23.69520	H	-3.30289	7.48048	21.08422
C	4.19228	8.98110	22.15702	H	-3.28588	6.96461	22.77895
H	4.34374	9.84691	21.51852	H	-1.78488	7.44879	21.98075
C	4.79283	7.70984	21.98195	C	-3.90448	4.81318	21.25140
H	5.50468	7.45586	21.20460	H	-4.50202	5.34965	20.50093
C	4.33547	6.86540	23.03605				

S58

H	-3.86809	3.75548	20.95880	H	7.74949	2.54582	6.49859
H	-4.45956	4.86868	22.20462	C	8.12371	1.92486	8.61503
C	-1.81649	4.77031	22.62272	H	8.53874	2.82668	9.06223
H	-2.41932	4.92294	23.53530	Si	4.67571	2.43643	10.34503
H	-1.69441	3.68586	22.49199	Si	3.14132	3.40328	11.85138
H	-0.82307	5.20067	22.81474	C	3.81864	2.92884	13.61890
C	2.88255	2.86446	17.57114	C	5.01446	3.80988	13.99550
H	2.27667	2.36994	16.79175	H	5.82255	3.75712	13.24837
H	3.59124	2.11687	17.94901	H	5.43639	3.45664	14.95324
H	2.20750	3.13498	18.38992	H	4.73950	4.86628	14.12790
C	2.53495	4.93486	16.25001	C	4.32060	1.47726	13.61882
H	2.98715	5.75446	15.67477	H	5.11651	1.31133	12.87274
H	1.96327	4.31277	15.53798	H	3.52843	0.74532	13.42066
H	1.81636	5.36983	16.96306	H	4.75293	1.23948	14.60728
C	4.57935	3.54074	15.92331	C	2.73783	3.07771	14.69495
H	5.35615	2.90606	16.37460	H	1.87698	2.41811	14.51457
H	4.02962	2.91406	15.19814	H	2.35979	4.10878	14.77297
H	5.07889	4.33116	15.34817	H	3.15641	2.80218	15.67972
C	5.28131	6.95712	16.30256	C	1.44089	2.56109	11.40011
H	5.95376	7.77234	15.98263	C	1.43163	1.11441	11.90738
H	5.24359	6.23402	15.47762	H	0.50300	0.61997	11.57379
H	4.27668	7.38237	16.41339	H	1.45999	1.04260	13.00326
C	7.12323	5.61881	17.26866	H	2.26941	0.52752	11.49866
H	7.63220	5.23451	18.16377	C	0.24792	3.30911	12.00601
H	6.98524	4.77990	16.57178	H	0.14520	4.32678	11.60037
H	7.81420	6.33230	16.78462	H	0.30520	3.38780	13.10211
C	6.11121	7.47576	18.57971	H	-0.68377	2.76764	11.76255
H	5.19746	7.98609	18.92620	C	1.26462	2.49354	9.87581
H	6.66012	7.12433	19.46468	H	2.10398	1.98344	9.37772
H	6.75264	8.22791	18.08634	H	1.14763	3.47761	9.40732
C	6.03835	2.81482	19.09850	H	0.36022	1.90583	9.63968
H	6.47985	2.19962	19.90291	C	3.22694	5.30251	11.43083
H	5.42148	2.14340	18.48696	C	4.68534	5.76427	11.29117
H	6.86706	3.17536	18.47248	H	5.23460	5.16866	10.54229
C	4.12883	3.37182	20.61448	H	5.24499	5.72212	12.23357
H	3.43418	2.72229	20.06972	H	4.70616	6.81117	10.93836
H	4.58432	2.76548	21.41777	C	2.52736	6.13193	12.51400
H	3.53670	4.16384	21.09381	H	2.51297	7.19797	12.22440
C	6.17266	4.72833	20.65745	H	3.04655	6.06672	13.48235
H	5.64181	5.53853	21.16738	H	1.48275	5.82340	12.67200
H	6.55782	4.04519	21.43531	C	2.56218	5.55896	10.07253
H	7.04358	5.15228	20.13889	H	3.00463	4.94821	9.26869
7				H	2.71033	6.61680	9.79237
W	5.76185	1.50307	8.62325	H	1.47887	5.37530	10.08346
C	4.67350	2.72465	7.51904	7 ^{Mo}			
O	4.06426	3.43429	6.83331	Mo	5.81411	1.52968	8.68367
C	4.20481	0.29797	8.59241	C	4.69836	2.72609	7.60947
O	3.30746	-0.43694	8.55388	O	4.05913	3.41569	6.93301
C	7.90567	0.68374	9.28237	C	4.28071	0.33780	8.81014
H	8.13274	0.46612	10.32478	O	3.39221	-0.40675	8.85187
C	7.34756	-0.22763	8.34890	C	7.95737	0.67483	9.18377
H	7.08646	-1.26413	8.55659	H	8.27805	0.50449	10.21031
C	7.22336	0.44320	7.09250	C	7.27848	-0.25865	8.35953
H	6.85422	0.00874	6.16541	H	6.99988	-1.27161	8.64612
C	7.69888	1.77736	7.26846	C	7.05210	0.35252	7.08664

S59

H	6.57750	-0.11337	6.22517	H	-0.27039	9.32147	22.34472
C	7.59777	1.66905	7.14038	C	1.27376	8.81336	23.88440
H	7.60021	2.39432	6.32801	H	2.02072	9.59217	23.73730
C	8.15263	1.86939	8.43058	C	1.34061	7.75887	24.84652
H	8.63857	2.77597	8.78774	H	2.14075	7.59135	25.56573
Si	4.80946	2.50780	10.40322	C	0.16564	6.96423	24.69869
Si	3.16964	3.41973	11.85448	H	-0.10546	6.09788	25.30035
C	3.79568	2.93874	13.64015	W	2.49451	8.80853	18.26328
C	4.96112	3.83737	14.06685	C	1.57038	7.93983	16.75208
H	5.79456	3.81047	13.34670	O	1.08249	7.49617	15.79660
H	5.35791	3.48051	15.03402	C	0.89109	9.01135	19.34846
H	4.66023	4.88629	14.20281	O	-0.01718	9.26253	20.03564
C	4.32324	1.49670	13.64217	C	4.16457	9.89352	16.95788
H	5.14634	1.35176	12.92144	H	4.60003	9.42062	16.07932
H	3.55003	0.75411	13.41119	C	3.01043	10.73616	16.97568
H	4.72727	1.25577	14.64184	H	2.39999	11.00511	16.11507
C	2.67747	3.05567	14.68143	C	2.80120	11.17052	18.31068
H	1.83863	2.37735	14.46985	H	1.99880	11.82287	18.65223
H	2.27335	4.07733	14.75295	C	3.81427	10.59714	19.12899
H	3.07001	2.78330	15.67783	H	3.94682	10.75205	20.19836
C	1.49199	2.56100	11.34899	C	4.64928	9.80100	18.29015
C	1.49784	1.10231	11.82187	H	5.53650	9.26274	18.61329
H	0.58361	0.60173	11.45901	Si	0.58200	5.89609	20.74426
H	1.50570	1.00569	12.91627	Si	-1.36565	4.87121	19.70311
H	2.35060	0.53681	11.41512	C	-1.31525	2.97072	20.14593
C	0.27238	3.27097	11.94889	C	-1.35232	5.21595	17.79840
H	0.15755	4.29628	11.56638	C	-2.84096	5.77652	20.62245
H	0.30362	3.32219	13.04737	Si	2.91272	6.70196	19.11845
H	-0.64276	2.71789	11.67089	Si	4.55117	4.87777	18.85462
C	1.34177	2.53059	9.82080	C	6.21761	5.91676	18.81866
H	2.21411	2.08538	9.31964	C	4.24299	4.06896	17.09526
H	1.17569	3.52156	9.38273	C	4.50300	3.55235	20.27987
H	0.47433	1.90244	9.55324	C	0.02284	4.85996	17.23012
C	3.22828	5.32718	11.46436	H	0.82614	5.42831	17.72556
C	4.67875	5.82491	11.38977	H	0.25248	3.79332	17.32469
H	5.27377	5.25004	10.65970	H	0.06485	5.11873	16.15954
H	5.20094	5.78883	12.35356	C	-1.60637	6.70248	17.52840
H	4.68831	6.87477	11.04530	H	-1.46438	6.91202	16.45528
C	2.46335	6.13161	12.52155	H	-2.62910	7.00800	17.78990
H	2.43865	7.19977	12.24016	H	-0.90491	7.35131	18.07363
H	2.93830	6.06870	13.51260	C	-2.41351	4.38959	17.06100
H	1.41959	5.79977	12.62847	H	-2.38845	4.64150	15.98588
C	2.61450	5.58381	10.08201	H	-2.23535	3.30700	17.14156
H	3.09218	4.98168	9.29221	H	-3.43394	4.58943	17.41832
H	2.76167	6.64470	9.81294	C	-2.72089	2.36712	20.03805
H	1.53361	5.38883	10.05235	H	-3.13826	2.45255	19.02377
Dimerization_Silyldyne TS				H	-2.67560	1.29187	20.28901
W	1.40311	6.73536	22.73563	H	-3.43569	2.82462	20.73379
C	1.91511	4.89353	23.19323	C	-0.39446	2.19558	19.19842
O	2.17314	3.82108	23.55267	H	0.62464	2.60564	19.18068
C	3.27500	7.28578	22.35007	H	-0.31844	1.14860	19.54159
O	4.32491	7.76027	22.26296	H	-0.77055	2.17180	18.16571
C	-0.62341	7.54164	23.66445	C	-0.78899	2.75370	21.57100
H	-1.60184	7.19925	23.34161	H	-1.34530	3.31336	22.33157
C	0.06171	8.68498	23.16227	H	-0.87232	1.68201	21.82576
				H	0.27147	3.03178	21.66916

S 60

C	-2.58142	7.28685	20.67454	C	5.33105	-0.31629	1.50694
H	-2.66100	7.76343	19.69085	H	6.27264	-2.55665	-0.87361
H	-3.32708	7.76737	21.33251	H	3.83136	0.97413	-1.25721
H	-1.58546	7.53655	21.06791	H	6.56216	-2.09143	1.54395
C	-4.18553	5.55487	19.91568	H	4.03899	1.38334	1.17715
H	-4.19944	5.98363	18.90374	H	5.45919	-0.10837	2.57253
H	-4.46523	4.49484	19.83878	C	5.13408	0.13110	-3.79916
H	-4.98077	6.06243	20.49053	C	4.70102	0.02497	-5.13611
C	-2.96467	5.26530	22.06266	C	5.67024	1.36957	-3.39131
H	-3.70142	5.88174	22.60730	C	4.78258	1.10224	-6.01385
H	-3.31821	4.22678	22.11710	C	5.76122	2.44906	-4.26438
H	-2.01093	5.31930	22.60684	C	5.31072	2.31783	-5.57840
C	3.19191	2.95915	17.16831	H	4.27222	-0.91722	-5.48599
H	2.96033	2.61038	16.14614	H	6.03575	1.48108	-2.36796
H	3.53881	2.08464	17.73582	H	4.42511	0.99663	-7.04127
H	2.25202	3.31007	17.61412	H	6.18977	3.39353	-3.91961
C	3.72521	5.10884	16.09480	H	5.37208	3.16523	-6.26606
H	4.38008	5.98192	15.98796	C	4.82252	-2.53415	-3.31938
H	3.63206	4.63859	15.09945	C	5.50541	-3.05132	-4.43687
H	2.73102	5.48474	16.37164	C	3.89812	-3.37693	-2.67394
C	5.53278	3.44248	16.54238	C	5.27049	-4.34657	-4.89286
H	5.96611	2.69064	17.21816	C	3.62539	-4.65630	-3.15195
H	5.30422	2.92994	15.59091	C	4.31357	-5.14349	-4.26282
H	6.30954	4.18620	16.32284	H	6.23891	-2.42659	-4.95408
C	6.31475	6.72080	17.51560	H	3.36995	-3.00762	-1.79062
H	7.18114	7.40466	17.57220	H	5.82560	-4.73413	-5.75100
H	6.46830	6.08379	16.63463	H	2.88129	-5.28120	-2.65194
H	5.41609	7.32957	17.33841	H	4.10077	-6.14695	-4.64123
C	7.46223	5.02515	18.92931				
H	7.55134	4.55899	19.92122				
H	7.49767	4.22518	18.17761				
H	8.36158	5.65059	18.78262	NHC_BPh₃			
C	6.24629	6.90972	19.98228	C	5.84621	4.71537	9.54301
H	5.38278	7.59048	19.96553	C	7.31519	6.39897	9.19188
H	6.25066	6.41859	20.96329	C	6.75407	6.08919	7.98710
H	7.16072	7.52793	19.92080	C	6.97449	5.71436	11.55327
C	5.40694	2.34916	19.97854	H	8.03502	5.96985	11.68726
H	5.31703	1.61383	20.79755	H	6.79950	4.75206	12.04390
H	5.12873	1.82840	19.05100	C	6.07893	6.78806	12.13787
H	6.46784	2.62863	19.90585	H	6.24418	7.76466	11.65809
C	3.06987	3.04097	20.45851	H	6.27388	6.89621	13.21476
H	2.73203	2.43909	19.60876	H	5.02167	6.51385	12.00778
H	3.00679	2.40933	21.35972	C	8.34933	7.40365	9.54800
H	2.35560	3.86904	20.59632	H	9.23677	6.92862	9.99613
C	4.95514	4.16130	21.61060	H	7.97389	8.14929	10.26602
H	4.36011	5.04065	21.89086	H	8.68290	7.94192	8.65166
H	4.82512	3.41792	22.41524	C	6.99510	6.68270	6.64619
H	6.01521	4.45156	21.59839	H	7.56455	6.00817	5.98930
				H	7.56757	7.61411	6.74125
BPh₃				H	6.05192	6.92294	6.13248
B	5.00819	-1.06686	-2.80148	C	4.97947	4.50570	7.20106
C	5.05365	-0.81168	-1.25563	H	4.46974	5.35463	6.71798
C	5.79497	-1.67835	-0.43042	H	4.20498	3.93499	7.72199
C	4.42658	0.29136	-0.64517	C	5.68486	3.63498	6.17989
C	5.95468	-1.42250	0.92934	H	4.93677	3.19546	5.50478
C	4.54577	0.52880	0.72174	H	6.21588	2.81158	6.67421
				H	6.40016	4.20101	5.56623

S61

N	6.74041	5.54652	10.12476	H	7.17904	6.10270	11.48303
N	5.85403	5.06147	8.22991	H	5.45507	6.48040	11.60552
B	4.93611	3.47425	10.16113	C	3.77043	5.36793	9.52643
C	5.32494	2.19308	9.20304	H	3.58437	5.92109	10.45696
C	4.37986	1.40350	8.53132	H	3.65476	4.29393	9.74703
C	6.67482	1.85494	8.98600	H	2.97487	5.64707	8.81806
C	4.74936	0.34558	7.69794	C	4.69023	4.88727	6.65552
C	7.06045	0.79019	8.16972	H	5.25537	5.00605	5.72194
C	6.09382	0.02791	7.51442	H	3.76570	5.47914	6.54488
H	3.31743	1.63853	8.64053	C	4.36067	3.42530	6.91574
H	7.45804	2.45981	9.45623	H	3.92529	2.96621	6.01565
H	3.97764	-0.23365	7.18382	H	3.63614	3.29657	7.73160
H	8.12060	0.55944	8.02958	H	5.26696	2.86544	7.18937
H	6.38793	-0.80015	6.86437	N	7.14972	6.45560	8.62992
C	3.35805	3.90409	10.09189	N	5.52003	5.48941	7.67693
C	2.37941	2.99299	10.53517	B	8.91246	4.21910	6.39204
C	2.89026	5.16842	9.70196	C	8.52870	3.34825	7.65008
C	1.02482	3.31449	10.56463	C	8.77536	3.80729	8.95853
C	1.53441	5.50746	9.72774	C	7.89712	2.09762	7.53048
C	0.59222	4.57716	10.15495	C	8.38123	3.09042	10.08258
H	2.69758	2.00959	10.89352	C	7.48572	1.37415	8.64933
H	3.60360	5.93238	9.37538	C	7.71874	1.87148	9.93039
H	0.29980	2.57719	10.91961	H	9.26998	4.76910	9.09647
H	1.21340	6.50413	9.41153	H	7.72157	1.67853	6.53696
H	-0.46927	4.83808	10.18063	H	8.58789	3.48861	11.08027
C	5.27997	3.12063	11.73548	H	6.97772	0.41472	8.51986
C	4.57365	3.74465	12.78218	H	7.38776	1.30812	10.80663
C	6.25350	2.18473	12.12592	C	8.43646	3.82053	4.94144
C	4.85168	3.49082	14.12486	C	9.34856	3.88123	3.87206
C	6.53744	1.91351	13.46536	C	7.14103	3.36488	4.64150
C	5.84369	2.57437	14.47646	C	8.98704	3.51356	2.57641
H	3.77426	4.44947	12.53595	C	6.75836	3.02850	3.34612
H	6.80525	1.63374	11.36264	C	7.68410	3.10087	2.30512
H	4.27828	4.00417	14.90180	H	10.36951	4.22152	4.06433
H	7.30023	1.17253	13.72024	H	6.41415	3.28029	5.44657
H	6.06407	2.36004	15.52594	H	9.72508	3.56083	1.77167
				H	5.73691	2.69345	3.14598
				H	7.38966	2.82415	1.28922
				C	10.04957	5.31013	6.48363
				C	9.96196	6.49024	5.71991
				C	11.18493	5.15241	7.29745
				C	10.93896	7.47889	5.79074
				C	12.17747	6.13153	7.36275
				C	12.05232	7.30300	6.61689
				H	9.08450	6.64156	5.08644
				H	11.30152	4.23989	7.88886
				H	10.83082	8.39343	5.20192
				H	13.05175	5.97608	8.00046
				H	12.82358	8.07588	6.67410
Addition NHC BPh₃ TS							
C	6.78199	5.93522	7.43181				
C	6.16955	6.31755	9.60464				
C	5.11403	5.70952	8.98982				
C	8.35769	7.22906	8.82937				
H	9.08519	6.89737	8.08076				
H	8.77195	6.98950	9.82173				
C	8.10587	8.72028	8.69656				
H	7.74562	8.95271	7.68307				
H	9.03029	9.28707	8.88239				
H	7.34436	9.06931	9.40969				
C	6.36554	6.69121	11.02849				
H	6.61741	7.75510	11.16400				

4. References

- [1] N. Kuhn, T. Kratz, *Synthesis* **1993**, 1993, 561-562.
- [2] W. Malisch, R. Lankat, S. Schmitzer, R. Piki, U. Posset, W. Kiefer, *Organometallics* **1995**, 14, 5622-5627.
- [3] G. Dübek, F. Hanusch, S. Inoue, *Inorg. Chem.* **2019**, 58, 15700-15704.
- [4] APEX suite of crystallographic software, APEX 3 version 2015.5-2; Bruker AXS Inc.: Madison, Wisconsin, USA, 2015
- [5] SAINT, Version 7.56a and SADABS Version 2008/1; Bruker AXS Inc.: Madison, Wisconsin, USA, 2008.
- [6] G.M. Sheldrick, SHELXL-2014, University of Göttingen, Göttingen, Germany, 2014.
- [7] C.B Hübschle; G.M. Sheldrick; B.J. Dittrich, *Appl. Cryst.* 2011, 44, 1281-1284.
- [8] G.M Sheldrick, SHELXL-97, University of Göttingen, Göttingen, Germany, 1998.
- [9] A.J .C. Wilson, *International Tables for Crystallography*, Vol. C, Tables 6.1.1.4 (pp. 500-502), 4.2.6.8 (pp. 219-222), and 4.2.4.2 (pp. 193-199); Kluwer Academic Publishers: Dordrecht, The Netherlands, 1992.
- [10] C.F. Macrae; I.J. Bruno; J.A. Chisholm; P.R. Edgington; P. McCabe; E. Pidcock; L. Rodriguez-Monge; R. Taylor; J. van de Streek; P.A.J. Wood, *Appl. Cryst.* 2008, 41, 466-470.
- [11] a) F. Neese, *Wiley Interdiscip. Rev.: Comput. Mol. Sci.* **2018**, 8, e1327; b) F. Neese, *Wiley Interdiscip. Rev.: Comput. Mol. Sci.* **2012**, 2, 73-78.
- [12] a) J. P. Perdew, M. Ernzerhof, K. Burke, *J. Chem. Phys.* **1996**, 105, 9982-9985; b) C. Adamo, V. Barone, *J. Chem. Phys.* **1999**, 110, 6158-6170.
- [13] a) S. Grimme, S. Ehrlich, L. Goerigk, *J. Comput. Chem.* **2011**, 32, 1456-1465; b) S. Grimme, J. Antony, S. Ehrlich, H. Krieg, *J. Chem. Phys.* **2010**, 132, 154104.
- [14] F. Weigend, R. Ahlrichs, *Phys. Chem. Chem. Phys.* **2005**, 7, 3297-3305.
- [15] a) D. Andrae, U. Häußermann, M. Dolg, H. Stoll, H. Preuß, *Theor. Chim. Acta* **1990**, 77, 123-141; b) K. Eichkorn, F. Weigend, O. Treutler, R. Ahlrichs, *Theor. Chem. Acc.* **1997**, 97, 119-124.
- [16] F. Weigend, *Phys. Chem. Chem. Phys.* **2006**, 8, 1057-1065.
- [17] https://comp.chem.umn.edu/freqscale/190107_Database_of_Freq_Scale_Factors_v4.pdf. Version from January 7, 2018.
- [18] a) E. v. Lenthe, E. J. Baerends, J. G. Snijders, *J. Chem. Phys.* **1993**, 99, 4597-4610; b) C. van Wüllen, *J. Chem. Phys.* **1998**, 109, 392-399.
- [19] Kaupp, M.; Buhl, M.; Malkin, V. (Eds) *Calculation of NMR and EPR Parameters. Theory and Applications*. Wiley-VCH, 2004.
- [20] C. J. Cramer, D. G. Truhlar, *Acc. Chem. Res.* **2008**, 41, 760-768.
- [21] G. Knizia, J. E. M. N. Klein, *Angew. Chem., Int. Ed.* **2015**, 54, 5518-5522.
- [22] Y. Zhao, D. G. Truhlar, *Theor Chem Acc* **2008**, 120, 215-241.
- [23] L. Goerigk, *J Phys Chem Lett* **2015**, 6, 3891-3896.
- [24] a) J. Tao, J. P. Perdew, V. N. Staroverov, G. E. Scuseria, *Phys. Rev. Lett.* **2003**, 91, 146401; b) V. N. Staroverov, G. E. Scuseria, J. Tao, J. P. Perdew, *J. Chem. Phys.* **2003**, 119, 12129-12137.

12.4 Licenses for Copyrighted Content

“Reactivity of an NHC-stabilized pyramidal hydrosilylene with electrophilic boron sources”

G. Dübek, D. Franz, C. Eisenhut, P. J. Altmann and S. Inoue, *Dalton Trans.*, 2019, **48**, 5756
DOI: 10.1039/C9DT00608G

If you are the author of this article you do not need to formally request permission to reproduce figures, diagrams etc. contained in this article in third party publications or in a thesis or dissertation provided that the correct acknowledgement is given with the reproduced material.

Reproduced material should be attributed as follows:

- For reproduction of material from NJC:
[Original citation] - Reproduced by permission of The Royal Society of Chemistry (RSC) on behalf of the Centre National de la Recherche Scientifique (CNRS) and the RSC
- For reproduction of material from PCCP:
[Original citation] - Reproduced by permission of the PCCP Owner Societies
- For reproduction of material from PPS:
[Original citation] - Reproduced by permission of The Royal Society of Chemistry (RSC) on behalf of the European Society for Photobiology, the European Photochemistry Association, and RSC
- For reproduction of material from all other RSC journals:
[Original citation] - Reproduced by permission of The Royal Society of Chemistry

If you are the author of this article you still need to obtain permission to reproduce the whole article in a third party publication with the exception of reproduction of the whole article in a thesis or dissertation.

“NHC-Stabilized Silyl-Substituted Chlorosilylene”**RightsLink®**

Home



Help



Email Support



Gizem Dübek ▾



NHC-Stabilized Silyl-Substituted Chlorosilylene**Author:** Gizem Dübek, Franziska Hanusch, Shigeyoshi Inoue**Publication:** Inorganic Chemistry**Publisher:** American Chemical Society**Date:** Dec 1, 2019*Copyright © 2019, American Chemical Society***PERMISSION/LICENSE IS GRANTED FOR YOUR ORDER AT NO CHARGE**

This type of permission/license, instead of the standard Terms & Conditions, is sent to you because no fee is being charged for your order. Please note the following:


- Permission is granted for your request in both print and electronic formats, and translations.
- If figures and/or tables were requested, they may be adapted or used in part.
- Please print this page for your records and send a copy of it to your publisher/graduate school.
- Appropriate credit for the requested material should be given as follows: "Reprinted (adapted) with permission from (COMPLETE REFERENCE CITATION). Copyright (YEAR) American Chemical Society." Insert appropriate information in place of the capitalized words.
- One-time permission is granted only for the use specified in your request. No additional uses are granted (such as derivative works or other editions). For any other uses, please submit a new request.

BACK**CLOSE WINDOW**

“An Air-Stable Heterobimetallic Si₂M₂ Tetrahedral Cluster”

Research Article |  Open Access |  

An Air-Stable Heterobimetallic Si₂M₂ Tetrahedral Cluster

Gizem Dübek, Franziska Hanusch, Dr. Dominik Munz, Prof. Shigeyoshi Inoue 

Publisher: John Wiley and Sons

© 2020 The Authors. Published by Wiley-VCH Verlag GmbH & Co. KGaA.

Open Access Article

This article is available under the terms of the Creative Commons Attribution License (CC BY) (which may be updated from time to time) and permits use, distribution and reproduction in any medium, provided that the Contribution is properly cited.

For an understanding of what is meant by the terms of the Creative Commons License, please refer to [Wiley's Open Access Terms and Conditions](#).

Permission is not required for this type of reuse.

Wiley offers a professional reprint service for high quality reproduction of articles from over 1400 scientific and medical journals. Wiley's reprint service offers:

- Peer reviewed research or reviews
- Tailored collections of articles
- A professional high quality finish
- Glossy journal style color covers
- Company or brand customisation
- Language translations
- Prompt turnaround times and delivery directly to your office, warehouse or congress.